THE PETROLOGY OF THE BASIC IGNEOUS ROCKS OF THE GARDAR PROVINCE, SOUTH WEST GREENLAND

by

Isobel C.F. Winstanley, B.Sc.

Thesis presented for the Degree of Doctor of Philosophy of the University of Edinburgh in the Faculty of Science.

1975

EX BIBL. UNIV. EDINBURGEN.

Page Number	Section Number and Heading
iii	SUMMARY
1	1. INTRODUCTION
1	1. The Gardar Province
2	2. Outline of the geological history of South Greenland
11	3. Review of work in the Gardar Province with special reference to the dykes
18	4. The present work
21	2. FIELD RELATIONS OF THE DYKES
21	1. Introduction
21	2. Zone 1, Ivigtut
25	3. Zone 2, Nunarssuit - Isortoq
30	4. Zone 3, Tugtutoq - Narssarssuaq
39	3. PETROGRAPHY
39	1. Introduction
39	2. Classification
41	3. Petrography
52	4. MINERALOGY
52	1. Feldspars
55	2. Olivine
57	3. Clinopyroxene
61	4. Ore minerals
62	5. Kaersutite
64	5. MAJOR-ELEMENT CHEMISTRY
64	1. Introduction
65	2. Statistical treatment
68	3. Variation diagrams
76	4. F-M-A diagram
77	5. CIPW norms
79	6. The trachydiorites
85	6. TRACE-ELEMENT CHEMISTRY
85	1. Statistical treatment
86	2. Variation diagrams
92	3. K/Rb ratios
94	4. The trachydiorites

Page Number	Section Number and Heading
97	7. PETROGENESIS
97	1. Low-pressure processes
100	2. The trachydiorites
102	3. Petrogenesis of the basaltic compositions
112	4. The incompatible elements
123	REFERENCES
133	ACKNOWLEDGEMENTS
	APPENDIXES
134	1. Preparation of rock-powders for chemical analysis
135	2. Analytical techniques
141	3. Key to analyses in Appendix 4
147	4. Rock analyses and CIPW norms
161	5. Mineral analyses
162	6. Optical determinations
Last Page	ERRATA

The rocks of the Precambrian Gardar province of south-west Greenland comprise an eroded continental sandstone and lava succession, now preserved in the eastern part of the region, a variety of alkaline igneous complexes and basic and salic regional dyke swarms. Faulting occurred during the Gardar period, subsequent erosion exposing the rocks at different structural levels. Anorthositic inclusions are common within the basic intrusions.

A study of the basic dyke swarms was undertaken to provide data on the variety of basic magmas available in the province during the Gardar period.

Magmatic activity was essentially confined within three narrow, ENE trending zones, which can be defined on the basis of the distribution of the ENE dyke swarms and alkaline complexes.

Despite a period of activity of some 150 my, strong petrographic and chemical similarities exist between the majority of the basic rocks, which comprise feldspathic olivine dolerites transitional to trachydolerites and syenogabbros. Although the salic rocks in the province are commonly highly alkaline, the basic rocks are only mildly alkaline, transitional between typical tholeiitic and alkaline compositions. The youngest ENE dyke swarm in the southeastern zone is an exception; petrographically these rocks may be termed trachydiorites and chemically they are considerably more alkaline and volatile-rich than the dolerites and trachydolerites.

The principal major and trace-element variation trends displayed by the dolerite/trachydolerite series can be satisfactorily explained in terms of the low-pressure fractionation of the observed phenocryst phases from transitional olivine basalt parent magmas. Some chemical variation, principally in K, Ba, Sr and Rb, results from the variation in composition of the basaltic parent magmas and is ascribed to high-pressure processes involved in the production of the basaltic parent magmas.

The delayed appearance of clinopyroxene phenocrysts (only in the trachydolerites) and the relatively low CaO and high Al_2O_3 content of the basaltic compositions is believed to be due to the prior fractionation of clinopyroxene at pressures of about 10 kb as the magma ascended.

It is suggested that the variation in incompatible-element abundances in the parental basaltic compositions may be due to variable degrees of melting producing the primary magmas, or to the effects of high pressure eclogite fractionation. The variation in K/Na ratios in the basaltic compositions indicates the latter alternative.

The compositional variation within the trachydiorite dykes cannot be explained in terms of fractionation of the observed phenocryst phases and it is believed that diffusion has altered the alkali contents of the magmas. The trachydiorites represent a fresh influx of basic magma after a period of salic volcanism and are believed to have resulted from a relatively minor melting episode producing a small

amount of alkali and volatile-enriched basic magma.

I. INTRODUCTION

The rocks belonging to the Gardar alkaline province occur in south-west Greenland principally between Sermiligarssuk (61° 30'N) and Julianehaab (N60° 20') and stretch from the coast to the Inland Ice. A probable extension of the province is seen in south-east Greenland between N61° and N62° latitude.

I.1. The Gardar province

C. E. Wegmann (1938) was the first to define two structural divisions in south Greenland. One consisted of folded and regionally metamorphosed 'old basement' rocks - the eroded remains of a mountain chain - which he called the 'Ketilides'. The other, 'younger formation', consisted of an unmetamorphosed and unfolded continental sandstone-lava sequence with associated basic and alkaline intrusions. The latter he called the 'Gardar formation'. A major unconformity separated the Gardar formation from the Ketilides. Thus the Gardar formation included all the rocks formed after the last orogenic period in south Greenland.

The name 'Gardar province' is used to cover the area affected by this period of faulting, sedimentation and volcanism.

The rocks of the Gardar province comprise:

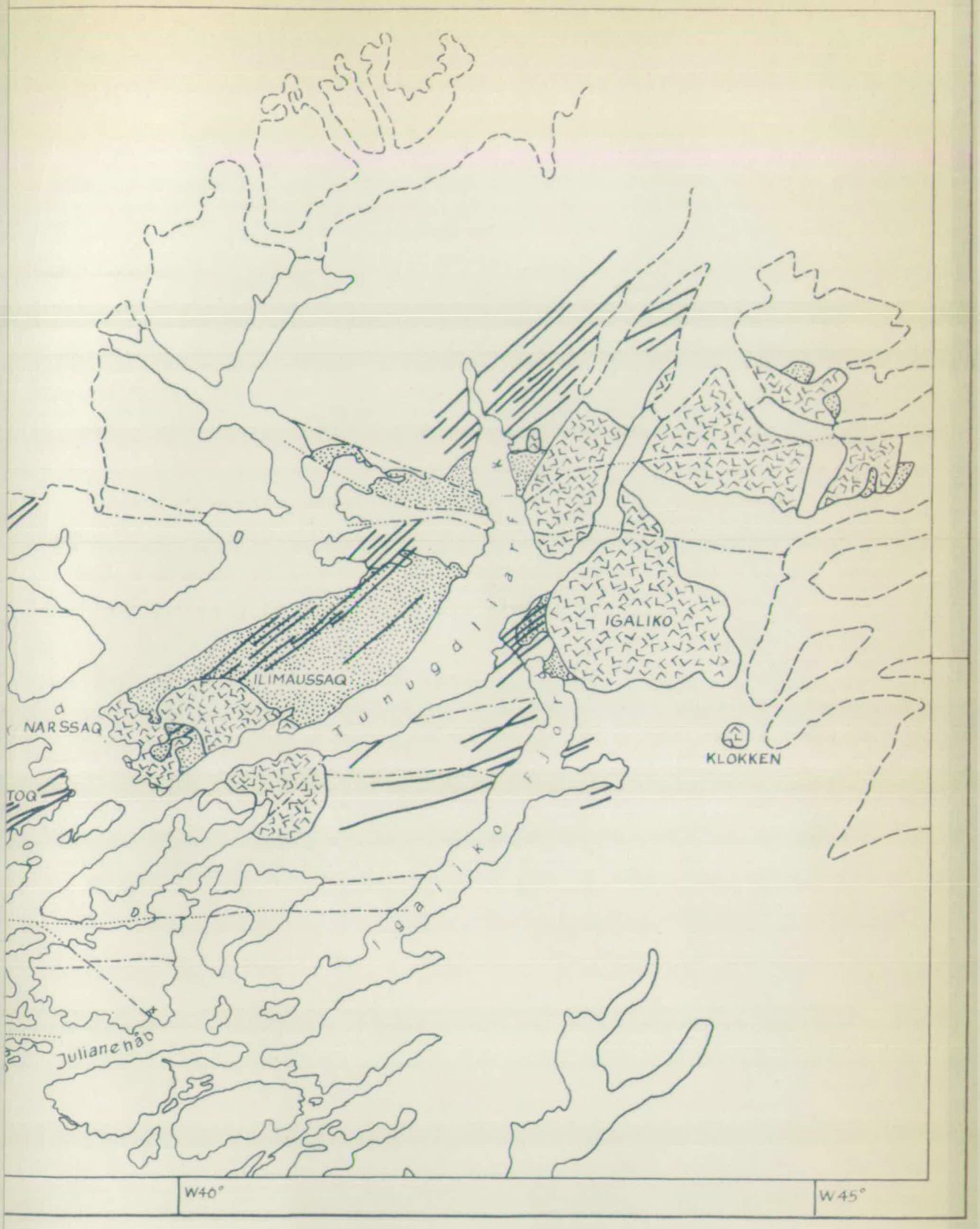
a. A continental sandstone and lava sequence preserved mainly in the area between Igaliko Fjord and Bredefjord (figure I.1.).

b. Swarms of unmetamorphosed basaltic to salic alkaline dykes intruded into the sandstones and lavas and also into the basement rocks throughout south Greenland.

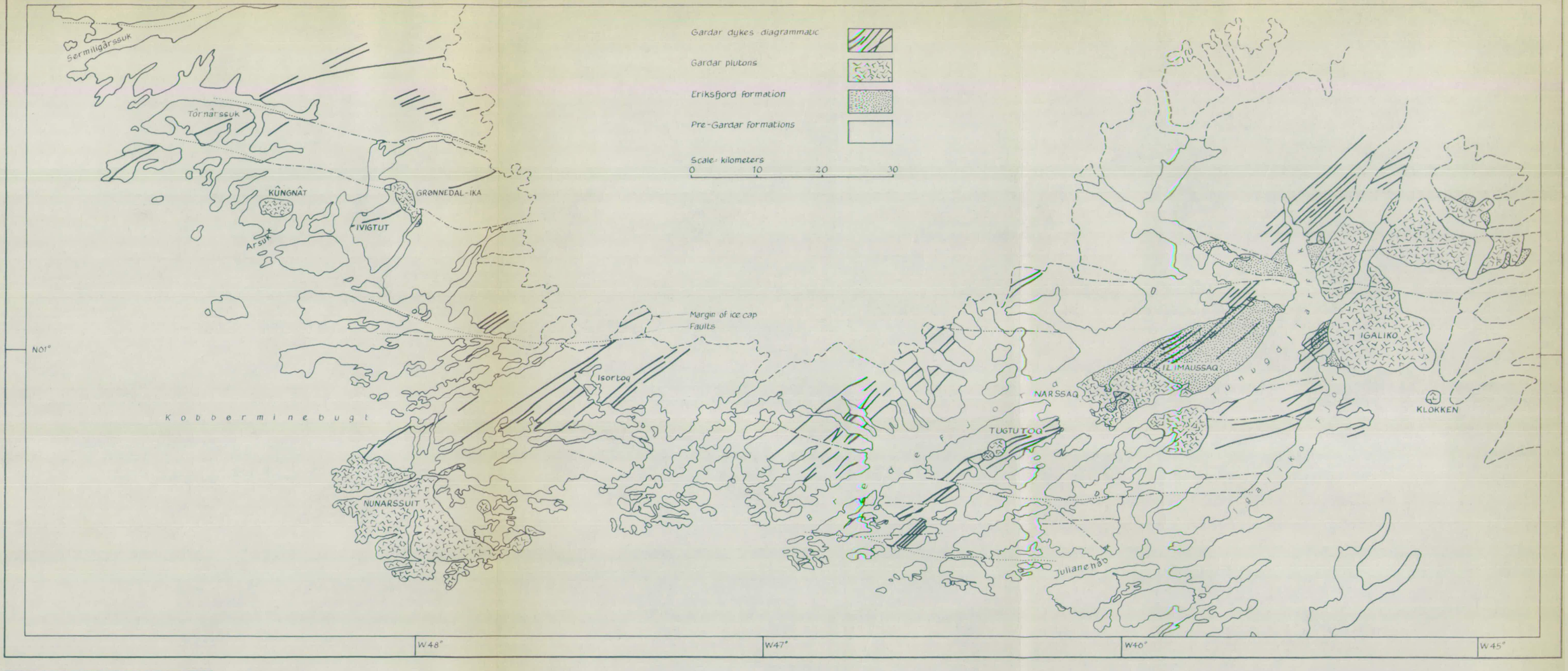
FIGURE 1.1:
A geological sketch-map of the Gardar province.

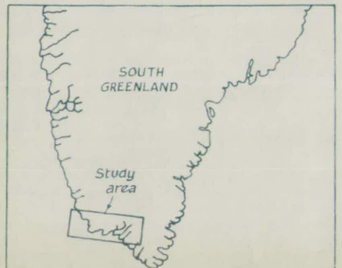
The location within south Greenland is shown by the inset, lower left.
Within the area of the map, the settlements of Arsuk, in the west, and Julianehaab, in the east, are shown.

For further description, see text.



Geological sketch map
of the Gardar province





Geological sketch map of the Gardar province

c. Diatremes and associated ultrabasic and carbonatitic plugs, sills and dykes which occur mainly in the eastern part of the province (Upton, 1962; Stewart, 1970).

d. Major central-complexes, largely composed of salic alkaline rocks ranging from alkali-granite to nepheline-syenite.

A south-east-trending swarm of basic dykes, younger than all other dykes and alkaline masses and unaffected by faults is now known to be of Mesozoic age (Larsen, 1966; Watt, 1968).

The igneous rocks of the Gardar province are Precambrian, within the limits 1350 to 1100 myrs (Blaxland et al., in prep., Bridgwater, 1965).

This study is confined to the basic dyke-swarms of the Gardar province, defined here as dykes with SiO_2 less than 54% and MgO more than 2%.

I.2. Outline of the geological history of south Greenland.

A chronology of the Precambrian of south Greenland is presented on Table I.1.

I.2.1. The basement complex.

In the Ivigtût region, slightly metamorphosed sedimentary and volcanic rocks of the Ketilidian period unconformably overlie pre-Ketilidian metasedimentary and metavolcanic rocks (the Tartoq Group) and Archaean Ivigtût gneisses (Higgins and Bondesen, 1966). A suite of basic dykes intruded the pre Ketilidian rocks and both Ketilidian and Pre-Ketilidian rocks became progressively more-deformed south and east of Ivigtût

TABLE I.1.

General chronology of the Precambrian in South Greenland.

(after Allart, 1967)

Name	Activity	Age
POST GARDAR	S.E. Dykes.	164my (approx.)
GARDAR	Late Alkaline Complexes: Salic Dykes (ENE); Basaltic Dykes (ESE); Lamprophyres. Early Alkaline Complexes: Lavas and Sandstones; ESE & NNW wrench faults.	1149±34my (4)* Age activity varied NW-SE 1327±17my (4)
KETILIDIAN	Tholeiitic Dykes	1590±70my (1)
	2nd Period Plutonic Activity: 3 phases, Granite Development; Reactivation Older Granites; Basic-Intermediate Intrusions	1780±20my (3)
	Dolerite Dykes in and around Julianehaab	
	1st Period Plutonic Activity: Older Granites; Repeated Deformation; Regional Metamorphism	1840±25my (3)
	Sediments, Volcanics, Basic Dykes	2000my (approx.)
PETILIDIAN	Basic Dykes; Regional Metamorphism; Repeated Deformation	2500my (approx.)
	Sediments and Volcanics (Tartoq Group)	
	Older Basement (Ivigtût Gneisses)	

*References for age

(1) Moorbath et al., 1960
(2) Van Breemen and Upton, 1972
(3)Van Breemen et al., 1974
(4) Blaxland et al., in prep.

during the Ketilidian orogeny (Bondesen and Henriksen, 1965).

Two main plutonic episodes can be recognised in the rocks affected by the Ketilidian fold belt. During the first, the main tectonic and metamorphic characters of the fold belt were formed, giving the NE to ENE foliation which is mainly seen in the basement rocks south of Ivigtut (Watterson, 1965; Allaart, 1967). Migmatisation and the formation of autochthonous and parautochthonous granites accompanied the first period of deformation (Bridgwater, 1965).

The second plutonic episode was called the Sanerutian by earlier workers (Bridgwater, 1965; Watterson, 1965) but was renamed the second Ketilidian episode by Allaart (1967). It involved reactivation of basement rocks and the formation of a suite of 'younger granites' in association with basic and intermediate intrusives (Allaart, 1967). Locally, 'hot shear belts' were formed with an ENE trend (Allaart et al., 1969).

The two plutonic episodes were separated by a period of intrusion of basic dykes (Allaart et al., 1969).

A further suite of north-west trending tholeiitic dolerite dykes was intruded towards the end of the second plutonic episode. They intersect all previous Ketilidian intermediate and basic intrusives, but are slightly metamorphosed and are displaced by Gardar faults. They are cut by the oldest Gardar dykes in the Sydprøven area (Allaart, 1967).

I.2.2. The development of transcurrent faults.

Following the Ketilidian orogeny, south Greenland underwent uplift and erosion and transcurrent faults were formed in two main directions: approximately north-south right-lateral faults and more dominant ESE left-lateral faults (Emeleus and Upton, in press). One of the left-lateral faults has been shown to have a long pre-Gardar history (Henriksen, 1960) but this may not be true of them all. These faults have broken south Greenland into large blocks (figure I.1).

Emeleus and Upton (in press) have suggested that crush zones found at the edges of principal fjords in south Greenland may indicate major ENE normal faults now largely submarine.

I.2.3. The Eriksfjord Formation.

The Gardar sandstone and lavas succession, some 3000 metres thick, is called the Eriksfjord Formation (Poulsen, 1964) and is preserved mainly in the downthrown Ilimaussaq fault-block (figureI.1). Isolated outcrops close to the Igaliko complex, together with stoped blocks preserved in Gardar intrusions, suggest that the Eriksfjord Formation once extended over a larger area (Emeleus and Harry, 1970; Upton 1962).

The sedimentary rocks comprise sandstones, siltstones and conglomerates which Poulsen suggested were deposited in a shallow water, non-marine environment. Sand-dunes are preserved at some levels (Poulsen, 1964), indicating an arid climate.

After a period of clastic sedimentation, volcanic activity began.

Ultrabasic and carbonatitic tuffs were erupted at an early stage in the

Qagssiarssuk area (Stewart, 1970). The volcanic activity involved the eruption of mainly basaltic lavas with trachyte lavas confined to the upper part of the succession (Stewart, 1964).

I.2.4. The intrusive igneous rocks.

Unmetamorphosed Gardar igneous intrusion, dykes, sills, plugs and central-type alkaline complexes, occur in south Greenland mainly between Julianehaab and Sermiligarssuk. Rock types vary from silica-deficient carbonatites and ultramafites through gabbroic rocks to syenites and alkali granites. The majority of the salic rocks are alkaline or peralkaline. Mineral layering is a common feature (Ferguson and Pulvertaft, 1963) and the widespread occurrence of inclusions of anorthosite and plagioclase megacrysts, particularly in basaltic and trachybasaltic rocks, has been taken to imply the existence of a large body of anorthosite at depth (Bridgwater and Harry, 1968).

I.2.4.1. Regional distribution of intrusive rocks.

South Greenland may be conveniently divided into three regions, each defined by a zone in which ENE dykes and central complexes are concentrated (figure I.1.). The three regions are: Ivigtut covered by the 1:100,000 GGU map sheet 61 V1 SYD), Nunarssuit (60 V1 NORD) and the Tugtutôq-Ilimaussaq area covered by the Julianehaab (60 V2 NORD) and Narsarssuaq (61 V3 SYD) map sheets.

Intrusive sequences between dyke swarms and alkali complexes can be established within each region but correlations between regions are not always possible because of the irregular distribution, both spatial and directional, of the dyke swarms.

There is evidence, moreover, that magmatic activity was not contemporaneous in the three regions. Rb/Sr age-determinations indicate a gap of 58±18 Myrs between the intrusion of the Kûngnât complex (1245±16 Myrs), the last intrusion in the Ivigtût region, and the Hviddal giant-dyke (1187±9 Myrs), the first of the ENE dykes in the Tugtutôq region (Van Breemen and Upton, 1972).

I.2.4.2. Dyke swarms.

A fuller account of the dyke swarms will be given in a later section; what follows is simply to serve the needs of the Introduction.

Several dyke swarms can be separated on the basis of contact relationships. The earliest swarm of dolerite dykes trends E to ESE, approximately parallel to the major, left-lateral transcurrent faults. Subsequent shearing along these dykes is not demonstrably due to further movement on the faults (Upton, 1962). Succeeding generations were emplaced sub-parallel to each other, with a general NE to ENE trend, in the same direction as the foliation of the basement rocks between Kobberminebugt and Julianehaab. However, north of Kobberminebugt, Gardar dykes of the trend are discordant to the basement structures (Upton, 1974). The ENE dyke swarms, too, have been affected by shearing subsequent to intrusion, eg. those crossing Tugtutôq island (Upton, 1962) and Ivigtût (Berthelsen, 1962).

Early members of the dyke swarms are doleritic and there is in the Tugtutôq - Ilimaussaq region an increase in the numbers of trachy-basaltic and alkalic dykes later in the intrusive sequences, although there is no strict progression from basic to alkaline rock types (Bridgwater and Harry, 1968).

The typical dolerite dykes, which weather to a reddish-brown rubble, were called 'brown dykes' by Wegmann (1938). Thus arose the 'BD' terminology, now current. Berthelsen (1962) distinguished three generations of dolerite dykes in the Ivigtût region which he called BD_0 BD_1 BD_2, and this grouping is now adopted by the Geological Survey of Greenland for dolerite dykes throughout the Gardar province. Thus the earliest swarm of essentially unmetamorphosed dykes, the E to ESE trending set, are classified as BD_0 dykes.

The BD dykes are invariably olivine dolerites in which plagioclase phenocrysts are common, although on occasion sparsely distributed. Synformal internal layering is common in the broader (over 100 meters) dykes of the younger generations but not in the BD_0 dykes.

Dyke widths range from under 1m to 150m with a median about 10 to 20m. Giant dykes up to 1000m thick occur at localities at Bangs Havn and Isortoq, N.E. of the Nunarssuit complex, on Tugtutôq and N. of Narsarssuaq (Harry and Pulvertaft, 1963; Bridgwater and Coe, 1970; Upton, 1962; Walton, 1965). The giant dykes are commonly composite with central portions of syenogabbro or syenite and marginal facies of

troctolitic gabbro or syenogabbro. Syenitic rocks form only a minor part of the younger Tugtutoq giant dykes. According to Bridgwater and Coe the Isortoq dykes have been intruded without dilatation of the basement rocks, probably by stoping. Evidence of emplacement of the syenitic portions in the Bangs Havn and Tugtutoq dykes prompted the suggestion by Upton (1974) that the giant dykes are intermediates in an evolutionary sequence from basic dyke intrusion by dilatation to ring-faulted and stoped central complexes.

Anorthosite xenoliths and plagioclase megacrysts are common in the dyke swarms and can comprise up to four-fifths of the dyke. Anorthosite xenoliths are present in the BD_O dykes but are more abundant in the later ENE swarms. Bridgwater and Harry (1968) link the type of inclusion with the composition of the host rock: gabbroic hosts contain anorthosite xenoliths and scattered calcic labradorite megacrysts; less-basic host rocks contain more-sodic megacrysts and secondary anorthosites. In the gabbroic hosts, the xenoliths are irregularly distributed, usually along the margins of the dykes or accumulated in small apophyses. Some unusual composite dykes, with microsyenite margins and trachydolerite centres, mainly found in the Tugtutoq area, carry abundant megacrysts in the basic centres.

The dykes that carry feldspathic inclusions have been referred to as 'BFD' (big feldspar dykes) dykes by the Greenland Survey.

Lamprophyre dykes are locally abundant, particularly in the ENE dyke zone that crosses Ivigtût (Berthelsen, 1962; Ayrton, 1963) where they were emplaced before the BD_0 dykes. Carbonatite dykes, sills and diatremes occur in an ENE zone north of Narssarssuaq (Walton, 1965) where most of them were intruded before the NE dolerite dyke swarms. Their relationship to the BD_0 dykes is uncertain.

Salic alkaline dykes, trachybasalts, trachytes, phonolites and rhyolites are concentrated in the vincinity of the alkaline complexes of Tugtutôq, Ilimaussaq, Igaliko and Grønnedal-Ika (Sørensen, 1969).

A swarm of basic ENE dykes, distinguished by flow-banding, has intruded the central Tugtutôq complex. These dykes are believed to be the latest Gardar intrusions in the area since the central complex itself cuts all other generations of ENE dykes, including the alkaline dykes of this region.

I.2.4.3. Major alkaline complexes.

The central complexes are mainly composed of salic alkaline rock types ranging from oversaturated alkali granite and augite syenite to undersaturated nepheline syenite and foyaites. Gabbroic rocks occur in minor amounts, for example the Alangorssuaq gabbro in the Nunarssuit complex (Harry and Pulvertaft, 1963) and the late basic ring dykes of the Kûngnât and Igaliko complexes (Upton, 1960; Emeleus and Harry, 1970). The gabbro-syenite Bangs Havn complex of Nunarssuit and the Narssaq gabbro are related to the ENE basic dyke swarms (Harry and Pulvertaft, 1963; Upton, 1964 b).

With the exception of the Klokken, Kûngnât and Tugtutôq centres, the

alkaline complexes are located at the intersections of the left-lateral wrench faults with the major ENE dyke swarms (fig. I.1.). Repeated intrusion of alkaline magma by ring-fracture and stoping formed steep-sided, arcuate complexes (Sørensen, 1969). Xenoliths of gneiss or of Gardar lavas and quartzites are present in many of the complexes below the level of the pre-Gardar unconformity (Upton, 1964 b), demonstrating the low density of the alkaline magmas. This is also shown by cumulates in which nepheline and alkali feldspar have settled.

Igneous layering is common in the complexes and cryptic and phase layering has been demonstrated in some of the intrusions. Trough banding and false bedding structures in some of the complexes suggest that convective overturn aided simple gravitative settling in forming accumulative rocks (Upton, 1960).

The majority of the alkaline complexes, with the exception of the Grønnedal-Ika and some members of the Igaliko complex, are later than the ENE dyke swarms amongst which they are located. The Grønnedal-Ika complex is intruded by the main dolerite dyke swarms in the Ivigtut region (Emeleus, 1964) and the Motzfeldt, north Qoroq and south Qoroq centres and three members of the Igdlerfigssalik centre (belonging to the Igaliko complex) are intruded by alkali trachyte and feldspathic (BFD) members of the main ENE dyke swarm. Four late members of the Igdlerfigssalik centre cut the majority of the ENE dyke swarms but have been intruded by trachyte and phonolite dykes. Thus the Igaliko complex

was intruded over a considerable period (Emeleus and Harry, 1970) but the latest syenites may be earlier than the latest members of the Ilimaussaq and central Tugtutôq centres. Alternatively the late alkaline dykes could be local products of the Igdlerfigssalik centre itself.

Mesozoic dykes

The latest manifestation of igneous activity in South Greenland was the intrusion of SE-trending basic dykes, which cut the Gardar intrusions and which are not affected by faults. These are now known to be of Mesozoic age (Larsen, 1966; Watt, 1969) and are believed to be associated with the opening of the Labrador sea (Allaart et al., 1969).

I.3. Review of work in the Gardar province, with special reference to the dykes.

Accounts of the geology of south Greenland have been published in connection with the regional mapping programme undertaken from 1955 by the Grønlands Geologiske Undersøgelse (Geological Survey of Greenland). Many publications dealt mainly with the Gardar alkaline plutons, although descriptions of the dyke swarms were included. Accounts of Gardar dyke swarms are given by Allaart, 1969; Watt, 1968; Upton, 1962. 1964; [redacted] Ayrton. 1963; Berthelsen, 1962; Walton, 1965. The dyke swarms containing abundant anorthositic inclusions were reported by Bridgwater and Harry (1968). Macdonald (1969) discussed the petrology of the Tugtutôq alkaline dykes and Gill (1972) described salic alkaline dykes near Grønnedal Ika and Ivigtût.

I.3.1. Chronological importance of the dykes.

Early workers followed Wegmann (1938) in assigning intrusions in south Greenland to the Gardar province by comparison with dykes and plutons that intruded the Eriksfjord formation, or because of their relationship to the regional dyke swarms (Harry and Pulvertaft, 1963).

Later, intersections between Gardar dykes and the alkaline plutons formed the basis for the chronological division of the Gardar period (i.e. the time during which Gardar rocks were being formed) and were, in fact, the only means by which intrusive sequences could be established for the plutons. Thus in the Ivigtût area, the Grønnedal-Ika complex is cut by a succession of dykes (Emeleus, 1964) but the swarms are cut by the Ivigtût cryolite body (Berthelsen, 1962) and the Kûngnât syentfie complex (Upton, 1960). In the Tunugdliarfik area, Gardar dykes are cut by the Tugtutôq central complex (Upton, 1962) and the Ilimaussaq complex (Ferguson, 1964). Some members of the Igaliko complex are intruded by dyke swarms, but these in turn are cut by later members of the complex as referred to in I.2. above.

Bridgwater and Harry (1968) tried to work out a detailed chronology for the Gardar period using the dyke swarms which are richest in anorthositic inclusions, as these dykes are widespread in the province and are easily recognisable in the field. However they found it difficult to make detailed correlations throughout the whole of the province as the spatial and temporal distribution of the swarms is irregular.

I.3.2. Tectonic environment.

There was a change in tectonic conditions in south Greenland after the end of the Ketilidian period. This change was from plutonic activity, involving formation of metamorphic, metasomatic and granitic rocks under orogenic conditions, to cratogenic activity, with processes affecting the crust comprising high-level faulting, intrusion of basic dyke swarms and extrusion of lavas and terrestial sedimentation. A long period of tectonic quiescence (ca. 300 my.) separated the Ketilidian and Gardar activity. It was recognition of the different environments which formed the basis for Wegmann's division of the Precambrian in south Greenland.

Tensional stresses were dominant in south Greenland during the Gardar period. In Ilordleq, Watterson (1965) calculated that intrusion of the dyke swarms involved crustal dilatation of between 10 and 20% in a zone 5km wide and Upton (1974) suggested total crustal dilatation in south Greenland may have been in excess of 10km.

Bridgwater (1965) and Watterson (1965) thought that Gardar cratogenic activity was related to the late stage of a 'tectono-magmatic' cycle and would therefore represent the last stage of development of the Ketilidian tectono-magmatic cycle rather than the beginning of a new one, as suggested by Wegmann (1938), or the marginal effects of the Grenville fold-belt, as suggested by Armstrong (1963). Watterson (1965) suggested that Gardar dyke emplacement could be related to the early stage of continental break up (cf. Sutton, 1963). The association in the Gardar province of basaltic volcanism and dyke

intrusion, alkaline and peralkaline plutons and carbonatite intrusions has been compared to activity within the east African rift eg. Stewart (1970), and Upton (1974) considered the Gardar province to be part of a Precambrian rift system analogous to the African occurrences.

I.3.3. Magmatic evolution of the province.

The main intrusive igneous rock types found in the Gardar province are dolerite, syenite and alkali granite (Sørensen, 1969). There is however, a marked preponderance of nepheline syenite and augite syenite and Watt (1969) estimated the areal extent of syenitic rocks to be ca. 67% of all rock types, although due to the difficulty of estimating the amount of doleritic rock represented by the dykes that figure may be too high. Watt quotes alkali granite and dolerite as each representing ca. 13% of the total. The doleritic/gabbroic rocks are present in only small amounts in the large complexes, being practically confined to the dyke swarms.

Trachybasalts and syenogabbros are common among the dyke rocks, but are scarce relative to the amount of doleritic/gabbroic and salic alkaline rocks. Frequency diagrams for silica content (SiO_2) and Thornton-Tuttle differentiation index (DI) of Gardar igneous rocks have mimima at SiO_2 50 to 55% and DI 60 to 65, thus corresponding to trachybasalt-syenogabbro composition (Upton, 1974).

The differentiation of a mildly alkaline basaltic magma to give syenogabbroic and syenitic rocks is illustrated by dykes in the Tugtutôq area (Upton, 1964b) and in the Isortoq area (Watt, 1966). Upton (1960) suggested that the Kûngnât syenite complex was formed by

tapping successively deeper levels of a stratified magma chamber which graded from transitional alkali olivine basalt in the lower part to trachyte. Sørensen (1969) suggested most of the Gardar rocks could have evolved by fractionation of early formed plagioclase, olivine and augite from an alkali olivine basalt in deep sub-crustal or crustal reservoirs. He suggested that the relative scarcity of rock types intermediate between dolerite and syenite and the predominance of syenite in the province could be explained if the magma reservoir were stratified with an upper part of trachytic magma, which was thus more readily available. Alternatively he suggested that the trachytic magma could have formed by partial melting of sub-crustal or crustal rocks, thus accounting for the relative abundance of syenitic and gabbroic rocks. However on the basis of Sr 87/86 data for the Gardar complexes, partial melting of crustal rocks to produce trachytic magmas can be ruled out (A. B. Blaxland, pers. comm.). The discussion of the relative abundance problem of Gardar rocks is further developed by Gill (1972) and Upton (1974).

Bridgwater and Harry (1968) explained the origin and distribution of anorthosite xenoliths and plagioclase megacrysts by postulating a magma chamber in which the liquids differentiated by liquid fractionation - a process which they claimed to be important in the formation of composite dykes that have syenitic margins and gabbroic centres.

Granular anorthosites accumulated at the top of a differentiating magma chamber of gabbroic composition. The resulting flotation cumulate was disrupted from time to time and partly differentiated magmas carrying anorthosite xenoliths were intruded at a higher level. As the magma at the top of the chamber became less basic with the operation of liquid and crystal fractionation (and possibly alkali diffusion), the density difference between magma and felspar crystals became less and the crystals hung suspended in the magma. Eventually the magma would no longer carry feldspar crystals in suspension and intrusions tapping the magma would not carry anorthosite xenoliths or plagioclase megacrysts. The critical magma composition appeared to be about 53% SiO_2, as few more-differentiated rocks carried feldspar xenoliths.

Upton (1962, 1970) pointed out that the primitive Gardar magma was relatively aluminous. This would minimise the difficulties of extracting large amounts of plagioclase from the parent magma to form the anorthosite body which is supposed to underlie the province. Plagioclase phenocrysts are observed in most Gardar dolerites and basalts; sometimes olivine phenocrysts are present but rarely clinopyroxene or hornblende. Clinopyroxene fractionation at moderately high pressure (greater than 10kb.) was suggested as a possible mechanism by which highly aluminous magmas could be produced (Upton 1971).

I.3.4. Comparisons with other provinces.

i. The shield areas of north America.

Wegmann (1938) compared the rocks of the Gardar provinces to the Precambrian Keweenawan formation, thus making the first suggestion of a Precambrian age for the Gardar rocks. The Keweenawan formation

consists of a continental sediment and lava succession, intruded by doleritic dykes and sills, with an age of approximately 1140 my. (Wanless et al. 1967). More recent work has confirmed Wegmann's suggestion.

Anorthosite xenoliths and plagioclase megacrysts occur in Keweenawan dykes, sills and lavas and the major rock type of the Duluth gabbro complex is anorthosite (Phinney, 1969; Grout and Schwartz 1939). Texturally and mineralogically these inclusions are similar to the Gardar occurrences although generally less alkaline than their Gardar counterparts: quartz tholeiites are common among the Keweenawan rocks and pigeonite is found in the groundmass of the intermediate varieties.

Upton (1964) and Bridgwater and Harry (1968) have pointed out the similarities between the Nain, Kiglapait and Michikamau anorthosite bodies in Canada and anorthosite inclusions in the Gardar province. The Canadian anorthosites were emplaced approximately 1500 to 1400my ago (Emslie, 1970; Morse, 1964). Layering is common, thus these bodies are similar in some respects to the layered anorthosites of the Assorutit body of Tugtutôq. The Canadian anorthosites, however, have tholeiitic affinities and carry both high and low-calcium pyroxene series. Bridgwater and Harry (1968) suggest the anorthosite body underlying the Gardar province may be similar to the Nain anorthosite.

ii. The Scandinavian shield areas.

Upton (1964) compared the Tugtutoq giant dykes to the large, east-west dykes of central Sweden described by Krokström (1932, 1936). These, the Breven and the Hallefors dykes, are Precambrian, possibly Jotnian (ca 1400 to 1100my - Welin and Blomqvist 1966) or post-Jotnian in age. The Breven dyke is doleritic with a later granophyric component; the Hallefors dyke was formed by repeated injections of gabbroic and more highly differentiated basic magma. Unlike the Greenland giant dykes, the Swedish examples have no internal layering reported, but the exposure is so poor that any layering is likely to be hidden.

Basic dykes belonging to the Jotnian province in the Eskilstuna region carry anorthosite inclusions and plagioclase megacrysts similar to the Gardar occurrences (Gorbatschev, 1961). The Jotnian intrusions, like the Gardar rocks, have transitional affinities and lack low calcium pyroxenes, however differentiates are commonly granophyric rather than syenitic ie. the Jotnian rocks are generally less alkaline than the Gardar rocks.

Anorthosites and related rocks of the Tjorn complex in Sweden were intruded during the Dalsandian orogeny approximately 1000my ago (Bergstrom, 1963). They show some features similar to the Gardar occurrences, but the dominant mafic mineral is hypersthene not olivine.

I.4. The present work

Mildly alkaline basaltic magma has played an important part in the evolution of the Gardar province. Although the basic rocks were

emplaced over a wide time and space interval, they have an overall chemical similarity. It may be assumed that the basic rocks are derived from a common source and that they have a common evolutionary history. Plots of analyses of Gardar rocks on total-iron:magnesium: alkali variation diagrams demonstrate relatively smooth curves (Watt, 1966), so this assumption is not unwarranted.

A variety of basaltic and trachybasaltic rocks was formed in the province over a period not exceeding 250my., possibly nearer 150my. Several processes may well have been operative in producing this variety:

1. Partial melting and segregation processes in the mantle to produce a variety of primary magmas.
2. Polybaric crystal fractionation.
3. Wall rock reaction processes.
4. 'Liquid fractionation' (which has been postulated to have operated in Gardar magmas), and 'alkali diffusion'.

An investigation of the evolutionary trends shown by the basic dykes will, it is hoped, help to distinguish between the processes which have been important in the formation of the Gardar alkaline rocks.

Attention has been drawn to the association of continental alkaline magmatism and faulting. In particular, parallels have been drawn between the east African rift volcanism and the Gardar volcanism. Modern theories of plate tectonics relating magma type to tectonic

environment have been much discussed in relation to the east African rift environment (eg. Mohr, 1970; Gass, 1970; Harris, 1969). The possibility must be considered that the Gardar province is the remains of such a rift system, thus implying that modern magmato-tectonic theories can be applied to processes that operated in the Precambrian.

A study of the basic dyke-rocks of the Gardar province has been undertaken, therefore, to provide a chemical and petrographic description of the rocks; to investigate the magmatic evolution of the Gardar province; to provide a comparison with other provinces of similar age and to give information about magmatic processes in the Precambrian.

2. Field relations of the dykes.

2.1. Introduction

Because of the sub-parallelism of the dyke swarms and the variation in age of intrusion from NW to SE, definite correlations cannot be established between the dyke swarms in the three dyke zones. The zones will therefore be described separately.

2.2. Zone 1. Ivigtût.

The northwesternmost and the least closely defined of the three zones, it extends from Sermiligarssuk to Sanerut Island. Dykes are less concentrated in this area than in the other zones. The major basic dykes are found in the region of the Tigssaluq granite (a late Ketilidian granite pluton), and crossing the Grønnedal-Ika alkaline complex. A summary of the chronology of the Ivigtût zone is given in Table 2.1.

Dyke types present in the Ivigtût zone include lamprophyres, several generations of basic dykes, including olivine dolerites and feldsparphyric dolerites and salic alkaline dykes. Gardar alkaline complexes are represented by the Kûngnât, Grønnedal-Ika and Ivigtût plutons.

There is some evidence for structural control on the location of the complexes and dykes; the dykes do not parallel the foliation of the basement rocks but are influenced by faults. A 15km wide ENE fault/crush zone crossing the Ivigtût peninsula is rich in dykes and is also the site of Th, Pb, and U mineral deposits (Berthelsen, 1962). The Grønnedal-Ika and Ivigtût intrusions lie in this dyke/fault zone, the

TABLE 2.1.

Kûngnât Complex.

W.N.W. Faulting.

Orthotrachytes.)
Phonolites.) Alkaline Dykes
Quartz trachytes)

Microporphyritic basalt dykes.

Movements in main fault zone of Ivigtut.

Cryolite mineralization.

Ivigtût granite.

Trachytic dykes.

Movements in main fault zone of Ivigtût.

Intrusion of olivine dolerite dykes (BD_0, BD_1, BD_2).

Intrusion of porphyritic dolerite dykes (BFD or big-feldspar dykes)

Lamprophyre dykes.

E.N.E. crush zone and faulting.

Grønnedal-Ika Complex.

Main events in Gardar Period, in region of Ivigtût (after Emeleus 1964).

former at the intersection of the zone with the Laksenaes fault, one of the major sinistral wrench faults which were active during the Gardar period. The Kûngnât complex, on the other hand, is located in relatively undisturbed gneisses (Upton, 1960). Movement on the ESE sinistral and ENE dextral wrench faults continued intermittently during the period, and it was through the relationships between dyke intrusion and displacement on the faults that a chronology was set up for the region.

ENE trending ultrabasic lamprophyres (kersantites, monchiquites and camptonites) are widespread in the Ivigtût zone and are particularly numerous in the ENE fault-zone crossing the Ivigtut peninsula (Berthelsen, 1962). Characteristically, the dykes are flow-banded, between 1 and 5m thick, and tend to be impersistent. They are carbonate and sulphide rich and may contain inclusions of augite and/or hornblende. They appear to be the oldest unmetamorphosed dykes around Kûngnât and Arsuk (Ayrton, 1963; Upton, pers. comm.), but they cannot be confined to one position within the chronology of the Ivigtût zone as in the Grønnedal-Ika area some lamprophyres postdate the syenite complex and others postdate the dolerite dykes (Emeleus, 1964).

Dolerite dykes characterised by considerable amounts of large plagioclase crystals (BFD's) form early members of the ENE dyke swarms throughout the Ivigtût zone. The plagioclase crystals range from 2cm to more than 15cm long and are sometimes corroded; they form 20 to 40% by volume of the dykes (Emeleus, 1964). Anorthosite xenoliths are present in some

dykes, notably those in the Tigssalup area.

In the Ivigtût peninsula BFD's cut the early lamprophyres and the Grønnedal-Ika complex, but are cut by olivine dolerite and salic alkaline dykes (Emeleus, 1964). The oldest of the doleritic dykes crossing the Tigssalup granite is a BFD (Upton, pers. comm.), but in the region between Tigssalup Ilua and Sermiligarssuk Ayrton (1963) found that feldspathic inclusions occurred locally in all doleritic dykes and were not confined to one recognisable swarm.

The olivine dolerite dykes range from 1m to 150m thick and thicknesses of 10 to 20m are common; some are traceable from the coast to the Inland Ice, a distance of approximately 60km. These are the 'Brown Dykes' of Wegmann's classification. Berthelsen (1962) recognised three separate generations of Brown Dykes which he classified as BD generation 0, 1 and 2. The relationships of the three generations are clearly displayed by the dykes crossing Grønnedal-Ika and Tigssalup (figs 2.1. a and b).

The BD dykes are composed of coarse, homogeneous olivine dolerite; igneous trough banding and gabbro pegmatite segregations are locally present (Ayrton, 1963; Upton, pers. comm.). Scattered plagioclase phenocrysts, sometimes flow-oriented, occur in the chilled margins. Contacts with the country rock are usually sharp but examples of rheomorphism and brecciation of the gneisses by large dykes have been observed near Kûngnât and on Tornarssuk Island. In the latter case the centre of the dyke contains small, partly resorbed gneiss xenoliths (Upton, pers. comm.). Contact effects of the large dolerite dykes crossing the Grønnedal-Ika complex led Emeleus (1964) to suggest these

FIGURE 2.1a:
Sketch-map of the dykes that cross the Grønnedal-Ika complex.
The complex is shown in blue.

Extracted from GGU 1:100,000 map sheet 61 V.1 Syd 'Ivigtut'.

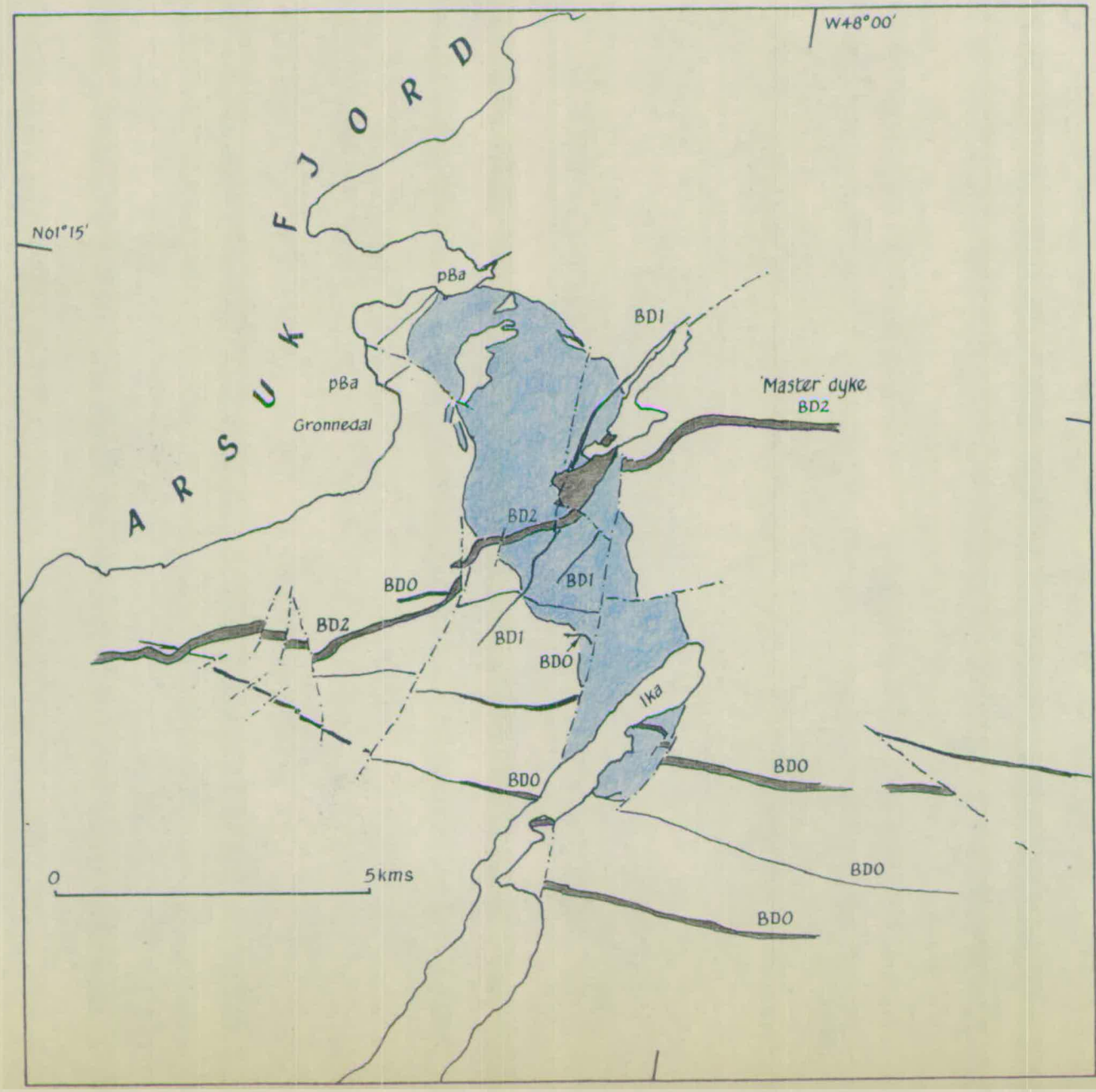
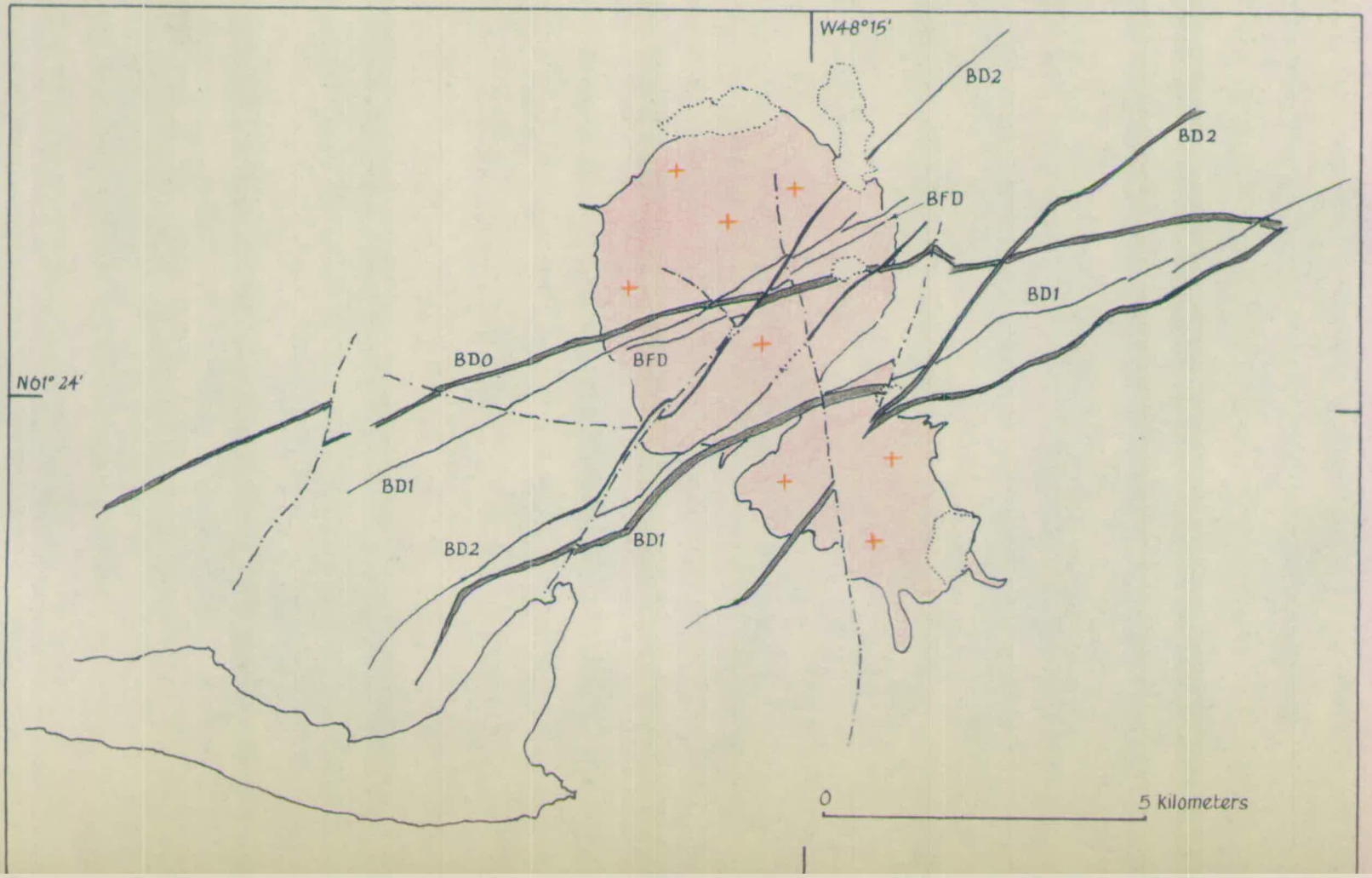

W48°00'
N01°15'
ARSUK FJORD
pBa
pBa
Gronnedal
BD1
'Master' dyke
BD2
BD2
BD0
BD2
BD1
BD1
BD0
Ika
BD0
BD0
BD0
0
5kms

FIGURE 2.1b:
Sketch-map of the dykes that cross the Tigssalup granite.
The biotite-granite is shown in pink.

Extracted from the GGU 100,000 map-sheet 61 V.1 Syd 'Ivigtut'.


W48°15'
N61° 24'
BD2
BD2
BFD
BD1
BD0
BFD
BD1
BD2
BD1
0
5 kilometers

dykes may have been feeders to surface flows. The large dykes fray out into swarms of smaller dykes as they die out (Ayrton, 1963). In the Ivigtût peninsula the oldest BD dykes (BD_0) strike approximately W and are broken up by N to NNE dextral faults (fig. 2.1a). The BD_1 dyke crossing the Grønnedal-Ika complex strikes NE and is cut by a large BD_2 dyke (the Ivigtût master dyke) which strikes ENE. With the exception of the early feldspathic dyke, successive basic dykes crossing Tigssalup strike further to the NW. Here the BD_0 dyke (known as Le Flic) trends ENE; the BD_1 NE and the BD_2 dyke NNE. A period of faulting on NNE dextral faults separated the intrusion of the BD_1 and BD_2 swarms (Ayrton, 1963). The BD_0 dykes are probably not represented in the Kûngnât area, but three generations of dolerite dykes are present, trending NE, ENE, and NE successively (Upton, 1960 and Upton, pers. comm). It is difficult to relate these dykes to others in the Ivigtût zone because of the lack of persistent major dykes in this area.

Thin (less than 1m thick) basic dykes containing 1 - 2 mm microphenocrysts of feldspar intrude fault and crush zones on the Ivigtût peninsula; similar dykes have been recorded in the Tigssalup area (Emeleus, 1964). They commonly form multiple intrusions, each member chilling cleanly against others and against the gneiss, with an aggregate width of up to 20m. The plagioclase phenocrysts are sometimes arranged in flow alignment, more commonly they form star-shaped aggregates.

With the exception of a swarm of trachytes which predate the Grønnedal-Ika complex, swarms of thin, salic alkaline dykes (trachytes and phonolites) postdate all the basic dykes in the Ivigtût zone. They are

concentrated in the dyke/fault zone crossing the Ivigtût peninsula; few are found near Sermiligarssuk (Berthelsen, 1962; Ayrton, 1963). They are rarely more than 5m thick and relatively impersistent, being traceable up to 2km only and some have been found to terminate against major faults (Emeleus, 1964). Some members of the alkaline dyke swarms intrude the Ivigtût granite but are not found in the cryolite ore body (Berthelsen, 1962).

The age of the Ivigtût granite is uncertain: Berthelsen found granophyre dykes which he believed were related to the intrusion of the complex intruding BD_2 dykes, implying the complex was intruded after the main episode of dolerite dyke intrusion. The Kûngnât complex may well be the youngest Gardar intrusion in the Ivigtût zone, as it cuts all the Gardar dyke swarms in the surrounding area (Upton, 1960).

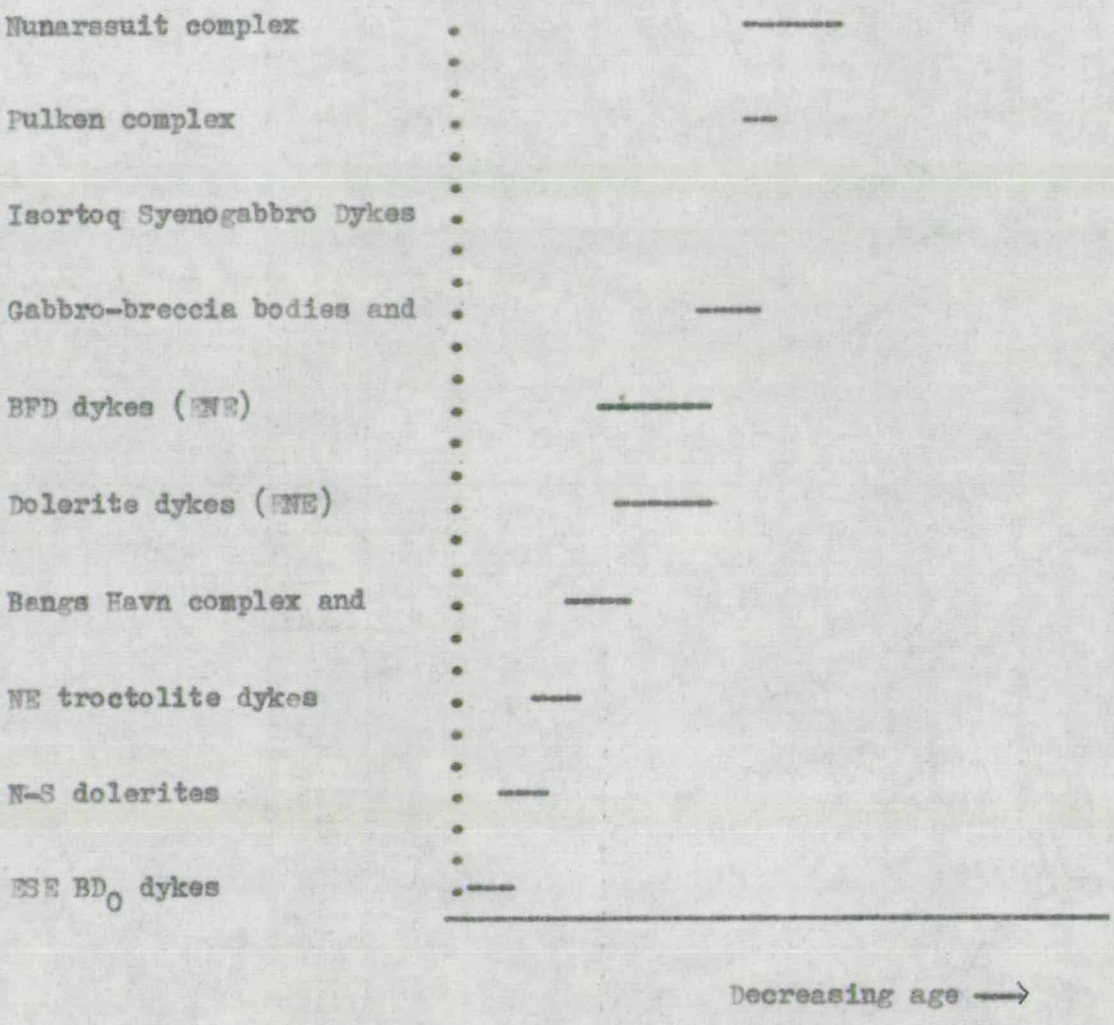
2.3. Zone 2. Nunarssuit-Isortoq.

A zone intensely intruded by ENE dykes crops out between Kobbermine bugt and Sermilik and stretches ENE from the Nunarssuit complex to the Inland Ice. In this zone, which represents crustal extension of 2.25km in a 14km wide belt, there is a striking abundance of basic dykes; dykes of intermediate or acid composition are rare (Harry and Pulvertaft, 1963). A summary of the chronology of the Nunarssuit-Isortoq zone is displayed in Fig. 2.2.

The direction of the main dyke swarms is approximately parallel to the strong foliation of the basement rocks. This zone has been less

Figure 2.2.

Chronology of the Nunarssuit - Isortoq Zone



Note: the horizontal axis is not to scale.

affected by faulting than the Ivigtût zone (Harry and Pulvertaft, 1963); the principal faults are the large, ESE sinistral faults which continued to be active after the end of the Gardar period and late NE dextral faults affecting all but the Isortoq syenogabbro giant dykes (Bridgwater and Harry, 1968). Minor ENE faulting affected some of the early ENE dykes but not the later dykes.

Several generations of dykes, intruded sub-parallel to each other in an ENE or NE direction, make up the main dyke zone. In places it is possible to distinguish 5 intrusive episodes, but most often only 3 or 4 may be seen, and the repeated intrusion of similar magmas makes correlation difficult. A few dykes have been traced for up to 35km, due mainly to their peculiar abundance of feldspathic inclusions (Bridgwater and Harry, 1968).

The majority of dykes are doleritic, micro-troctolites to alkali dolerite. They are normally between 10m and 150m thick, but individual dykes range up to 500m thick. Synformal internal layering is common in dykes more than 100m thick. Contacts of the thicker dykes with country rock may be diffuse, with rheomorphism and back veining, but normally the dykes chill cleanly, with little metamorphic effect. Anorthosite xenoliths and plagioclase megacrysts occur locally in all the dykes and in spectacular concentrations in some (BFD dykes), but in the Nunarssuit - Isortoq zone these are not all the same generation (Bridgwater and Harry, 1968).

The oldest Gardar intrusions in this zone are homogeneous, brown

dolerite dykes (BD_0), striking ESE, approximately parallel to the sinistral wrench faults. They are not numerous, with no more than 4 or 5 dykes throughout the area, but members of this swarm have been traced intermittently for more than 100km south-eastwards. They are broad dykes, up to 70m thick, of mildly feldsparphyric olivine dolerite, with occasional patches of dolerite pegmatite.

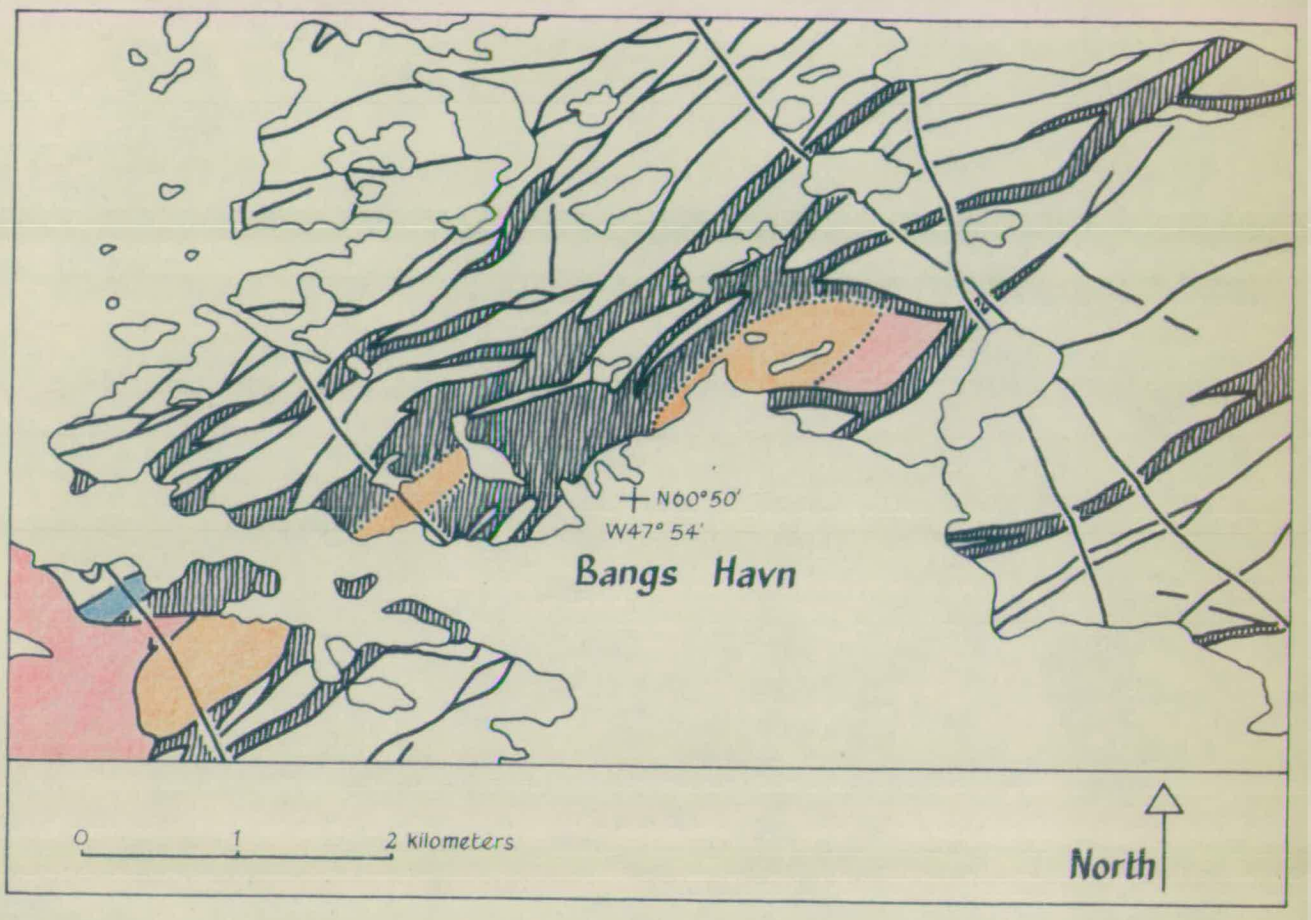
Subsequent swarms trend ENE, NE or N; thin, rare, N - S dolerite dykes were the earliest, followed by ENE trending microtroctolitic dykes often more than 100m thick (Harry and Pulvertaft, 1963; Bridgwater and Coe, 1970). The main ENE swarm comprises a large number of sinuous, anastomosing basic dykes which coalesce in the Bangs Havn complex (fig. 2.3a). Many of these dykes contain large volumes of anorthosite blocks or large crystals of plagioclase up to 60cm long (Harry and Pulvertaft, 1963). The distribution of feldspathic inclusions in the dykes has been described by Bridgwater and Harry (1968). They may be concentrated in the centre or at either margin of the dykes, or in apophyses and form up to 85% of the rock. Some dykes appear to have been formed by repeated intrusion of inclusion-rich magma, with little chilling between each pulse; they are heterogeneous and streaky, vertically banded with zones of inclusions (Upton, pers.comm.).

Some dykes belonging to this swarm are composite with central components of granite or syenite, which are not completely continuous along the length. Normally, the central component displays little chilling against the basic margin; sometimes there is hybridisation at the contact. Anorthosite xenoliths and plagioclase crystals are rare in

FIGURE 2.3a:
Sketch map of the Bangs Havn complex and related dykes.
Enlarged from GGU 1:100,000 map-sheet 60 V.1 Nord 'Nunarssuit'.

Red: granite.
Orange: syenite.
Blue: appinitic rocks.

The four youngest dykes, trending NW to SE, are Mesozoic.


N60°50'
W47° 54'
Bangs Havn
0
1
2 kilometers
North

the acid components. Partly digested xenoliths of Julianehaab granite are sometimes found in the basic components (Watterson,1965; Bridgwater and Harry, 1968) and where abundant appear to exclude feldspathic xenoliths. Rare in this zone are composite dykes with microsyenite margins containing phenocrysts of alkali feldspar and basic, trachydoleritic centres containing abundant plagioclase megacrysts. These dykes vary between 5m and 80m wide and the basic component may take up 80% of the width. The boundary between the two components is usually sharp but not chilled (Bridgwater and Harry, 1968).

Small, oval composite bodies (less than 1.5km long and 300mwide), with gabbro margins and breccia filled centres trend ENE from Ikerassagssuaq. The breccia units are composed mainly of fragmented basement rock (granites and metasediments) and have a sharp contact against the gabbro. The gabbro units are between 4 and 20m wide and are sharply chilled against the country rock (Upton, pers. comm.). Steep, complex layering was observed in one gabbro unit. The age of these bodies is uncertain: one is cut by a NE dolerite dyke, possibly belonging to the main swarm.

The Bangs Havn complex (fig. 2.3a) is an elongate body, 6km long by 1km wide, composed of anastomosing gabbro dykes enclosing units of syenite and granite. The contact of syenite with granite tends to be gradational, but the gabbro/ syenite contact is usually sharp with some alteration and development of a marginal pegmatitic facies in the gabbro (Bridgwater and Harry, 1968). The contact of the complex

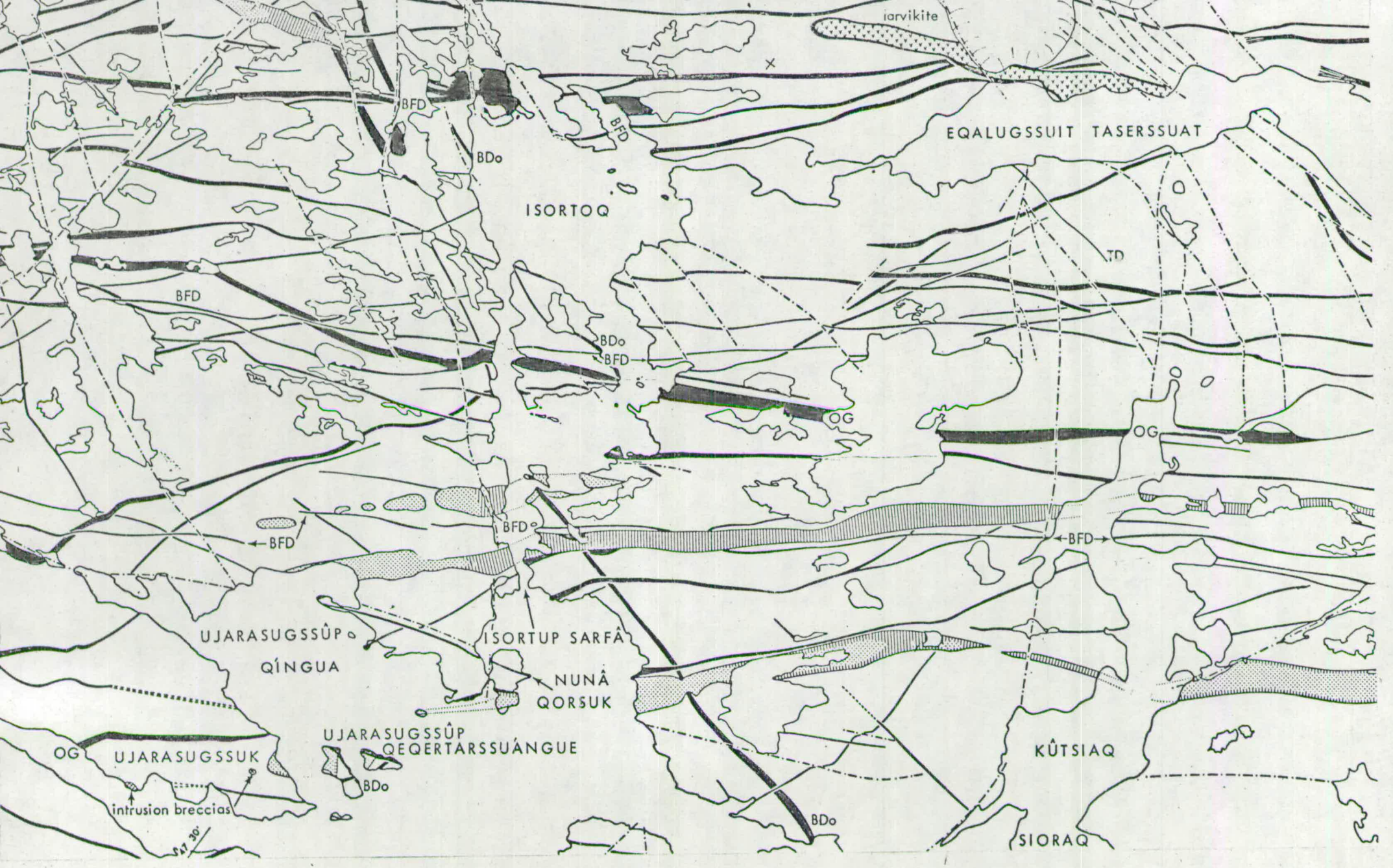
with country rock is sheared and crushed in places and some of the marginal gabbro has a vertical fluxion lamination (Upton, pers. comm.). Trough banding has developed in both the gabbro and mafic syenite units. Masses of anorthosite up to 50m broad and broken plagioclase megacrysts up to 35cm long are abundant in the gabbro surrounding the western syenite unit, but less common in the east. The feldspathic material is often concentrated in well-defined areas up to 50m wide in which it forms more than 75% of the rock (Bridgwater and Harry, 1968). At one locality the gabbro contains xenoliths of gabbro which in turn contain pieces of anorthosite and plagioclase megacrysts (Upton, pers. comm.).

The youngest intrusions in the Isortoq region are very large ENE trending composite bodies up to 500m broad, referred to as 'giant dykes' by Bridgwater and Coe (1970). They form elongate, discontinuous masses, the largest of which is 25km long (fig. 2.3b). The giant dykes are composed of gabbro, syenogabbro and syenite; the syenite units are normally central, with basic marginal units but locally syenite has broken through the marginal facies and may have filled the whole width of the dyke. Internal contacts are normally gradational and layered cumulates may have developed, showing the body to have formed from a single pulse of magma (Bridgwater and Coe, 1970). In some dykes however, there is evidence of multiple intrusion, where the trachytic magma has disrupted cumulate structures in already solidified basic units. Where cognate xenoliths are found they are more basic than the host. Chilled contacts between the basic

FIGURE 2.3b:
Geology of the Isortoq area.
Figure 1 from Bridgwater and Coe, 1970.

Solid black: Gardar dolerite dykes, BFD dykes and post-Cambrian dykes.
Ruled: gabbro or syenogabbro.
Stippled: syenite.
'v' ornament: larvikite.

The last three rock-types comprise the 'giant' dykes.


iarvikite
EQALUGSSUIT TASERSSUAT
ISORTOQ
BFD
BDo
TD
OG
UJARASUGSSÛP QÍNGUA
ISORTUP SARFÂ
NUNÂ QORSUK
UJARASUGSSÛP QEQERTARSSUÁNGUE
UJARASUGSSUK
intrusion breccias
KÛTSIAQ
SIORAQ

marginal units of the giant dykes and the country rock have been observed in places, but commonly the marginal facies are poorly chilled, with marginal hybridisation and extensive metamorphism of the basement rock (Bridgwater and Coe, 1970; Upton, pers. comm.).

According to Bridgwater and Coe, the relationship of the giant dykes with earlier Gardar dykes provides evidence for emplacement by stoping: the giant dykes are in part bridged by older dykes (fig. 2.3b), so that the older dykes appear to cut the giant dykes. Bridgwater and Coe believe the giant dykes are transitional between dilatational dyke intrusion and the 'permissive' intrusion of central complexes. The age relationship between these dykes and the Nunarssuit complex is not known.

The age of the rare salic dykes relative to the other dykes is uncertain - one is cut by a NE dolerite dyke, another cuts a similar dyke (Harry and Pulvertaft, 1963). Some thin trachytes in the Ilordleq area may be related to the intrusion of the Nunarssuit complex (Watterson, 1965).

The Nunarssuit complex is younger than the dyke swarms in the area (Harry and Pulvertaft, 1963). The small Pulklen complex nearby has intruded dykes of the main NE swarm, but its relationship to the Nunarssuit complex is uncertain.

2.4. Zone 3. Tugtutôq-Narssarssuaq.

A 25 to 30km wide zone stretching from Tugtutôq NE to the Inland Ice is intensely intruded by NE to ENE trending dykes. Upton (1962) has

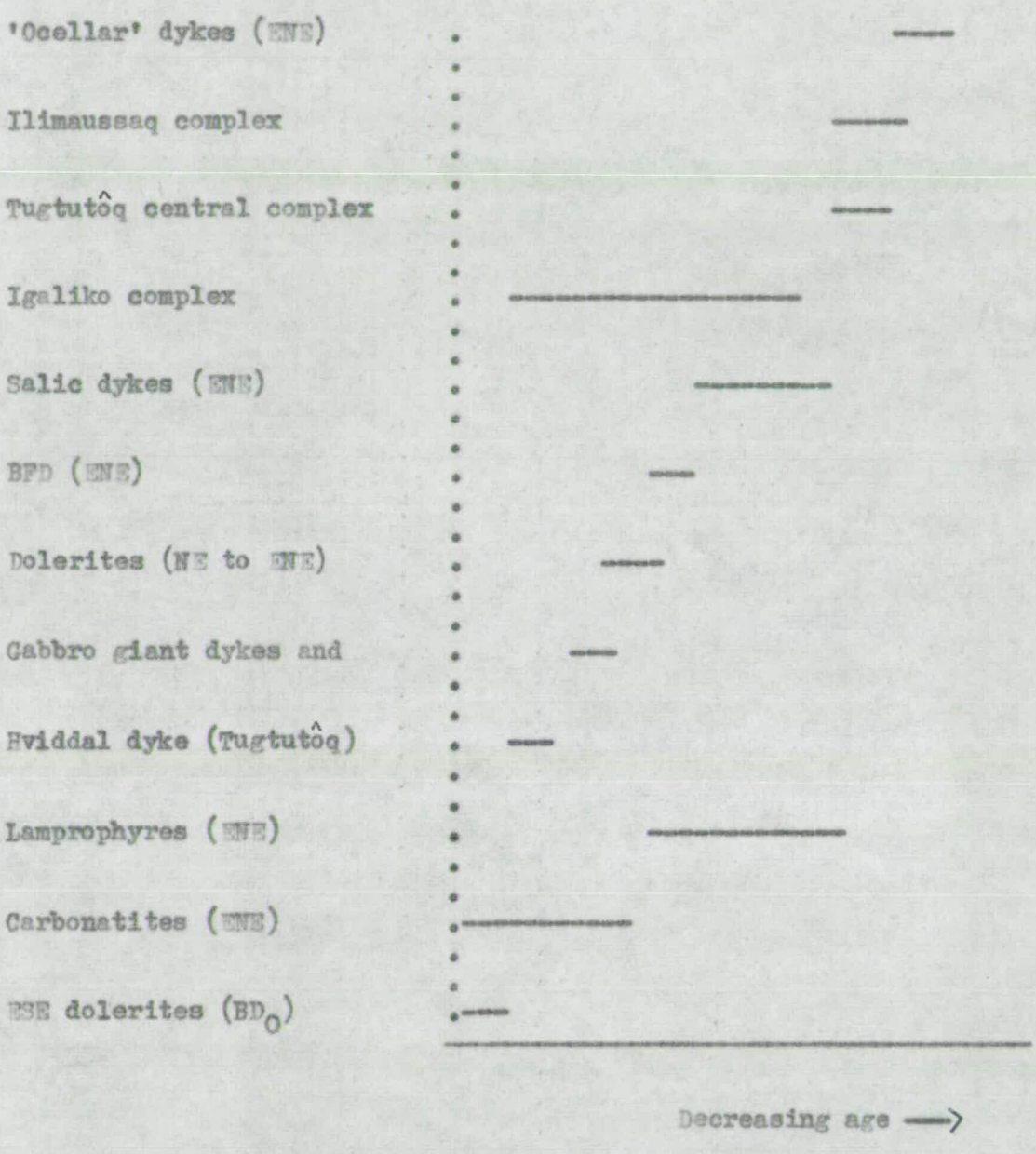
calculated the ENE dyke swarms on Tugtutôq involved crustal extension of 10 to 20% in a zone 11km wide. There is a great variety of dykes from lamprophyres to phonolites and trachytes, but fewer dolerite and gabbro dykes than in either the Ivigtût or the Nunarssuit - Isortoq zone (Allaart, 1973). A summary of the chronology of the zone is given in fig. 2.4.

Throughout most of this area the foliation of the basement trends approximately NE. The area is affected by the major sinistral wrench faults referred to in previous sections, striking E-W, and approximately NNW or N dextral faults (see fig.1.1.,section 1.1.2). In addition it has been suggested that important ENE normal faults lie along the principal ENE fjords (Emeleus and Upton, in press). The Ilimaussaq, Igaliko and Dyrnaes-Narssaq complexes appear to be located at the junction of the left-lateral faults with the ENE dyke-zone, but the Tugtutôq central complex and the Klokken intrusion are located in relatively undisturbed basement.

Ultramafic, carbonatitic and lamprophyric dykes, sills and diatremes are concentrated in a 6km wide zone trending ENE north of Narssarssuaq (fig. 2.5a) and in Qagssiarssuk. Some carbonatite and lamprophyre dykes occur in the Igaliko area, and biotite pyroxenite and biotite peridotite bodies intrude the Narssaq gabbro (Walton, 1965; Stewart, 1970; Emeleus and Harry, 1970; Upton, 1962, gabbro). The quantity of ultramafic magma erupted during the Gardar period was small compared with the amounts of basaltic and trachytic magmas. Generally carbonatite dykes are less than 1m thick and impersistent, while

Figure 2.4.

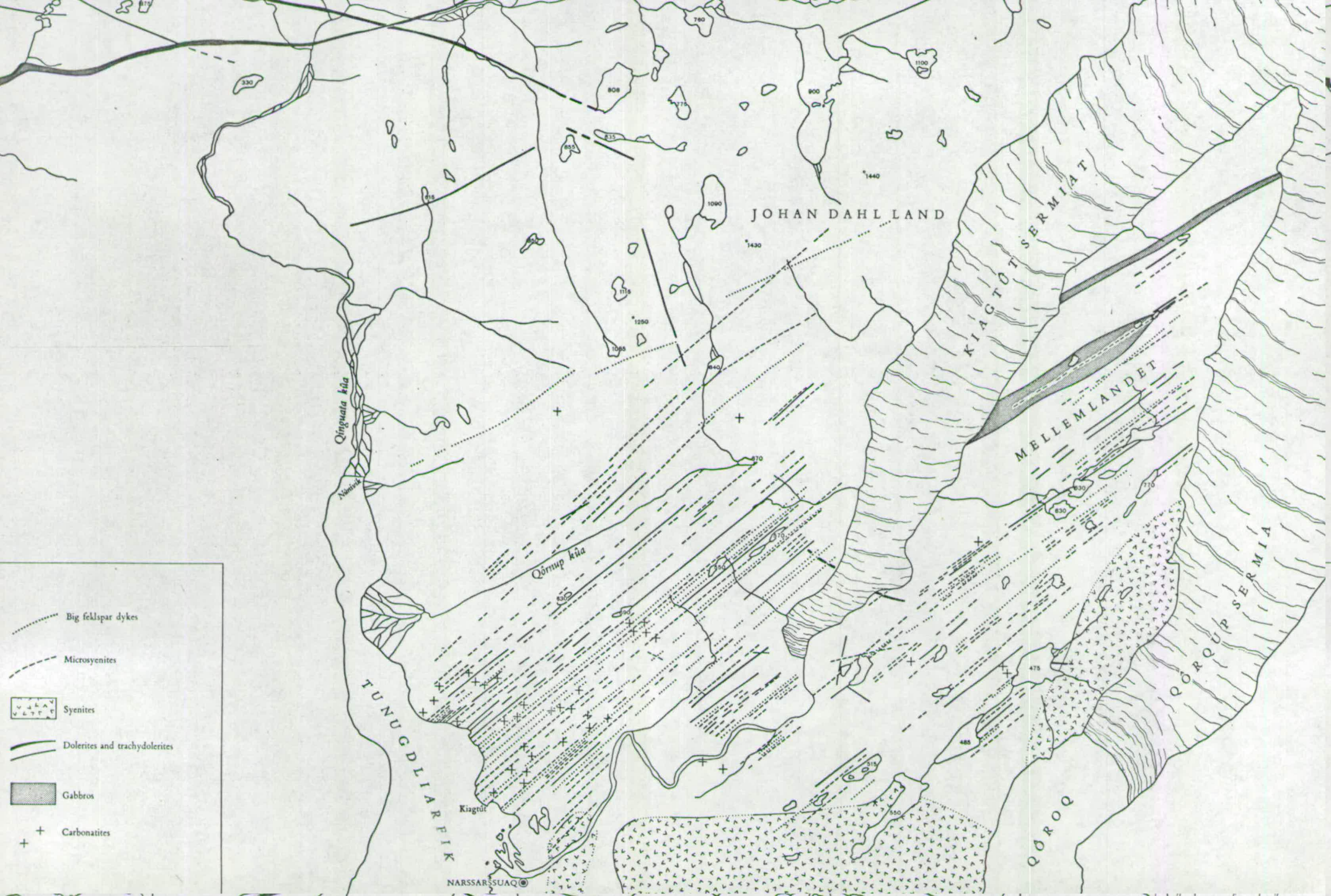
General chronology of intrusions in the Tugtutôq-Narssarssuaq zone.



Note: the horizontal axis is not to scale.

FIGURE 2.5a:
The ENE dyke swarm in the Narssarssuaq region.

Plate 3 from Walton, 1965: scale 1:100,000.


JOHAN DAHL LAND
KIAGTÛT SERMIAT
MELLEMLANDET
QÔROQ SERMIA
QÔROQ
TUNUGDLIARFIK
Qôrnup kûa
Qinguata kûa
Nûnârik
Kiagtût
NARSSARSSUAQ
Big feldspar dykes
Microsyenites
Syenites
Dolerites and trachydolerites
Gabbros
Carbonatites

lamprophyre dykes may be up to 10m thick; the largest of the Narssarssuaq diatremes is approximately 300m by 100m. The ultramafic intrusions are not confined to one part of the magmatic sequence: some of the Narssarssuaq carbonatites predate the main NE dolerite dyke swarms, others cut NE dolerites (Walton, 1965). Carbonatite dykes and lamprophyres intrude both early and late members of the Igaliko complex, but since intersections are few it is not possible to say if they all belong to the same generation (Emeleus and Harry, 1970).

A dispersed swarm of dolerite dykes (BD_0 dykes) trending approximately ESE was possibly the earliest Gardar intrusion in this zone. The relationship of these dykes to the early carbonatite intrusions near Narssarssuaq is uncertain (Walton, 1965). The trend of the BD_0 dykes changes to approximately E-W in the eastern part of the area. They are sometimes found intruding shear zones and are themselves sheared (Allaart, 1973). Individual members of this swarm are up to 150m thick, and like BD_0 dykes elsewhere in the province they are composed of mildly feldsparphyric olivine dolerite, homogeneous but for occasional patches and veinlets of dolerite pegmatite. The larger dykes have caused substantial melting of the wall-rock granite, with rheomorphic veining of the marginal dolerite (Upton, pers. comm.). An E - W dolerite dyke intruded by the Motzfeldt centre of the Igaliko complex - the earliest of the Igaliko centres - is thought to be a BD_0 (Emeleus and Harry, 1970).

On Tugtutôq the BD_0 dykes were followed by the intrusion of a composite dyke, 500 to 600m broad and 22km long striking ENE, which is called the

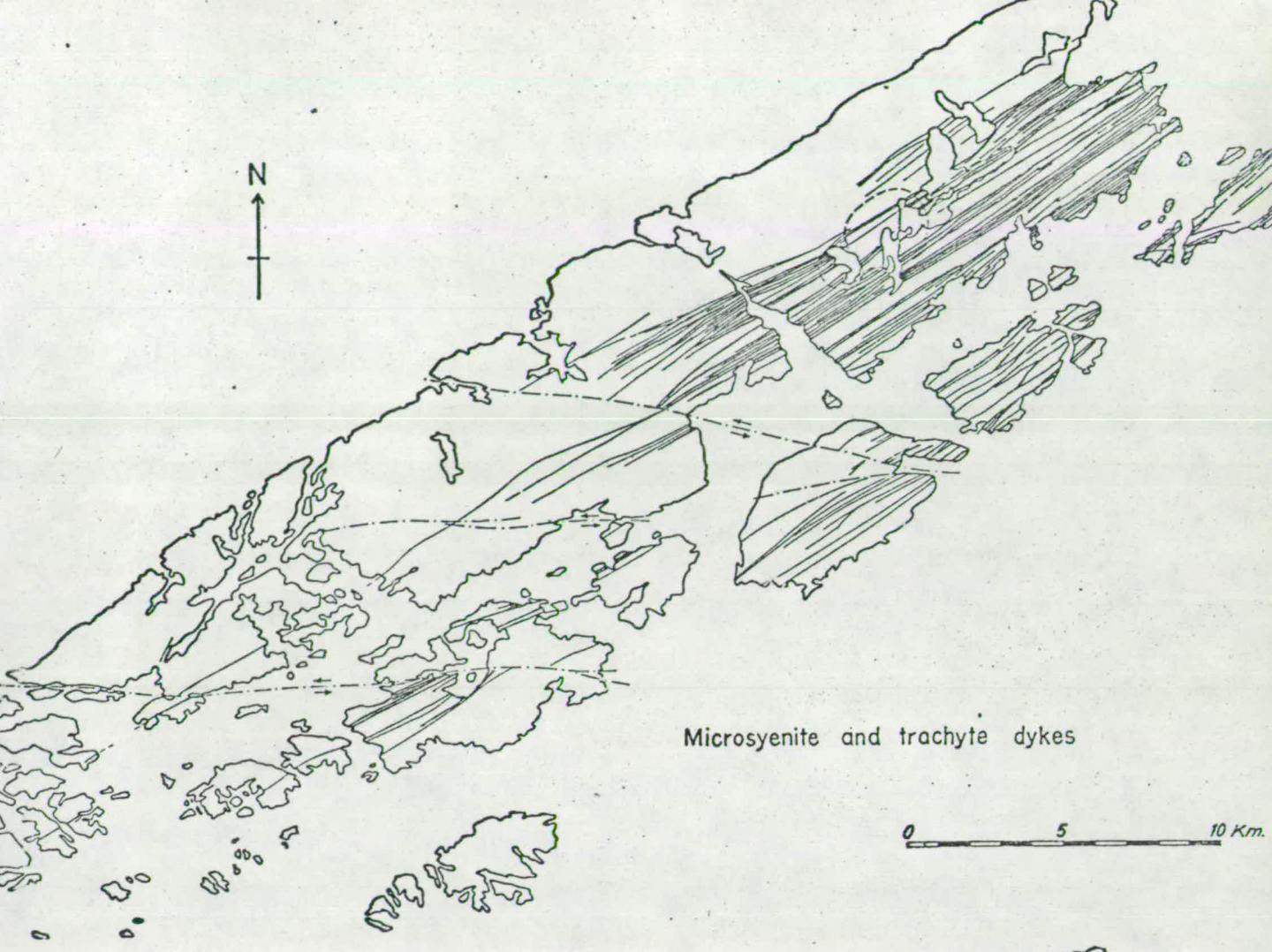
Hviddal giant dyke (Upton, 1962) (fig,2,5b). This dyke has syenogabbro margins between 50 and 100m wide and a central syenite unit which grades from augite syenite at the western end to nepheline syenite at the eastern end. The basic margins are well chilled against the basement granite but the contact with syenite is hybridised and the syenite unit develops a marginal pegmatitic facies close to the syenogabbro (Upton, 1962). It is thought that two separate pulses of magma were involved in the formation of the dyke, the first forming a gabbroic dyke 100 to 200m wide, along the centre of which trachytic magma was intruded before crystallisation was complete. Layered structures are largely absent from the Hviddal dyke, with the exception of local feldspar lamination and a few vertical cylindrical structures in the syenite.

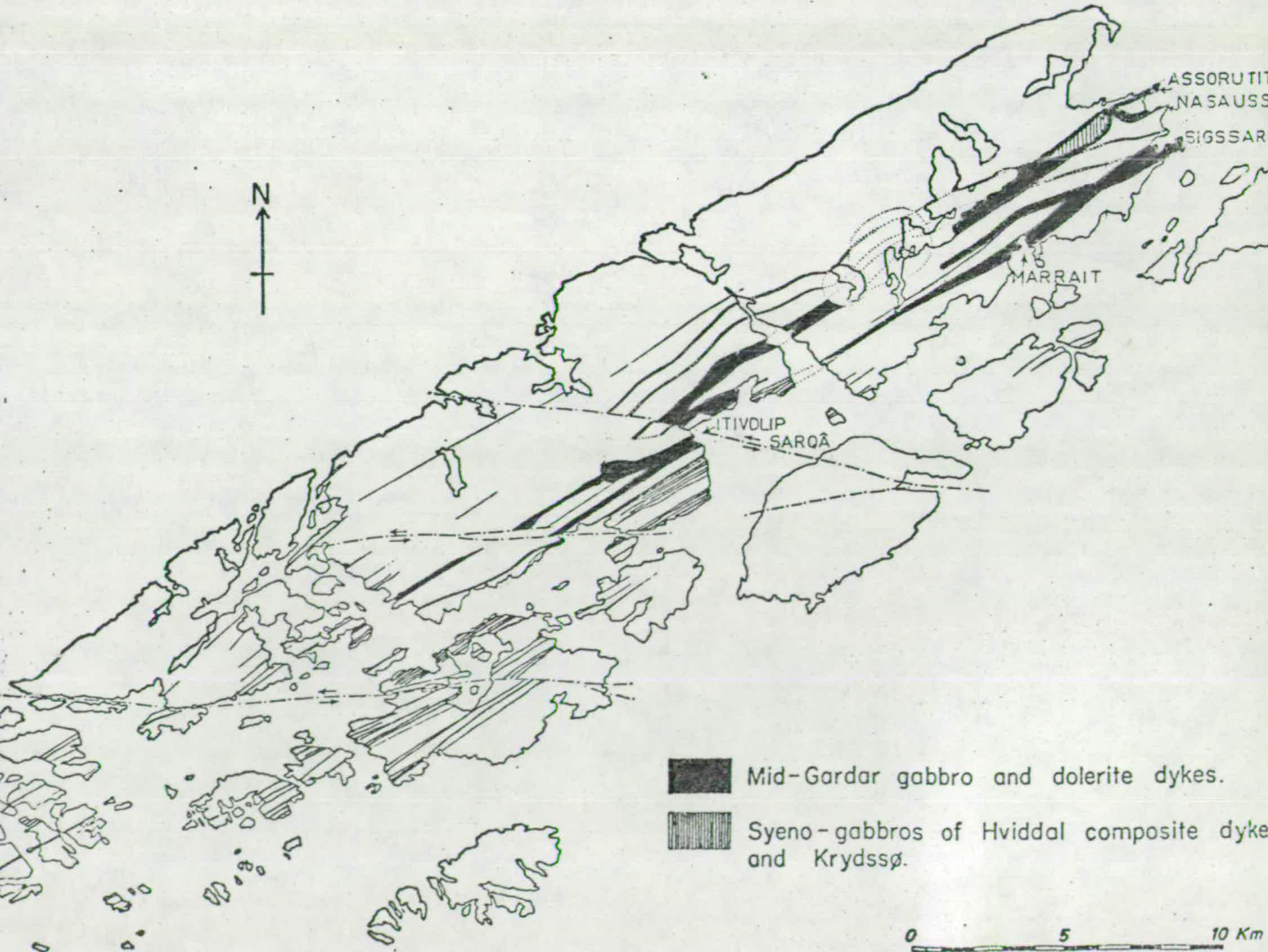
Two large ENE branching gabbro dykes and a swarm of small dolerite dykes succeeded the Hviddal dyke. The gabbro dykes are up to 800m broad in the eastern part of the island; the northern dyke can be traced for 45km to the SW, where the thickness diminishes to 40m. The southern dyke splits into two branches, one of which terminates abruptly against old crush lines in the basement while the other frays out into a swarm of small dolerite dykes (fig. 2.5b). To the NE the the gabbro giant dyke system continues onto the mainland at Narssaq, where the gabbro body has no obvious dyke-like form, the contacts changing from vertical on Tugtutoq to low-angled above the basal Gardar unconformity near Narssaq (Upton, 1962). The Narssaq gabbro was

FIGURE 2.5b:
Sketch-map of the dyke swarms on Tugtutoq island.

The upper map is plate 7 from Upton, 1964a, the lower map is plate 6 from Upton, 1964b.

Not shown are the BFD's, but their distribution is similar to that of the other swarms.


N
Microsyenite and trachyte dykes
0
5
10 Km.


N
ASSORUTIT
NASAUSS
SIGSSAR
MARRAIT
ITIVDLIP
SARQÂ
Mid-Gardar gabbro and dolerite dykes.
Syeno-gabbros of Hviddal composite dyke and Krydssø.
0
5
10 Km

subsequently intruded by syenite and alkali granite units, the whole constituting the Dyrnaes-Narssaq complex (Emeleus and Upton, in press).

The gabbro dykes are well-chilled against the basement granite with only minor melting, but in some places gradational contacts are found where the granite has been melted for approximately 20cms from the contact (Upton, pers. comm.). There is evidence that more than one pulse of basic magma was involved in the formation of the giant dykes, in that internal chilled contacts have been found at one locality. The northern gabbro dyke is composite at the eastern end, where it has been intruded by lenticular bodies of syenite and syenogabbro. The internal contacts are gradational and hybridised, thus similar to the Hviddal dyke (Upton, 1962; 1964). The southern gabbro dyke is gabbroic along the whole length. Synformal layering is locally present; the chilled facies are virtually aphyric with scattered phenocrysts of olivine and plagioclase, but patches of gabbro pegmatite are frequently developed (Upton, 1964).

Inclusions of anorthosite and plagioclase megacrysts in these dykes occur principally near Assorutit on the east coast of Tugtutoq and around Narssaq (Upton, 1962; 1964). The inclusions range from masses of anorthosite up to 100m across to small crystal fragments up to 20cm across. The Assorutit anorthosite blocks are layered, units of anorthosite in which the feldspars are laminated alternating with units of gabbro anorthosite. The gabbro is chilled against the inclusions, and both gabbro and inclusions are unaltered. Laminated anorthosites also occur in the Narssaq gabbro, but most of the inclusions are of broken, unsorted plagioclase crystals. Both the inclusions and the

gabbros are extensively altered, in contrast to the Assorutit occurrences.

Walton (1965), described two broad gabbro dykes occurring NE of Narssarssuaq, which may have been intruded at the same time as the Tugtutoq dykes. Like the Tugtutoq dykes, the Narssarssuaq dykes strike ENE; one is 200m wide, the other 700m wide, thinning to the east. Both are well chilled against the basement, and some internal synformal layering is developed, with a foliation due to the preferred orientation of plagioclase. Lenses and patches of anorthosite are found in the dykes, and a thin microsyenite dyke is intruded along the axis of the thicker dyke.

Subsequent swarms included a variety of doleritic, BFD and salic dykes - trachytes, phonolites and alkali rhyolites. Oversaturated salic dykes occur principally on Tugtutoq: on the Ilimaussaq peninsula and in the Narssarssuaq area both over and undersaturated varieties are found (Walton, 1965; Upton, pers. comm.) while in the Igaliko area and on Qarssuarssuk the salic dykes are mainly undersaturated (Watt, 1968; Allaart, 1969; Emeleus and Harry, 1970).

On Tugtutôq the later swarms are concentrated in the vicinity of the giant dykes and in the Skovfjord district: few dykes are found NNW of the Hviddal dyke (Upton, 1962). There is a concentration of dykes towards the N coast of the Ilimaussaq peninsula (Allaart, 1973), in the 6km wide zone N of Narssarssuaq (Walton, 1965), and several

generations of dykes intrude all but the late members of the Igdlerfigssalik centre in the Igaliko complex (fig.2.5c). In the ground between Qoroq and Tunugdliarfik the swarms are defined* from ENE to approximately N-S, due perhaps to the modification of the regional stress pattern by the early stages of development of the Igdlerfigssalik centre, or to the effect of contemporaneous transcurrent faulting (Emeleus and Harry, 1970).

Dykes belonging to these later swarms are generally less than 20m broad, although individual members range up to 40m broad. The earliest post giant-dyke intrusions on Tugtutoq were basic dykes and most subsequent dykes were salic. However in the Skovfjord area a group of thin, scarcely porphyritic dolerites was intruded after a group of trachyte dykes (Upton, 1962) and a swarm of flow-banded basic dykes was possibly the last Gardar intrusion in the area.

Most of the basic members of these later ENE dyke swarms are BFD's, containing large volumes of feldspathic inclusions which are usually concentrated at the centre of the dyke. Less commonly the inclusions are concentrated in one or both margins (Upton, 1962; pers. comm.). In many BFD's the inclusion-free margins are trachytic and contain alkali feldspar phenocrysts. In these cases the central basic unit was intruded after the trachytic margin before crystallization was complete and internal contacts are gradational. The inclusions consist of cataclased anorthosite blocks and broken plagioclase crystals up to 50cms across. The inclusions in these dykes are frequently

* see Errata.

FIGURE 2.5c:
Figure 34 from Emeleus and Harry, 1970.

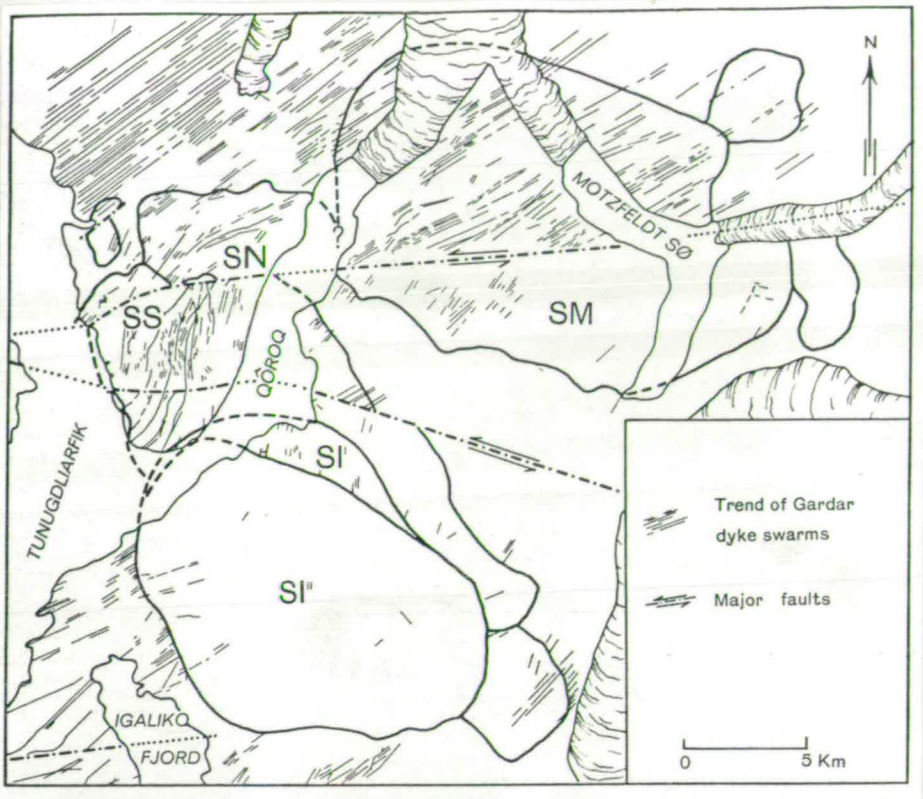


Fig. 34. Sketch map of the Gardar dykes (all generations) in and around the Igaliko nepheline syenites. Note (a) the absence of dykes cutting the late Igdlerfigssalik syenites (SI″), and (b) the approximately N–S trend of all dykes in the country between Qôroq and Tunugdliarfik.

altered cf. the inclusions in the earlier dolerite and gabbro dykes.

Several members of the later alkali rhyolite swarms form the central unit of composite dykes but unlike the composite dykes described above the rhyolites are chilled against the doleritic margins (Upton, pers. comm.), ie. in this case the rhyolitic magma was intruded some time after the basic magma.

In the Narssarssuaq area the NE dolerite dykes are cut by NE trachytes which in turn are cut by BFD's (Walton, 1965). A further group of trachytes intrude the BFD's and these later trachytes are mainly sodic while the earlier group are mainly potassic.

ENE dolerites, BFD's and trachytes intrude the lavas and sandstones of the Ilimaussaq peninsula, but of these groups the trachytes are the most common. They intrude the BFD's and are cut by members of the late, flow-banded basic dykes (Upton, pers. comm.: Emeleus and Stevenson, 1969). Some of the dykes are very similar to certain of the lavas - for example, one dyke carried aggregates of plagioclase phenocrysts arranged in a stellate fashion similar to the 'star basalt' lavas, and may have acted as a feeder to some of these lavas (Upton, pers. comm.).

Porphyritic trachytes are the most abundant ENE dykes in the Igaliko area, although porphyritic dolerites and BFD's are present. These dykes cut the Motzfelt, N and S Qôroq and the first three of the

Igdlerfigssalik centres, but are cut by the late Igdlerfigssalik centres (Emeleus and Harry, 1970). Phonolite, trachyte and lamprophyre dykes intrude the late Igdlerfigssalik centres.

The central Tugtutôq and Ilimaussaq complexes formed later than the main ENE dyke swarms, but are intruded by flow-banded ENE basic dykes characterised by 'ocelli' of feldspar and epidote which are the last Gardar intrusions in the area (Upton, 1962; 1964). These dykes are usually thin (less than 5m) and contain inclusions of anorthositic material. The dark internal banding may show evidence of multiple intrusion, with internal chilling (Upton, pers. comm.).

3. Petrography

3.1. Introduction

Because of the petrographic similarities of different generations of dykes and because intrusion sequences in different parts of the province cannot be related, the dykes have been grouped according to their petrographic characteristics. Most of them are doleritic to trachydoleritic (syenogabbroic) rock types, feldspathic and generally characterised by ophitic augite. In the late, flow-banded dykes from the Tugtutoq zone augite is characteristically idiomorphic and chlorite and calcite are common.

3.2. Classification

The classification and nomenclature of the rocks is based on both petrographic and chemical characteristics as outlined in table 3.1. The basaltic/doleritic types are classified according to their normative mineral composition and subdivisions in the more evolved rocks are made on the basis of DI (differentiation index- Thornton and Tuttle, 1960). The subdivisions correspond approximately to the fields of hawaiite and mugearite in basalts as defined by Wilkinson, (1974).

Strictly speaking, the more evolved syenogabbros should be termed 'syenodiorites' as their modal plagioclase is in the range andesine-oligoclase, but they grade into syenogabbroic types so will not be distinguished from them. The modal plagioclase in the late Tugtutôq dykes is always in the range andesine-oligoclase and the potassic and

Table 3.1.

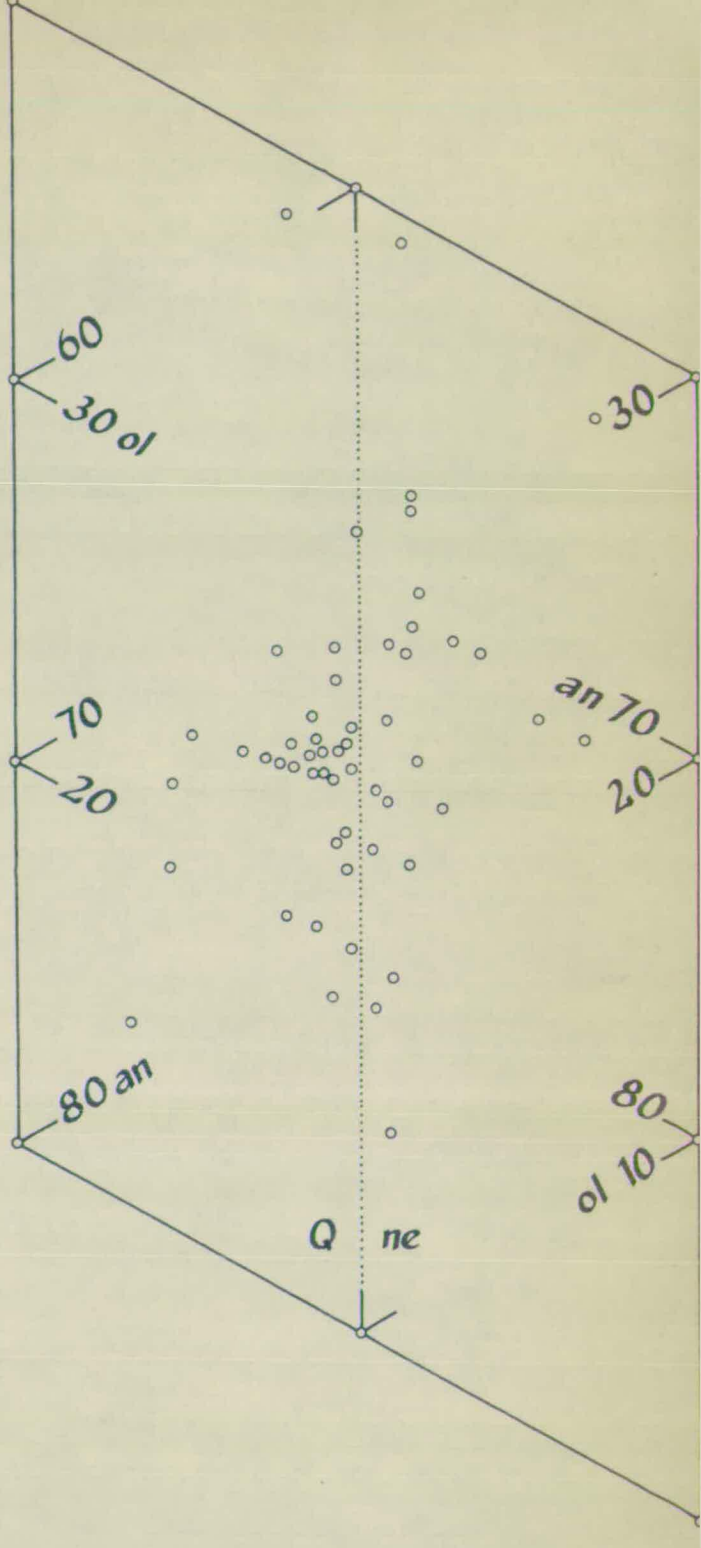
Classification of Gardar rocks

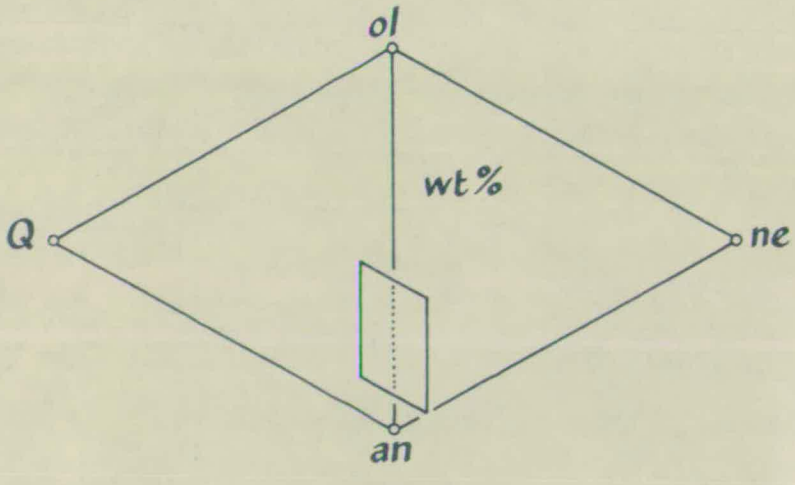
DI < 35 alk. fsp. < 10% total feldspar. K_2O/Na_2O < 1/2	Transitional olivine basalt/dolerite (fine → medium grained) Phenocrysts: plag.; plag. + ol. groundmass: plag., ol., ophitic cpx., mt., bi., ap.	% of Analysed Rock Types 45%
DI 35 → 50, alk. fsp. 10 – 40% total fsp.	Trachybasalt/trachydolerite (fine → medium grained) Phenocrysts: plag.; plag. + ol. + mt. ± ap. groundmass: plag., alk. fsp., ol., cpx., mt., bi., ap.	38%
DI 50 – 65, alk. fsp. ~40% total fsp.	Trachydolerite (evolved) (fine → medium grained) Phenocrysts: plag., ol., cpx., mt., ? ap. groundmass: plag., alk. fsp., cpx., ol., mt., bi., ap. Syenogabbro (coarse grained) matrix: plag., alk., fsp., cpx., ol., mt., bi., ap., ± qz., ep.	10%
DI 65 alk. fsp. 10 → 40% total fsp. K_2O/Na_2O > 1/2	Trachydiorite (fine → medium grained) Phenocrysts: plag. (and - olig.), ol., mt., ± cpx. groundmass: plag., alk. fsp., cpx., bi., chl., calc., ep., mt., ap.	7%

plag.	plagioclase	calc.	calcite	Average matrix grain-size	
alk.fsp.	alkali feldspar	ep.	epidote	fine grained	<1mm
ol.	olivine	qz.	quartz	medium grained	1–5mm
cpx.	clinopyroxene	DI	differentiation index	coarse grained	>5mm
mt.	magnetite				
bi.	biotite				
ap.	apatite				
chl.	chlorite				

FIGURE 3.1:
Normative projections of basaltic compositions from clinopyroxene into the planes quartz(Q)-plagioclase(an)-olivine(ol) and nepheline(ne)-plagioclase(an)-olivine(ol) of the expanded basalt tetrahedron.

See text for further explanation.


60
30 ol
30
70
20
an 70
20
80 an
80
ol 10
Q
ne


ol
wt%
Q
ne
an

alkaline nature of these dykes requires that they be distinguished from the dolerite-series rocks. They have therefore been named 'trachydiorites'.

3.2.1. Basaltic/doleritic rocks.

Figure 3.1. shows the basaltic compositions projected from clino-pyroxene (cpx) into the planes quartz (qz) - olivine (ol) - plagioclase (plag) and nepheline (ne) - ol - plag of the expanded normative basalt tetrahedron qz-ol-cpx-ne. This system, derived from the iron-free system diopside-forsterite-nepheline-quartz, contains the principal components of the major phases of basaltic rocks (Yoder and Tilley 1962) and can therefore be used as a basis for classifying basaltic rocks.

Two points may be noted about the use of this tetrahedron. First, to avoid distortion, only compositions in which qz + ol + plag + cpx + ne form more than 80% of the normative minerals are plotted in the system. Second, normative composition is influenced by post-magmatic alteration, the main effect of which is to increase the amount of normative hypersthene at the expense of nepheline. This is critical for compositions which plot close to the plane of critical silica undersaturation. The Fe_2O_3/FeO ratios of the analyses were therefore reduced according to the ratios in the freshest rocks.

The Gardar rocks plot close to and on either side of the plane ol-plag-cpx, the plane of critical silica undersaturation, which

approximates to a thermal divide at low pressure (ca.8kb). The thermal divide is not exactly coplanar with ol-plag-cpx (O'Hara 1968), so compositions containing minor normative nepheline may fractionate to give silica saturated residua. Compositions containing normative olivine plus hypersthene have been termed mildly alkaline and transitional basalts (Coombs, 1963). and the term may be extended to include those containing minor normative nepheline. The Gardar rocks may be classified as transitional basalts, containing normative olivine plus hypersthene or minor normative nepheline and characterized by their alkaline mineralogy: lack of olivine reaction relationship, one high-calcium pyroxene series, interstitial alkali feldspar and association with a trachybasaltic - trachytic assemblage.

3.3. Petrography

This section will be confined to the textural and mineralogic features of the rocks; mineral compositions will be given in chapter 4.

The rocks examined all have alkaline tendencies: no low-calcium or subcalcic pyroxene was found and all the rocks with the exception of some syenogabbros and possibly one BD_0 lack free primary quartz and granophyric mesostasis. The clinopyroxenes are commonly pink to brown mildly titaniferous augites. Biotite, apatite and alkali feldspar are relatively abundant minor components and occasionally brown amphibole occurs. All the rocks are feldspathic and olivine (fresh or

pseudomorphed) occurs in all, although in some cases as a minor component. Neither nepheline nor analcite was found.

70% of all the rocks examined were aphyric (ie. contained less than 5% phenocrysts). The matrix grain size of the porphyritic varieties ranges from an average of 1mm down. The phenocryst content varies up to 30% by volume and plagioclase phenocrysts are ubiquitous. Where accompanied by olivine and magnetite, plagioclase phenocrysts make up more than 60% of the phenocryst species.

The finer grained chills are severely altered and composed of a mixture of feldspar, chlorite, biotite and iron ore which may have formed on devitrification; specimens from the centre of the same dyke are not so altered. Table 3.2 lists the phenocryst assemblages in the Gardar rocks.

The feldspar crystals described as 'megacrysts' by Bridgwater and Harry (1968) have been grouped with the phenocrysts here. In many cases it is difficult to decide whether particular feldspars should be called 'megacrysts' or phenocrysts, when evidence of unusual size or corrosion is lacking. Bridgwater and Harry established a genetic connection between the host-dyke composition and the 'megacryst' composition and suggested the 'megacrysts' crystallized from magmas related to the hosts. The material derived from disrupted anorthosite xenoliths can be distinguished from phenocrysts as they are anhedral and show evidence of deformation in distorted twin planes. Inclusions in the phenocrysts are distributed throughout the crystal or in a

Table 3.2.

Phenocryst assemblages

1. Dolerite-trachydolerite series.

   Plagioclase

   Plagioclase + olivine

   Plagioclase + olivine + magnetite

   Plagioclase + magnetite + apatite

   Plagioclase + olivine + magnetite + clinopyroxene

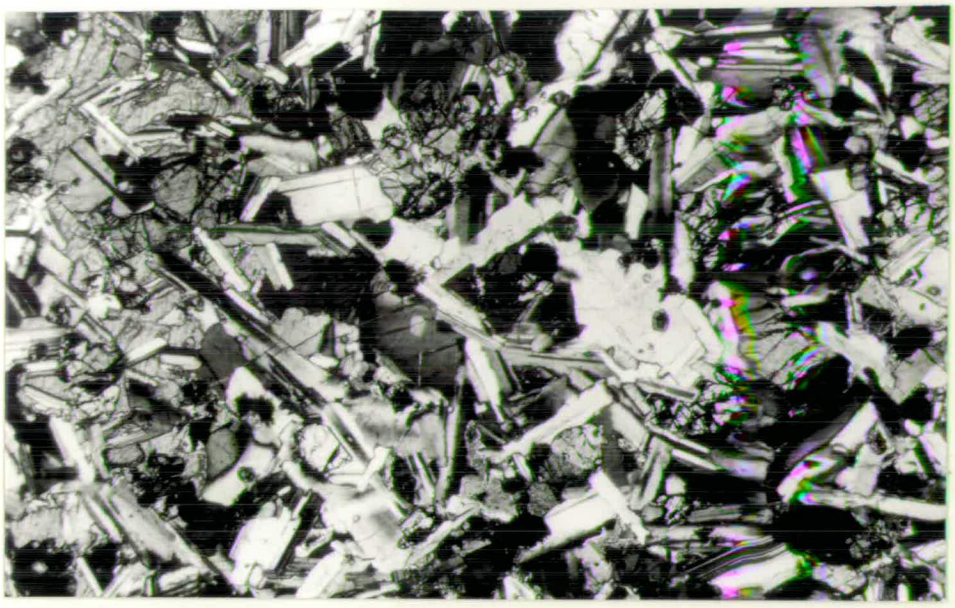
   + ? apatite.

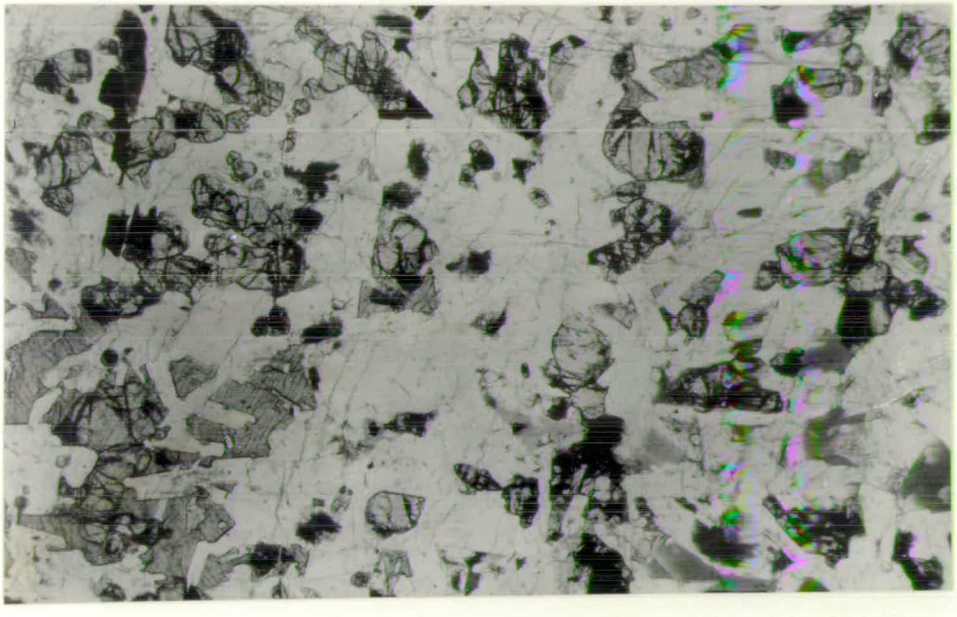
2. Trachydiorite series.

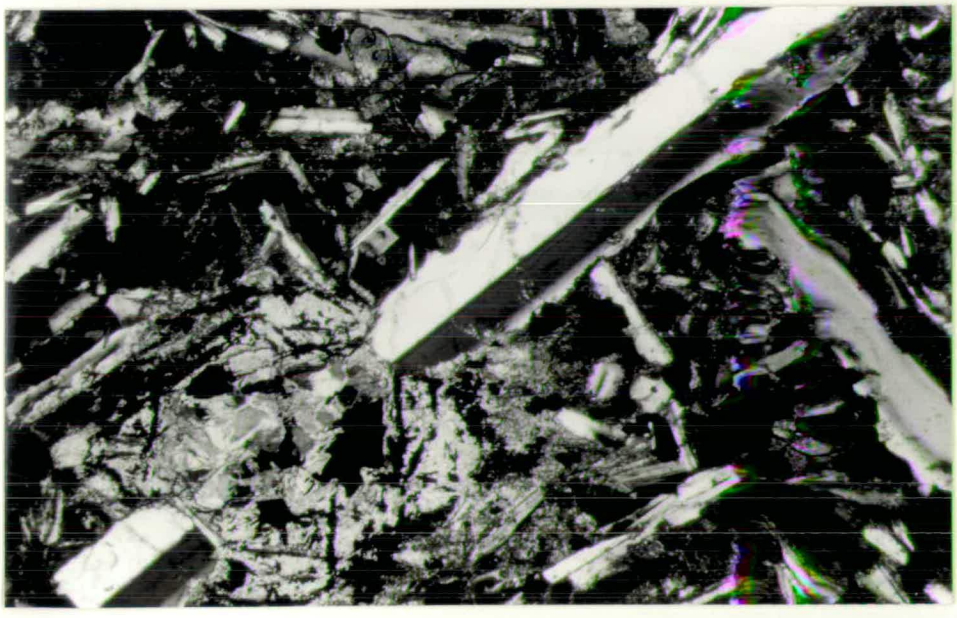
   Plagioclase + olivine + magnetite $\pm$ clinopyroxene

PLATE 3.1:
GGU specimen number 101413: porphyritic olivine dolerite with phenocrysts of plagioclase and olivine (now altered) and groundmass of plagioclase, olivine, clinopyroxene and magnetite. Crossed nicols. Width of field 6mm.

PLATE 3.2a & b:
GGU specimen number 101403: feldspathic olivine dolerite, aphyric with plagioclase, olivine, clinopyroxene and magnetite. (a) plane-polarised light, (b) crossed nicols. Width of field 6mm.







rim round an inclusion-free core, but in disrupted anorthosite feldspars is confined to the crystal edges (Bridgwater and Harry, 1968).

3.3.1. Transitional olivine dolerites. (plates 3.1 and 3.2)

Only 13% of the transitional basalts are porphyritic, with phenocrysts of plagioclase or plagioclase and olivine. Phenocrysts constitute up to 9% of the rock with olivine forming less than 40% of the phenocryst species.

Plagioclase phenocrysts typically form idiomorphic laths averaging 2mm long, but can be up to 7mm long by 2mm wide. They sometimes form star-shaped aggregates. Normal zoning is common, and there is sometimes evidence of partial resorbtion, with euhedral overgrowths on a rounded core. Prismatic, sub-hedral olivine phenocrysts have an average size of 1.0mm. There is no obvious compositional zoning. Frequently the crystals are partly or completely altered to a mixture of serpentine and magnetite, which forms at low temperatures ($<400^{\circ}$ C.) when water is present (Deer et al, 1966). There is no evidence of resorbtion or reaction with the liquid.

The aphyric rocks, and the groundmass of the porphyritic varieties, are composed of 50 to 60% labradoritic plagioclase, 8 to 20% subhedral olivine, very variable amounts of anhedral brownish clinopyroxene and accessory magnetite, biotite, apatite and interstitial alkali feldspar. The feldspar, which sometimes displays

reversed zoning, is frequently sericitized. Rarely the feldspars are clouded by finely disseminated iron oxide. Poldervaart and Gilkey (1954) suggest the clouding is due to thermal metamorphic effects causing exsolution of iron ores incorporated in the plagioclases; although Brown (1967) suggests the exsolution of ore may be connected with inversion to a different structural state because iron enters more readily into the higher temperature disordered structures. As the specimens displaying clouded plagioclases are from dykes close to the Nunarssuit complex it may be that the clouding is due to thermal metamorphism. There is a variation in size of olivine crystals within one thin section, the smaller crystals forming clusters. Opaque, needle-like inclusions, possibly of rutile, are sometimes found. The pyroxene is neutral or pale brown, faintly pleochroic to pale pink, and sometimes displays a patchy zonation. It occurs as anhedral plates fully or partly enclosing plagioclase, olivine, magnetite and apatite. No exsolution lamellae of orthopyroxene were found, even in the coarser-grained rocks. The principal ore mineral is titaniferous magnetite, although rare ilmenite and some sulphides also occur in the rocks. Deep red-brown biotite and acicular apatite are constant accessories.

3.3.2. Inclusions (plate 3.3)

A xenolith of porphyritic gabbroic anorthosite (specimen 101394) was found in one dyke in the Kobberminebugt area. The xenolith is composed of 84% plagioclase, 11% olivine and 5% clinopyroxene, magnetite and

apatite. The euhedral, tabular plagioclase phenocrysts, 3 to 4cms long, are set in a gabbroic matrix of small (2 to 7mm), strongly zoned plagioclase laths in sub-ophitic texture with olivine and interstitial clinopyroxine, magnetite and apatite. The plagioclase phenocrysts are unzoned and contain small inclusions of olivine and pyroxene along the twin-planes. Anhedral olivine crystals up to 4mm across are partly enclosed at the edges of the phenocrysts. No deformation of this xenolith is noted and alteration is minor.

This appears to be a type of 'secondary anorthosite' xenolith (cf. Bridgwater and Harry, 1968) in that the early-formed phenocrysts were enclosed in a gabbroic matrix then later disrupted and included in the host dyke. The mineralogy of the xenolith groundmass is similar to the host dyke, although the average grain-size is greater and it is possible the 'groundmass' represents an earlier phase of the host dyke. No phenocrysts were found in the host dyke but similar rocks carry phenocrysts of plagioclase or plagioclase plus olivine. The presence of inclusions throughout the plagioclase phenocrysts and the lack of deformation suggest they were not derived from the disruption of the granular anorthosites.

3.3.3 Trachydolerites.

With increasing alkali feldspar content the rocks grade into trachydolerites. The proportion of ore increases in the trachydolerites and enters the phenocryst species, reflecting the iron-rich nature of the rocks. The textural and mineralogical features are similar to those of the dolerites, so the description will be brief.

Porphyritic varieties (ca. 30%) contain up to 26% phenocrysts of plagioclase (generally a sodic labradorite to calic andesine) and olivine, plus or minus magnetite and apatite. Euhedral to subhedral, slightly rounded plagioclase crystals up to 1cm long and often flow-aligned form 70 to 80% of the phenocryst species. Some crystals have a seive texture formed of a network of holes filled with groundmass material. Sericitic alteration is frequently far advanced. The subhedral olivine phenocrysts (ca. 3mm) may be completely pseudomorphed by serpentine and magnetite. Idiomorphic magnetite forms less than 4% of the phenocryst species and apatite phenocrysts occasionally occur.

The groundmass is composed of up to 65% plagioclase zoned to cryptoperthite, 4 to 15% olivine, 5 to 15% pinkish clinopyroxene, 5 to 10% magnetite plus ilmenite and accessory biotite and stumpy apatite prisms. Cryptoperthite can form up to 40% of the total feldspar content. The finer-grained rocks may display flow-alignment of the feldspar microlites while the coarser rocks are dominated by ophitic textures.

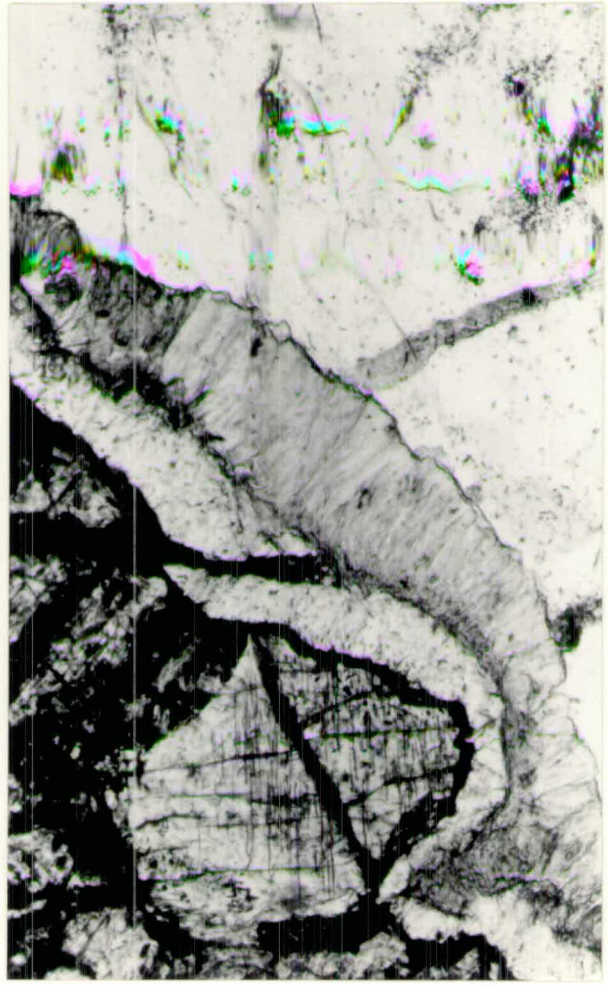
Narrow corona structures rimmed the olivine in one rock (101430) (plate 3.4). The coronae are composed of an inner rim of a neutral, low-birefringent mineral (? orthopyroxene) and an outer rim of a greenish, acicular mineral (? actinolite). The crystals were too small for definite identification. Only olivine enclosed in plagioclase was affected. Such corona structures are considered to be the result of thermal metamorphism, producing reaction in the solid state (Murthy,

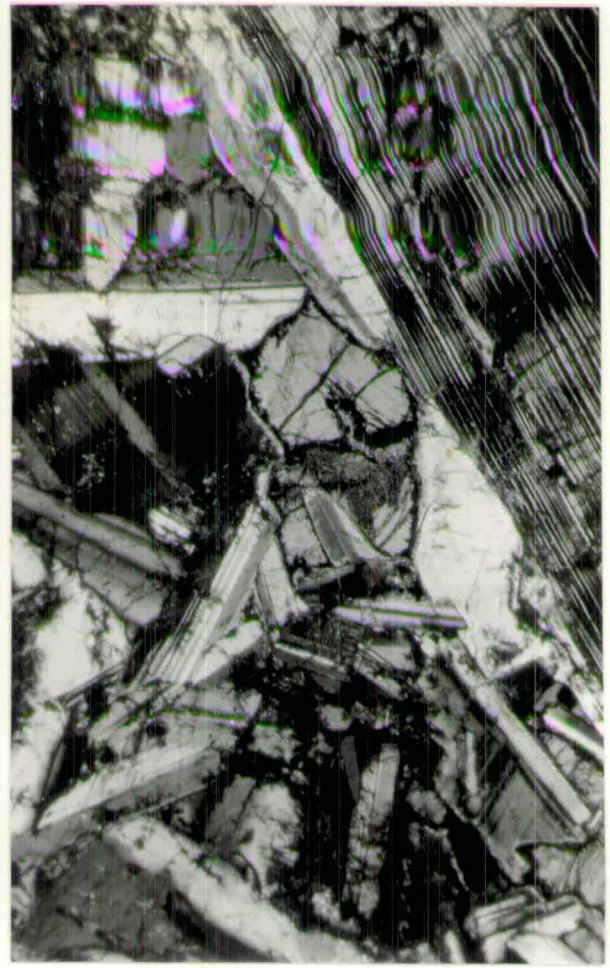
PLATE 3.3:
GGU specimen number 101394: porphyritic gabbroic anorthosite showing 'phenocryst' plagioclase and gabbroic 'groundmass'.
Crossed nicols. Width of field 6mm.

PLATE 3.4:
GGU specimen number 101430: detail of corona-structure developed at the contact of olivine and plagioclase. Outer rim - amphibole, inner rim - ?orthopyroxene.
Plane-polarised light. Width of field 3mm.

PLATE 3.5:
GGU specimen number 86029: an evolved trachydolerite with phenocrysts of fayalitic olivine, clinopyroxene and magnetite.
Plane-polarised light. Width of field 6mm.







1958). Both olivine and plagioclase in this rock are clouded with iron ores, which is characteristic of the rocks described by Murthy and indicative of thermal matamorphism.

Rarely quartz was observed in some dykes where, however, it appeared to be secondary, replacing alkali feldspar in myrmekite intergrowths with plagioclase or pseudomorphing olivine crystals. Only in one rock (101406) did quartz appear to be a primary mineral; this is the coarse, central facies of a BD_0 dyke. The quartz occurs interstitally.

3.3.4. Inclusions in Trachydolerites.

A single xenolith of anorthosite was found in one dyke (101280 - dyke and xenolith). More than 90% of the xenolith is plagioclase, which is very badly sericitized but shows some relict albite twinning. The crystals (0.5 to 1cm) are anhedral and the xenolith has a granular texture. Other minerals - iddingsitised olivine and magnetite - are confined to the boundaries between the plagioclase crystals. No cataclasis of the xenolith was noted but otherwise the xenolith is similar to the granular anorthosite xenoliths described by Bridgwater and Harry (1968). The alteration of the xenolith probably took place after its inclusion in the host dyke: iddingsite forms at low temperatures and has an upper stability limit of 140°C (Haggerty and Baker, 1967). The host dyke too is badly affected by sericitic alteration.

3.3.5. Evolved trachydolerites. (plate 3.5)

Few of the specimens examined fall in this category: these rocks are transitional to trachytes. They are confined to the Nunarssuit and

Tugtutoq zones. Phenocrysts (up to 31% of the rock) are predominantly plagioclase (andesine) with minor amounts of fayalitic olivine, clinopyroxene, magnetite and apatite, these forming up to 10% of the phenocrysts. The plagioclase phenocrysts are up to 7mm across, and may show strong zoning. Pyroxene and olivine phenocrysts are ca. 2mm across. The groundmass is composed of plagioclase zoned to alkali feldspar, subhedral pinkish clinopyroxene, biotite, magnetite, apatite and minor brown amphibole.

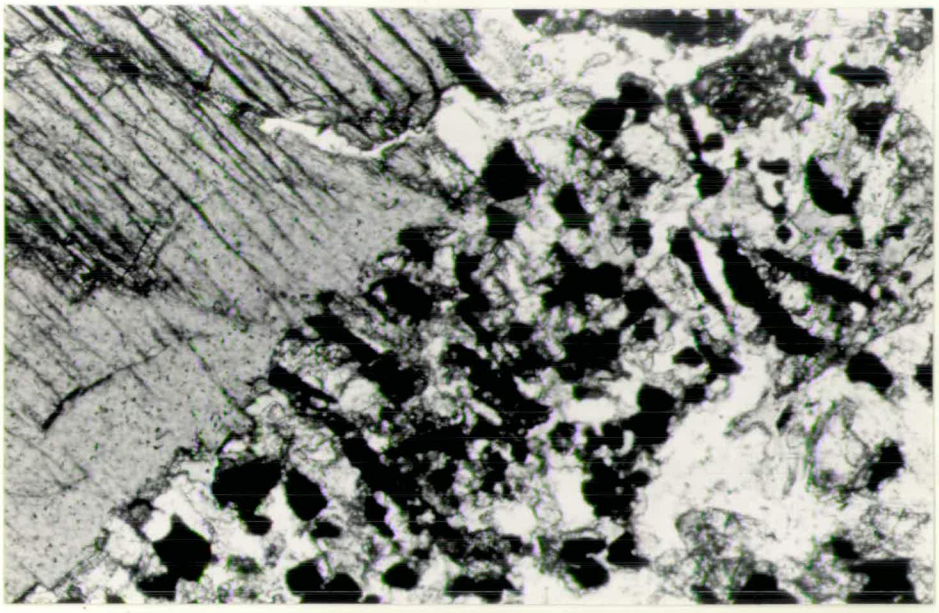
3.3.6. Syenogabbros (plate 3.6)

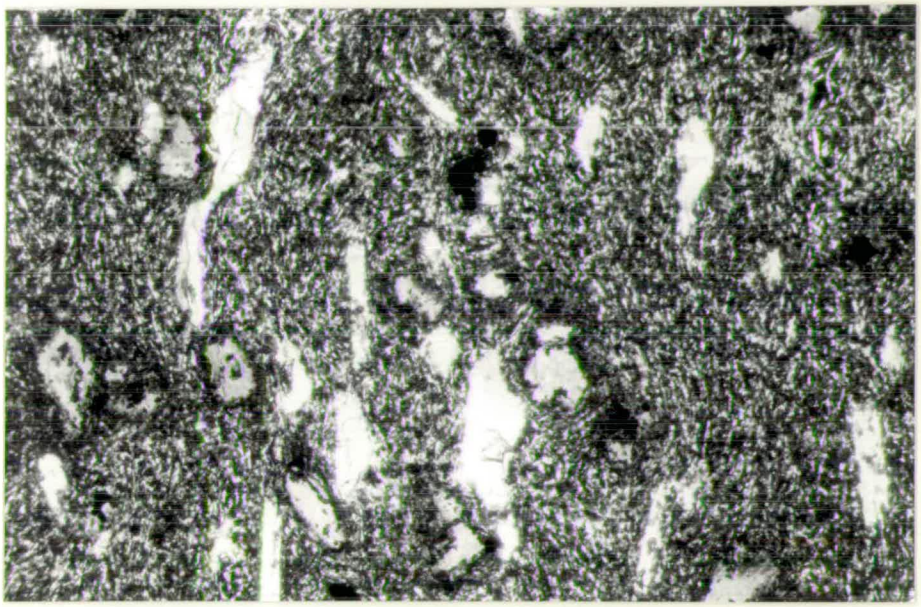
The syenogabbros are all specimens from the composite dykes in the Nunarssuit-Isortoq zone and the majority of them are from the Isortoq giant dykes. They are thoroughly evolved rocks (DI 50 to 65) transitional to syenites, coarse grained and have hypidiomorphic textures. Feldspar is the principal constituent, forming ca. 75% of the rock. Alkali feldspar (antiperthite) constitutes ca. 40 to 60% of the feldspar and in the more evolved syenogabbros is rimmed by albite. Plagioclase (andesine-oligoclase) forms the core of the feldspar crystals. The clinopyroxene, forming 10 to 15% of the rock, is idiomorphic but the edges of the crystals are partly penetrated by plagioclase. Narrow green rims form on the pinkish clinopyroxene adjacent to alkali feldspar, reflecting the uptake of Na^+ into the pyroxene structure. Fayalitic olivine is a minor constituent (<10%) and is commonly altered to serpentine and magnetite. Magnetite fringed by biotite and accompanied by prismatic apatite is a constant accessory. Minor amounts of interstitial quartz and epidote occur in

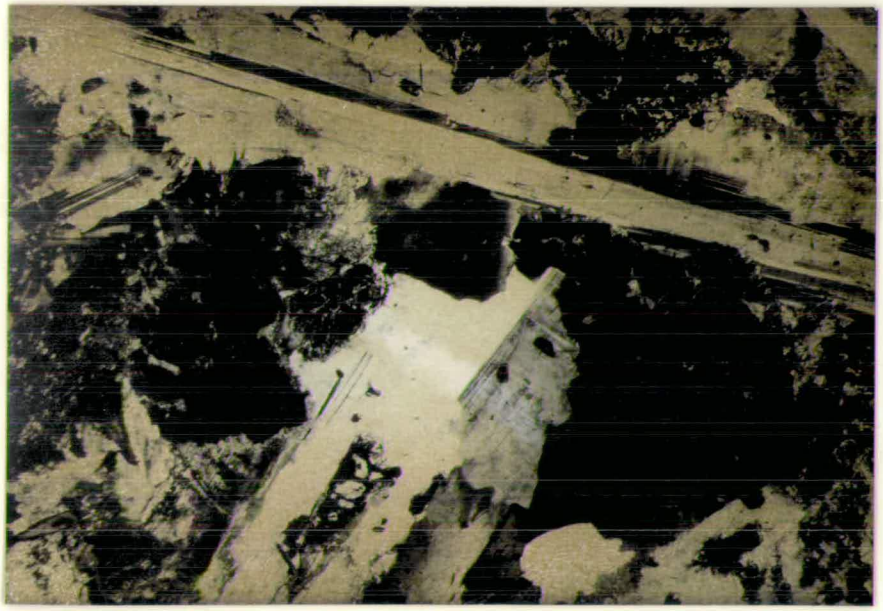
PLATE 3.6:
GGU specimen number 101361: syenogabbro with strongly-zoned plagioclase, altered olivine and magnetite.
Crossed nicols. Width of field 6mm.

PLATE 3.7:
GGU specimen number 101312: chilled facies of trachydiorite with plagioclase, altered olivine and magnetite phenocrysts and irregular ocelli filled with calcite and chlorite.
Plane-polarised light. Width of field 6mm.

PLATE 3.8:
GGU specimen number 101319: kaersutite phenocryst with a corrosion rim of clinopyroxene, plagioclase and ore, about 1mm wide.
Plane-polarised light. Width of field 3mm.







some of the syenogabbros.

3.3.7. Trachydiorites. (plate 3.7)

The trachydiorites represent the resurgence of basic volcanism after a period of salic volcanism.

The trachydiorites are commonly porphyritic with up to 25% phenocrysts of andesine (45 to 70% of the total), olivine (< 30%) and magnetite, plus or minus clinopyroxene (<25%). Apatite phenocrysts are occasionally present and corroded kaersutite phenocrysts were found in one rock (101319). The large (1.5cm) strongly pleochroic kaersutite crystals were not in equilibrium with the liquid at the time of intrusion and have developed a thick, radial rim of ilmenite plates, pyrite, clinopyroxene and plagioclase. The plagioclase phenocrysts (2mm long) are frequently flow-oriented and the olivine phenocrysts (0.5mm) are invariably pseudomorphed by serpentine. The idiomorphic clinopyroxene phenocrysts are zoned from pink, titaniferous core to green rims; hourglass zoning is common. See plate 3.8.

In the chill facies are sub-spherical structures filled with calcite and chlorite, which form up to 5% of the rock. These are possibly amygdales but the presence of primary chlorite and calcite in the trachydiorites suggests that the calcite and chlorite in these structures has formed from a separate CO_2 rich fluid phase during the cooling history of the rock and not as a later infill. These structures should therefore be called ocelli rather than amygdales.

The groundmass is composed of idiomorphic augite, strongly zoned andesine, alkali feldspar, biotite, magnetite and acicular apatite.

The finer-grained chills have a strong trachytoid texture. In the coarser-grained rocks chlorite, calcite and occasionally epidote occur interstitially, characteristically in areas enriched in feldspars. There is no clear boundary to these areas, which grade into more normal groundmass. It appears that they were formed through enrichment in the low-temperature components of the liquid. They may be equivalent to the ocellar structures in the chill facies, blurred by slower cooling. The proportion of interstitial calcite and chlorite in the coarser rocks is approximately similar to the proportion of ocelli in the chilled facies (ca. 5 to 7%).

3.3.8. A few specimens cannot be assigned to any of the categories so far described.

Dolerite pegmatites.

Segregation patches and veinlets of pegmatite are common in the coarser dolerite dykes (see chapter 2). A specimen from one such pegmatite (101267) is described briefly below.

The rock is very coarse grained, with plagioclase laths up to 1cm long. Brownish clinopyroxene is the principal mafic mineral, forming ca. 28% of the rock. It forms sub-ophitic intergrowths with the plagioclase, which is considerably sericitised. Plagioclase plus alkali feldspar together form 60% of the rock, with alkali feldspar (antiperthite), forming more than half of the total feldspar. The iron ore - an ilmenite/magnetite intergrowth - forms large (2 - 3mm), skeletal crystals which show some leucoxene alteration after ilmenite. Euhedral apatite (2mm long) generally occurs near the ore crystals and both may be enclosed by pyroxene. Minor biotite occurs as fringes on the ore. No olivine was found.

Trachydiorite from the Ivigtût zone.

An unusual dyke (101409) from the Kungnat area has no equivalents in the rest of the province. It is the only dyke of intermediate composition in the Ivigtût zone and the principal mafic mineral is hornblende not clinopyroxene or olivine. It is aphyric, medium grained and contains oligoclase in addition to cryptoperthite, together forming ca. 70% of the rock, euhedral hornblende (ca. 10%), biotite (ca. 7%) forming fringes on the magnetite and accessory apatite and interstitial epidote, calcite and chlorite. It is a thoroughly evolved rock (DI = 60) and has been classed as a trachydiorite although completely unlike the Tugtutôq trachydiorites, except in the content of epidote, calcite and chlorite.

EX BIBL. UNIV. EDINBURGEN.

4. Mineralogy

Phenocryst assemblages and groundmass minerals from a range of Gardar dykes were analysed by electron microprobe. The analyses are presented in Appendix 5 and summarised in figures in this chapter and where appropriate the individual analyses in Appendix 5 are referred to by bracketed specimen numbers. A description of the analytical technique is given in Appendix 2.

4.1. Feldspars.

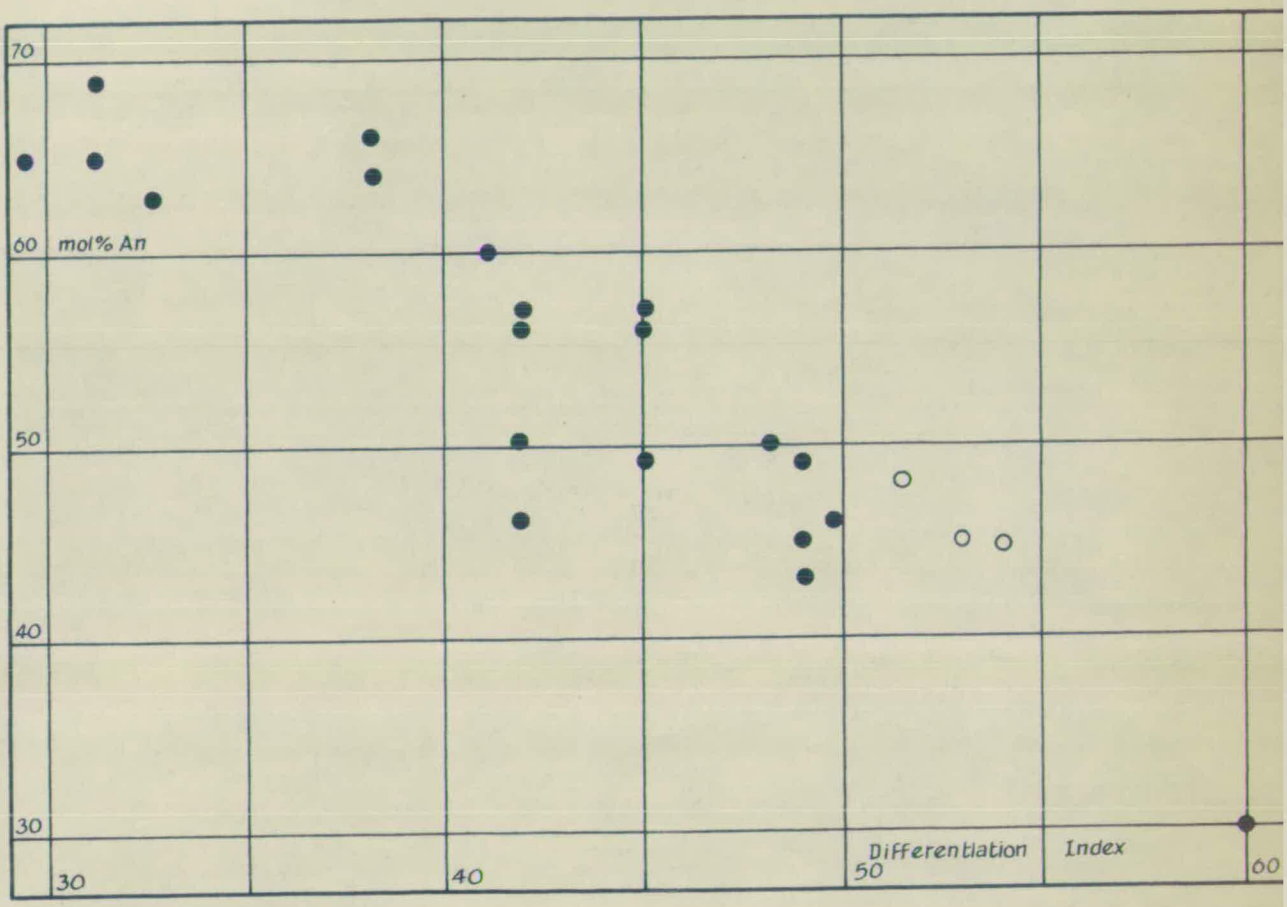
Plagioclase is the principal phenocryst phase in the Gardar rocks and together with interstitial alkali feldspar forms more than 50% of the groundmass in the dolerites and trachydolerites.

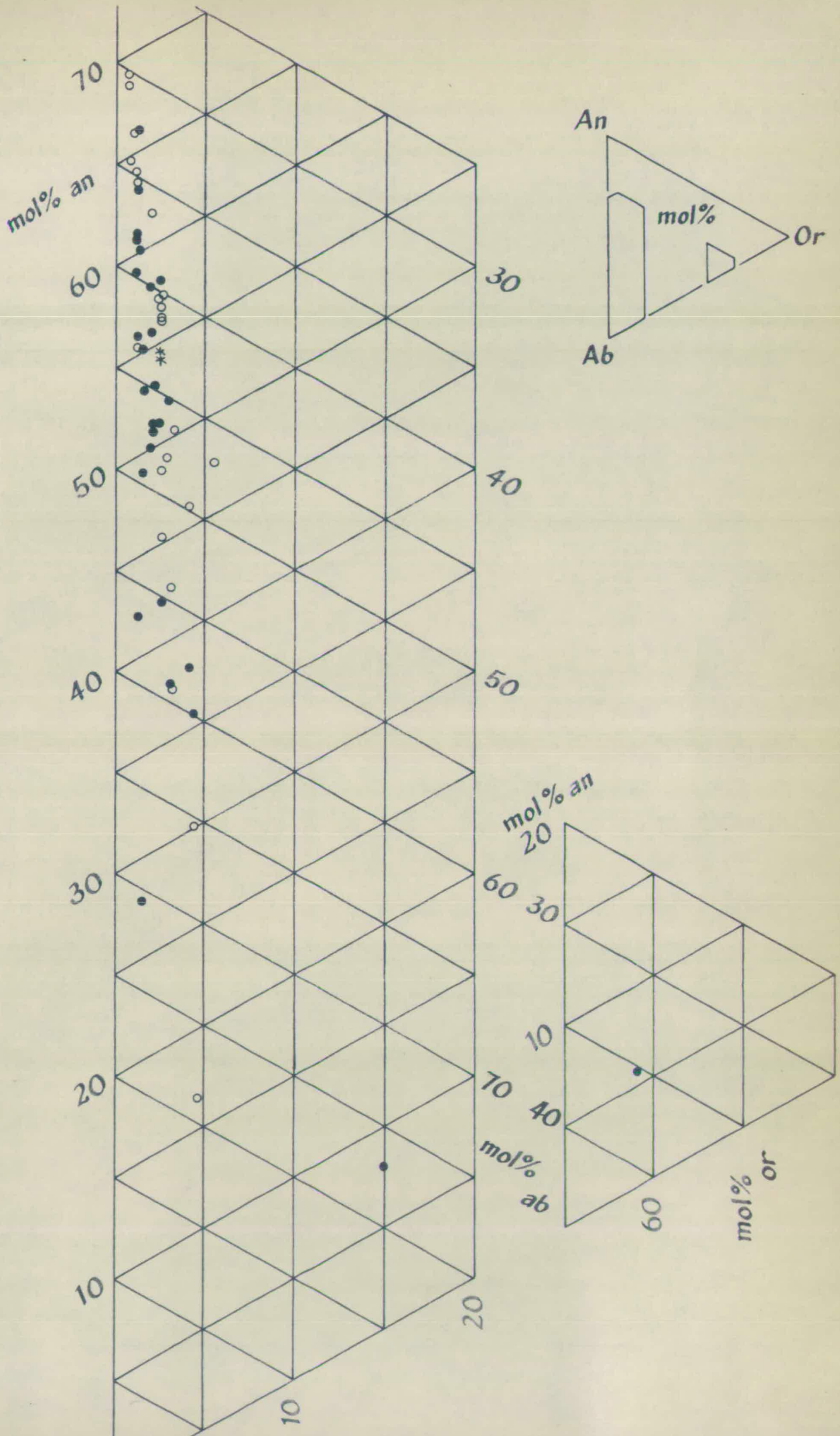
The 25 phenocryst analyses reported in Appendix 5, table A.5.1 are from 10 separate dykes. Groundmass feldspar in these dykes was also analysed and a further 17 analyses are of feldspars from the aphyric rocks. Since these are relatively rapidly chilled they are unlikely to represent equilibrium compositions, but they cover the same range of compositions as the feldspars from the porphyritic rocks.

The variation in phenocryst composition with differentiation is shown in fig.4.1 and the molecular proportions Anorthite-Albite - Orthoclase of each analysis are shown in fig.4.2. Pulvertaft (1965) reported plagioclase compositions up to An 75 in the Equaloqarfia dyke, Nunarssuit and Upton (1964) has found plagioclase compositions up to An 72 in the Tugtutoq gabbro dykes. The compositions of phenocrysts from the dolerites reported here range

FIGURE 4.1:
Variation in anorthite content of the plagioclase phenocrysts with differentiation. Both optical and chemical data used. Filled circles: dolerite-series rocks; open circles: trachy-diorites.

FIGURE 4.2 (following figure 4.1):
Variation in molecular proportions of anorthite, albite and orthoclase for the analysed feldspars listed in Appendix 5. Filled circles: groundmass feldspars; open circles: phenocryst feldspars; stars: phenocrysts from the gabbroic anorthosite xenolith.


70
60
mol% An
50
40
30
30
40
50
Differentiation
Index
60


mol% an
70
60
50
40
30
20
10
30
40
50
60
70
mol% ab
10
20
An
mol%
Or
Ab
mol% an
20
30
10
40
60
mol% or

from An 60 to An 66, but optical determinations gave values up to An 70 in the aphyric dolerites.

Zoning in the phenocrysts is usually slight; however a phenocryst from one dyke (101419a to d) displays continuous reversed zoning from An 65 to An 69, while strong normal zoning from An 30 to An 17 is seen in a phenocryst from a trachydolerite dyke (86029). Lofgren (1975) found that continuous reversed zoning could be produced experimentally with substantial supercooling of the liquid. Reversed normal and oscillatory zoning has also been noted in plagioclases from the aphyric rocks and here the rate of diffusion of ions in the melt may be the principal control. Feldspars in the syenogabbro dykes are strongly zoned from andesine through oligoclase to untwinned (cryptoperthitic) alkali feldspar (eg. 101361).

In fig.4.2 the scarcity of compositions more sodic than An 30 is a reflection of the scarcity of evolved compositions in the sample studied. There is very limited substitution of K^+ in the feldspars (less than 5 mol. % or), but the tendency for increased substitution in the more sodic compositions (Deer et al. 1966) is clear. The analysed andesine phenocryst from the trachydiorite dyke (101319) contains more Or (6%) than comparable andesines from the trachydolerites. The groundmass feldspar in the trachydiorites is anorthoclase, reflecting the potassic nature of these dykes.

The minor oxides present in the feldspars, TiO_2, FeO and MgO, generally contribute less than 1% by weight to the analysis. There

is a noticeable increase in these oxides in the small groundmass feldspars, or at the phenocryst rim, perhaps reflecting impurities in the rapidly chilled plagioclase.

The 'phenocryst' plagioclases in the gabbroic anorthosite xenolith (101394) are more sodic than the 'groundmass' plagioclases, at An 55 cf. An 64. The 'groundmass' plagioclases are not directly derived from the host dyke (101393), but may be an early phase of the host dyke. Most plagioclases from Gardar anorthosites range from An 52 to An 62, more calcic plagioclases being found only in anorthosites from Tornarssuk, in the Ivigtut zone (Bridgwater and Harry, 1968). By contrast, the early-formed plagioclase in the host rocks generally ranges from An 60 to An 75 (Bridgwater and Harry, 1968; this study).

The Gardar anorthosites are presumed to have formed at a depth of at least several kilometres, since nowhere are they exposed despite the strong faulting and differential erosion of the province, and to have been disrupted and carried up to higher levels as inclusions in the subsequent magma batches (Bridgwater and Harry, 1968). The fact that the xenocrysts and xenoliths contain plagioclase more sodic than those apparently in equilibrium with the host rocks at low pressures may be explained in terms of experimental studies. Thus, Cohen et al. (1967) and Green and Ringwood (1967a) showed that plagioclase crystallising in basaltic compositions becomes more sodic with increasing pressure. This behaviour is associated with increasing entry of normative An into the clinopyroxene as

calcium Tschermak's component. The feldspar forming at depth is therefore expected to be more sodic than the feldspar precipitated from similar magma at shallower depths. The calcic 'groundmass' feldspars in 101394 may thus have formed at lower pressures than the 'phenocrysts'.

In this context the reverse zoning seen in 101419 could have formed as the phenocryst was carried up in the magma, implying relatively rapid ascent rates.

Increasing pressure diminishes the stability field of olivine and plagioclase while that of clinopyroxene expands (Cohen et al. 1967). Olivine is the commonest mafic mineral found in the anorthosites (Bridgwater and Harry, 1968), although clinopyroxene and very rarely orthopyroxene may also occur. This would imply that the anorthosites formed at a pressure below that at which clinopyroxene became stable on the liquidus, which, in the case of the Gardar basaltic compositions, occurs at approximately 10kb. (Upton, 1971).

4.2. Olivine

Olivine phenocrysts occur in some of the more basic dyke compositions and thereafter they remain as a phenocryst phase throughout the trachydolerites. However, in many cases deuteric alteration is considerable and the olivines are pseudomorphed by serpentine and magnetite. Thus of the 17 analyses presented in Appendix 5, table A.5.2, only 6 are analyses of phenocrysts, from 4 separate dykes. The remaining 11 analyses are principally from aphyric rocks and

indicate the variation in olivine composition throughout the range of rock-types.

The Fo content of the olivines decreases through the series from a maximum of Fo 75 in a phenocryst from a dolerite dyke (101413) to Fo 27 in a syenogabbro (101361). No compositional zoning was detected in any of the phenocrysts. ~~The compositional range of olivines from the anorthosite xenoliths (Fo 73 to 60, Bridgwater and Harry, 1968) overlaps that of the dolerites and the composition of olivines in the groundmass of the gabbroic anorthosite xenolith (101413), believed on petrographic grounds to be an early phase of the host-rock, (101393).~~ The phenocryst olivine (101413) is considerably more magnesian than the most magnesian olivine compositions previously reported in Gardar dolerites and gabbros (Fo 68, Upton, 1964) and is comparable with the composition of olivines from the anorthosite xenoliths (Fo 73 to 60, Bridgwater and Harry, 1968). The groundmass olivines in the gabbroic anorthosite xenolith (101394), believed on petrographic grounds to be an early phase of the host (101393), are slightly more magnesian than the olivines in the host, at Fo 68 to 65 cf. Fo 61 and 60 and thus are also comparable to the olivines in anorthosites. It is not certain whether the anorthosite olivines were cumulus minerals with the plagioclase and thus they may not represent equilibrium compositions.

In those olivines in which the MnO content was measured, MnO increased with decreasing Fo from 0.35 weight % at Fo 67 to 1.6%

at Fo 27, reflecting the diadochy between Fe^{2+} and Mn. The MnO contents are slightly lower than in comparable olivines from the South Qoroq centre of the Igaliko complex, which have 2.16% at Fo 32 (Stephenson, 1974).

Simkin and Smith (1970) have suggested that the CaO content of olivines may be affected by the pressure and environment of crystallisation and have reported that in general, olivines of slowly cooled and deep-seated rocks have a low CaO content. They also report that the CaO contents of olivines in undersaturated rocks tend to be higher. The CaO contents reported in Appendix 5 range from 0.13 to 0.49 weight %, approximately within the range for volcanic olivines (0.28 to 0.56%). The low CaO contents of 101331, 101266 and 101361 (0.13 - 0.19) cannot be due to the pressure of crystallisation since this should be similar for all the dykes, but may reflect the degree of undersaturation, since these rocks have hypersthene or in the case of 101361, quartz in the norm, cf. the other specimens. The high level of CaO in 101394 at 0.31%, similar to that in 101393, (0.34 - 0.38%) suggests a comparatively high level of crystallisation.

4.3. Clinopyroxene.

Clinopyroxene is present only in the groundmass of the dolerites and basic trachydolerites, appearing in the phenocryst phase in the more-evolved trachydolerites, ie. at a comparatively late stage in the compositions studied. Clinopyroxene phenocrysts are also present in the trachydiorites. The 17 analyses presented in

table A.5.3 (Appendix 5), therefore, are mainly of groundmass clinopyroxene.

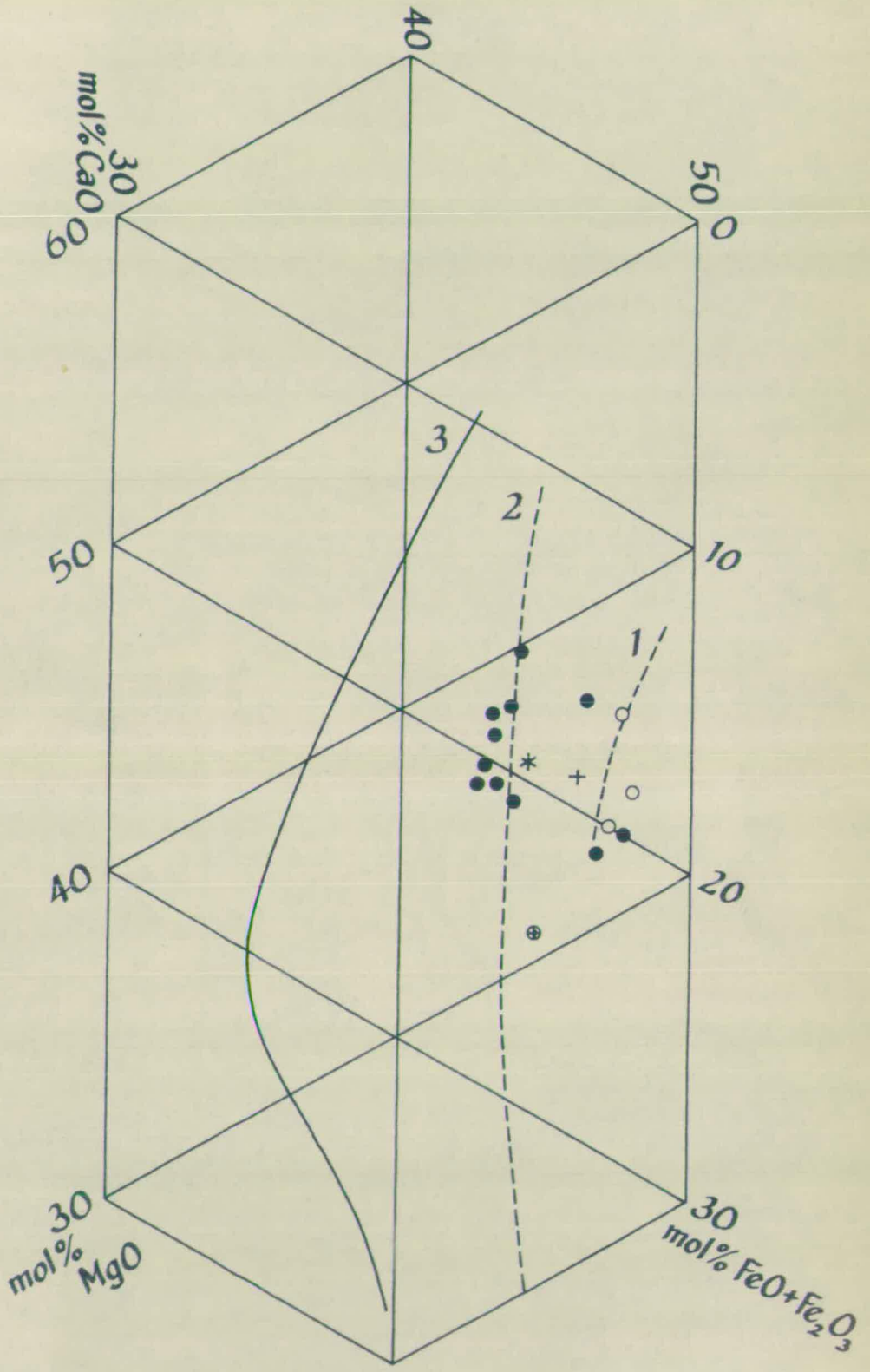
The formula of each analysis calculated on the basis of 6 oxygen atoms is also presented in table A.5.3. Electron microprobe analysis does not distinguish between Fe_2O_3 and FeO, so the Fe_2O_3 content was estimated by making the ionic amount of Fe^{3+} equivalent to the amount of Na plus K (cf. Carmichael, 1967). Calculation of the end-member molecules theoretically present in the clinopyroxenes (table A.5.4) was carried out by using matrix algebra to solve the simultaneous equations involved in apportioning the elements to each end-member molecule. This method gives similar results to that outlined by Kushiro (1962). Jadeite was not calculated; Kushiro has suggested that it is usually absent from igneous clinopyroxenes. The norms of the clinopyroxenes are presented in table A.5.5.

The clinopyroxenes from the dolerites and trachydolerites are calcium-rich varieties, lying close to the augite-salite-ferrosalite boundary at 45 mol% CaO as defined by Deer et al., (1966). Since the TiO_2 content varies from 0.82 to 3.13% they should not be described as titanaugite, which typically has between 3% and 6% TiO_2 (Deer et al., 1966). The variation in composition in terms of the molecular proportions CaO: MgO: FeO is shown in fig.4.3, with pyroxene trends in several well-known igneous series shown for comparison. There is only limited substitution of Fe^{2+} for

FIGURE 4.3:
Variation in the molecular proportions CaO-MgO-FeO in the analysed clinopyroxenes listed in Appendix 5.
'$FeO+Fe_2O_3$' means total iron expressed as FeO.

Full circles: groundmass pyroxenes in the dolerite series.
Open circles: groundmass pyroxenes in the trachydiorites.
Circled cross: trachydiorite phenocryst.
Cross: dolerite phenocryst.
Star: clinopyroxene from the groundmass of the anorthosite xenolith.

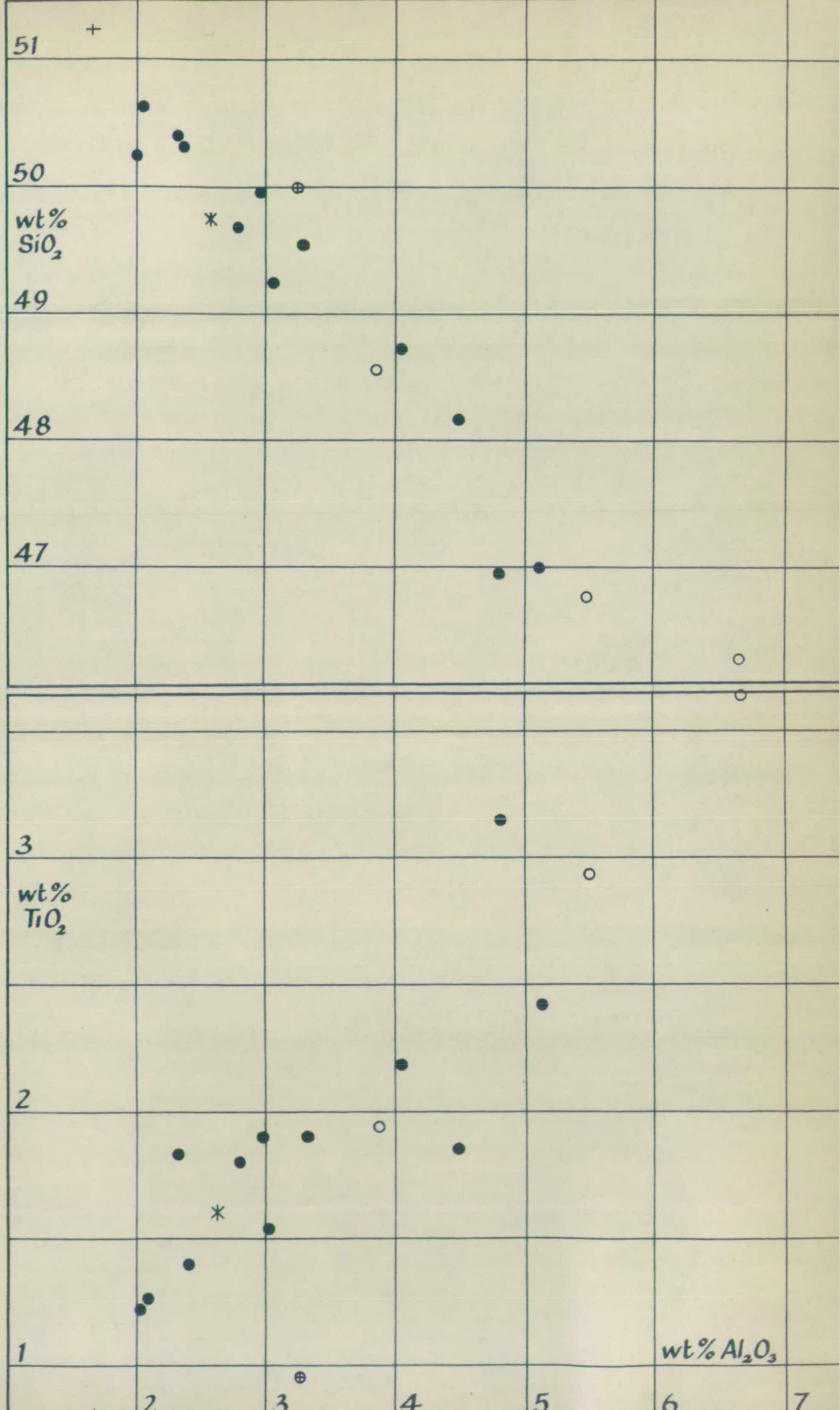
Line 1: compositional variation in pyroxenes from the Black Jack sill. Wilkinson (1956).
Line 2: compositional variation in pyroxenes from the Shiant Isles sill. Gibb (1973).
Line 3: compositional variation in pyroxenes from the Skaergaard intrusion. Brown and Vincent (1963).


40
30
mol% CaO
60
50
0
50
10
40
20
30
30
mol% MgO
mol% FeO+Fe2O3
3
2
1

Mg^{2+}, up to 22 mol% FeO, reflecting the limited compositional range of the rocks. There is no obvious tendency for Ca to decrease with increasing Fe/Mg as in many tholeiitic differentiation trends. The composition of the groundmass pyroxene from 101394 is within the compositional range of the pyroxenes from the dykes. The optically determined compositions reported by Bridgwater and Harry (1968) for clinopyroxenes from anorthosite xenoliths (Ca 33.5, Mg 36.5, Fe 30 to Ca 40.5, Mg 30, Fe 29.5) are poorer in calcium and richer in iron than any of the analyses reported here, or the phenocryst compositions reported by Boyd (1974) from the composite BFD dykes (Ca 44, Mg 35, Fe 21).

Up to 5.1% Al_2O_3 is present in the Gardar clinopyroxenes, within the limits quoted by Brown (1967). Most of the Al_2O_3 is in tetrahedral co-ordination (Al_z). The controlling factor is the Si content of the parent melt, as Al^{3+} substitutes for Si^{4+} (Le Bas, 1962) and there is a pronounced negative correlation between Al_2O_3 and SiO_2 in the clinopyroxenes (fig. 4.4). TiO_2 varies sympathetically with Al_2O_3 (fig.4.5) and Yagi and Onuma (1967) suggest that Al_z and Ti are present as $CaTiAl_2O_6$. Al in octahedral co-ordination is present as Ca-Tschermak's molecule ($CaAl_2SiO_6$), which is favoured by increasing pressure (Clark et al., 1962), while the solubility of $CaTiAl_2O_6$ decreases with increasing pressure (Yagi and Onuma, 1967). However, Hytonen and Schairer (1961) have shown that at atmospheric pressure diopside can contain up to 11.7% Al_2O_3 as $CaAl_2SiO_6$. The Gardar clinopyroxenes contain only small amounts of $CaAl_2SiO_6$, usually less than 2%,

FIGURES 4.4 and 4.5:
Variation in SiO_2 and TiO_2 with Al_2O_3 in the analysed clinopyroxenes.
Symbols as in figure 4.3.


51
50
wt%
SiO2
49
48
47
3
wt%
TiO2
2
1
wt% Al2O3
2
3
4
5
6
7

though one groundmass pyroxene contains 4.7%. The phenocryst pyroxene, 86029a, and xenolith pyroxene (101394) both contain less than 2 mol% $CaAl_2SiO_6$, and thus probably formed at relatively low pressures (Aoki and Kushiro, 1968).

No substantial enrichment in Na is noted in these pyroxenes and the acmite content is always less than 6% (table A.5.4). However, Boyd (1974) reports acmite contents of 18% for clinopyroxene phenocrysts in the composite BFD'S. Coombes (1963) showed that there is a relationship between magma type and the normative composition of the pyroxene. The norms of the Gardar clinopyroxenes contain small amounts of either hypersthene or nepheline, emphasing the transitional nature of the rocks.

Analyses of clinopyroxenes from the trachydiorites are presented in the Appendix. These clinopyroxenes are slightly more calcic than the basaltic clinopyroxenes, with up to 48 mol% CaO (fig.4.3). They display varying amounts of Mg^{2+} - Fe^{2+} substitution but the phenocryst (101319a) is unusual in containing more FeO and less MgO than the groundmass pyroxene (101319b). The phenocryst displays some evidence of disequilibrium in being somewhat rounded and corroded. The proportion of Al in octahedral co-ordination is higher than in clinopyroxenes of comparable Fe enrichment, so that the content of $CaAl_2SiO_6$ is 4.6 mol%. This cannot be taken as evidence for a high pressure origin however, since the groundmass pyroxene contains 4.3% $CaAl_2SiO_6$, although this is accompanied by 10% $CaTiAl_2O_6$.

The norms of these pyroxenes are listed in table A.5.5. The phenocryst contains a small amount of normative hypersthene but the other pyroxenes are nepheline normative.

4.4. Ore minerals

An extensive study of the ore minerals is beyond the scope of this thesis. This section is based on the examination of several polished specimens which were thought to be representative of the rock-types.

The principal ore mineral in the Gardar basic rocks is titaniferous magnetite, typically containing exsolution lamellae of ilmenite parallel to (111) of the host. In some of the coarse grained rocks a discrete ilmenite phase is commonly intergrown with the magnetite implying coprecipitation, while in the fine-grained trachydolerites platelets of ilmenite form a grid-like pattern in the groundmass. The magnetite is completely oxidised to maghemite, a process which takes place at low temperatures (approximately 200°C). Maghemite inverts to haematite at temperatures above approximately 375°C (Haggerty and Baker, 1967).

Disseminated sulphides are comparatively abundant in the dykes. In the coarse-grained rocks the sulphides are a mixture of pentlandite ($(Fe,Ni)_9S_8$) and cubanite ($CuFe_2S_3$). However in the dolerites and trachydolerites the sulphide is pyrite. The reason for this difference is not clear; the coarse-grained rocks examined are comparatively little differentiated and the Cu sulphides may

separate at an early stage (eg. Wager et al., 1957). Or this may be an indication of significant compositional differences in the magmas which produced the dykes (eg. Ade-Hall & Lawley, 1969). The Ni and Cu contents of the coarse-grained rocks are slightly higher but if the level of differentiation is taken into account this may not be significant. Clearly, more information on the distribution of the sulphides in the dykes is required to resolve this problem.

The trachydiorites contain altered titaniferous magnetite with ilmenite exsolution lamellae, and abundant pyrite.

4.5. Kaersutite.

Deep red-brown amphibole has been found as rare, strongly corroded anhedral phenocrysts in the trachydiorites. The crystals are surrounded by a thick radial growth of ilmenite plates, pyrite blebs which sometimes enclose the ilmenite, titaniferous pyroxene and plagioclase. The pyrite may have formed inclusions in the kaersutite, since it encloses the ilmenite which is an alteration product.

The amphibole analysis is given in the Appendix, table A.5.6. It is a kaersutite as defined by Wilkinson (1961), with more than 2 Mg atoms per formula unit, and a high Ti content. There is considerable replacement of Si by Al in the tetrahedral site, with 2.2 atoms per formula unit. Kaersutite commonly occurs in alkaline basalt-trachyte suites and in camptonites (Aoki, 1963; Deer et al., 1966). According to Holloway and Burnham (1972), it may occur as a

liquidus phase in basaltic liquids at pressures between 2 and 5 kb. and temperatures between 950 and 1060°C, when p_{H_2O} is less than p_{tot}. Instability at lower pressures is the probable cause of the alteration.

5. Major Element Chemistry

5.1. Introduction

In this chapter the distribution of the major elements within the dykes is discussed, comparing the distributions within each of the three zones Ivigtut, Nunarssuit and Tugtutoq by statistical methods. Simple variation diagrams are then used to illustrate the evolution of the magmas and the role of crystal fractionation discussed. Finally the variation in C.I.P.W. normative components of the basic rocks is described by means of projections within the 'simple basalt tetrahedron' (Yoder and Tilley 1962).

5.1.1. Sampling

The Greenland Geological Survey in 1969 made the cutter 'Steenstrup', under the direction of Captain Hvidstein, available to Dr. B.G.J. Upton specifically for sampling Gardar basic dykes over as wide an area as was feasible. Some 150 specimens were collected between Narssarssuaq and Tigssalup (fig. A.3.1 in Appendix 3 shows the distribution of the specimens). The majority of the specimens are from coastal exposures. Composite dykes, and dykes which are traceable over long distances are represented by several specimens.

In choosing specimens for analysis an attempt was made to include specimens representative of the different rock types and different generations. Relatively few analyses are of chill facies because of the possibility of contamination by country rock; Fratta and Shaw (1974) find evidence of diffusion of K and related elements from granitic wall-rocks into the marginal facies of Canadian

basaltic dykes. Although the main purpose of this study was to investigate the basic dykes, some salic rocks closely associated with the basic rocks, for example in composite dykes, have been analysed. These analyses are presented in the appendix, but are not discussed further.

5.2. Statistical Treatment.

The 88 specimens chosen for analysis have the following distribution: 25 specimens from the Ivigtut zone, 38 from the Nunarssuit zone and 25 from the Tugtutoq-Narssaq zone.

5.2.1. Cumulative proportion diagrams.

The chemical characteristics of the basic dykes (SiO_2 less than 54%) from each region are summarised and compared with data from Manson, (1967) in fig. 5.1. Twenty analyses of specimens from the Bangs Havn complex supplied by J. Engell are included in the diagrams. The statistical test used to test the differences between the samples is the Kolmogorov-Smirnov test, which is briefly described in section 5.2.2. The height of the line (D_{xy}) shown on the diagrams indicates the level at which differences in the distributions of two samples (x and y) are significant at the 0.05 level. The following points may be noted:

a. The MgO content of the Gardar sample is significantly low, reflecting the incidence of trachydolerites, whereas Manson considered

only basaltic rocks.

b. The CaO content is significantly low but the Al_2O_3 contents of both samples are similar.

c. The SiO_2 content of the Gardar rocks is low and correlates with the significantly higher FeO compared with Manson's sample.

d. The Na_2O content of the Gardar sample is higher than in Manson's sample and is also positively skewed. The K_2O contents are similar but the Gardar sample has a wider range of K_2O values.

e. The TiO_2 and P_2O_5 contents are significantly higher in the Gardar rocks and the dispersion is greater.

f. The MnO content is less dispersed in the Gardar sample.

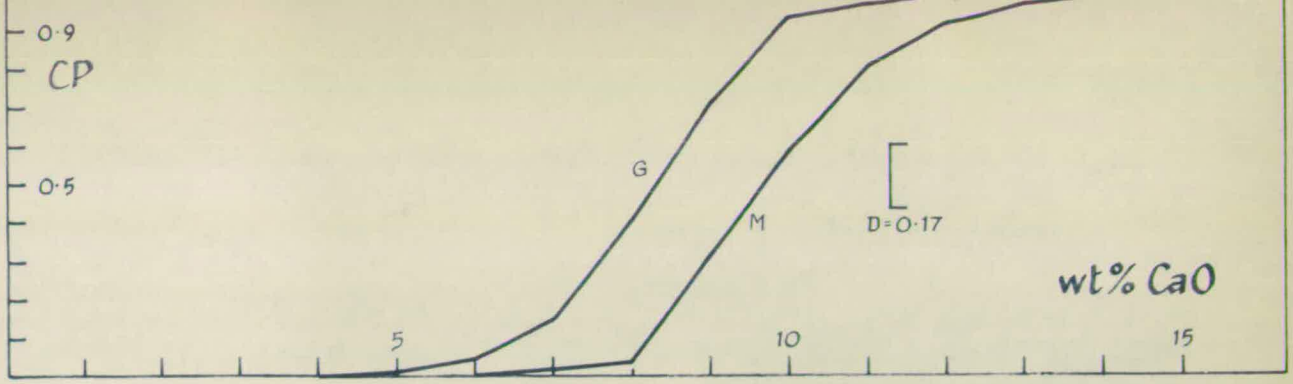
a., c., and e. relate at least in part to the incidence of trachydolerites in the Gardar sample. The significance of the similarity of Al_2O_3 contents depends on the variation during differentiation.

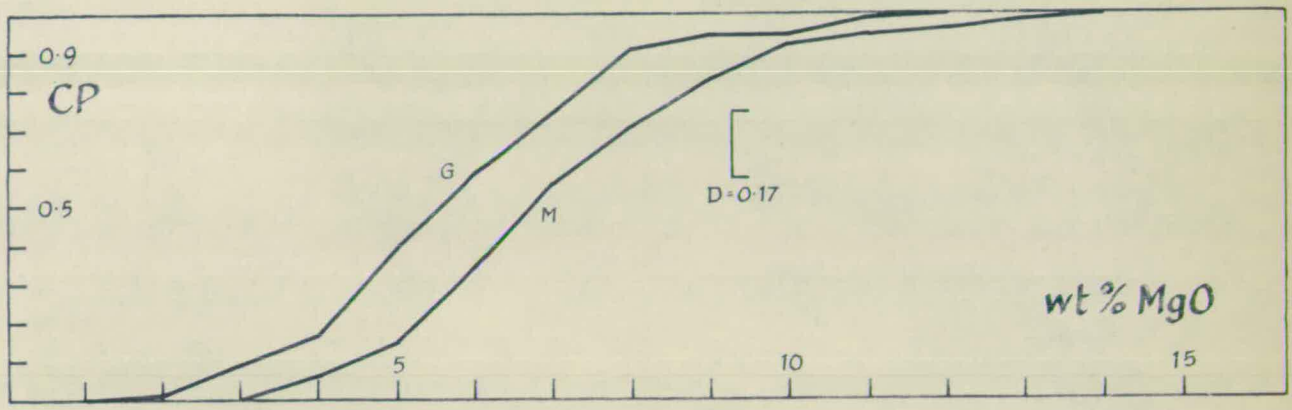
Figures 5.2a and b show the chemical characteristics of the dykes in each of the three zones Ivigtut, Nunarssuit-Isortoq and Tugtutoq-Narsarssuaq. There are significant differences between the three

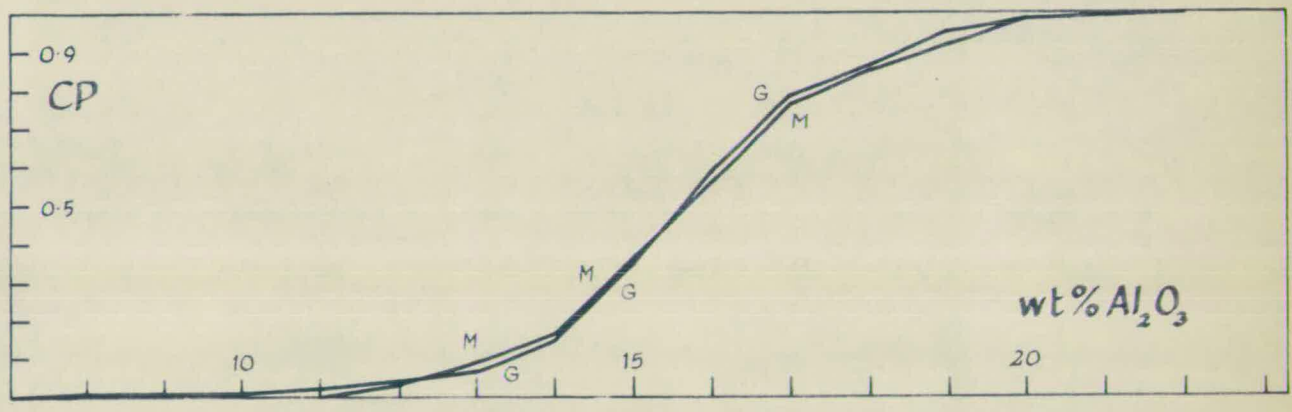
FIGURE 5.1 (two pages):
Cumulative-proportion graphs comparing the major-element chemistry of the Gardar sample with data for the basaltic rocks given by Manson, 1967).

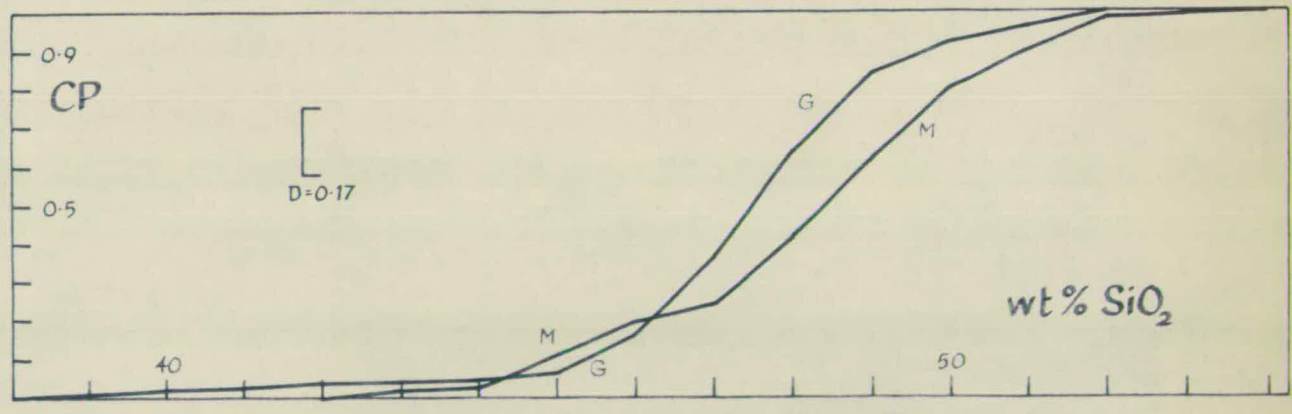
G: graph for the Gardar sample of 88 specimens.
M; graph for the Manson sample of 130 dolerites.

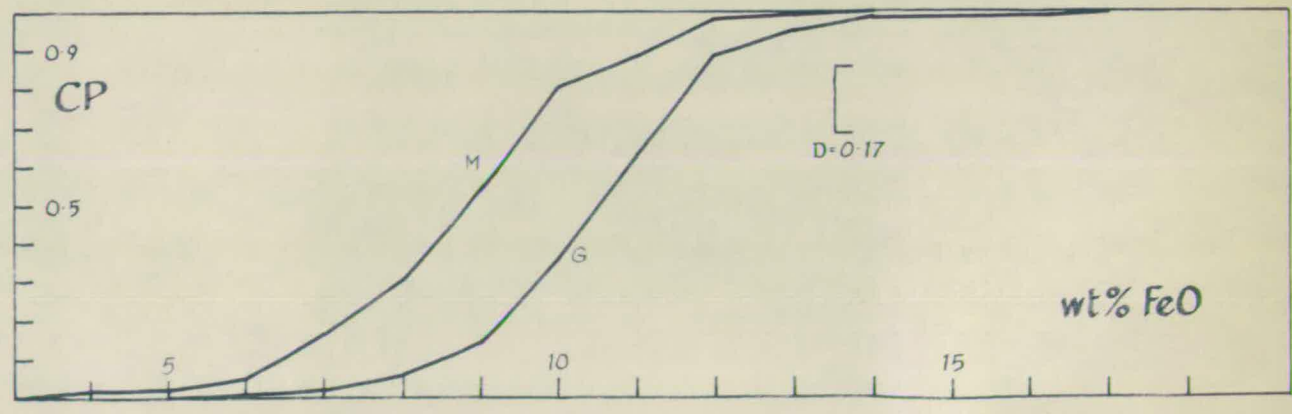
The graphs show the proportion of the sample having values of the variate equal to, or less than, the specified value.

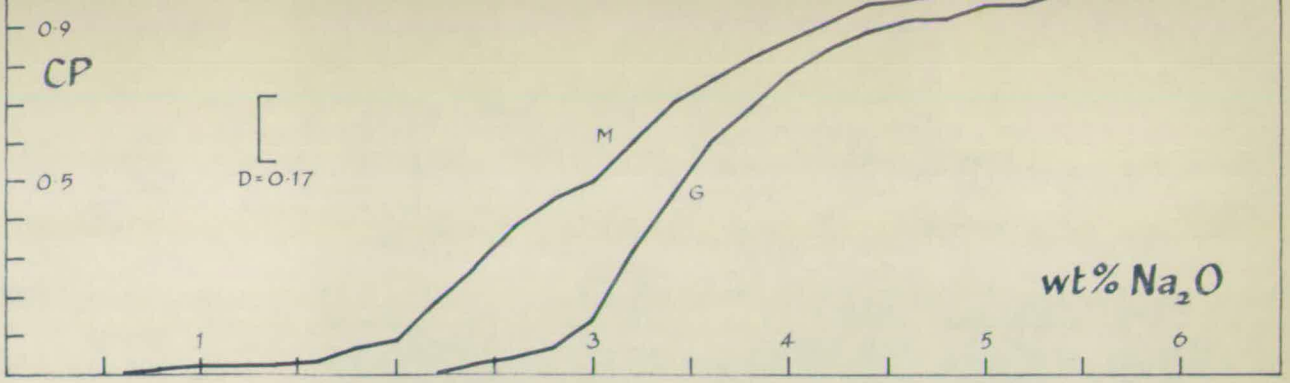

0·9
CP
0·5
G
M
D=0·17
wt% CaO
5
10
15

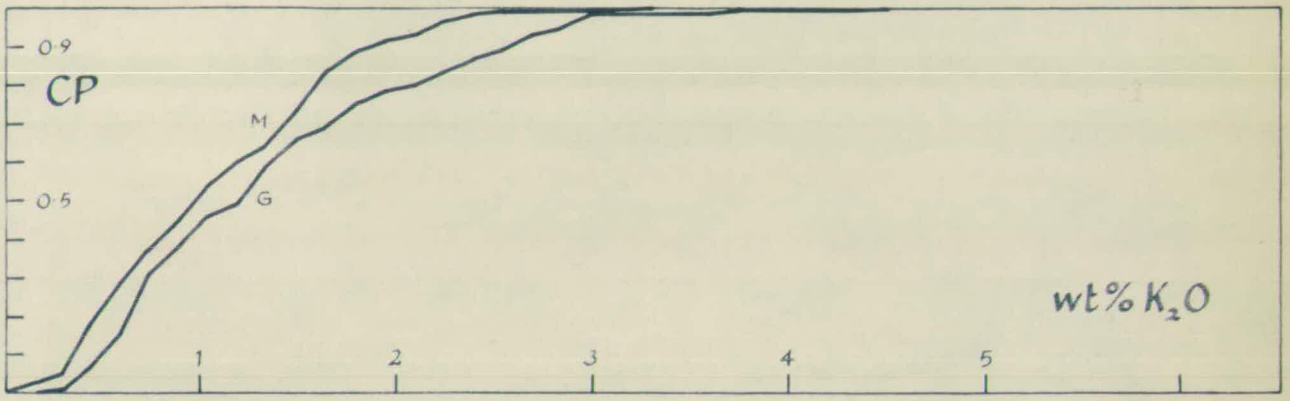

0·9
CP
0·5
G
M
D=0·17
wt% MgO
5
10
15

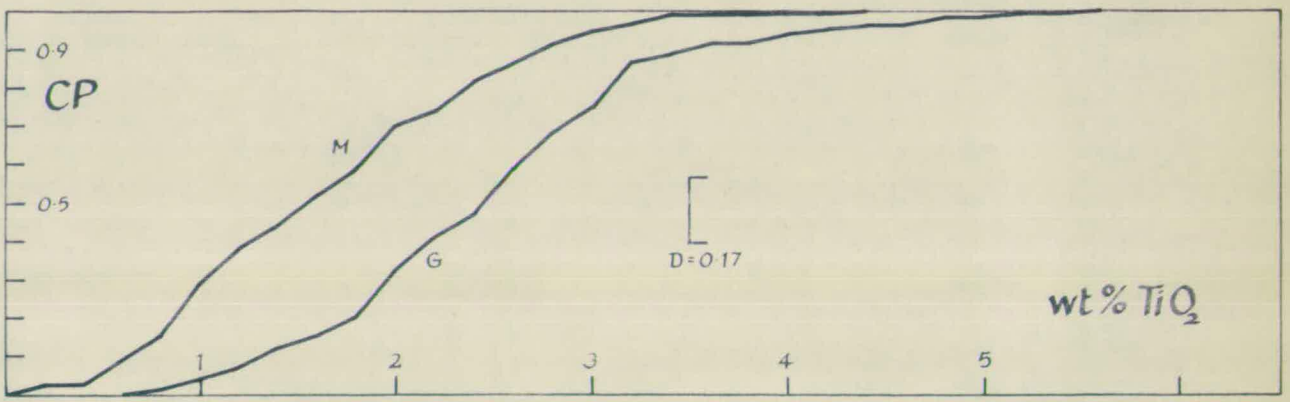

0·9
CP
0·5
G
M
M
G
M
G
wt% Al_2O_3
10
15
20

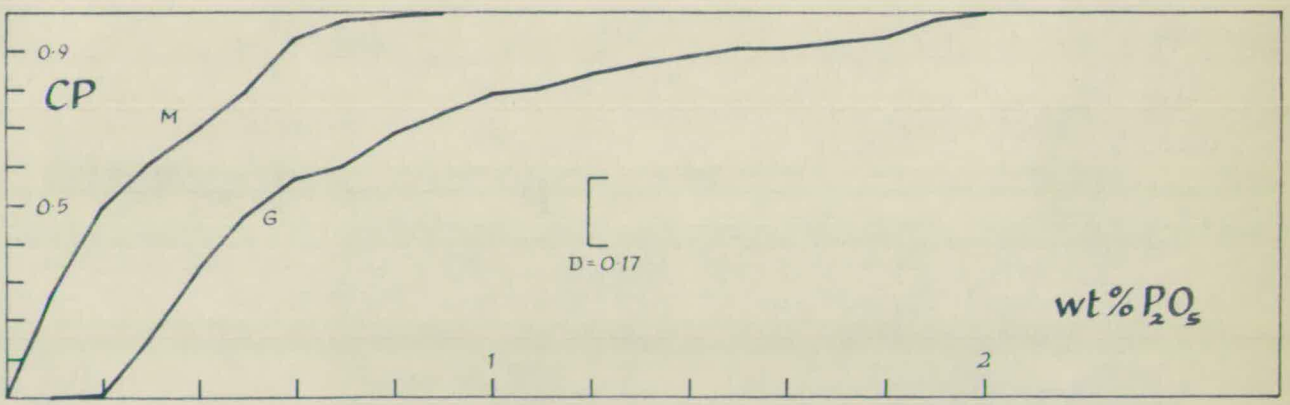

0·9
CP
0·5
D=0·17
G
M
M
G
wt% SiO_2
40
50

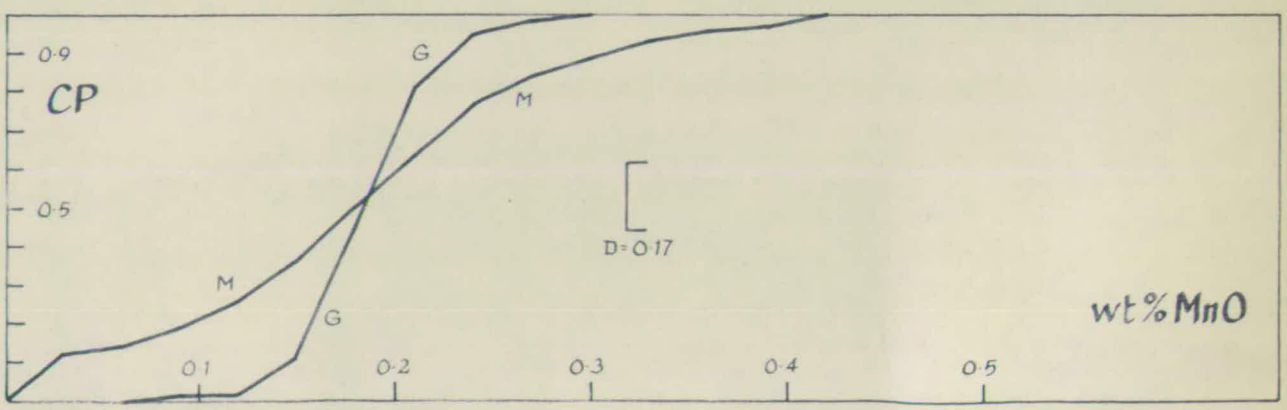

0·9
CP
0·5
M
G
D=0·17
wt% FeO
5
10
15


0·9
CP
0·5
D=0·17
M
G
wt% Na_2O
1
3
4
5
6


0·9
CP
0·5
M
G
wt% K_2O
1
2
3
4
5


0·9
CP
0·5
M
G
D=0·17
wt% TiO_2
1
2
3
4
5

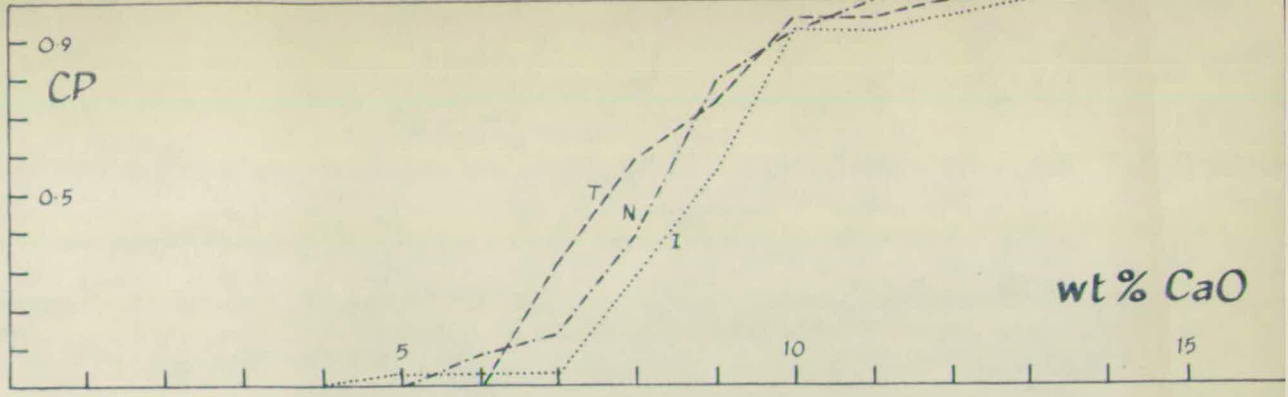

0·9
CP
0·5
M
G
D=0·17
wt% P_2O_5
1
2

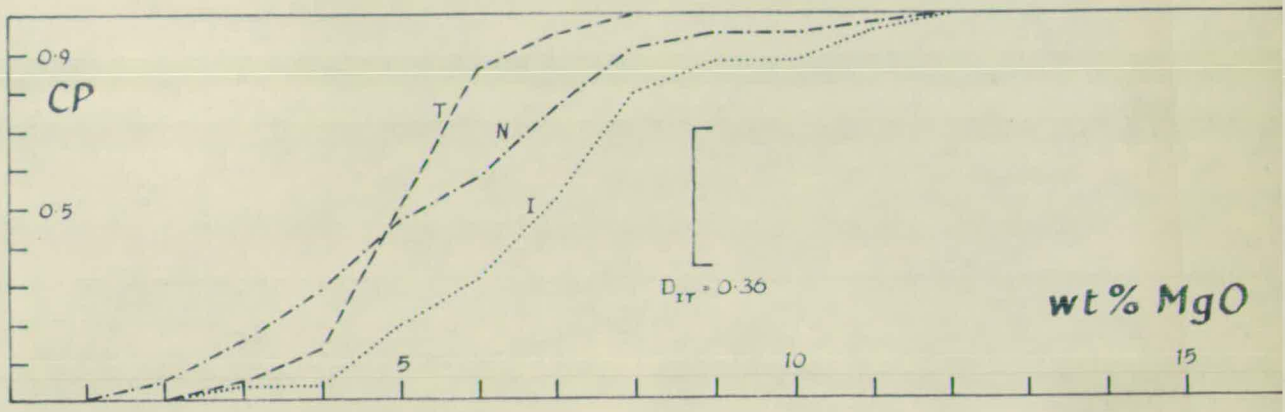

0·9
CP
0·5
G
M
D=0·17
M
G
wt% MnO
0·1
0·2
0·3
0·4
0·5

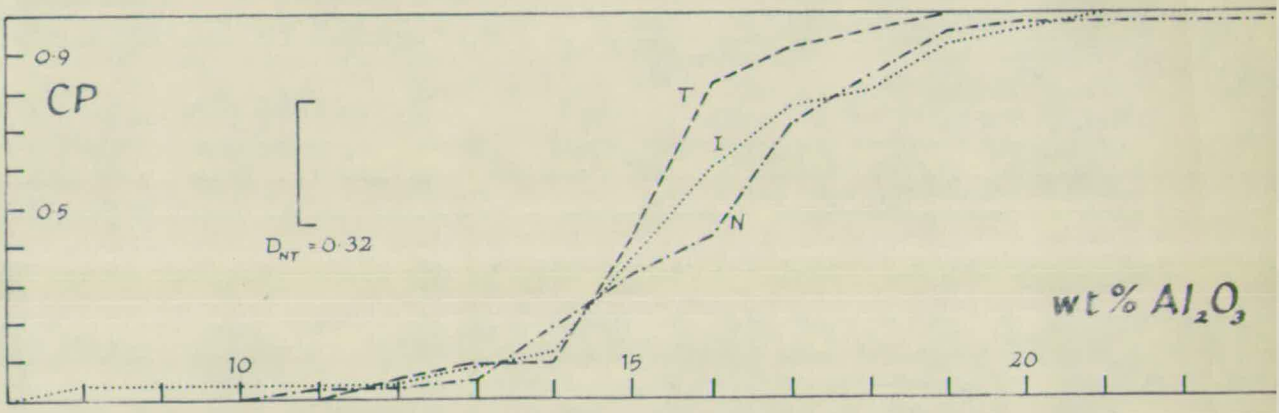
FIGURES 5.2a & b (two pages):
Cumulative-proportion graphs comparing the major-element chemistry between the three dyke-zones of the Gardar province.

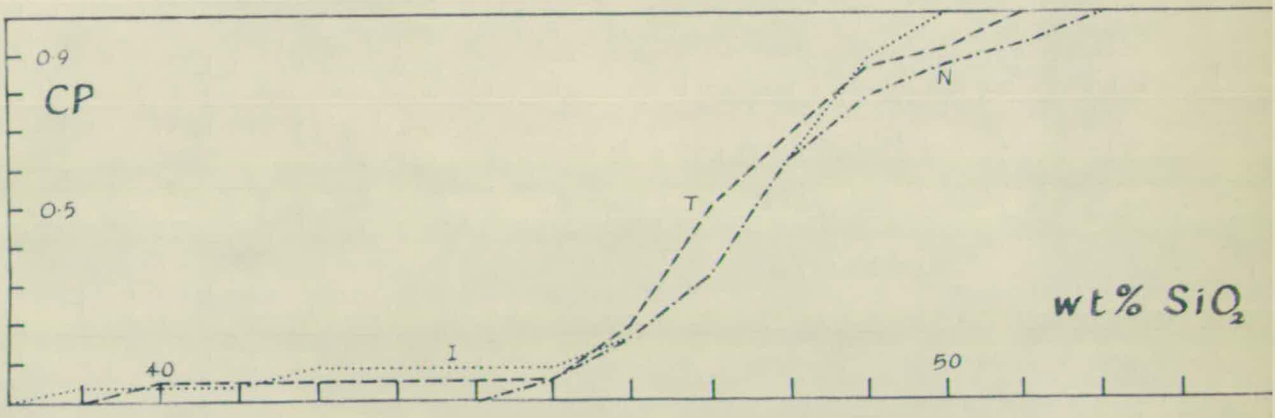
T: graph for the Tugtutoq-Narssarssuaq sample of 25 specimens.
I: graph for the Ivigtut sample of 25 specimens.
N: graph for the Nunarssuit sample of 38 specimens.

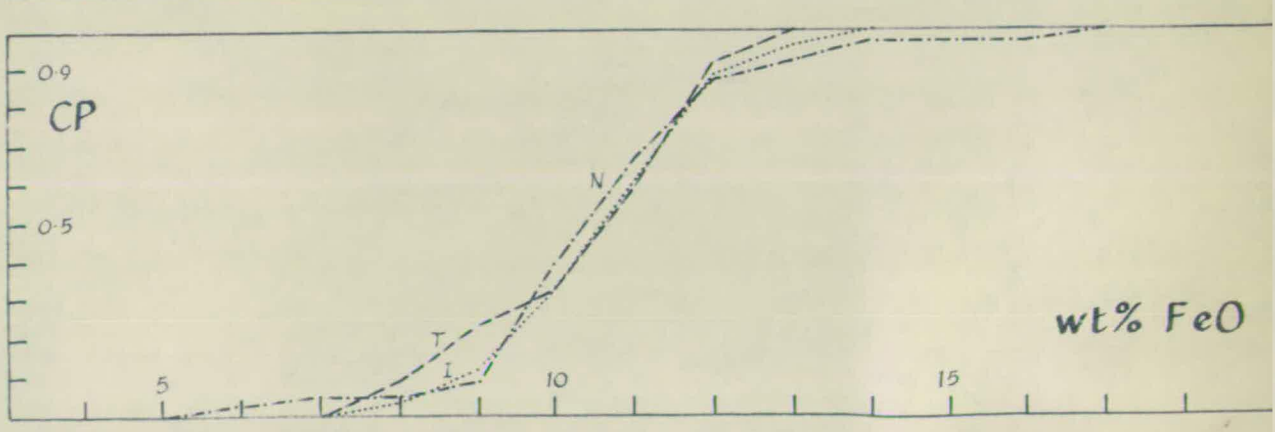
The graphs show the proportion of the sample having values of the variate equal to, or less than, the specified value.

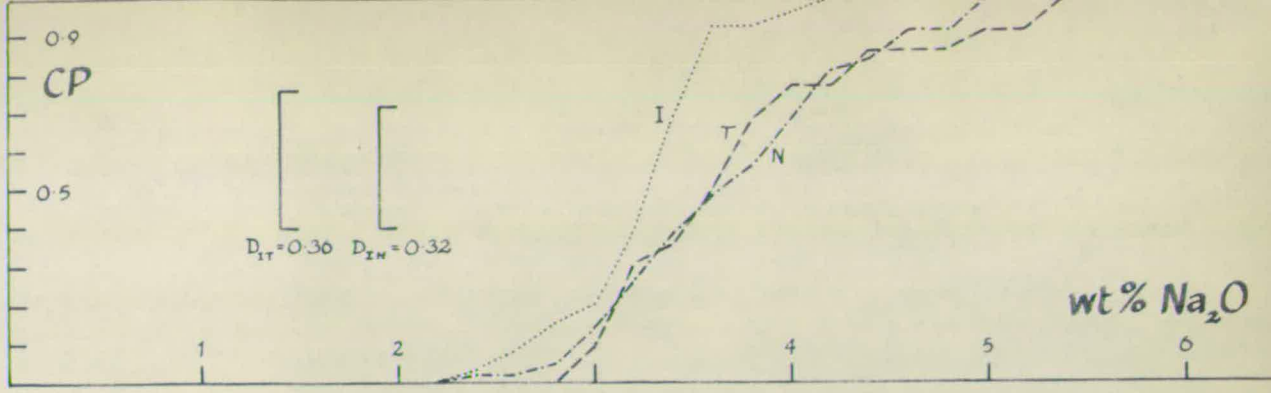

0·9
CP
0·5
T
N
I
wt% CaO
5
10
15

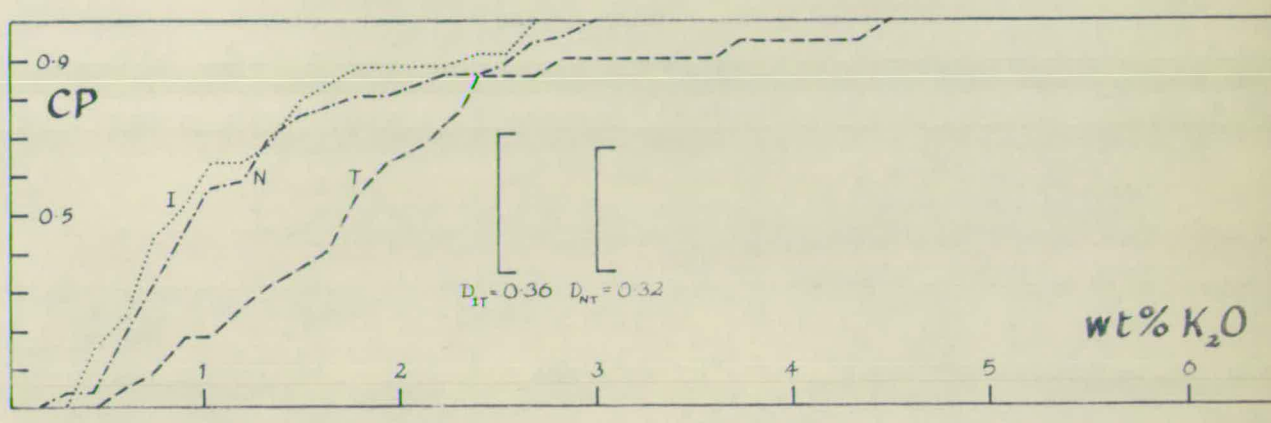

0·9
CP
0·5
T
N
I
D_{IT} = 0·36
wt% MgO
5
10
15

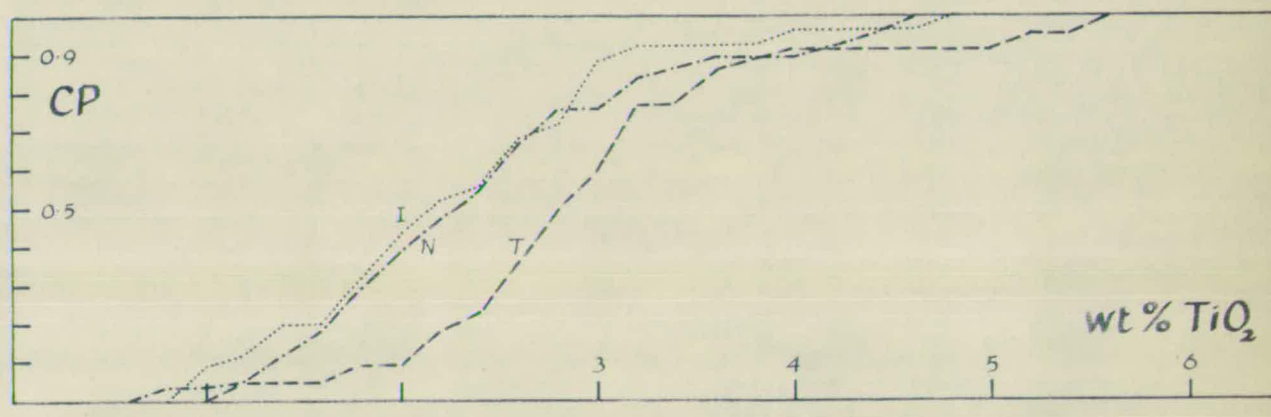

0·9
CP
0·5
D_{NT} = 0·32
T
I
N
wt% Al_2O_3
10
15
20

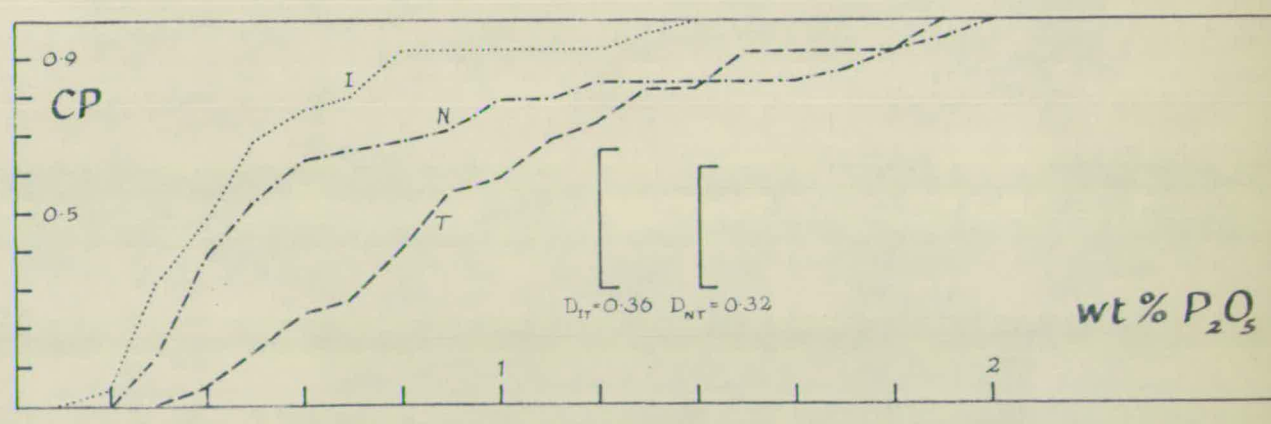

0·9
CP
0·5
N
T
I
wt% SiO_2
40
50

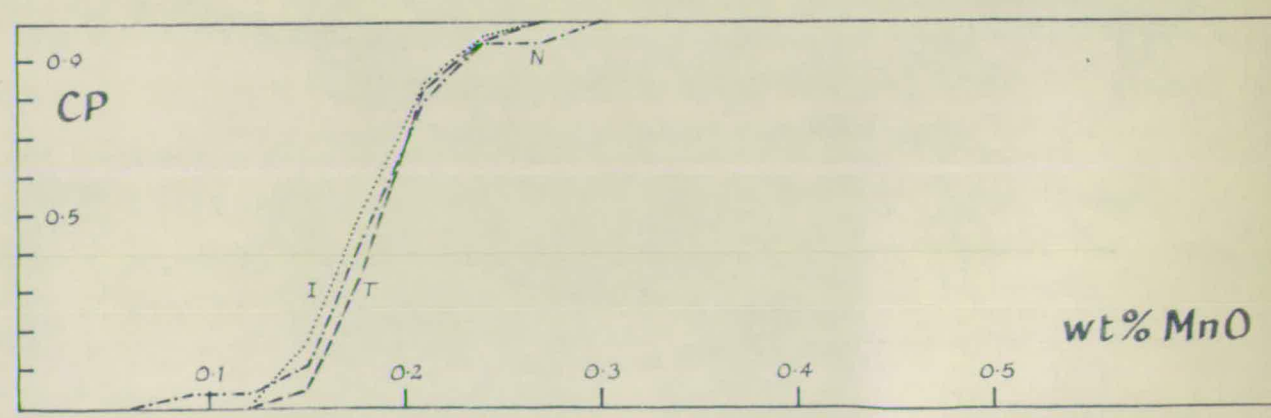

0·9
CP
0·5
N
T
I
wt% FeO
5
10
15


0·9
CP
0·5
I
T
N
D_{IT}=0·36 D_{IN}=0·32
wt% Na_2O
1
2
4
5
6


0·9
CP
0·5
I
N
T
D_{IT}=0·36 D_{NT}=0·32
wt% K_2O
1
2
3
4
5
6


0·9
CP
0·5
I
N
T
wt% TiO_2
3
4
5
6


0·9
CP
0·5
I
N
T
D_{IT}=0·36 D_{NT}=0·32
wt% P_2O_5
1
2


0·9
CP
0·5
N
I
T
wt% MnO
0·1
0·2
0·3
0·4
0·5

zones in the distribution of some of the elements. If these differences are not due to a defective sampling plan but reflect differences in the chemistry of the basic rocks in the three zones, then they carry important implications about the evolution of the Gardar province.

5.2.2. Kolmogorov-Smirnov Test.

The hypothesis of two independent samples being drawn from the same population can be tested by the Kolmogorov-Smirnov two sample test (see Siegel 1956 p.127 for a full description). The difference in the cumulative frequency distribution of the two samples is measured, and the probability of that difference occurring if the two samples are drawn from the same population tested. If the probability is small, then that hypothesis can be rejected at the chosen level of significance, ie. the samples are drawn from different populations. The test of significance can be chosen to determine that the values for one sample are 'larger' than the values for the other sample (a one - tailed test of significance), or simply to determine that they are different, without specifying the direction.

Figures 5.2 a to c show no significant differences in the distribution of SiO_2, CaO, FeO, TiO_2 and MnO in the three zones, but there are differences in the distributions of MgO, Al_2O_3, Na_2O, K_2O, P_2O_5 and DI. The Tugtutoq sample has significantly lower MgO and DI than the Ivigtut sample, higher K_2O and P_2O_5 than both Ivigtut and Nunarssuit and lower Al_2O_3 than the Nunarssuit sample. Ivigtut and

Nunarssuit differ significantly only in the Na_2O content, which is higher in the Nunarssuit sample.

The differences in the Tugtutoq sample appear to imply a greater incidence of more evolved magmas there. Assuming that the observed differences are not due to inadequate sampling - there is not a great variety of basic rocks in the Tugtutoq zone, so the analysed specimens are probably representative of the dykes from this zone - the differences may be linked with the fact that rocks in the Tugtutoq zone are exposed at a higher level than those in the Nunarssuit and Ivigtut zones (Upton, 1974). The apparently greater incidence of evolved magmas may thus relate to the level of exposure. There was a gap of some 60 my between the intrusion of the dykes in the Ivigtut and Tugtutoq zones (van Breemen and Upton, 1972), which may also be a significant factor.

5.2.3 Correlation Coefficients

A correlation matrix for the basic dykes is presented in table 5.1. Because of the constant sum effect strong negative correlations may not be as significant as they appear. Notable strong positive correlation exists between MgO and both Al_2O_3 and CaO; between K_2O, Na_2O, TiO_2 and P_2O_5 and between TiO_2 and FeO.

5.3. Variation diagrams

Variation diagrams plotting oxides versus MgO (Powers, 1955) have been chosen to display the chemical variation in the dykes. The trachydiorites have not been plotted in these diagrams because they appear to form a distinctive separate suite. They are

Table 5.1

Correlation Coefficients for Major Elements

Basic Dykes

	SiO_2	Al_2O_3	FeO*	MgO	CaO	Na_2O	K_2O	DI	TiO_2	P_2O_5	MnO
SiO_2	-	-	-.24	-.22	-	.28	-	.21	-	-	-
Al_2O_3		-	-.34	.31	-	-	-.30	-.26	-.51	-.44	-.51
FeO*			-	-	-	-	-	-	.38	.24	.47
MgO				-	.42	-.55	-.57	-.69	-.45	-.56	-.20
CaO					-	-.48	-.50	-.61	-.19	-.34	-
Na_2O						-	.37	.67	.24	.38	-
K_2O							-	.70	.45	.61	-
DI								-	.40	.57	-
TiO_2									-	.62	.25
P_2O_5										-	.25
MnO											-

FeO* = total Fe as FeO

Correlation coefficient is Kendall's Tau

described in a separate section.

The variation diagrams are presented in fig.5.3. The slight variations in chemistry between the three zones demonstrated in the previous section are not apparent on these diagrams, due to the overlap of the composition fields. Thus the rocks may have originated in a similar manner from similar parent magmas.

The distribution of the phenocryst minerals in the rocks, plotted versus MgO, is displayed in fig.5.4. Olivine and plagioclase are the principal phenocryst minerals in the dykes but tie-lines between olivine and plagioclase have not been drawn on the diagrams as this would obscure the variation trends. Inspection of the diagrams reveals the following points:

a. Al_2O_3 falls continously with falling MgO from ca. 8% MgO, consistent with a hypothesis of plagioclase fractionation. The increase in Al_2O_3 from 12% MgO to 8% MgO may indicate that plagioclase was not precipitated at that stage or that the proportion of plagioclase in the extract was less.

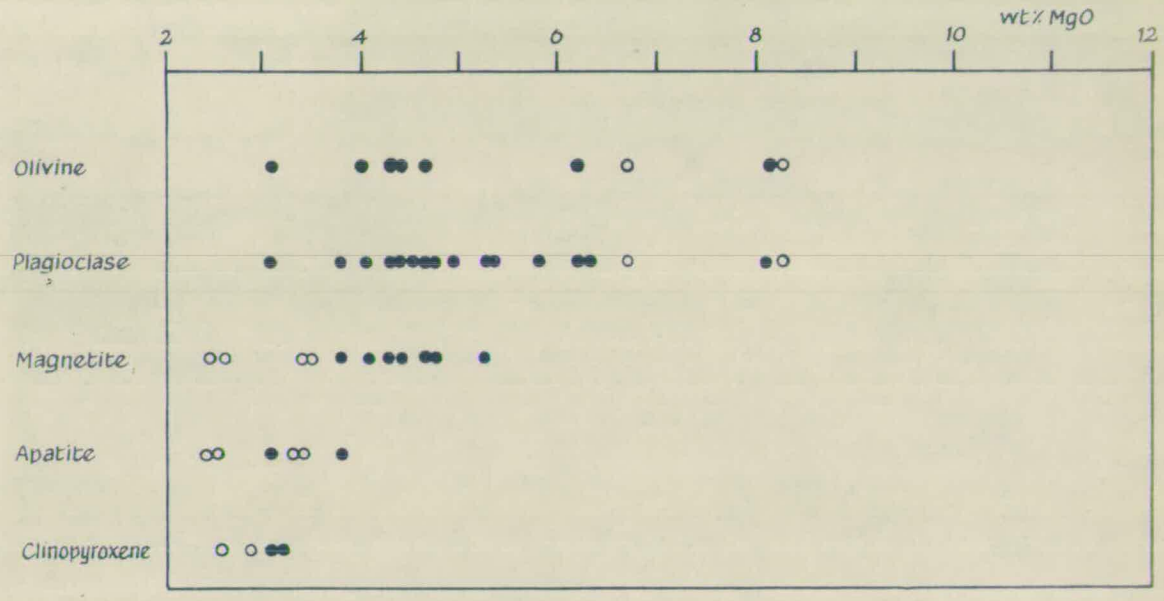
b. CaO remains approximately steady until ca.6% MgO, when it begins to decrease. Clinopyroxene phenocrysts have been found only in the more evolved trachydolerites (fig.5.4) and thus

FIGURE 5.3 (end pocket):
Major-element variation diagrams with wt% MgO as abscissa.

Filled circles: dolerites and basalts with DI less than 35.
Crosses: trachydolerites with DI in the range 35 to 50
Triangles: trachydolerites and syenogabbros with DI greater than 50.

FIGURE 5.4:
Phenocryst-distribution diagram showing phenocryst occurrence plotted vs. wt% MgO. of the rock analysis.

Filled circles: rocks from this study.
Open circles: rocks from other studies.


wt% MgO
2
4
6
8
10
12
Olivine
Plagioclase
Magnetite
Apatite
Clinopyroxene

cannot explain the variation in CaO at this stage, which may therefore depend critically on the proportion of plagioclase in the extract.

c. TiO_2 and FeO increase with falling MgO until the MgO level is between 4 and 4.5% MgO; beyond this value they begin to decrease. Titaniferous magnetite phenocrysts occur in the trachydolerites, hence at this stage the precipitation of magnetite begins to affect the composition of the residual liquids.

d. K_2O, Na_2O, P_2O_5 and SiO_2 increase sharply at approximately 4.5% MgO, coinciding with the onset of magnetite fractionation. P_2O_5 becomes highly variable but although apatite phenocrysts occur in the trachydolerites (fig.5.4), there is no obvious decrease in P_2O_5 in the compositions studied. Apatite appears to enter the phenocryst phase later than magnetite and the effect of apatite crystallisation may be noticeable only in compositions more evolved than those studied.

The variation of these oxides in the Gardar rocks thus appears consistent with a hypothesis of crystal fractionation controlling the variety of basic rock types.

In choosing to plot the oxides versus MgO it was assumed that some

of the chemical variation was controlled by an MgO rich mineral, most likely olivine. The contribution of olivine fractionation to the variation in chemistry is demonstrated in the following sections.

5.3.1.1 Olivine crystallisation

Emslie and Roeder (1970) found that since the partition of Fe^{2} and Mg^{2} between olivine and coexisting liquid is essentially independent of temperature and possibly of pressure, it may be regarded as a constant (K_D), thus:

$$K_D = \frac{X_{ol}^{FeO}}{X_{liq}^{FeO}} \cdot \frac{X_{liq}^{MgO}}{X_{ol}^{MgO}} = 0.33 \qquad \text{EQ 1}$$

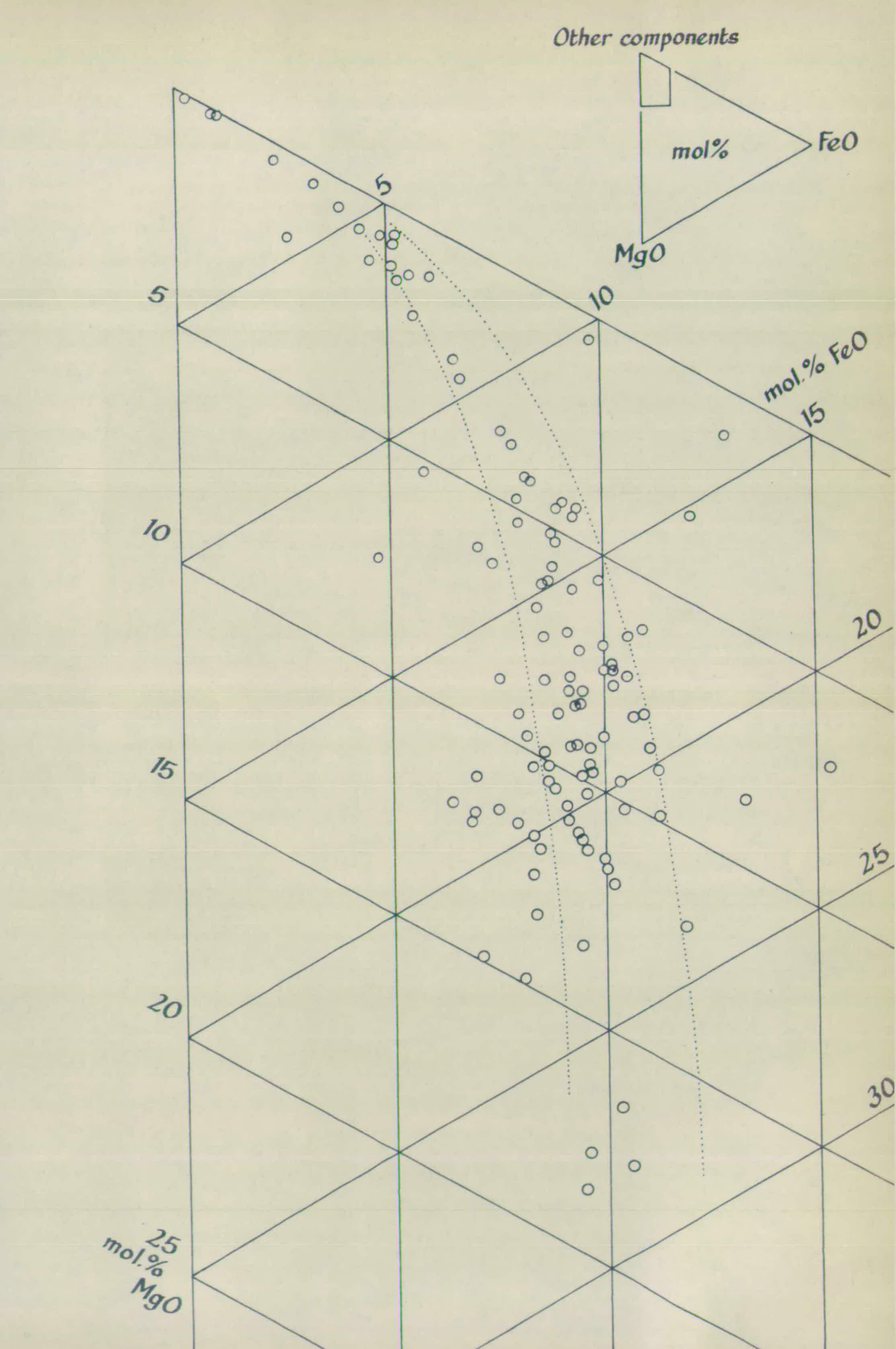
(where X = concentration in moles). The value of KD was taken from Cawthorne et al., 1973.

This implies that the fractionation of olivine can be represented by a differential equation:

$$\frac{dFeO}{dMgO} = \frac{FeO(0.33x2/3-0.33FeO-MgO)}{MgO(2/3-0.33FeO-MgO)} \qquad \text{EQ 2}$$

(R.F. Cheeney pers. comm.). This equation can be solved to give a family of curves for olivine fractionation in the system moles FeO: MgO: Rest (fig.5.5). If a suite of rocks plotted in this system falls along one of these curves, then olivine fractionation has been involved in the evolution of that suite and has been the

FIGURE 5.5:
Gardar rocks plotted with respect to two solutions to EQ 2, p. 71, shown as dotted lines.


Other components
mol%
FeO
MgO
5
10
15
20
25
30
mol.% FeO
mol.% MgO

only ferromagnesian mineral to affect it. Fractionation of an other ferromagnesian mineral having different FeO/ MgO ratio, and a different crystal/liquid distribution coefficient would produce residual liquids along a different path. The Gardar rocks plotted in fig.5.5 lie along olivine fractionation curves, agreeing with the hypothesis of olivine fractionation controlling the variation in iron and magnesium in the dykes. The composition of the olivine precipitating from the most primitive liquids can be predicted by Emslie and Roeder's method and is Fo 80 to Fo 75; olivine phenocrysts with the composition Fo 75 have been found in one dyke, while olivines from anorthosite xenoliths range from Fo 73 to Fo 62. The olivine is more iron rich than the liquid, so residual liquids should be depleted in iron; the F.M. A. diagram fig.5.8 shows iron enrichment in the early stages which can only be produced if the fractionating assemblage contains less iron than the liquid, hence a non iron-bearing mineral must be precipitating together with the olivine.

5.3.1.2 Extract calculations.

Traditional extract calculations depend on a linear relationship between the extract or additive and the suite of rocks. If the composition of the extract changes continuously with changing liquid composition, as when solid solution series minerals precipitate, then the path taken by residual liquids is not linear. The path of residuals in this system can be approximated if the change in liquid composition during a short time interval is considered. See fig.5.6a. Extract of composition C_1 is fractionating

from a liquid composition L_1; after a time the liquid composition is L_2, the extract C_2, and so on. Providing the time interval is sufficiently short, the calculated liquid compositions lie on a curved path.

A computer programme was written to carry out these calculations, using the most primitive dyke compositions as starting liquid. The results are shown in fig.5.6(b). Removal of olivine plus plagioclase in varying amounts is capable of producing the major element variation in the dyke rocks down to approximately 5% MgO, where magnetite must be added to the extract. From 8% MgO to 5% MgO the proportions of olivine to plagioclase in the extract are approximately 30:70, while the few rocks containing more than 8% MgO may be related to those with 8% MgO by removal of an extract containing 55 to 100% olivine. The variation in K_2O content of the rocks is not explained by the fractionation scheme. The majority of the little-differentiated rocks have low K_2O contents, ca.0.5%, but some have considerably higher levels of K_2O, ca.1%. It is not possible to derive these K_2O-rich doleritic rocks by fractionation of the observed phenocryst minerals from the K_2O-poor doleritic rocks.

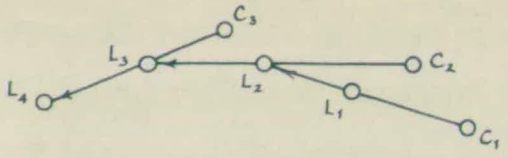
Fractionation of olivine plus plagioclase from both the K_2O rich and the K_2O poor compositions can give the range of K_2O compositions found in the Gardar rocks. Thus it appears that there is an initial variation in K_2O in the parental Gardar magmas which cannot be explained in terms of low pressure crystal fractionation. This will be discussed in a later section.

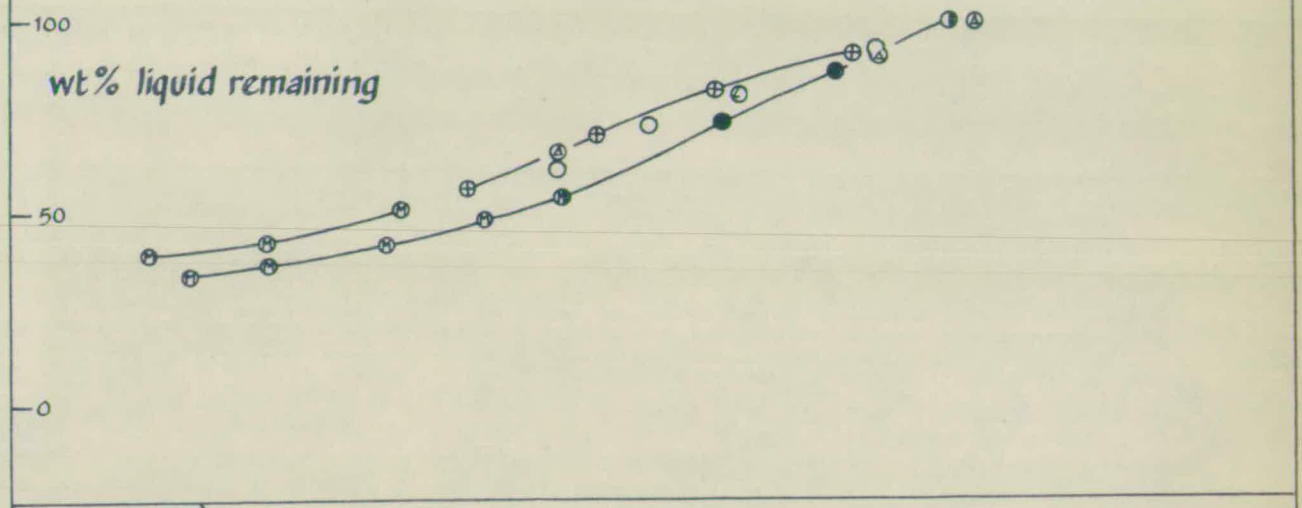
FIGURE 5.6a (small diagram at head of page):
Illustrating the finite-elememt method of solving the partial differential equations describing generalised fractional crystallisation. See text for brief explanation.

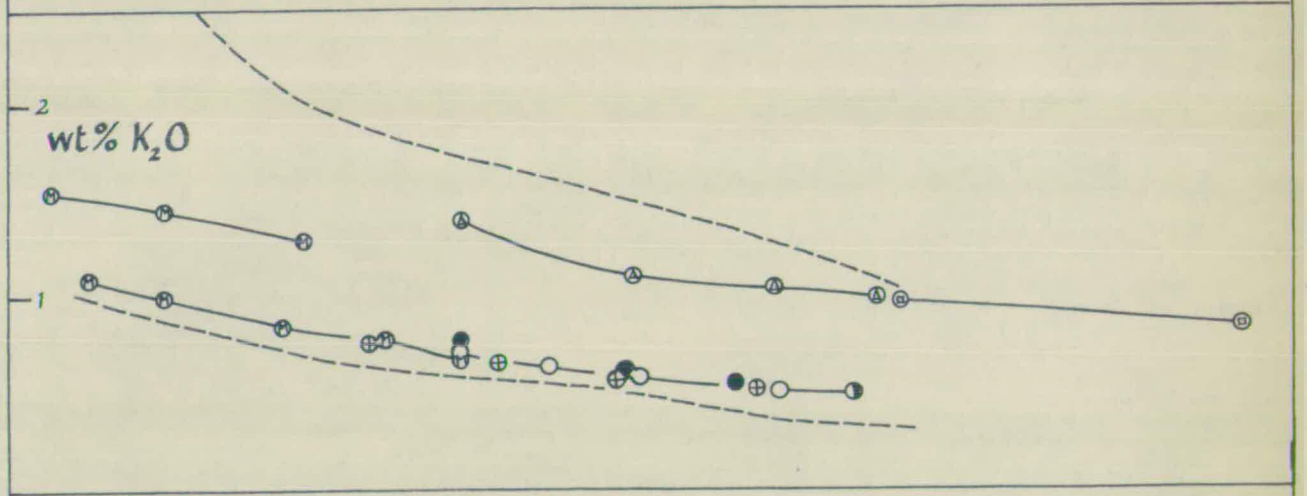
FIGURE 5.6b (extending over two pages):
A set of solutions to the above equations, illustrating variation in composition of liquids due to fractional crystallisation as a function of wt% MgO in the residual liquid.

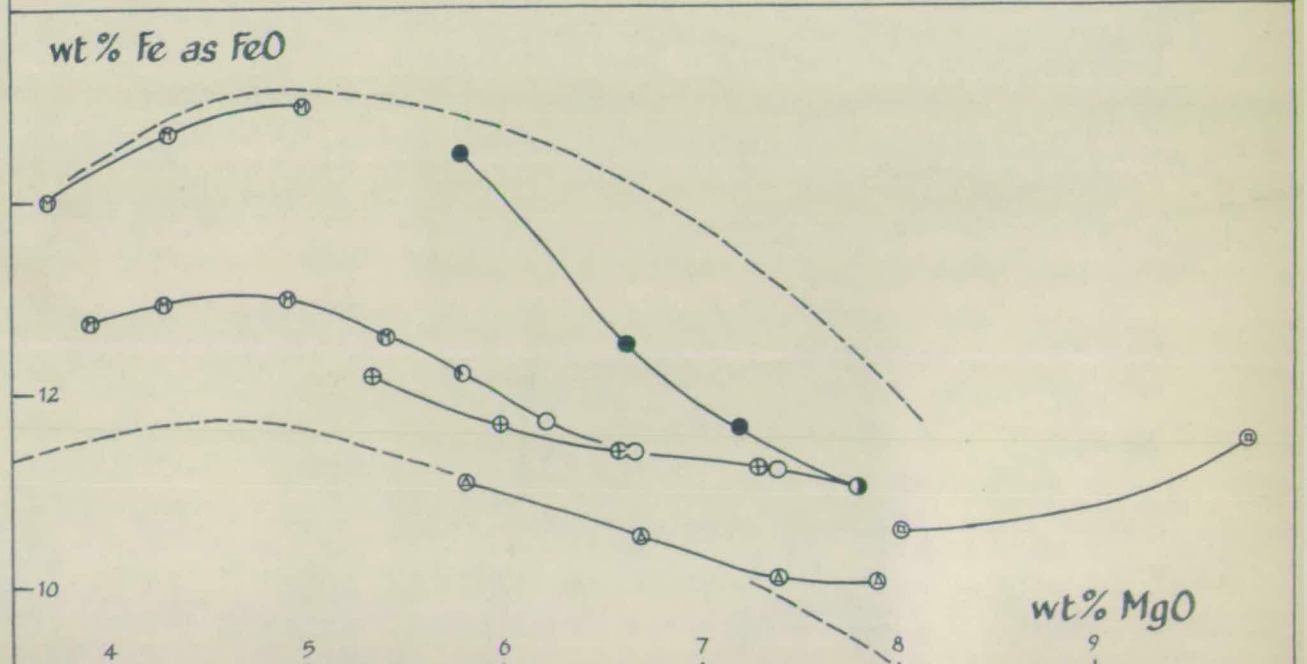
Circled square: fractionation of olivine only.
Circled 'M': fractionation of magnetite, plagioclase and olivine.
Remaining symbols: fractionation of plagioclase and olivine.

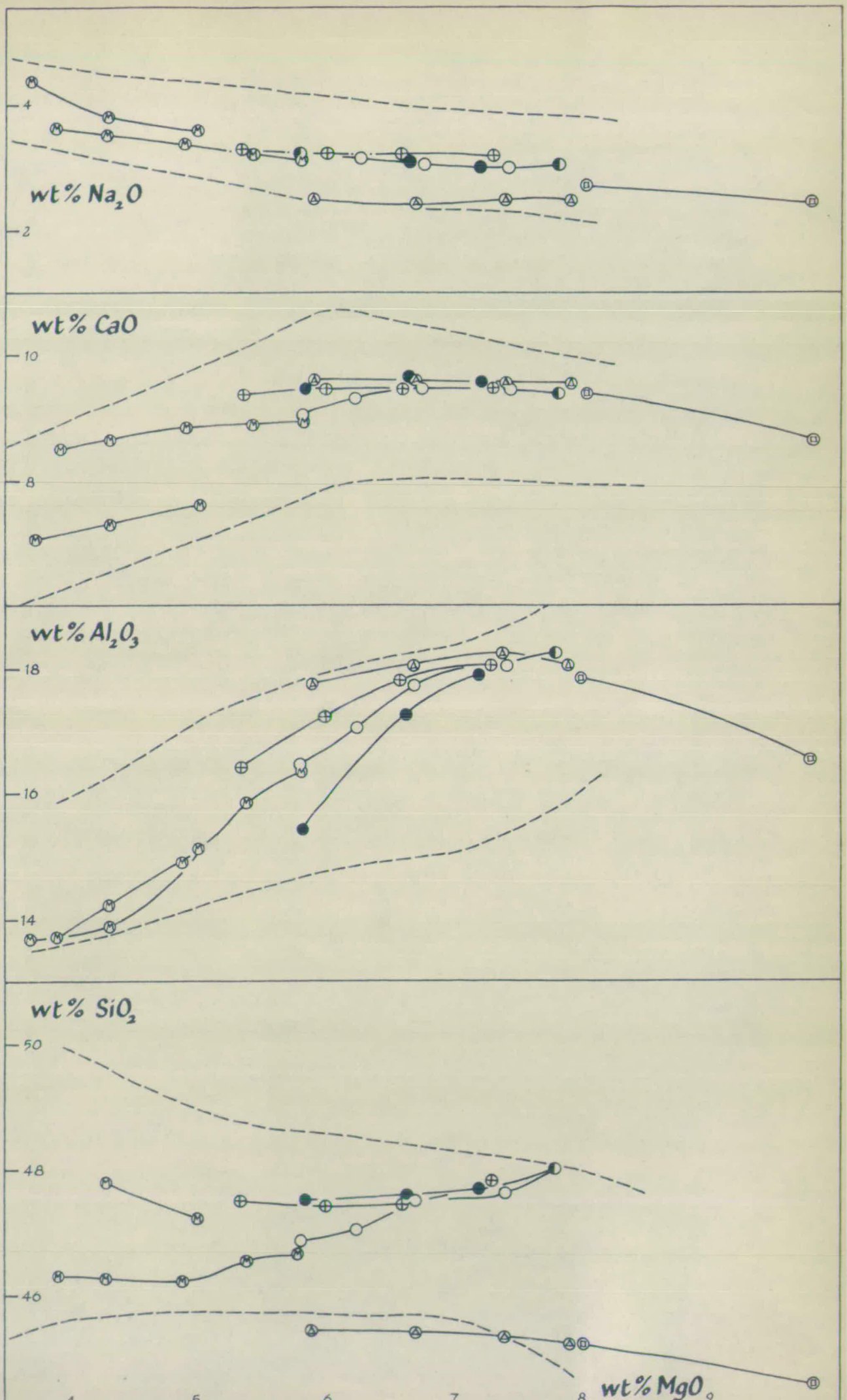
The pecked lines show the compositional limits of the Gardar dyke-rocks.


C3
L3
C2
L4
L2
L1
C1


100
wt% liquid remaining
50
0


2
wt% K2O
1


wt% Fe as FeO
12
10
wt% MgO
4
5
6
7
8
9


wt% Na_2O
4
2
wt% CaO
10
8
wt% Al_2O_3
18
16
14
wt% SiO_2
50
48
46
wt% MgO

It has been proposed (Bridgwater and Harry, 1968) that the feldspathic inclusions crystallized from the Gardar magmas at an early stage and the large proportion of plagioclase in most of the extract provides a ready source for the formation of the anorthosite. The relative amounts of olivine and plagioclase may also explain the lack of ultramafic inclusions in the Gardar rocks.

The density contrast between plagioclase and basaltic liquids at liquidus temperatures is small, andesine-labradorite having a density of 2.63 g/cc, labradorite-bytownite a density of 2.67 g/cc (Martignole, 1974). Bottinga and Weill (1970) have suggested that iron enrichment during differentiation increases the density of the magmas and that plagioclase flotation is therefore possible. Enrichment in H_2O in the residual liquids, however, would decrease the density.

The density of some of the Gardar magmas has been calculated, using a computer programme written by W. Boyd, and the results are shown in table 5.2. There is no obvious increase in density in the trachydolerites, which are iron-enriched, but this may relate to the H_2O content of the rocks.

The densities of the magmas between 5 and 10kb which may approximate to the pressure of formation of the anorthosites, vary from 2.57 to 2.66 g/cc. The density of the anorthosite plagioclase (An 56 to An 61) is approximately 2.64 g/cc, thus plagioclase flotation is a possibility. Bridgwater and Harry (1968) report

Explanation of table 5.2.

Calculated densities are given for pressures varying from atmospheric pressure up to 10 kilobars. For each specimen the top line gives the density at 1200°C, the second line the density at 1150°C.

The specimens are classified as D = dolerite or TD = trachydolerite.

Table 5.2

Density of Gardar Magmas

Specimen No.	At.Press.	1KB	2KB	5KB	10KB	Fe as FeO
101413	2.644	2.623	2.629	2.642	2.655	2.664
D	2.652	2.631	2.637	2.650	2.663	2.673
101407	2.660	2.594	2.600	2.613	2.625	2.661
D	2.668	2.603	2.609	2.621	2.634	2.669
101426	2.635	2.591	2.597	2.610	2.623	2.652
D	2.643	2.599	2.605	2.618	2.630	2.660
101419	2.613	2.587	2.593	2.606	2.618	2.626
D	2.621	2.595	2.601	2.614	2.626	2.634
101393	2.643	2.591	2.597	2.610	2.623	2.647
D	2.651	2.600	2.606	2.619	2.631	2.655
20632	2.578	2.626	2.632	2.646	2.653	2.589
D	2.588	2.635	2.642	2.655	2.668	2.599
40452	2.715	2.663	2.669	2.683	2.696	2.725
OB	2.724	2.672	2.678	2.692	2.705	2.733
121301	2.711	2.646	2.652	2.666	2.679	2.722
D	2.720	2.655	2.662	2.675	2.688	2.731
101469	2.620	2.607	2.613	2.626	2.639	2.632
TD	2.628	2.615	2.621	2.634	2.646	2.640
101375	2.588	2.549	2.555	2.568	2.580	2.600
TD	2.595	2.557	2.563	2.575	2.587	2.608
101412	2.625	2.602	2.608	2.621	2.634	2.646
TD	2.634	2.610	2.616	2.629	2.642	2.655
101277	2.546	2.585	2.591	2.604	2.617	2.564
TD	2.555	2.593	2.599	2.612	2.624	2.573
101356	2.603	2.585	2.591	2.604	2.616	2.614
TD	2.611	2.593	2.599	2.612	2.624	2.622
101408	2.622	2.601	2.607	2.620	2.632	2.639
TD	2.630	2.608	2.614	2.627	2.640	2.647

Specimen No.	At.Press.	1KB	2KB	5KB	10KB	Fe as FeO
101415	2.633	2.616	2.622	2.635	2.648	2.650
TD	2.641	2.624	2.630	2.643	2.656	2.659

that the anorthosites have textures suggesting the feldspars floated in the magmas from which they crystallised.

However textures in the layered Assorutit anorthosite demonstrate that plagioclase sank in the liquid (Upton, 1964). In view of the high Al_2O_3 contents of the compositions at 8% MgO (up to 19% Al_2O_3), it is possible that plagioclase was on the liquidus at that stage, and the anorthosites could equally well be a bottom accumulate from a liquid precipitating predominantly plagioclase. The density data is not conclusive.

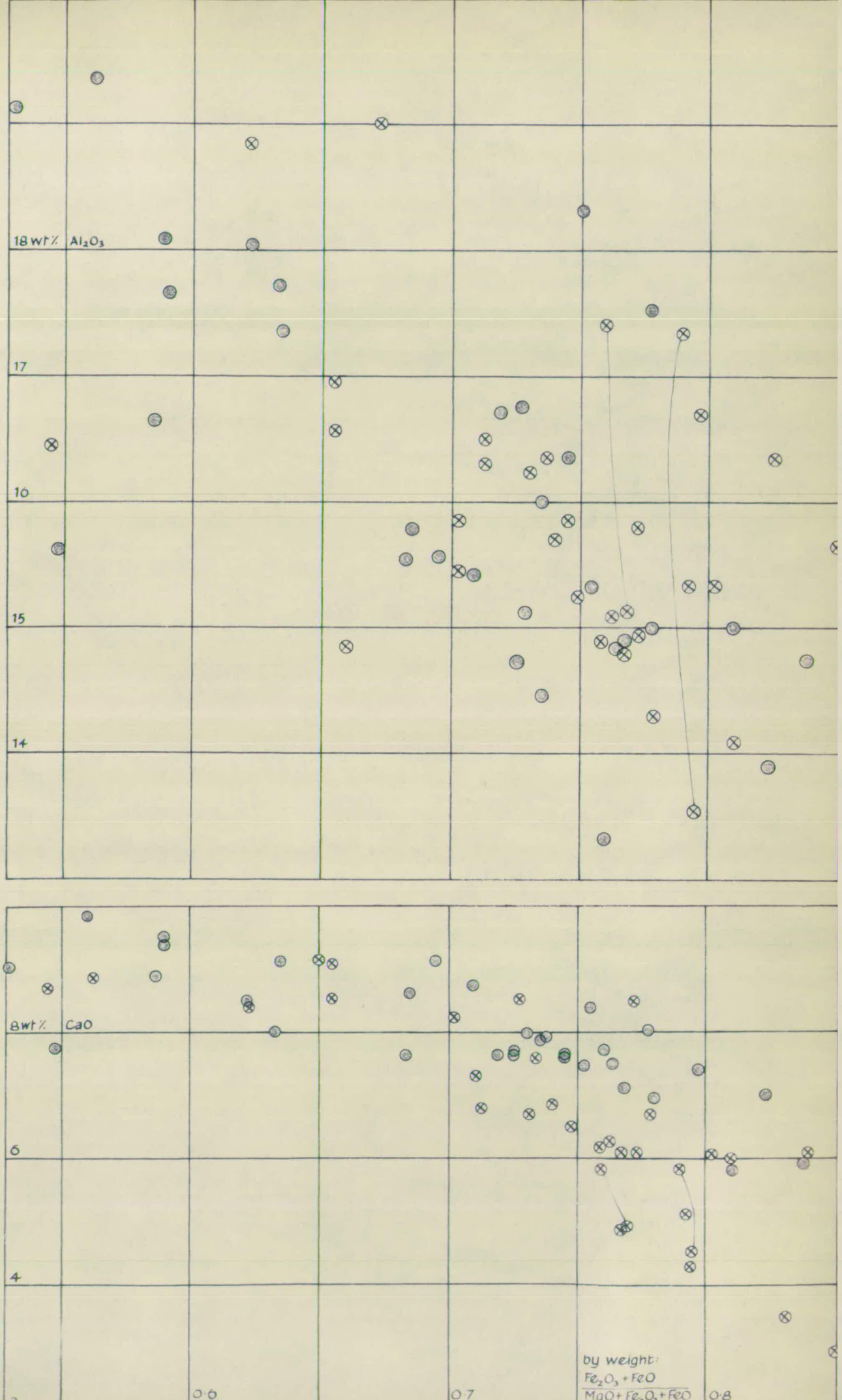
In their study of the composite BFD dykes, Bridgwater and Harry (1968) noted that the CaO contents of these dykes appeared to be lower at the same level of differentiation than in dykes which did not contain inclusions. They thought this could be due to the early formation of labradoritic magacrysts. A plot of CaO vs the iron/magnesium ratio (fig.5.7) for BFD and non-BFD dykes shows the CaO contents differ in the later stages. Use of the Kolmogorov-Smirnov test showed that in the dykes with iron/magnesium ratio greater than .70, the BFD dykes contain significantly less CaO than the non-BFD dykes.

The Al_2O_3 contents of the dykes did not show similar differences, although this may be partly due to the greater variation of Al_2O_3 contents in all the dykes compared with the narrow range of CaO. The two analyses of host rock plus included feldspar have higher

FIGURE 5.7:
The calcium and aluminium contents of BFD and non-BFD dykes with a function of FeO and Fe_2O_3 and MgO as abscissa.

Filled circles: non-BFD dykes.
Circled crosses: BFD dykes.

Lines connect pairs of analyses corrected and uncorrected for the content of plagioclase phenocrysts.


18 wt% Al_2O_3
17
10
15
14
8 wt% CaO
6
4
0·6
0·7
by weight:
$\frac{Fe_2O_3 + FeO}{MgO + Fe_2O_3 + FeO}$
0·8

Al_2O_3 contents than the non-BFD dykes, but the CaO contents are still lower than in the non-BFD dykes. This may suggest that the low CaO contents of the BFD dykes is not wholly due to the early crystallisation of plagioclase.

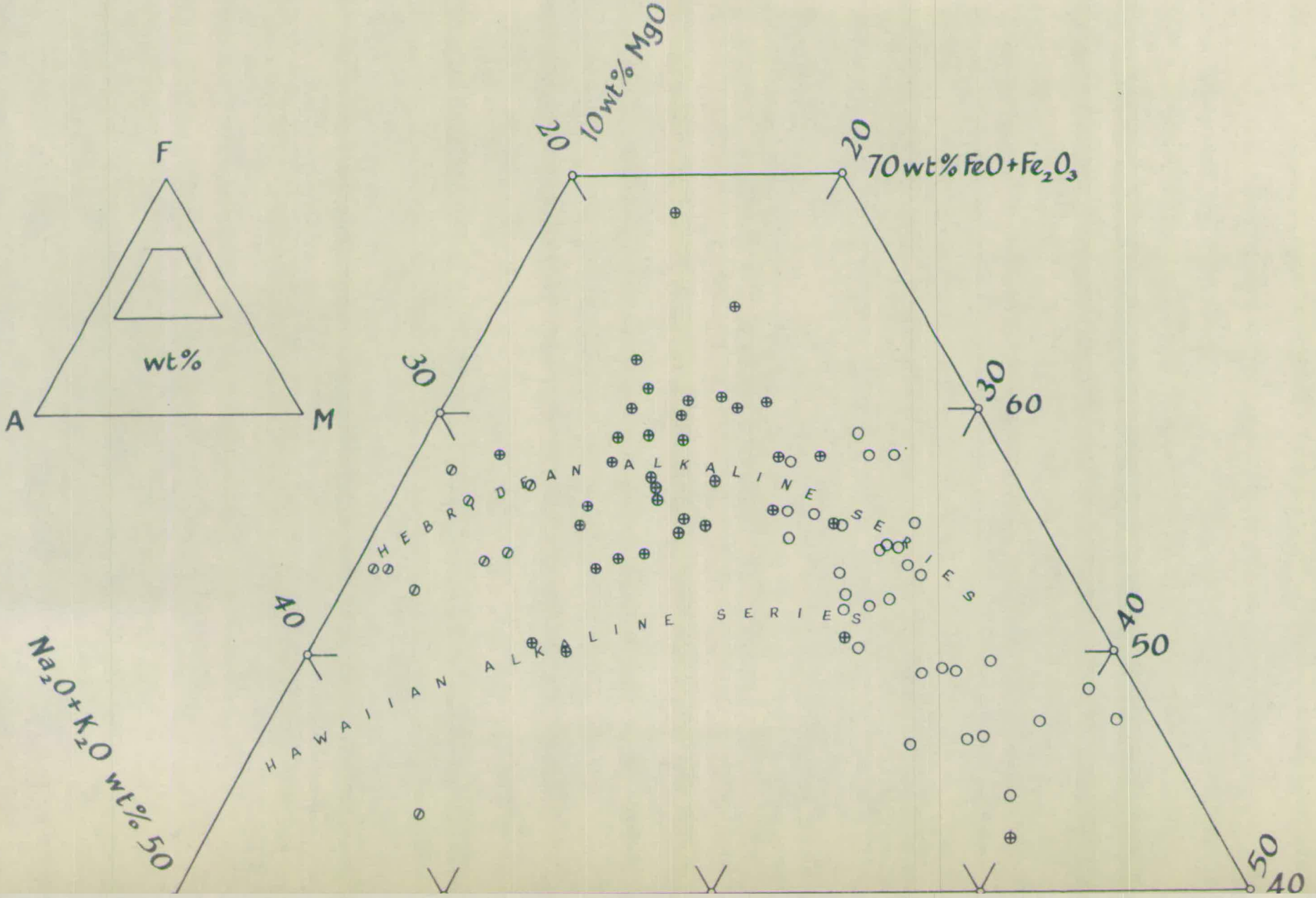
Clinopyroxene phenocrysts appear at a later stage than the onset of low-calcium dykes, so the differences cannot be attributed to variation in clinopyroxene fractionation at low pressures. It is conceivable that the liquids which gave rise to the BFD's suffered a period of aluminous clinopyroxene fractionation at higher pressures (approximately 10kb), increasing the Al_2O_3 content and decreasing the CaO content of the liquid. The problem here is that the basic members of the two series do not differ in CaO and Al_2O_3 content and there is no way by which the intermediate members of the BFD series can be derived from the basic members by fractionation of aluminous clinopyroxene. A possible solution is that if only minor amounts of cpx fractionation occurred the decrease in CaO content and increase in Al_2O_3 content might not be obvious at the basic end, but might be enhanced by olivine plus plagioclase fractionation, particularly if more plagioclase could be fractionated because of increased Al_2O_3.

5.4 FMA diagram (fig.5.8)

The Gardar rocks differentiated with moderate iron enrichment in the intermediate stages, followed by alkali enrichment. The oxidation ratios of the basic rocks are very low (ca.0.12 - 0.18) and Upton (1965) has pointed out the reduced nature of the magmas. Low initial fO_2 in the magma leads to iron enrichment in the late stages (Hamilton and Anderson, 1967; Kennedy, 1955). The decrease in iron

FIGURE 5.8:
F-M-A diagram.

Open circles: basaltic compositions.
Circled crosses: trachydolerites with DI less than 50.
Circles with diagonals: trachydolerites with DI over 50.


F
wt%
A
M
10wt% MgO
70wt% FeO+Fe2O3
Na2O+K2O wt%
HAWAIIAN ALKALINE SERIES
HEBRIDEAN ALKALINE SERIES
20
30
40
50
60

after the intermediate stages may imply an increase in fO_2, or simply that the liquid became saturated in the components of Fe-Ti minerals.

5.5 CIPW norms

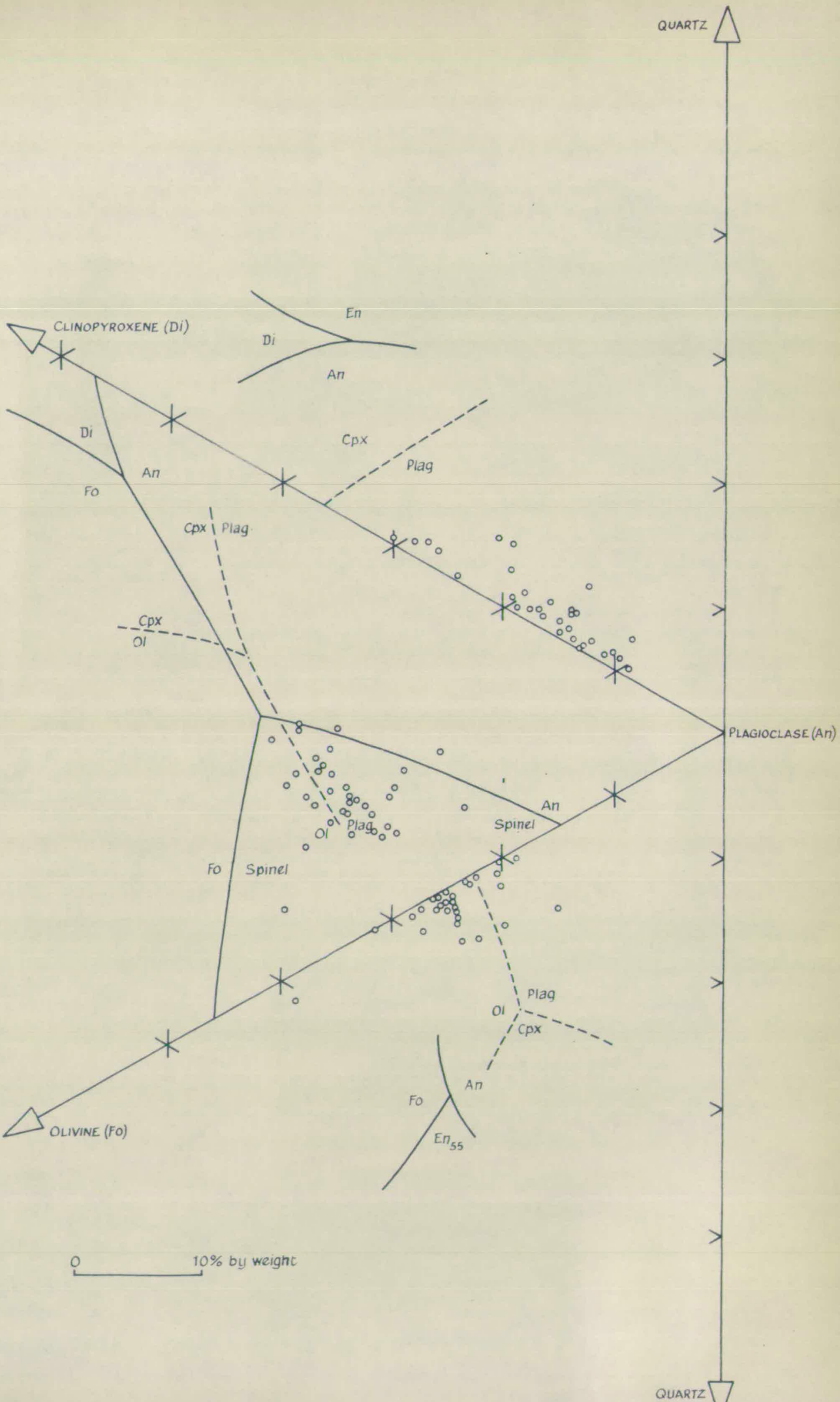
Norms for the dykes are presented in the appendix. To offset the effect of alteration on the norms the Fe_2O_3/FeO ratios were reduced as described in chapter 3. The rocks are critically undersaturated, rarely containing more than 2% nepheline or 6% hypersthene in the norm, and retain this character during evolution to the mugearite stage. Only in the late syenite-trachyte stage do the rocks become highly under - or oversaturated.

5.5.1 Projections in the 'Simple Basalt Tetrahedron'

The compositions in which the normative minerals qz + ol + cpx + plag + ne make up more than 80% of the total normative content of the rocks were plotted in the expanded 'normative basalt tetrahedron' fig.5.9 (see O'Hara 1965). The 1 atmosphere dry cotectics of the synthetic system silica-forsterite-diopside-anorthite and of the natural system qz-ol-cpx-plag are marked (cotectics taken from Clarke 1970). The Gardar rocks plot close to the plag apex on either side of the plane cpx-ol-plag, the plane of critical silica undersaturation which approximates to a thermal divide at low pressure (O'Hara 1968). Evolution produces both undersaturated and oversaturated residua and as evolution through the thermal divide can

FIGURE 5.9:
Projections in the normative basalt tetrahedron: from top to bottom, the olivine, quartz and clinopyroxene projections respectively.

Cotectics from Clarke, 1970, are for 1 atmosphere pressure.
Solid: the synthetic system silica-forsterite-anorthite-diopside.
Pecked: the natural system quartz-olivine-plagioclase-clinopyroxene.


QUARTZ
CLINOPYROXENE (Di)
En
Di
An
Di
An
Fo
Cpx
Plag
Cpx
Plag
Cpx
Ol
PLAGIOCLASE (An)
An
Spinel
Ol
Plag
Fo
Spinel
Plag
Ol
Cpx
An
Fo
En_{55}
OLIVINE (Fo)
0
10% by weight
QUARTZ

only readily take place at pressures above 8kb. (O'Hara 1968) if the basalts are considered to be derived from the same parent magma, then their position relative to the divide must be inherited from higher pressure.

Since the rocks plot in or near the plane cpx-ol plag projections from ne or qz into this plane will cause the least distortion and therefore will be most informative on the 1 atmosphere phase relations. Projections from plagioclase cause too much distortion and will not be used.

a. Quartz projection fig.5.9

Most points lie along the natural system ol-plag cotectic, ie. the locus of liquids in equilibrium with olivine and plagioclase, agreeing with the deduced order of crystallisation in the dykes.

b. Olivine projection

The points form a narrow band along the plag-cpx edge due to projection of the trend along the ol-plag cotectic.

c. Clinopyroxene projection

The cotectic boundaries are nearly vertical in this projection and all the points lie below the clinopyroxene primary phase volume. They project in a narrow band along the olivine-plagioclase edge, being more clustered than in the olivine projection due to projection down the ol-plag cotectic. The thickest cluster of points lies midway between the synthetic and natural cotetic boundaries, and is probably the true position of the

ol-plag cotectic for the Gardar rocks.

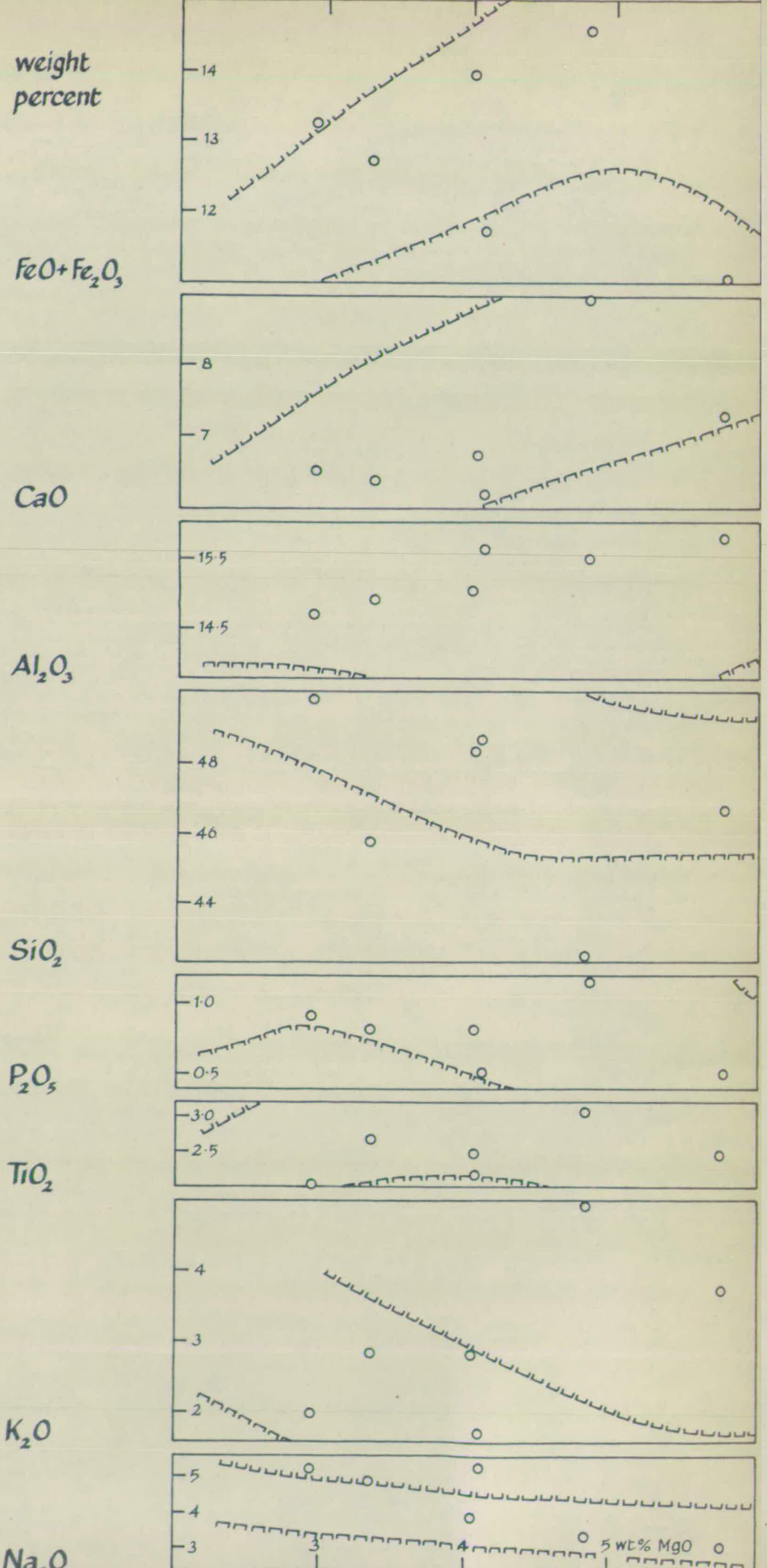
Projections in the natural basalt tetrahedron demonstrate that the basaltic rocks are controlled by low-pressure olivine - plagioclase equilibria, agreeing with evidence from the simple oxide variation diagrams.

5.6. The trachydiorites

The trachydiorites are banded, the banding displaying sharp outer edges grading in towards the centre (Upton, pers.comm.), which suggests that the dykes formed from several pulses of magma, although no internal chills were noted. The central unit of one such dyke (101313) is more magnesian than the chilled margin (101312), indicating, as in the case of the BFD's, the presence of a compositionally zoned magma chamber prior to intrusion. This situation may not be true of all trachydiorite dykes however, and more specimens are required from each dyke to be certain on this point. Three or more phenocryst species (andesine + altered olivine + magnetite ± clinopyroxene ± apatite ± corroded kaersutite) may occur in the dykes, thus crystal fractionation must be considered as a mechanism of differentiation.

Kaersutite occurs in a variety of alkaline basic and intermediate rocks and frequently displays evidence of resorbtion and breakdown, attributable to its instability upon decrease of water pressure and probably a concomitant rise in temperature, during ascent to a high crustal environment (Coombes and Wilkinson, 1969; Wilkinson, 1974).

FIGURE 5.10:
Variation diagrams of the major elements in the trachydiorites. Wt% MgO as abscissa. Lines of buckets show the limits of the composition field for the dolerite-series rocks.


weight percent
FeO+Fe2O3
14
13
12
CaO
8
7
Al2O3
15·5
14·5
SiO2
48
46
44
P2O5
1·0
0·5
TiO2
3·0
2·5
K2O
4
3
2
Na2O
5
4
3
3
4
5 wt% MgO

Aoki (1970) reported the presence of xenoliths containing kaersutite and kaersutite magacrysts, associated with aluminous clinopyroxenes, calcic plagioclase and magnetite, in alkaline lavas on Iki island, Japan. He suggested, on the basis of the Al_2O_3 content of the pyroxene, that these minerals crystallised from a hydrous alkali basaltic magma at depths of 25 to 30 km (approximately 10kb). Le Maitre (1969) considered gabbroic xenoliths containing kaersutite in the lavas of Tristan da Cunah to have formed at pressures between 1.5 and 6kb.

That the kaersutite in the trachydiorites is unstable in its present environment is shown by the corrosion rim of pyroxene, plagioclase and ore minerals. The pressure of formation of the kaersutite may have been greater than approximately 2 kb (Holloway and Burnham, 1972), with p_{H_2O} less than p_{tot} due to the CO_2 content of the magma.

Aluminous clinopyroxene and calcic plagioclase, which are often reported in association with kaersutite, have not so far been identified in the trachydiorites. The clinopyroxene phenocryst occurring in the specimen containing kaersutite is also not in equilibrium with the magma, but is not particularly aluminous, with only 3.6% Al_2O_3 and therefore probably formed at comparatively low pressures. The plagioclase phenocrysts present are andesine, whereas

the plagioclase crystallising under high p_{H_2O} might be expected to be more calcic, labradorite or bytownite (Green and Ringwood, 1967a). Thus there is little evidence on the pressure of formation of the kaersutite. The effect of any high pressure fractionation episode is difficult to assess in the relatively few specimens available, but may well have been minor; the TiO_2 content of the rocks shows little decrease in the compositions studied.

Chemically the trachydiorites are generally similar to the dolerite/trachydolerite series rocks, except in their high content of H_2O, CO_2 and alkalis, and in most variation diagrams plot within the trachydolerite field (fig.5.10) They are all nepheline normative with between 2 and 8% nepheline in the norm. The sample is small, (6 specimens), but significant correlations exist between certain of the oxides: Al_2O_3 has a positive correlation with MgO (coefficient = 0.87, probability = 0.008), Na_2O has a negative correlation with MgO (coefficient = -0.6, probability = 0.068) and K_2O has a negative correlation with Na_2O (coefficient = -0.87).

The variation in Al_2O_3 could be explained by the fractionation of the observed phenocrysts but the relationship between Na_2O and K_2O cannot. Fractionation or possibly the resorbtion of kaersutite cannot explain the variation since it contains only 1.5% K_2O compared with between 1.7 and 3.7% in the trachydiorites, and the TiO_2 content of the trachydiorites does not vary sympathetically with K_2O.

There is no evidence, in the specimens examined, for the crystallisation and fractionation of a K_2O rich mineral, which could explain the

variation in K_2O and Na_2O. If crystal fractionation is to appealed to, any such mineral must be completely lost by fractionation or resorbtion.

In a magma column of considerable vertical extent, the minerals crystallising near the top of the chamber would not be in equilibrium with the magma at lower levels, because of temperature and pressure differences and, if they sank, would react with the magma and be resorbed. This is a process whereby compositional zoning in the column may be produced or enhanced, but the effects might be confined to a relatively narrow chamber where convective mixing would be inhibited. It might therefore be possible for a mineral such as alkali feldspar to crystallise in the higher levels of the column and be resorbed in the lower levels, thus increasing the K_2O content of the magma at depth. This is not a satisfactory mechanism for producing the compositional variation in the trachydiorites, however, since alkali feldspar does not crystallise early in the compositions examined, and it must therefore be postulated that the compositions capable of crystallising alkali feldspar existed at a higher level than is now seen, and also that the feldspar was completely resorbed in the lower levels.

The mechanism of fractional melting, proposed by Yoder (1973) to account for the association in composite intrusions and flows of compositionally dissimilar magmas, which cannot be related by fractional crystallisation, does not produce intermediary magma types. Therefore modification of the initial compositions by mechanisms such as crystal fractionation or diffusion would be necessary prior

to intrusion to produce the compositional variation in the trachydiorites.

It appears that the alkali content of a magma may be altered by a number of processes. Saether (1948) and Kennedy (1955) considered that in response to pressure and temperature gradients within a magma, alkalis and volatiles would diffuse to the higher parts of the magma chamber. Experimental work by Burnham (1967) and Jahns and Burnham (1969) did not find diffusion to occur in geologically realistic times and they favoured the transport of alkalis through separation of a vapour phase. Alkalis, in particular Na_2O, are enriched in the aqueous vapour in equilibrium with granitic melts (Luth and Tuttle, 1969), thus the separation of a vapour phase would be capable of changing the K/Na ratio in the magma. However Kogarko (1974) has shown that water and volatiles are more soluble in alkaline and peralkaline melts and thus a water - rich phase might not separate. In these cases Kogarko et al. (1974) believe that alkali diffusion could be an important process.

The presence of ocelli in the trachydiorites demonstrates the presence of a separate fluid phase, which appears to have been CO_2 rich as well as water-rich. CO_2 is more soluble in basic melts than acid melts, and more will dissolve in hydrous melts (Eggler, 1973) but if a vapour phase is present CO_2 will preferentially enter the vapour phase.

The effect of CO_2 in an aqueous fluid coexisting with granitic liquids

is to decrease the concentration of alkalis in the fluid phase (Burnham, 1967), hence it appears that transfer of the alkalis in the trachydiorites may not have proceeded through the vapour phase. Alkali diffusion within the magma remains a possible mechanism, however; diffusion rates within the magma are influenced by the ionic size (Carmichael et al., 1974) and hence Na should be enriched over K in the lower temperature and pressure regions of the magma column. If the ascent of the trachydiorite magma was comparatively slow, diffusion might be expected to be more effective than during rapid ascent.

Alteration of the alkali contents of the magma by alkali-ion exchange or loss of the vapour phase on crystallisation has been proposed in compositionally more-evolved peralkaline dykes by Macdonald (1969). Loss of a vapour phase, however, should preferentially remove Na_2O.

If alkali diffusion occurred, relatively rapid rates of diffusion are thus implied by the alkali contents of the dykes. This is not an entirely satisfactory mechanism for producing the variation in K_2O and Na_2O in the trachydiorites, but lacking evidence for the fractionation of a K_2O-rich phase, diffusion remains a possible mechanism.

6. Trace-element chemistry

6.1. Statistical treatment

Figure 6.1 shows the distribution of 8 selected trace elements in the basic dykes from the three dyke zones. The cumulative proportion diagrams reveal the following points.

a. Many of the distributions are positively skewed (ie. the longer tail of the variate lies towards the higher values). This is particularly noticeable for Rb, Ba, Sr, Ni and Cr, although the long 'tail' in the Rb and Sr diagrams are produced by a small number of unusually high values.

b. There are significant differences in the distribution of some trace elements between the three zones, these differences appearing in Ba, Sr, Zr, Ni and Cr.

The Tugtutoq sample has significantly higher levels of Sr and lower levels of Ni than both the Ivigtut and the Nunarssuit samples, higher Ba and Zr than the Nunarssuit sample and lower Cr than the Ivigtut sample. The differences are not thought to be due to inadequate sampling, for the reasons explained in chapter 5. The observed differences are such as to imply a higher incidence of evolved magmas in the Tugtutoq zone.

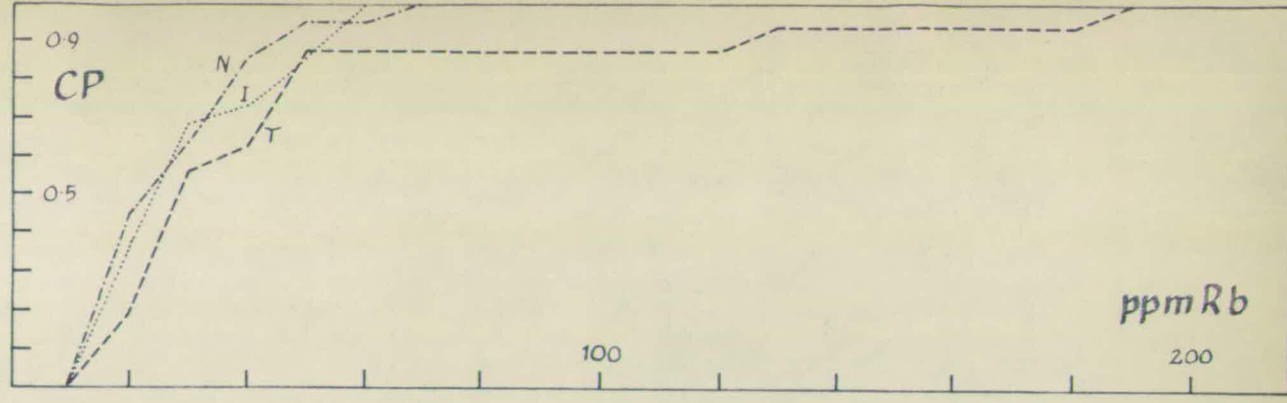
6.1.1 Correlation Coefficients

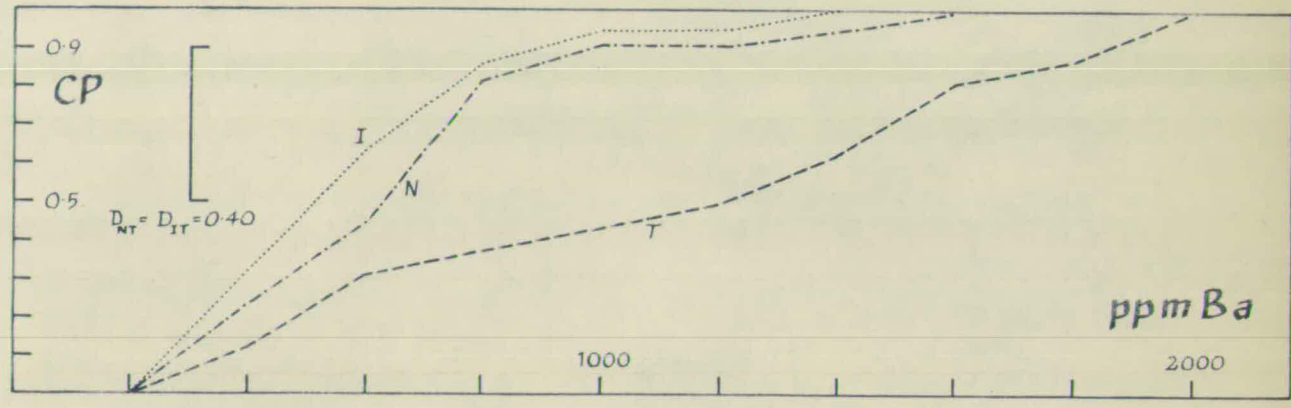
A correlation matrix for the trace elements has been computed and is presented in table 6.1. The coherence of Ba, Zr, Yt, Sr and Rb, and of K_2O, TiO_2, and P_2O_5 with these trace elements and each other (see also table 5.2) is notable. The coherence of this group of

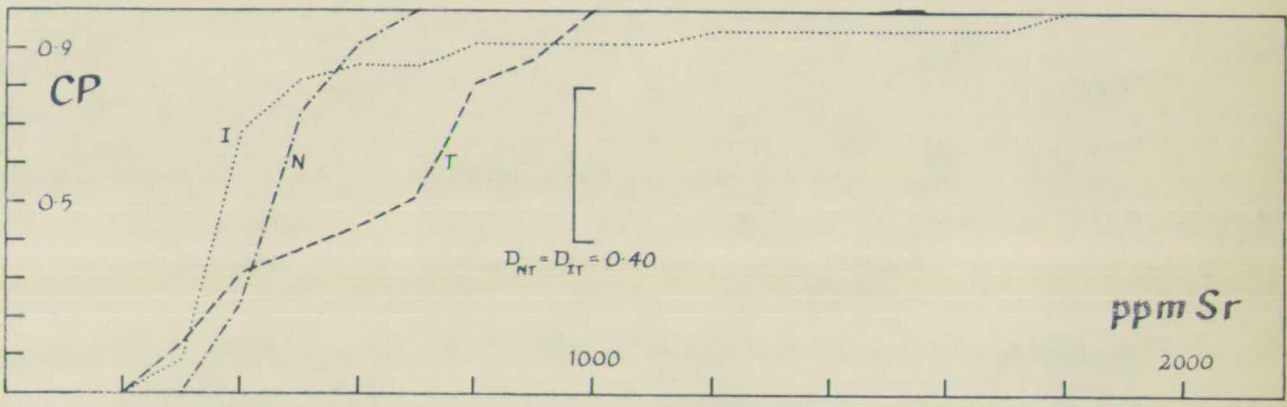
FIGURE 6.1 (two pages):
Cumulative-proportion graphs comparing the trace-element chemistry between the three dyke-zones of the Gardar province.

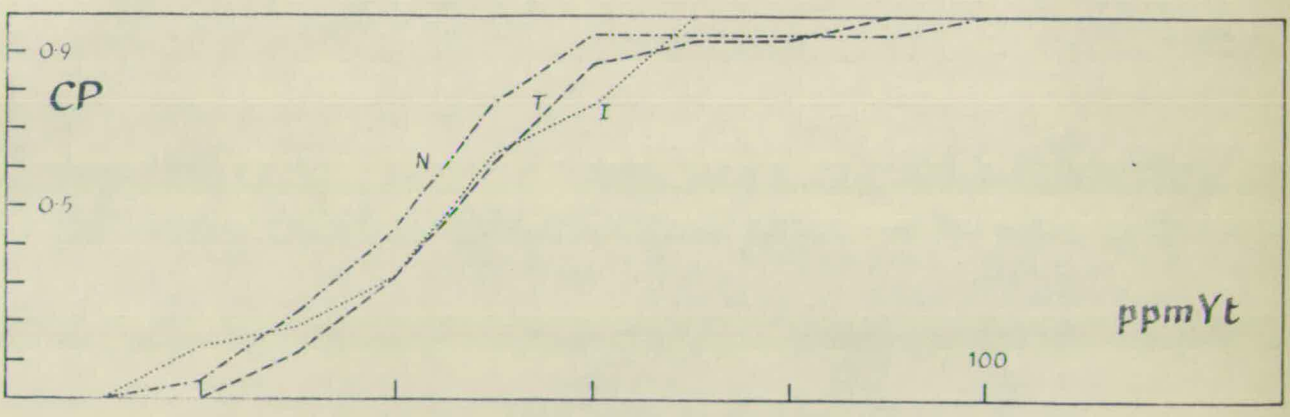
T: graph for the Tugtutoq-Narssarssuaq sample of 25 specimens.
I: graph for the Ivigtut sample of 25 specimens.
N: graph for the Nunarssuit sample of 38 specimens.

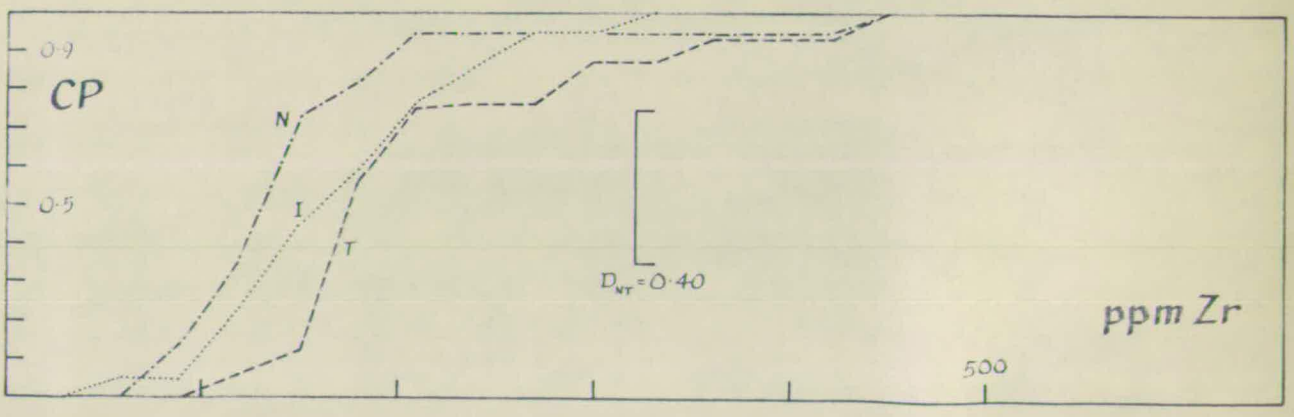
The graphs show the proportion of the sample having values of the variate equal to, or less than, the specified value.

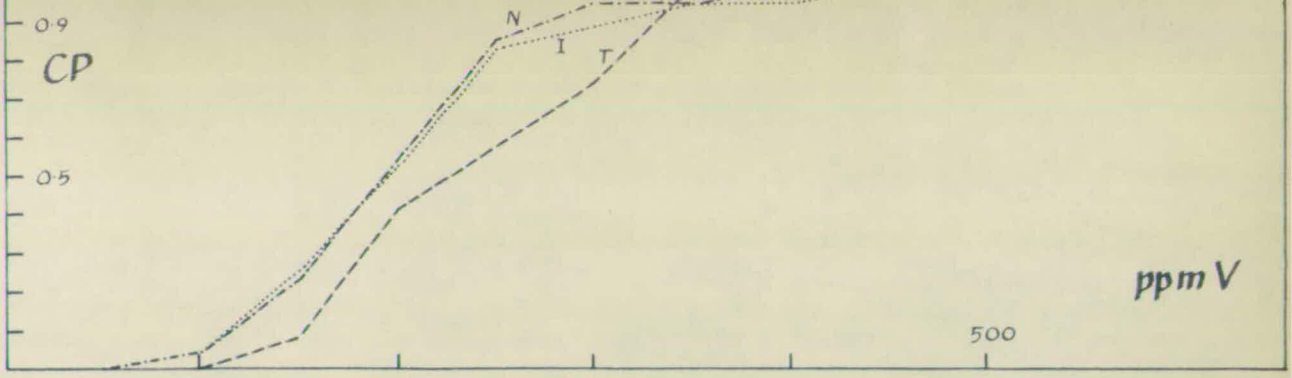

0·9
CP
0·5
N
I
T
100
200
ppm Rb

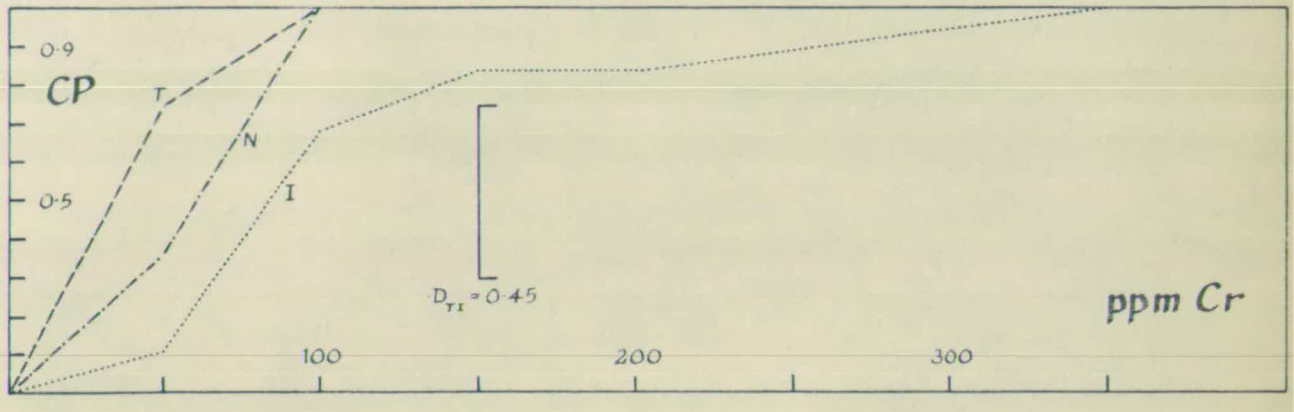

0·9
CP
0·5
$D_{NT} = D_{IT} = 0·40$
I
N
T
1000
2000
ppm Ba


0·9
CP
0·5
I
N
T
$D_{NT} = D_{IT} = 0·40$
1000
2000
ppm Sr


0·9
CP
0·5
N
T
I
100
ppm Yt


0·9
CP
0·5
N
I
T
$D_{NT} = 0·40$
500
ppm Zr


0·9
CP
0·5
N
I
T
500
ppm V


0·9
CP
0·5
T
N
I
D_TI = 0·45
100
200
300
ppm Cr

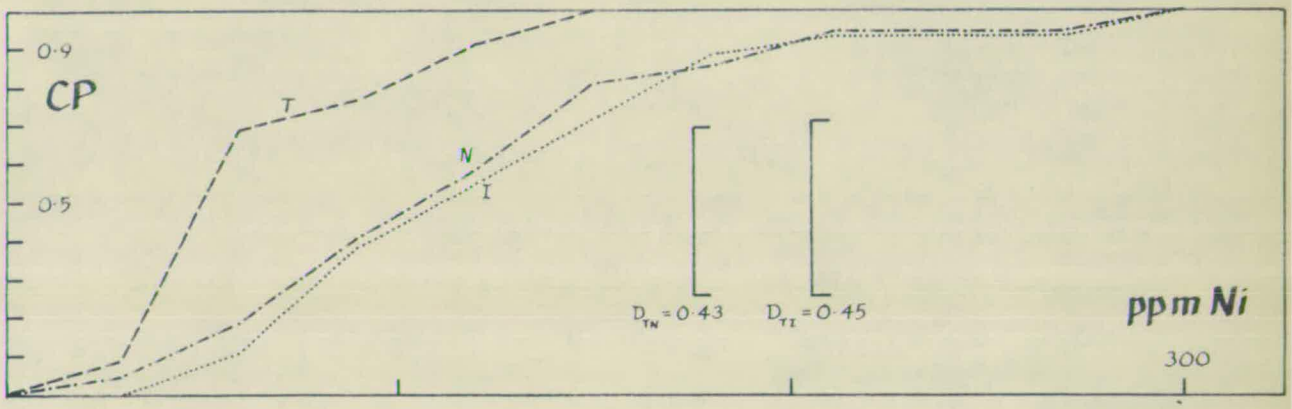

0·9
CP
0·5
T
N
I
D_TN = 0·43
D_TI = 0·45
300
ppm Ni

Table 6.1.

CORRELATION COEFFICIENTS FOR TRACE ELEMENTS

GARDAR BASIC DYKES

	Ba	Zr	Yt	Sr	Rb	Zn	Cu	Ni	Cr	V
SiO_2	-	-	-	-	-	-	-	-	-	-
Al_2O_3	-.3 1	-.58	-.49	-	-.32	-.38	-	.43	-	-.35
FeO*	-	.34	.31	-	-	-	-	-.31	-	.49
MgO	-.54	-.53	-.51	-	-.50	-.31	-	.77	.34	-.27
CaO	-.51	-.33	-.28	-	-.44	-	-	.38	.37	-
Na_2O	.42	.37	.26	-	.25	-	-	-.50	-	-
K_2O	.76	.47	.49	.31	.64	-	-	-.53	-.30	-
DI	.68	.48	.43	-	.50	.31	-	-.60	-.36	-
TiO_2	.47	.63	.56	-	.38	.26	-	-.59	-	.44
P_2O_5	.66	.59	.50	-	.49	.31	-	-.60	-.30	.25
MnO	-	.25	.29	-	-	.30	-	-.27	-	.28

	Ba									
Ba	-	Zr								
Zr	.40	-	Yt							
Yt	.39	.66	-	Sr						
Sr	.35	-	-	-	Rb					
Rb	.50	.48	.44	-	-	Zn				
Zn	-	.33	.25	-	.33	-	Cu			
Cu	-	-	-	-	-	-	-	Ni		
Ni	-.52	-.52	-.51	-	-.42	-.27	-	-	Cr	
Cr	-.29	-	-	-	-	-	-	.33	-	V
V	-	.32	.32	-	-	-	-	-.27	-	-

FeO* = FeO total

Correlation coefficient is Kendall's Tau

Note: coefficients shown are different from zero at the 0.01 level of significance.

FIGURE 6.2 (end pocket):
Variation diagrams for the trace elements.

Filled circles: dolerites and basalts with DI less than 35.
Crosses: trachydolerites with DI 35 to 50.
Triangles: trachydolerites and syenogabbros with DI over 50.

elements, the incompatible elements, will be discussed in a later section.

6.2. Variation Diagrams

Variation diagrams plotting the trace elements against MgO are presented in fig.6.2. Except in the Ni vs MgO diagram, there are no trends which can be clearly related to olivine and plagioclase fractionation. The distribution and behaviour of the trace elements in the dyke rocks is summarised below.

6.2.1. Barium

Barium substitutes for potassium, mainly in feldspars and feldspathoids and is enriched in alkali feldspar relative to plagioclase (Prinz, 1967; Berlin and Henderson, 1969). The distribution coefficient for Ba in plagioclase is less than 1 hence, the residual liquid is not depleted in Ba by precipitation of plagioclase (Philpotts and Schnetzler, 1970).

The increase in Ba throughout the compositions studied, from 300 ppm at 8% MgO to more than 2000 ppm at 2% MgO reflects the exclusion of Ba from the fractionating phases. The greater increase in Ba in compositions with less than 5% MgO coincides with the onset of magnetite crystallisation. There is, however, a variation in Ba content for the same level of MgO which probably reflects the variation in K_2O content noted in chapter 5, since there is a strong positive correlation between Ba and K_2O in the Gardar rocks. Hence it is suggested that there was a variation in the Ba content of the parent liquids.

The Ba content of dyke-rock plagioclase and plagioclase in inclusions differs, the former frequently having the higher Ba content (Bridgwater and Harry, 1968). The differences are not simply due to the variation in An content of the feldspar, since there is not a good correlation between Ba and An content in the feldspars (op cit.), but may reflect differences in the Ba content of the liquids from which the feldspars precipitated. This in turn will depend on both the Ba content of the parent liquid and the differentiation stage reached by the liquid when the feldspars precipitated.

6.2.2. Strontium

Because of diadochy between strontium and calcium, strontium is mainly found in plagioclase, clinopyroxene and apatite. It is also present in high-temperature potassium-bearing minerals such as K feldspar and the feldspathoids (Prinz, 1967).

The Sr content of plagioclase may not vary consistently with An content, as the distribution ratio for Sr between plagioclase and liquid is strongly dependent on temperature and bulk composition of the liquid (Sun et al., 1974) and Prinz (1967) finds the highest Sr content in intermediate plagioclases. The precipitation of plagioclase should deplete the liquid in Sr and decrease the Sr/Ca ratio, as plagioclase is enriched in Sr compared with Ca(Sun et al. 1974). The Ba/Sr ratio increases with differentiation when plagioclase precipitates as Ba is not removed from the liquid (Berlin and Henderson 1968).

The Sr content and Sr/Ca ratio in the Gardar rocks is very variable

in the dolerites and trachydolerites but begins to decrease with falling MgO between 3 and 4% MgO (figs.6.2 and 6.3). The Ba/Sr ratio increases steadily with differentiation. Thompson et al. (1972) have suggested that plagioclase fractionation may in fact cause considerable variation in the Sr content of a rock series, but the variation in the Sr/Ca ratio in the dolerites and trachydolerites is anomalous if plagioclase has been fractionated throughout as it appears to be. Imperfect fractionation of the plagioclase, discussed by Cox and Bell (1972), should be reflected in the Al_2O_3 content of the rocks. This, however, decreases with decreasing MgO throughout the series, indicating effective fractionation of the plagioclase.

Some variation in the Sr/Ca ratio may be caused by a variation in D_{sr}^{pl} (the distribution ratio for Sr between plagioclase and liquid) with temperature and magma composition as suggested by Sun et al. Precipitation of olivine with the plagioclase can increase the Sr content of the residual liquid but will not affect the Sr/Ca ratio. The Sr/Ca ratio in a magma series may rise in spite of plagioclase fractionation if clinopyroxene is also fractionated, since D_{sr}^{cpx} is less than 1 (Berlin and Henderson, 1968). However, as noted in chapter 5, clinopyroxene phenocrysts do not occur in rocks with more than ca. 3% MgO, hence low pressure clinopyroxene fractionation could not have affected the Sr/Ca ratios in more basic rocks. The variation in Sr/Ca ratios in the dolerites could, however, be an indication that clinopyroxene fractionation has occurred at moderately high pressures.

FIGURES 6.3 and 6.4 (end pocket):
The variation of Sr with CaO is shown in the first together with the compositions of three plagioclases and a clinopyroxene. Plagioclase 1 is from the younger Tugtutoq gabbro giant dyke. Plagioclase 2 is from an early ESE dolerite in the Isortoq region. Plagioclase 3 is from a granular anorthosite xenolith from the Kobberminebugt region. The clinopyroxene is mentioned in the text, page 89.

The second shows the variation of Y with CaO.

The compositions of some plagioclases from Gardar basic dykes and anorthosite inclusions (reported by Bridgwater and Harry, 1968) are plotted in fig.6.3. The Sr content of the pyroxene is taken from Berlin and Henderson (1968), and the Ca content is that of an aluminous clinopyroxene in equilibrium at moderate pressures (ca. 10kb.) with the Skye basaltic lavas (Thompson, 1974). It is obvious that plagioclase fractionation could not increase the Sr/Ca ratios in the rocks. Clinopyroxene fractionation however, modified by subsequent plagioclase fractionation, is apparently capable of producing the observed variation. However, it should be noted that the weak positive correlation between Sr, K and Ba may indicate that the Sr content of the parental liquids, like the K_2O and Ba contents, varied.

The decrease in Sr content and Sr/Ca ratio in compositions with less than 3-4% MgO may reflect increased partition of Sr into the plagioclase and/or the fractionation of apatite, which is relatively Sr-rich (Prinz, 1967).

6.2.3. Rubidium

Rubidium, being a large ion, is excluded from most mafic minerals but is accepted into the alkali feldspar lattice and feldspathoids, where it substitutes for potassium (Prinz, 1967). The exclusion of Rb from the phases crystallising in the basic dykes is reflected in the increase with decreasing MgO throughout the compositions studied.

6.2.4. Zirconium

Zirconium is discriminated against by most of the major phases of basaltic rocks (Jamieson and Clarke, 1970), although it does enter pyroxenes and apatite (Prinz, 1967). Chao and Fleischer (1960) suggest that Zr is more soluble in alkaline magmas, since the increase in Zr from mafic to salic compositions is greater in these rocks than in tholeiitic rocks. The Zr content of the Gardar basic dykes rises from 100 ppm at 8% MgO to 250-300 ppm at 2% MgO. Macdonald and Parker (1969) report Zr contents of more than 3000 ppm in alkaline rocks from the Gardar province, but the Zr contents of the basic rocks are not significantly higher than the values reported by Prinz (1967), who found a median value of 125 ppm for all alkali basalts. The median values for the Gardar rocks vary from 100 ppm for the Ivigtut zone to 150 ppm for the Tugtutoq zone, where however, there appears to be a greater incidence of more-differentiated compositions.

6.2.5. Yttrium

Yttrium is believed to substitute for calcium as Y^{3+}, with an ionic radius of 0.98 Å, is similar to Ca^{2+} at 0.94 Å (Lambert and Holland 1974). Augite and plagioclase do not accept yttrium preferentially over calcium and in differentiation controlled by plagioclase and/or augite the Ca/Y ratio falls, as Y is enriched and Ca depleted in the magma. With decreasing MgO, Y increases steadily in the dykes from approximately 20 ppm at 8% MgO to 70 ppm at 2% MgO. There is a weak negative correlation between Y and CaO (table 6.1), the Ca/Y ratio falling with differentiation (fig.6.4), consistent with

plagioclase or augite fractionation.

6.2.6 Nickel

Nickel enters most abundantly into the olivine structure, less so into orthopyroxene and clinopyroxene (Deer et al 1966, Prinz 1967), thus olivine fractionation has a marked influence on the nickel content of rocks. Table 6.1 shows a strong positive correlation between Ni and MgO in the dykes and olivine control is apparent in the Ni vs MgO variation diagram, Ni decreasing rapidly with decreasing MgO.

6.2.7 Chromium

The bulk of the chromium in basic rocks is contained in chrome spinels or diopsidic pyroxene; later pyroxene and magnetite have low levels of Cr (Prinz 1967). The Cr contents of Gardar dykes are low, generally less than 100 ppm: Prinz finds a median value of 140 ppm for alkali basaltic rocks but admits a wide variation. The dykes with moderately high Cr values contain large amounts of pyroxene (101401, 101287, 101417) or ore minerals (101418, 101427, 101428). Cr remains relatively steady at 50 to 75 ppm until 5 to 4% MgO, when it decreases to 25 ppm, probably due to magnetite fractionation.

6.2.8 Vanadium

Vanadium substitutes for Fe^{3+}, entering magnetite rather than ilmenite (Prinz 1967, Brown 1967). The behaviour of V in the rocks is similar to that of TiO_2 and total FeO, ~~and~~ rising, with decreasing MgO, from 100 to 340 ppm at 5% MgO and declining thereafter.

6.2.9 Copper and Zinc

The precision of the Cu and Zn determinations is poor; none the less it is clear that Cu decreases and Zn increases with decreasing MgO. Zn is camouflaged by FeO, but there can be strong geochemical separation during differentiation, to produce enrichment in Zn in the late stages (Wood 1968). Cu sulphides are the principal Cu-bearing minerals (Prinz 1967) and the decline in Cu content of the rocks may be due to the early separation of an immiscible sulphide liquid.

6.3 K/Rb ratios

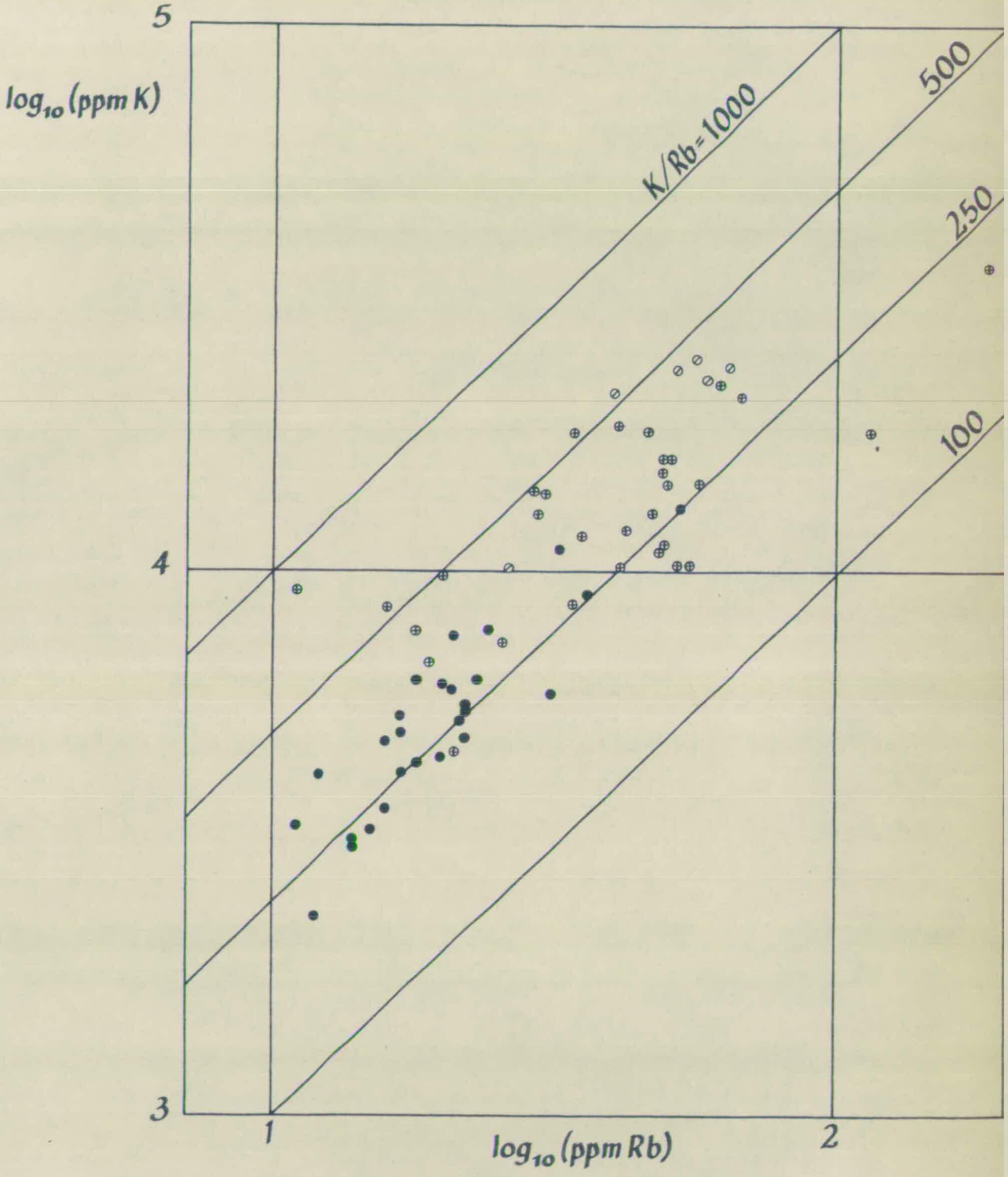
There is a wide variation in K/Rb ratios in the dykes (ca.200 to 500) but some of this is undoubtedly due to the comparatively poor precision of the Rb determinations, which gives a standard error of 2.2 at 24 ppm Rb, equivalent to 24 ± 4 ppm. Fig. 6.5 shows K ppm plotted versus Rb ppm (log scale).

The K/Rb ratios of the dolerites are between 200 and 350, ie. low compared with Prinz's average values for olivine-normative tholeiites and alkali basalts (414 and 346 respectively) although close to his average of 253 for nepheline-normative basalts.

Gast (1968) showed that K/Rb ratios in basaltic rocks are largely controlled by the nature of the source material, degree of partial melting and by crystal fractionation processes. Because of the large size of the Rb ion it should be discriminated against in early crystal fractions, so the K/Rb ratio should decrease with fractionation, but this effect may be apparent only under conditions of

FIGURE 6.5:
K/Rb ratios for the Gardar dykes.

Filled circles: basaltic compositions with DI under 35.
Circled crosses: trachydolerites with DI between 35 and 50.
Circles with diagonals: trachydolerites and syenogabbros with DI over 50.


5
log10 (ppm K)
K/Rb=1000
500
250
100
4
3
1
2
log10 (ppm Rb)

extreme fractionation (Erlank 1968).

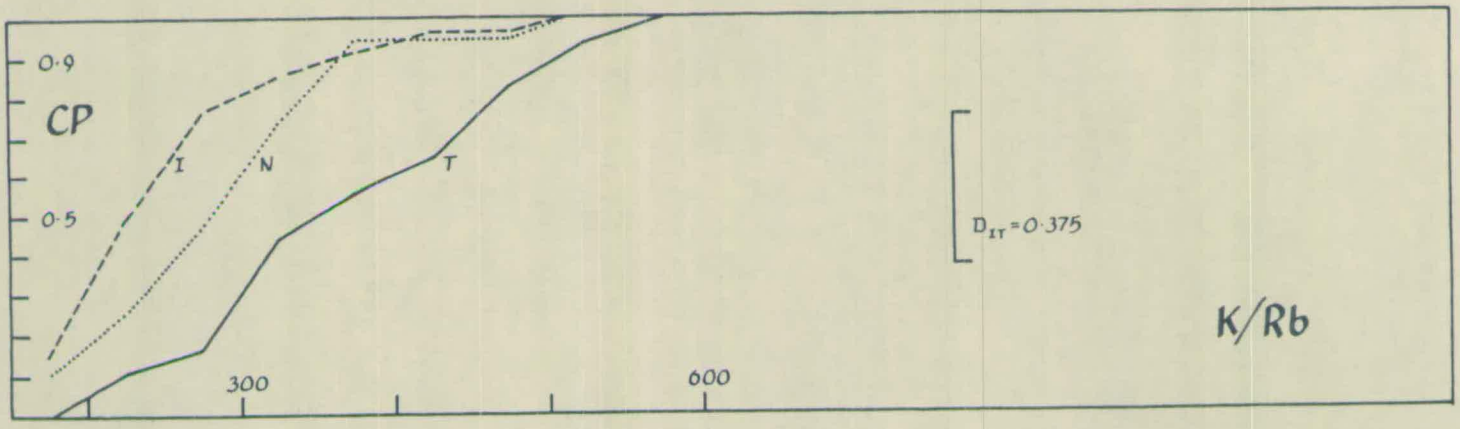
The K/Rb ratios of the Gardar rocks rise during fractionation to ca. 500 in the trachydolerites. If the concentration of K_2O in the rock is insufficient for the formation of K feldspar the K/Rb ratio may rise (Shaw 1968); the initial increase in the dolerites may be attributable to this. Fractionation of mica, which preferentially accepts Rb (Shaw 1968) can increase the K/Rb ratio. But the concomitant entry of K into mica (D_K^{mica} is greater than 1 : Philpotts and Schnetzler, 1970) would deplete the K content of the liquid.

There is some suggestion that K/Rb ratios vary between the three zones: A cumulative proportion diagram (fig.6.6) for K/Rb in rocks with DI less than 50 shows that the K/Rb ratios for the Ivigtut sample are significantly smaller than those for the Tugtutoq sample, with a median value of 220 compared with 350 for the Tugtutoq sample. The significance of this is open to doubt in view of the variation of K/Rb in the rocks, and the slight increase in the trachydolerites, but it may indicate a variation in K/Rb in the parent magmas supplying the three zones. The K/Rb ratios of the basaltic compositions (DI less than 35) were not significantly different, but this may be attributable to the small sample size.

The K/Rb ratio of some syenogabbros (101339, 101351, 101355) is high, ca. 550, but since these are from the Isortoq syenogabbro dyke,

FIGURE 6.6:
Cumulative-proportion graph comparing the K/Rb ratios between the three dyke-zones of the Gardar province.

Explanation as for figure 6.1, which follows page 85.


0·9
CP
0·5
I
N
T
300
600
D_{IT} = 0·375
K/Rb

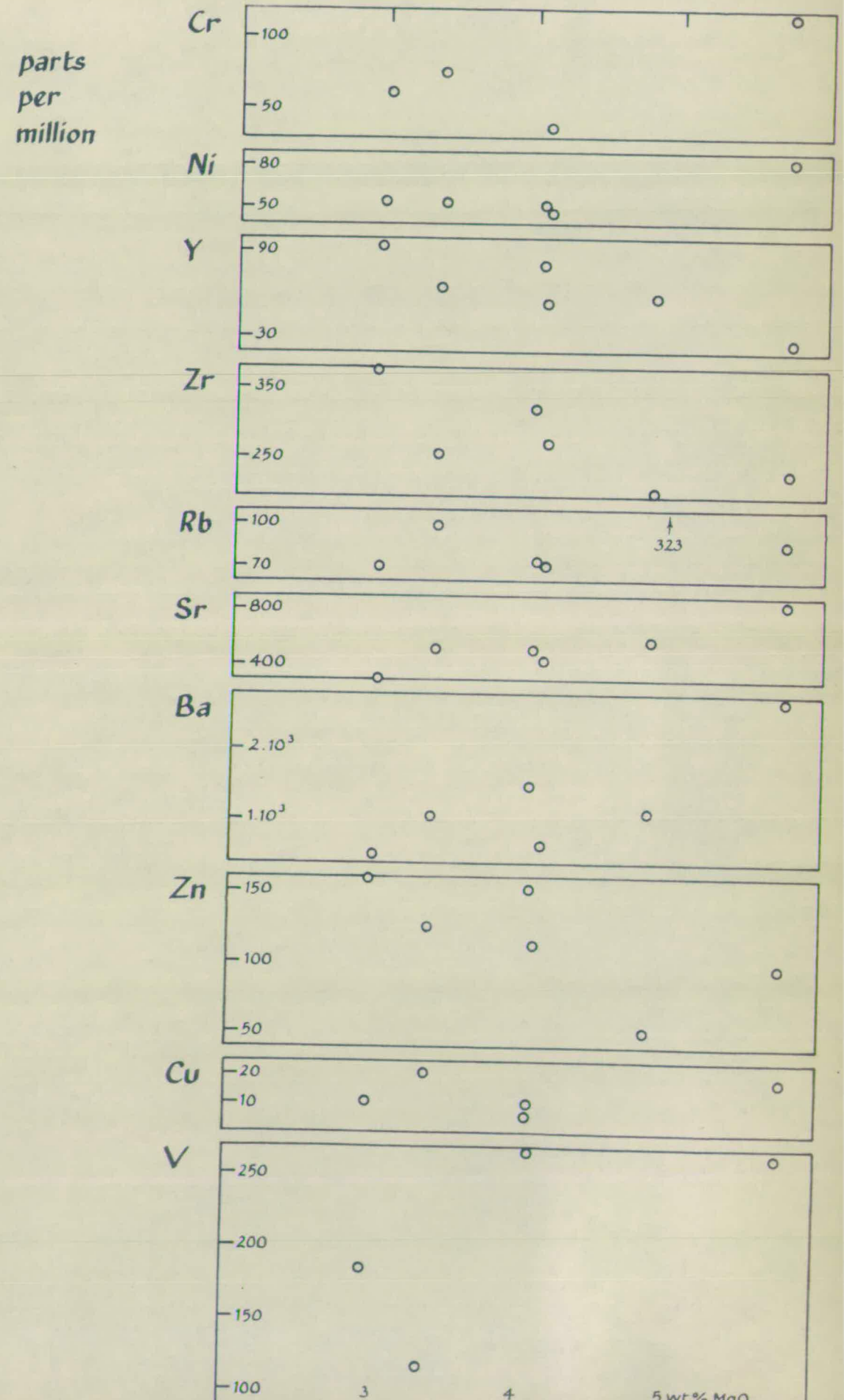
where layered cumulate structures indicate in situ fractionation, and in view of the coarse grain-size of the rocks in question, it may be doubted whether these represent liquid compositions. These rocks contain large amounts of sodic alkali feldspar (antiperthite) (45 to 55 vol%) which discriminates against Rb (Taylor, 1965).

6.4. The Trachydiorites

Ba decreases with decreasing MgO from 2700 ppm at 6% MgO to 530 ppm at 3% MgO (fig.6.7). Sr decreases similarly from 800 ppm to 300 ppm, but the Rb content of the rocks varies little. Both Ba and Sr have correlation coefficients of 0.6 with MgO and with K_2O.

Sr depletion can be caused by the crystallisation of either plagioclase or alkali feldspar, but Ba depletion can be produced only by the crystallisation of alkali feldspar or mica (Philpotts and Schnetzler, 1970). The behaviour of Rb may perhaps be an indication of alkali feldspar fractionation, since Rb will enter alkali feldspar but is not accepted preferentially over K_2O and Ba (Taylor 1965) and hence the liquid may not be depleted in Rb. However, as described in chapter 5, there is no evidence of alkali feldspar fractionation in the compositions examined. The lack of variation in Rb is anomalous if a diffusion mechanism is operative as suggested in chapter 5 section 6, although the fact that Rb does not increase in the more-evolved rocks, as it should if excluded from the fractionating phases, may be an indication that Rb too is partly affected by diffusion.

FIGURE 6.7:
Trace-element variation diagrams for the trachydiorites.


parts per million
Cr
100
50
Ni
80
50
Y
90
30
Zr
350
250
Rb
100
70
323
Sr
800
400
Ba
2.10³
1.10³
Zn
150
100
50
Cu
20
10
V
250
200
150
100
3
4
5 wt% MgO

Zr and Y both have a negative correlation with MgO (coefficients of 0.6 and 0.73 respectively, probability (i.e. significance +0.068 and +0.028), behaviour similar to that found in the dolerites and trachydolerites.

The Ni content of the trachydiorites is low, less than 85 ppm, but similar to the trachydolerites at the same MgO content. Ni decreases slightly with fractionation and the presence of altered olivine phenocrysts shows that the liquids have probably undergone extensive olivine fractionation.

The Cr content too is generally low, decreasing from 117 ppm Cr at 6% MgO to 60 ppm at 3% MgO. The values are higher than in the trachydolerites, reflecting the dominance of clinopyroxene in the trachydiorites. The decrease in Cr is consistent with clinopyroxene and /or magnetite fractionation and phenocrysts of both minerals occur in the rocks.

Vanadium is extremely variable in the trachydiorites, as is Fe, but there is not a good correlation between V and Fe. This may relate to the high content of iron pyrite in the trachydiorites, since V^{3+} substitutes for Fe^{3+}, in preference to Fe^{2+}, and should therefore be contained in magnetite, (Prinz, 1967). The Cu content is very low, less than 25 ppm. No Cu sulphides were observed in polished sections. The increase in Zn with decreasing MgO to 150 ppm at 3% MgO (correlation coefficient -0.73, probability 0.028) is similar to the behaviour in the dolerites and trachydolerites.

The K/Rb ratio of the trachydiorites varies from 130 to 353, slightly lower than in the trachydolerites. As might be expected, K/Rb shows no significant correlation with either K_2O or MgO.

7. Petrogenesis.

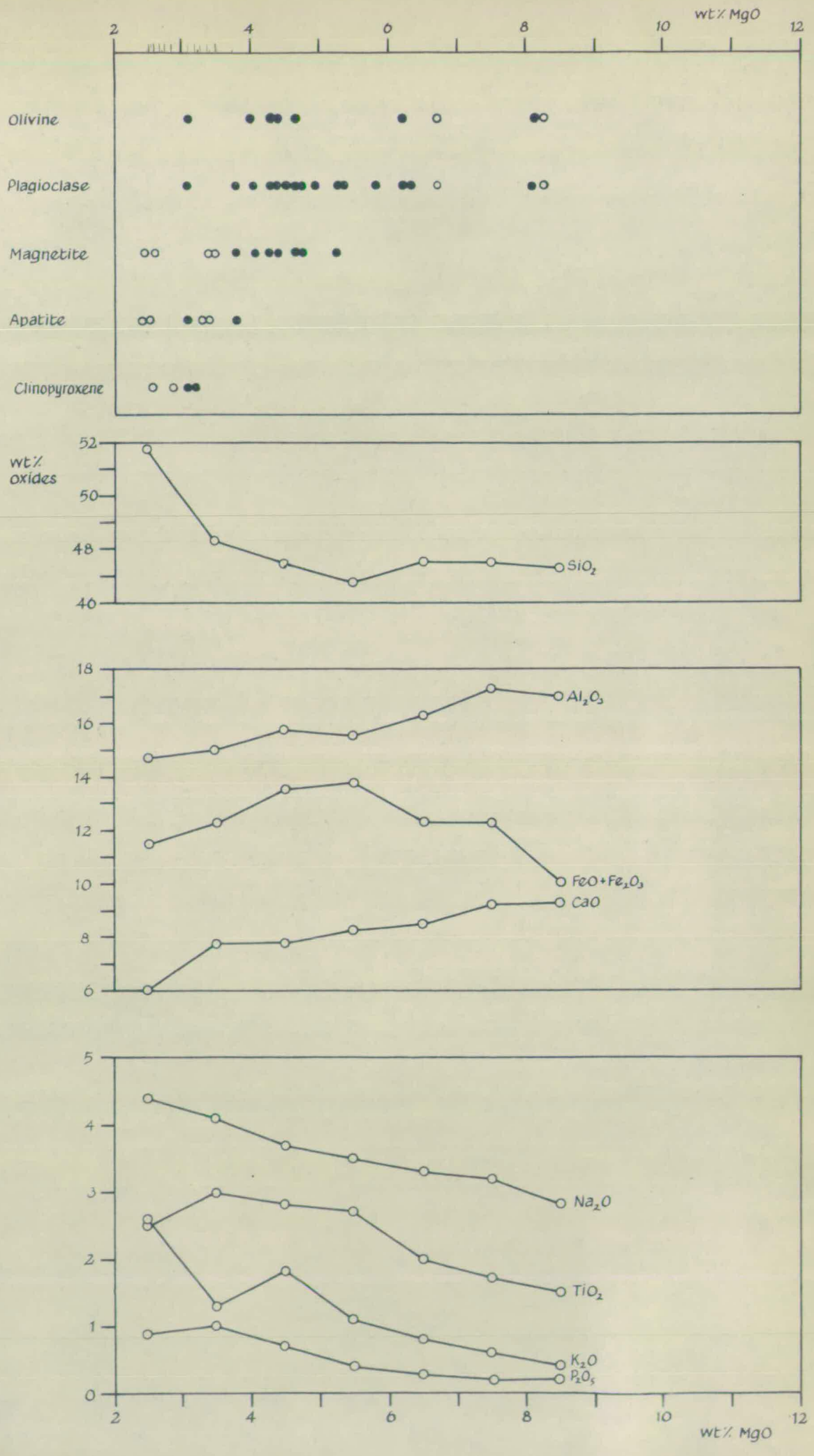
7.1. Low pressure processes.

The majority of the rock-types present in the Gardar basic dykes constitute a series from dolerite to trachydolerite, with complete gradation between the end members. The volatile-rich trachydiorites may represent an alkali-enriched variant of the normal series.

The coherence between major-element trends and phenocryst assemblages in the basaltic series rocks suggests that the major process of differentiation from dolerite to trachydolerite has been crystal fractionation at relatively low pressures (ca. 5kb or less) (fig.7.1). Thus the following features may be seen:

1. The decline of TiO_2 and $FeO + Fe_2O_3$ with decreasing MgO in the trachydolerites commences with the appearance of titaniferous magnetite phenocrysts.
2. From this point there is a concomitant increase in SiO_2, P_2O_5, Na_2O and K_2O.
3. Apatite phenocrysts appear in the trachydolerites at ca. 3.5% MgO, but the effect of apatite fractionation on the P_2O_5 content of the rocks is not noticeable in the relatively basic compositions studied.
4. Clinopyroxene appears as a phenocryst at ca. 3% MgO but, as with apatite, there is little obvious

FIGURE 7.1:
Relationship of major-element trends to phenocryst occurrences in the Gardar dykes.
The open circles on the graphs are median values of oxides for one percent intervals of wt% MgO.
Open circles on the top diagram are phenocryst occurrences from the literature; filled circles are phenocryst occurrences from this study.


wt% MgO
2
4
6
8
10
12
Olivine
Plagioclase
Magnetite
Apatite
Clinopyroxene
wt% oxides
52
50
48
46
SiO_2
18
16
14
12
10
8
6
Al_2O_3
$FeO+Fe_2O_3$
CaO
5
4
3
2
1
0
Na_2O
TiO_2
K_2O
P_2O_5
2
4
6
8
10
12
wt% MgO

effect in these basic compositions. The precipitation of clinopyroxene can only enhance the decline of CaO with decreasing MgO.

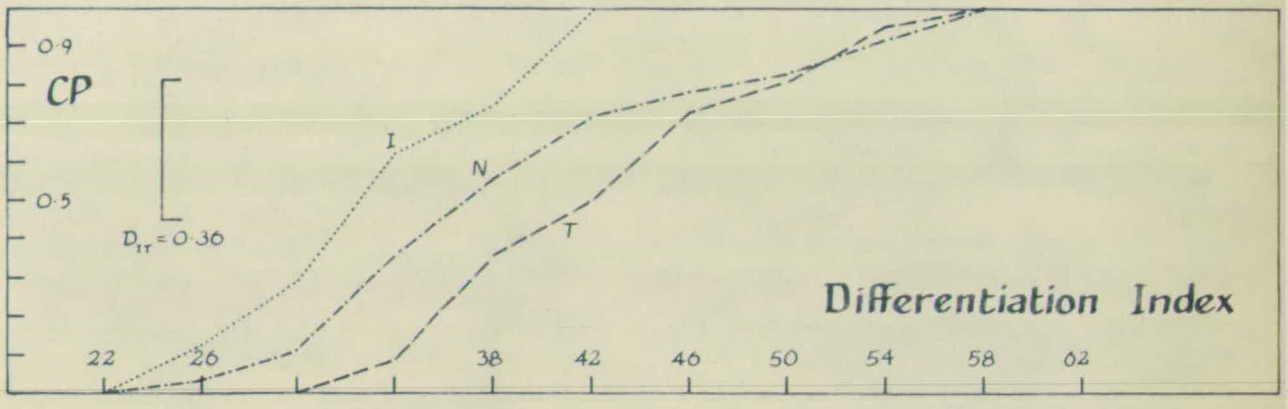
5. In rocks containing between 5 and 8% MgO, olivine and plagioclase are the only phenocrysts present and, as demonstrated in chapter 5, the major element trends between 8 and 5% MgO can be related to the fractionation of olivine and plagioclase in the approximate proportions 30% olivine to 70% plagioclase. These are the proportions in which olivine and plagioclase phenocrysts occur in the rocks. Olivine forms a major portion of the extract in deriving compositions with approximately 8% MgO from the few more magnesian compositions. Of these, some contain olivine phenocrysts and may be cumulus-enriched, for example the chill of a Tugtutoq gabbro dyke (40452 - Upton, 1964) but others are virtually aphyric and thus probably represent liquid compositions.

6. The widespread occurrence of anorthosite xenoliths which may be cumulates formed at depth: Bridgwater and Harry (1968) demonstrated a genetic connection between the type of inclusion and the host rock-type.

FIGURE 7.2:
Cumulative-proportion graphs comparing differentiation index between the three Gardar dyke-zones.

T: graph for the Tugtutoq-Narssarssuaq sample of 25 specimens.
I: graph for the Ivigtut sample of 25 specimens.
N: graph for the Nunassuit sample of 38 specimens.

The graphs show the proportion of the sample having values of the variate equal to, or less than, the specified value.


0·9
CP
0·5
I
N
T
$D_{IT} = 0.36$
Differentiation Index
22
26
38
42
46
50
54
58
62

As was noted in chapter 5, there is considerable variation in the K_2O content of the dykes, which cannot be produced by low-pressure fractionation, so it appears that the parent magmas varied in K_2O content. This will be discussed in a later section. The action of crystal fractionation on these variable basaltic liquids is to produce trachydolerites with a range of K_2O contents.

7.1.2. Relative abundances.

This study has been confined to basic rocks with more than 2% MgO and less than 54% SiO_2, so that discussion of the possible existence of and significance of the so-called 'Daly gap' at 50 to 55% SiO_2 has no place here. However it is relevant to studies of the salic rocks to point out that there is a comparative scarcity of the more-evolved trachydolerites and syenogabbros (those with more than 48% SiO_2 and less than 3.5% MgO, corresponding approximately to those with DI greater than 50). This is particularly true of the Ivigtût zone, as the cumulative proportion diagram for DI shows (fig.7.2). The smaller proportion of these compositions could be related to crystal fractionation processes producing successively smaller volumes of differentiated liquids, but if the large volumes of salic rocks in the province are to be derived by differentiation from a basaltic parent, the lack of intermediate types is significant. Thus the scarcity of rock types intermediate between gabbro and syenite noted by Watt (1966) in a planimetric estimation of

abundances, and later by Upton (1974) in a discussion of the published analyses, is confirmed in the basic dyke swarms.

Many of the more-evolved trachydolerites and syenogabbros occur in the giant dykes, for example the Isortoq giant dykes and the Bangs Havn complex, where the internal layering shows that in situ fractionation has occurred. Others occur in the BFD's (Bridgwater and Harry, 1968, p.150), which are believed to have formed through the serial tapping of a compositionally stratified magma column. Intrusions formed in this manner would be expected to contain a series of rocks representative of the compositional gradation within the column. Diminishing eruptive energy or increasing viscosity would operate to discriminate against the more basic magma near the base of the column, but a compositional gap between the salic and basic magmas would not be expected in this case.

7.2. The trachydiorites

The alkali and volatile-rich trachydiorites intruded towards the end of the Gardar period, after a long period of salic volcanism, nevertheless appear to be compositionally related to the earlier dolerites and trachydolerites, plotting within the same composition field in variation diagrams.

Fractionation of the observed phenocryst phases is not capable of explaining the variation of Na_2O and K_2O in these rocks: K_2O falling and Na_2O rising with falling MgO in the more differentiated rocks. The trace element data for Ba and Rb would appear to

indicate the involvment of alkali feldspar in fractionation, but alkali feldspar phenocrysts were not found in any of the specimens examined. It therefore appears that the Na_2O, and K_2O, Ba and possibly Rb contents of the rocks may have been affected by diffusion in response to pressure and temperature gradients within the magma. There is some evidence for the existence of a compositionally-zoned magma column prior to intrusion.

The trachydiorites were intruded towards the end of the Gardar period, after a long period of alkaline volcanism, so that the opportunity existed for the contamination of basaltic magmas by alkalis and volatiles derived from the alkaline magmas. However the presence of carbonatite intrusions in the province indicates that the likely source for the CO_2 and alkalis is the mantle itself.

Since no rocks containing more than 6% MgO which are obviously genetically related to the trachydiorites have been found, the character of the parent magmas is uncertain. Hence it cannot be ascertained whether the parent magmas were themselves rich in water, CO_2 and alkalis, or if the trachydiorites were produced from a less volatile-rich basaltic magma after a considerable period of crystallisation of anhydrous minerals at depth. It seems probable, however, that as magmatic activity waned in south Greenland, a fresh batch of basic magma could be produced from the mantle perhaps in response to a local rise in the geo-isotherms. If the heat flux were comparatively small, only a small proportion of melt would be formed, which would be enriched in the

incompatible elements (K and related elements, Ti, P and Zr, Gast, 1968) and volatiles which preferentially enter the melt. The trachydiorites could represent the residual liquid formed after fractionation of such a magma. The trachydiorite dykes are generally less than 5m broad and are not particularly abundant (Upton, 1964b), implying that the volume of magma involved in their production was not great.

7.3. Petrogenesis of the basaltic compositions

7.3.1. It is unlikely that the Gardar dykes, which were intruded over a period of approximately 150 my, were all derived from the same parent magma, although it is possible that only a few melting episodes were involved. The dykes in the Ivigtût zone were intruded between 1327 ± 17 my and 1233 ± 16 my. The principal dykes in the Tugtutôq zone were intruded between 1175 ± 9 and 1168 ± 37 my and the Nunarssuit zone dykes were intruded prior to 1164 ± 18 my (van Breemen and Upton, 1972; Blaxland et al., in prep.). The variety of the least differentiated dolerites may be taken to represent the variety of parent magmas available.

Chemically the most primitive rocks (those containing more than 7% MgO) have a general similarity, with moderate to high Al_2O_3, (15% to 19%), moderate to low CaO (7% to 10%) and generally low K_2O (0.2% to 0.6%) but some comparatively rare specimens are more potassic with ca. 1% K_2O (table 7.1). These potassic rocks are not confined to any one zone, although all the ENE dykes in the Tugtutôq zone are rich in potassium, and may have been derived

Table 7.1.

A selection of analyses showing the most primitive compositions among the Gardar dolerite dykes

The specimen numbers with the prefix 101 - refer to specimens analysed during this study. A brief description of the specimens, together with trace element analyses and CIPW norms, is presented in the appendix.

121301* Analysis supplied by J. Engell. see appendix.

40452* Chill of Tugtutoq gabbro giant dyke. Upton, 1964b.

20632* Dolerite from Equaloqarfia dyke. Pulvertaft, 1965.

Table 7.1.

Specimen No.	101431	121301*	101407	101345	101331	101403	101471	40452*	20632*
SiO_2	45.43	44.05	47.40	46.72	47.98	47.83	47.62	44.41	44.60
Al_2O_3	15.62	15.40	19.15	16.67	18.91	16.81	17.72	16.80	16.46
Fe_2O_3	1.54	2.13	0.17	2.12	1.35	1.94	1.68	1.97	2.28
FeO	12.23	10.25	9.41	9.48	9.79	10.70	10.75	12.95	9.44
MgO	11.38	10.84	8.50	8.20	7.76	7.16	7.21	8.26	9.77
CaO	7.76	7.65	9.05	8.91	9.44	9.24	8.04	7.42	8.68
Na_2O	2.98	2.34	3.30	2.82	3.14	3.20	3.64	3.10	2.50
K_2O	0.28	0.54	0.39	0.59	0.53	0.44	1.18	0.92	0.85
H_2O^+	0.46	-	0.33	1.73	0.89	0.55	0.62	0.79	2.06
TiO_2	1.32	0.65	0.96	1.52	1.34	1.65	2.21	2.44	1.49
P_2O_5	0.24	0.17	0.22	0.32	0.23	0.22	0.85	0.65	0.32
MnO	0.21	0.09	0.14	0.17	0.16	0.17	0.15	0.22	0.16
Sum.	99.45	95.23	99.02	99.25	100.80	99.91	101.67	99.93	98.61

solely from a K_2O-rich parent.

The overall similarity of the more primitive compositions implies a considerable homogeneity in the source mantle and in the conditions under which the magmas were produced. For example, the Kûngnât basic ring dyke, postdating the Kûngnât syenite complex, was intruded some time after the regional basic dyke swarms in the Ivigtût zone, which predate the complex (Upton, 1960). The major element chemistry of the basic rocks is, however, similar, although the Kûngnât dyke is possibly slightly more potassic than some members of the regional swarm (see table 7.2).

It might be imagined that the production of considerable volumes of magma over a period of some 150 my would result in severe depletion of the underlying mantle in the low-melting constituents. Hence the magma composition might be expected to change with time, becoming poorer in those constituents which preferentially enter the early melt fraction. There is no evidence for this in the Gardar province. There may even be evidence for some enrichment in K_2O in the later intrusions, (for example, the ENE dykes in the Tugtutôq zone). However, the occurrence of K_2O enriched dykes is irregular.

The lack of evidence for depletion of the mantle during the Gardar period would appear to imply the continual supply of fresh undepleted mantle to the region, possibly through convective circulation.

Table 7.2

Comparison of the compositions of the Kungnat basic ring dyke and basic dykes from the earlier regional swarms

Specimen No.	26040	86186	101425	101428
SiO_2	45.40	45.2	47.39	46.70
Al_2O_3	18.0	17.34	14.76	18.03
Fe_2O_3	3.1	2.33	4.19	1.87
FeO	11.9	13.58	11.35	10.19
MgO	5.1	7.51	5.40	6.91
CaO	7.6	7.45	7.65	8.86
Na_2O	3.7	3.22	3.55	3.33
K_2O	0.91	0.79	1.22	0.66
H_2O^+	0.35	0.41	1.04	0.58
TiO_2	3.5	2.74	2.82	1.83
P_2O_5	0.25	0.34	0.43	0.39
MnO	0.19	0.19	0.21	0.15
Sum	100.03	101.13	100.01	99.50

26040 Kungnat basic ring dyke (Upton, 1960)

86186 " " " " (Upton, 1971)

101425 BD_2 regional dyke swarm, Tigssalup area

101428 BD_0 " " " " "

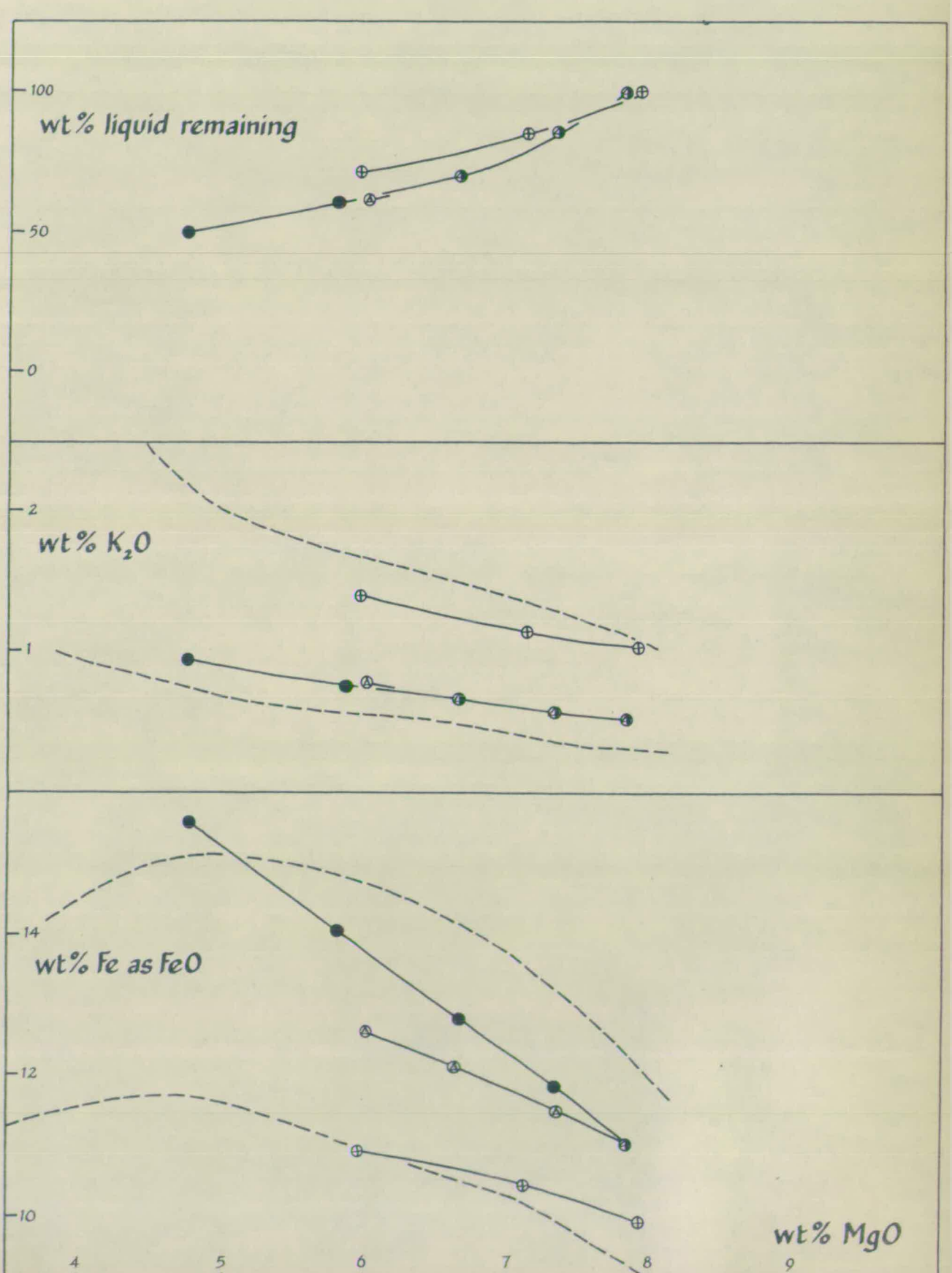
7.3.2.

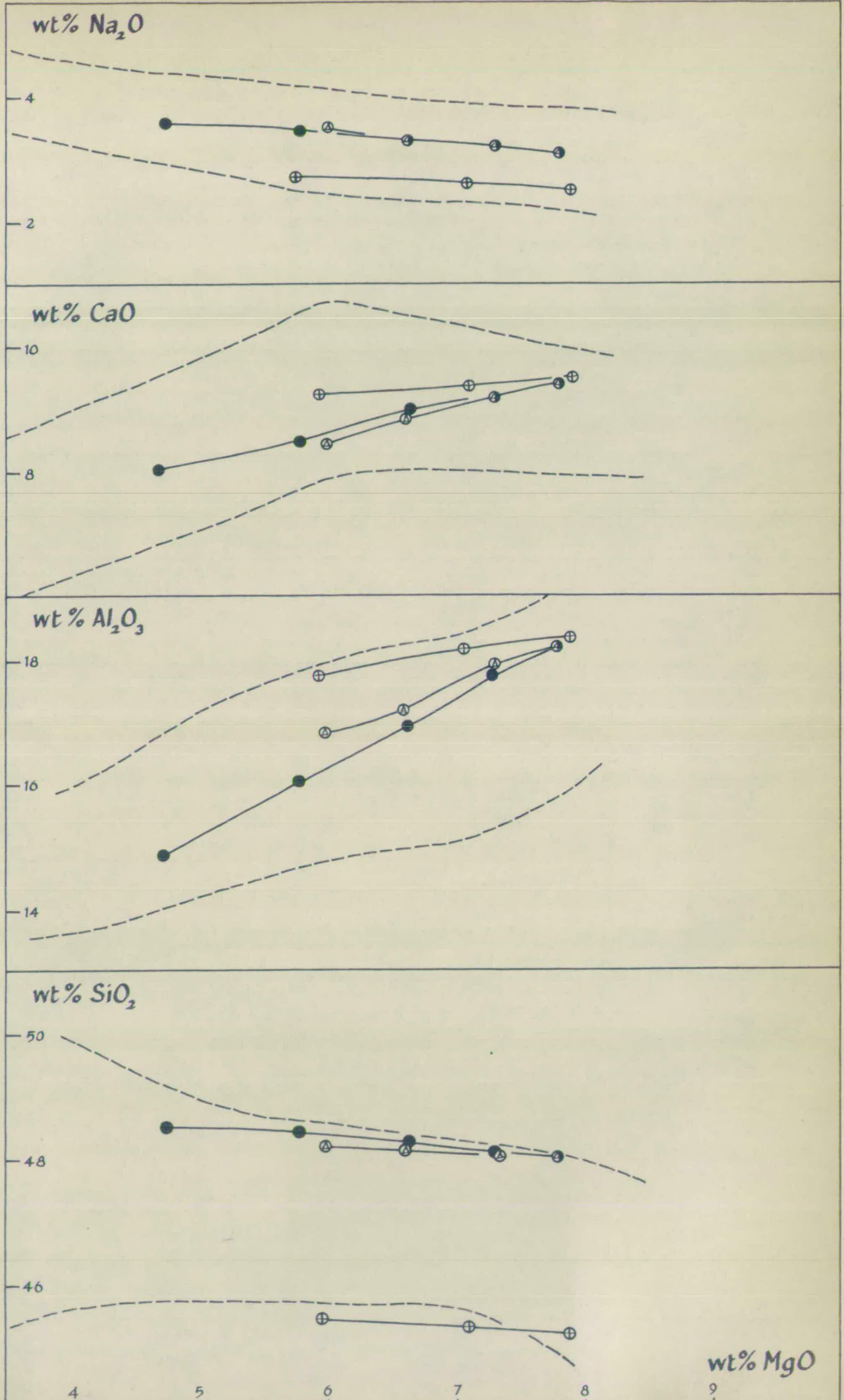
The parental basaltic magmas were below their liquidus temperatures when intruded and carried phenocrysts of plagioclase or olivine plus plagioclase, which suggests they lay in the plagioclase volume or on the olivine-plagioclase cotectic surface and may have suffered some olivine or plagioclase or olivine plus plagioclase fractionation prior to intrusion.

Clinopyroxene does not appear as a phenocryst in the basaltic compositions and its (low pressure) entry is delayed until after that of magnetite and possibly apatite in the trachydolerites (hawaiite-mugearite compositions). Thompson (1972) described similar behaviour for clinopyroxene in some basaltic suites, notably Skye and Snake River, Idaho but suggested that clinopyroxene was involved in the fractionating assemblage at high pressures.

Melting experiments on Gardar dyke rocks have shown that, in the basaltic compositions, the crystallisation of clinopyroxene is delayed relative to that of olivine and plagioclase at low pressures, and that clinopyroxene replaces olivine as the liquidus phase at pressures between 5 and 10 kb (Upton, 1971). Hence the basaltic compositions could have been affected by clinopyroxene fractionation at moderately high pressures (ca. 10kb), although to what extent is uncertain since it is likely that the compositions have been modified during ascent to the present environment.

FIGURE 7.3 (two pages):
Compare with figure 5.6, following page 73; this figure illustrates the effects of adding up to 20 percent aluminous clinopyroxene to the 'normal' extract of olivine and plagioclase.


100
wt% liquid remaining
50
0
2
wt% K_2O
1
14
wt% Fe as FeO
12
10
4
5
6
7
8
9
wt% MgO


wt% Na_2O
4
2
wt% CaO
10
8
wt% Al_2O_3
18
16
14
wt% SiO_2
50
48
46
4
5
6
7
8
9
wt% MgO

If, as is likely, there has been an episode of clinopyroxene fractionation at moderately high pressures it must have occurred prior to the eruption of the basaltic compositions and all subsequent differentiation from basaltic to hawaiitic compositions took place at low pressures. Clinopyroxene fractionation at moderately high pressures has been suggested as one mechanism whereby basaltic magmas can be enriched in Al to produce magmas capable of crystallising anorthosite (Emslie and Lindsley, 1969). The Gardar rocks are most aluminous at approximately 8% MgO, the Al_2O_3 content decreasing at higher and lower levels of MgO. The decrease in Al_2O_3 with decreasing MgO is an indication that clinopyroxene cannot be involved in the fractionating assemblage to any great extent during the production of the hawaiitic compositions from the basaltic compositions, since the Al_2O_3 content would then be likely to rise.

In fact, up to 20% aluminous clinopyroxene could be added to the 'normal' extract of olivine and plagioclase without producing residual liquids outside the field of Gardar compositions, but the CaO content would fall throughout instead of remaining steady at the basaltic stage as it appears to do (fig.7.3).

Turning now to the possibility of clinopyroxene fractionation prior to the ascent of the basaltic magmas to higher levels in the crust, O'Hara (1968) has suggested that the fractionation of clinopyroxene alone at moderate pressures is confined to liquids committed to the nepheline normative volume. If this restriction

is valid, then any clinopyroxene fractionation occurring in the critically undersaturated Gardar magmas at high pressures should have been accompanied by olivine fractionation.

7.3.3. Formation and fractionation of magmas at high pressures

Continental basalts may be assumed to originate in the upper mantle, although the possibility exists for the modification of the magmas by interaction with the continental crust. There is little information available as yet on the Sr^{87}/Sr^{86} ratios of the basic dykes. Van Breemen and Upton (1972) report an initial ratio of 0.7024 $\pm$ 0.0010 for the chilled syenogabbro facies of the Hviddal dyke, which is consistent with a mantle or deep crustal origin. Thus significant crustal contamination seems unlikely to have occurred.

Experimental work at high pressures sets some limitations on the nature of the processes influencing the production and evolution of magmas at high pressures in the mantle, although the processes are but poorly known.

Current estimates of the composition of the upper mantle are based on geophysical and experimental evidence and on the evidence of naturally occurring peridotites which bear evidence of equilibration at very high pressures, as nodules in volcanic rocks or as Alpine-type peridotite bodies (Ringwood, 1966; Harris, 1967; O'Hara, 1968, 1970; O'Hara et al., 1971). All converge on a peridotitic upper mantle composition. Reviews of various upper mantle models are given by O'Hara (1968, 1970) who proposes

an upper mantle model based on the composition of garnet lherzolite nodules found in kimberlite.

Because of the geometrical complexities involved in portraying phase relationships in natural rock compositions, O'Hara (1968) devised a projection scheme whereby the major components of natural rocks were reduced by recalculation to four end member components thus:

$$wt\%\ C = 56.08\ x(\text{molar prop. } CaO - 3\tfrac{1}{3}P_2O_5 + 2Na_2O + 2K_2O)$$

$$wt\%\ M = 40.311\ x\ (\text{molar prop. } MgO + FeO + MnO + NiO - TiO_2)$$

$$wt\%\ A = 101.961\ x(\text{molar prop. } Al_2O_3 + Cr_2O_3 + Fe_2O_3 + TiO_2 + Na_2O + K_2O)$$

$$wt\%\ S = 60.085\ x(\text{molar prop. } SiO_2 - 2Na_2O - 2K_2O)$$

This system is an analogue of the synthetic system $CaO - MgO - Al_2O_3 - SiO_2$. Basic and ultrabasic rock compositions and mineral compositions can be represented within the tetrahedron and their phase relationships and crystallisation paths displayed by projections towards or from mineral compositions onto suitable planes within the tetrahedron. Experimental data on the melting of natural and synthetic peridotites and basalts were used to contruct phase diagrams showing the character of the liquid formed on partial melting of peridotite of likely mantle composition at various pressures (O'Hara, 1968).

This projection scheme could be used to investigate the relationship of suites of basaltic rocks to the experimentally determined phase boundaries at different pressures and to show the possible fractionation paths, under isobaric and polybaric conditions, of

the initial partial melts formed at high pressures.

The composition of the liquid produced on partial melting of mantle peridotite is influenced by a number of factors, including: the pressure (depth) at which melting occurs and therefore the character of the phases stable; the degree of melting and order in which minerals are withdrawn into the melt; the presence of H_2O and CO_2 and the bulk composition of the peridotite.

The initial melt under hydrous conditions is silica-rich (Kushiro et al. 1972; Nicholls and Ringwood, 1973; Green, 1973). As the proportion of H_2O in the melt drops the melt becomes less silica-rich. The presence of CO_2 in the hydrous system, however, increases the solidus temperature of peridotite and tends to produce a less silica-saturated melt (Eggler, 1973).

The position of the cotectics shown in figures 7.4 and 7.5 are taken from O'Hara, (1968) and demonstrate the variation with pressure in the composition of the initial partial melt formed in equilibrium with the four phases of an anhydrous aluminous lherzolite (olivine + clinopyroxene + orthopyroxene + garnet, spinel or plagioclase, depending on pressure). The composition of the initial liquid formed becomes increasingly picritic and undersaturated, from hypersthene normative at pressures less than 8 kb to (just) nepheline normative between 10 and 20 kb (Ito and Kennedy, 1967; O'Hara, 1968; Kushiro, 1972). At pressures greater than 20 kb, Kushiro believed that the degree of

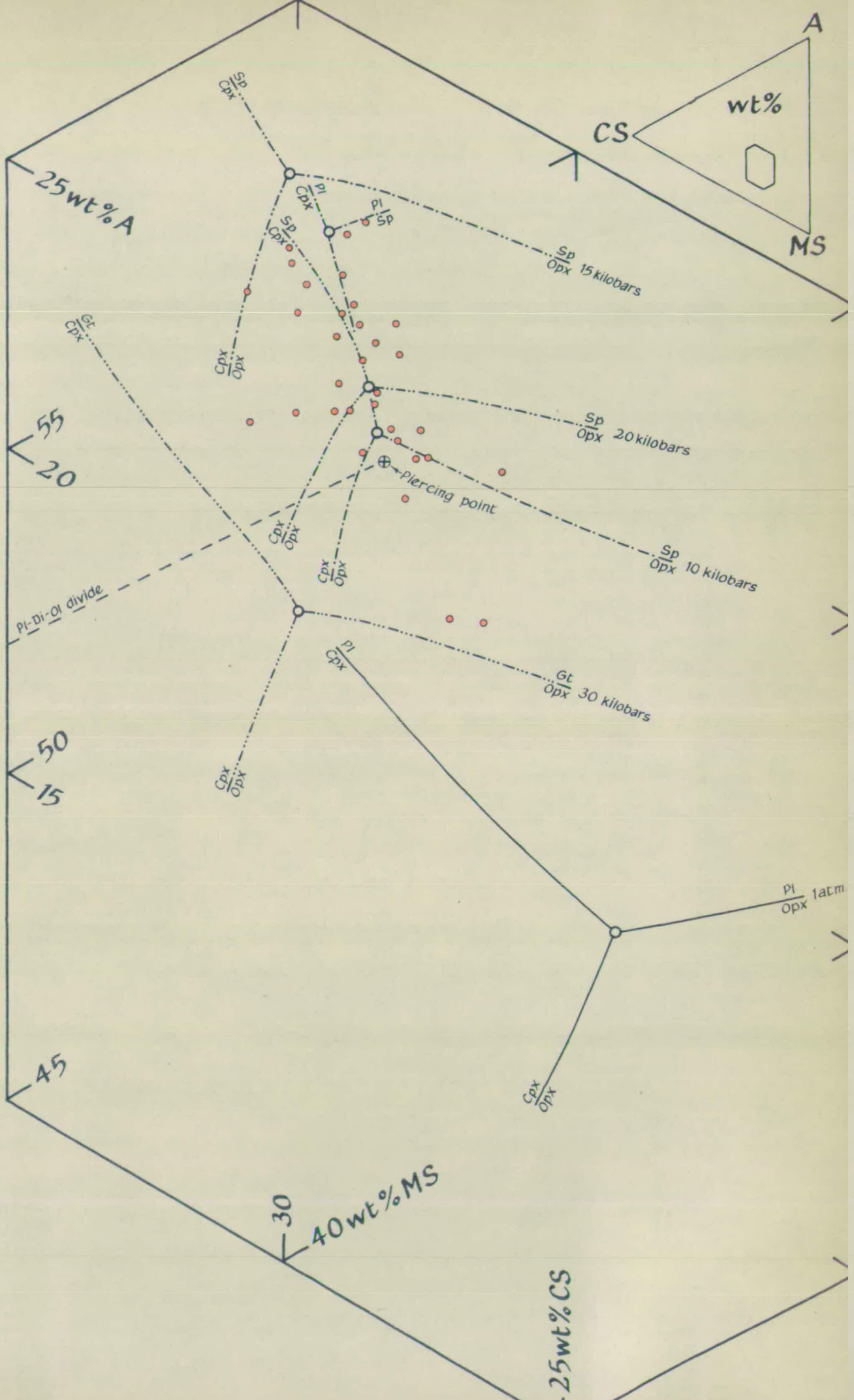
undersaturation continued to increase, but Davis and Schairer (1965), Ito and Kennedy and O'Hara found that at 30 kb the initial melt was hypersthene normative and picritic. As the degree of melting increases, the liquid becomes increasingly picritic and is hypersthene normative at all pressures (O'Hara, 1968).

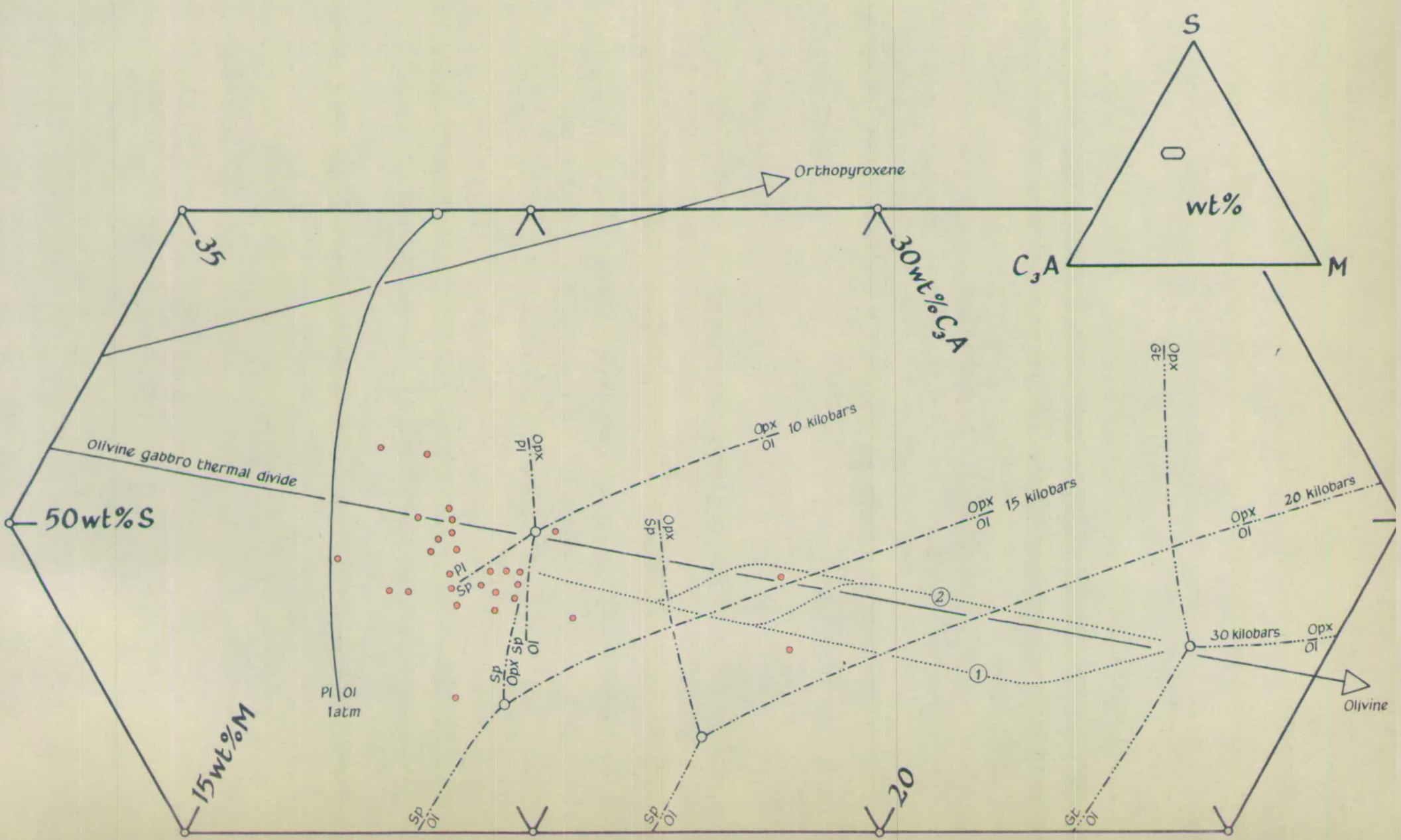
The movement of the invariant point with decreasing pressure potentially allows hypersthene-normative liquids formed at higher pressures to fractionate across the olivine-diopside-plagioclase join to silica undersaturated compositions, if the ascent is slow enough to allow the liquids to equilibrate to the ever-changing invariant point.

The liquid in the intermediate pressure range (ca. 10 to 20 kb.) has a high ratio of plagioclase to augite in the norm because of the expansion of the clinopyroxene volume to compositions poor in normative augite, this ratio decreasing at pressures above 20 kb and below 10 kb. Thus the liquid formed in the pressure range 10 to 20 kb., if brought to the surface rapidly with only olivine fractionation, would tend to show the phenocryst sequence, 1: olivine, 2: olivine plus plagioclase (O'Hara, 1968).

Figures 7.4 and 7.5 show the Gardar rocks (DI less than 35) projected in CMAS (after O'Hara, 1968). Figure 7.4 is a projection from olivine (M_2S) into the plane CS-MS-A of CMAS, figure 7.5 a projection from diopside (CMS_2) into the plane C_3A-M-S of CMAS. Only compositions with DI less than 35 have been projected, because the projection scheme breaks down with increasing Na/Ca

FIGURES 7.4 and 7.5 (two pages):
Gardar basaltic compositions projected in CMAS after O'Hara, 1968. See text for details.
Dotted lines labelled '1' and '2' on figure 7.5 relate to paragraphs, similarly numbered, on page 112.


A
wt%
CS
MS
25wt%A
Sp/Cpx
Pl/Cpx
Pl/Sp
Sp/Opx 15 kilobars
Gt/Cpx
Cpx/Opx
55
20
Sp/Opx 20 kilobars
Piercing point
Cpx/Opx
Sp/Opx 10 kilobars
Pl-Di-Ol divide
Pl/Cpx
Gt/Opx 30 kilobars
50
15
Cpx/Opx
Pl/Opx 1atm
45
30
40wt%MS
25wt%CS


S
wt%
C3A
M
Orthopyroxene
35
30wt%C3A
50wt%S
15wt%M
20
Olivine gabbro thermal divide
Pl/Ol 1atm
Opx/Ol 10 kilobars
Opx/Ol 15 kilobars
Opx/Ol 20 kilobars
30 kilobars
Opx/Gt
Pl/Opx
Sp/Opx
Sp/Ol
Gt/Ol
Olivine

ratios.

An essential feature of the Gardar rocks is that they are critically undersaturated, ie. lie close to the olivine-gabbro divide, which approximates to a thermal divide at pressures less than 8 kb. They are also poor in normative diopside and have high Al/Ca ratios, and this is shown by their position in fig.7.4.

This character was presumably attained in the intermediate pressure range, but as it has been noted above that the least-differentiated Gardar compositions do not have olivine on the liquidus at 10 kb., they cannot be in equilibrium with mantle peridotite at that pressure or above.

The elongated trend towards orthopyroxene displayed by the projected points in fig.7.4 is due to the obliquity of the plane CS-MS-A to olivine. If the elongation is ignored it can be seen that the points form a tight cluster around the projected positions of the 10 and 20 kb. cotectics, suggesting that fractionation of olivine from an appropriate liquid in this pressure range could produce compositions like the parental Gardar liquids.

In fig.7.5 the projected points again form a relatively close cluster, and most are not within the olivine primary phase volume at pressures greater than 10 kb. Those which do lie within the primary phase volume of olivine at higher pressures are relatively coarse grained dolerites and may not represent liquid compositions.

It has been suggested in a previous section that the Gardar basalts could have suffered a period of olivine plus clinopyroxene fractionation at comparatively high pressures (ca. 10kb or greater) prior to their intrusion. There is no evidence of clinopyroxene control on the distribution of the points in fig 5.4 and it may be argued that since high Al/Ca ratios are characteristic of liquids in the intermediate pressure range, there is no need to postulate clinopyroxene fractionation to explain the calcium-poor nature of the rocks. However this does not rule out the possibility of clinopyroxene + olivine (± spinel) fractionation having occurred at these pressures, followed by eruption to lower pressures with concomitant olivine fractionation, as the primary phase volume of olivine expanded and that of clinopyroxene contracted with decreasing pressure. Gabbro fractionation at slightly lower pressures (ca. 8 kb.) prior to eruption is unlikely, since the early fractionation of plagioclase would modify the Al/Ca ratios and clinopyroxene phenocrysts are characteristically absent.

Formation of the primary magmas by partial melting in the intermediate pressure range would demand a high geothermal gradient, but a similar liquid would be obtained if a liquid formed at some higher pressure underwent equilibration in the intermediate pressure range, or had risen slowly enough to modify its composition to remain in equilibrium with the mantle. Thus possible evolutionary paths could involve: formation and segration of the liquid at high pressure, possibly 30 kb. or greater, then:

1. Relatively slow ascent with fractionation of harzburgite then lherzolite, sufficient to keep the liquid close to the olivine gabbro divide, followed by a period of olivine + clinopyroxene fractionation, possibly at the base of the crust and subsequent more rapid ascent within the primary phase volume of olivine.
2. Alternatively the liquid could ascend more rapidly to pressures less than 20 kb with fractionation of olivine alone, followed by a period of lherzolite fractionation to modify the liquid towards critically undersaturated compositions before the onset of olivine + clinopyroxene fractionation.

However, lacking high pressure xenoliths which could be cumulate sequences, these fractionation paths are speculative.

7.4. The incompatible elements

The abundance patterns of the incompatible elements K, Ba, Sr, Rb, P, Zr and Ti may be expected to give information about the processes involved in the production of the Gardar magmas. Because of their high liquid-crystal distribution coefficients the incompatible elements are strongly concentrated in the first liquid fraction on partial melting (Gast, 1968; Griffin and Murthy, 1969) and further melting has a dilution effect. The inter-element abundance ratios can vary considerably during the first

few degrees of melting (Gast, 1968), but such liquids are unlikely to be easily extracted. During fractional crystallisation the incompatible elements are concentrated in the residual liquid and, providing perfect incompatibility is maintained, the residual liquid retains the ratios of the primary magma. Variations in the content of minor phases such as phlogopite, amphibole, zircon and apatite, in which the incompatible elements are principally contained, may be expected to have a considerable effect on the abundance patterns in the derivative liquids (eg. Thompson, et al. 1972).

Amphibole is believed to be stable at depths less than approximately 100 km in the upper mantle, under hydrous (vapour present) conditions, (Varne, 1970; Kushiro, 1969). Phlogopite is believed to be stable to greater depths, up to 175 kms depending on the geothermal gradient (Modreski, 1972). Yoder and Kushiro (1969) found that the stability field of phlogopite was extended under vapour-absent conditions and similarly in the presence of CO_2 (Yoder, 1969). Titaniferous phlogopite is more stable than the Ti-free variety and does not break down at the temperature of the peridotite solidus at pressures less than 25 kb (Forbes and Flower, 1974). Hence the initial partial melt of a phlogopite-bearing peridotite would be depleted in those elements which are preferentially held in phlogopite (K, Rb, Ba and Ti). This implies it is possible to produce liquids having Rb/Sr ratios lower than those of the source mantle (O'Nions and Pankhurst, 1974). With increasing temperature the Rb/Sr ratio of the melt

would increase, as the phlogopite was withdrawn into the melt.

Thus there are four principal influences on the content of incompatible elements in magmas: the composition of the source mantle, the degree of partial melting and the pressure at which it occurs and any subsequent fractionation. In continental areas high levels of K and related elements may result from assimilation of sialic material; the extent of assimilation can be judged from the values of Rb/Sr and Sr^{87}/Sr^{86} ratios.

7.4.1. Abundance variations

It has been suggested in section 7.1 that there is a variation in the content of K in the Gardar parental magmas, although the proportion with high K contents is comparatively small. High levels of K are generally accompanied by high levels of P, Ti, Ba, Sr and Rb.

Contamination with crustal material on any but a small scale can be eliminated: the Rb/Sr ratios are low in all the basaltic rocks (less than 0.08) which rules out significant contamination by a Rb-enriched source: van Breemen et al. (1974) report Rb contents of 53 to 137 ppm. for the Julianehaab granite, the country rock for the southern (Tugtutoq) swarm and part of the Nunarssuit swarm.

Significant inhomogeneity in the source mantle can be ruled out: K-rich rocks occur in all three zones and the linear relationships between the incompatible elements (fig.7.6) implies there

FIGURE 7.6 (end pocket):
Incompatible-element variation diagrams.

Filled circles: basaltic compositions with DI under 35.
Crosses: trachydolerites with DI between 35 and 50.
Triangles: trachydolerites and syengabbros with DI over 50.

were not significant differences in the ratios of these elements in the source magmas. This in turn may indicate that the rocks are related by partial melting and/or fractional crystallisation mechanisms. Very small degrees of melting are ruled out, however, because of the similarity of the inter-element ratios.

The limitations imposed on partial melting and fractional crystallisation models by the incompatible element content of the most primitive Gardar rocks will be considered in terms of an estimated mantle composition (given in table 7.3a). Also given are the estimated contents of K, Rb, Sr and Ba in a mantle containing minor amounts of phlogopite (from Griffin and Murthy, 1969).

The minimum amount of liquid which was capable of segregation will be taken to be approximately 5%, since the inter-element abundance ratios do not vary in the Gardar rocks. 5% melting can produce liquids enriched in incompatible elements by a factor of 17 over the source mantle; the enrichment factor drops to 4 at 20% melting (Jamieson and Clarke, 1970; O'Hara, 1968). Table 7.4 shows the enrichment factors for the incompatible elements in a range of the most primitive Gardar rocks.

Enrichment factor: $E = \frac{\text{concentration in liquid (rock)}}{\text{concentration in mantle}}$

The enrichment factors which can be produced by different degrees of melting are shown in table 7.3b.

A maximum of 40% fractionation (principally of olivine $\pm$ clinopyroxene) will be assumed to have occurred since the liquids were

Table 7.3a

Trace element abundances in Mantle peridotites

TiO_2	0.26% by wt.	
P_2O_5	0.02%	Carswell and Dawson, 1970
Na_2O	0.17%	

K ppm	106	
Ba	14	Griffin and Murthy, 1969
Sr	15	
Rb	0.48	

Zr	30	Vinogradev, 1962

Hydrous mantle with 0.2% phlogopite

K	248
Ba	17
Sr	15
Rb	0.98

Griffin and Murthy, 1969

Hydrous mantle with 0.5% phlogopite

K	464
Ba	21
Sr	15
Rb	1.76

Table 7.3 b

Enrichment factors for K, Ba, Sr and Rb during partial melting

	5% melting	10% melting	20% melting
K	18	10	5
Ba	18	9	5
Sr	17	9	5
Rb	16	9	4
Mean	17	9	5

Table 7.4

Enrichment factors in a range of Gardar Basaltic compositions (calculated relative to the phlogopite-free mantle composition)

	101407	101338	101345	101369	101347	101426	20632	101471	40452	50033	86107
TiO_2	4	7	6	6	7	7	6	9	9	10	10
P_2O_5	11	14	16	16	19	16	16	43	33	42	45
Na_2O	19	19	17	19	21	20	15	21	18.2	19	19
K ppm	30	32	46	73	60	57	67	92	72	89	99
Ba	22	21	21	44	47	46	34	81	-	81	74
Sr	26	27	24	30	44	26	37	61	-	60	55
Rb	29	23	45	50	37	44	31	42	-	35	38
Zr	3	4	4	-	3	5	4	5	-	5	5
MgO*	8.50	7.18	8.20	6.79	6.67	6.29	9.77	7.21	8.2	6.60	6.08
E*	23	23	28	37	38	35	33	57	-	54	55

20632 Equaloqarfia dyke, Nunarssuit: major elements from Pulvertaft (1965), trace elements from Boyd (1974)

40452 chill of a Tugtutoq giant gabbro dyke (Upton, 1964)

86107 chill of a Tugtutoq gabbro dyke (Upton, pers.comm.)

50033 " " " " " " " " "

Specimen numbers with the prefix 101 refer to analyses in Appendix 4.

E* = average enrichment factor calculated after exclusion of values less than 10.

(MgO* wt. %. these figures are not enrichment factors.)

Table 7.5.

Enrichment factors for some parental compositions calculated on the basis of the phlogopite-bearing mantle compositions

Mantle with 0.2% phlogopite

Specimen No.	101407	101388	20632
K	13	14	28
Ba	18	18	30
Sr	26	27	35
Rb	14	11	15

Mantle with 0.5% phlogopite

K	7	7	15
Ba	15	15	24
Sr	26	27	35
Rb	8	6	9

segregated (cf. O'Hara, 1968) and the limits to melting will be taken as 5 to 20%. 40% fractionation from liquids with enrichment factors in the residual liquid of 8 to 28. **

Considering first the K-poor parents (ie. those with K_2O contents of ca. 0.5%) which constitute the majority of the Gardar parent magmas: the average E for these rocks is 25, excluding those elements with E less than 10 since these have probably not behaved as true incompatible elements. Both Zr and Ti have very low enrichment factors, suggesting that pyroxene may have been involved in fractionation at some stage. With the limits to partial melting and fractionation suggested above, the K-poor parents can be produced from the phlogopite-free mantle composition by approximately 7% melting and up to 40% further fractionation.

Turning now to the K-rich compositions (those with ca.1% K_2O), it can be seen that the average E for these compositions is larger by factors between 1.4 and 1.6 than in K-poor compositions with a similar MgO content. This level of enrichment would require 33% further fractionation from a parent magma similar to that producing the K-poor compositions, and the major element compositions would not be similar. The differences in E could possibly be accounted for by different degrees of melting, since the average E for the most primitive K-rich composition, 20632, of 33, is only slightly greater than the limit suggested above (E = 28 for 5% partial melting and 40% fractionation). Such variations in the degree of melting should produce the enriched liquids at

** See 'Errata'.

the beginning of a cycle of melting, thus the Tugtutoq rocks could be explained as the products of a new melting episode, but the rare occurrences of K-rich rocks as later intrusions in other zones could not.

If the mantle contained minor amounts of a K-bearing phase such as phlogopite, the levels of enrichment could be more easily accounted for by a partial melting model. The calculated degrees of melting seem somewhat low for the major magmatic episodes involved, although the volume of the products cannot be estimated since the province is deeply dissected.

The liquids produced by partial melting of a phlogopite-bearing assemblage will be enriched in K, Rb and Ba relative to Sr and will have a high Rb/ Sr ratio (Appleton, 1972; O'Nions and Pankhurst, 1974). If the phlogopite remains in the solid phase the initial liquid will be depleted in K, Rb and Ba and enriched in Sr and P compared with the more-advanced melt product and the Rb/Sr ratio will rise as melting continues (O'Nions and Pankhurst, 1974; Forbes and Flower, 1974). If it breaks down at the peridotite solidus the initial melt will be enriched in K, Rb, Ba, P and Ti and the Rb/Sr ratio will be high, decreasing in the more advanced melts.

Neither pattern is apparent in the Gardar compositions. The enrichment of Sr in the parental compositions is not easily accounted for by assuming that the mantle contained minor amounts of phlogopite. Enrichment factors calculated using the

phlogopite-bearing mantle compositions show that the enrichment factor for Sr is nearly double that of the factors for K, Rb and Ba and the discrepancy increases with increasing phlogopite content (table 7.5).

Both K and Rb are enriched in the initial melt of an amphibole-bearing assemblage, with Rb enriched relative to K and as melting proceeds the K/Rb ratio rises, while the absolute values of K and Rb fall (Gast, 1968). Although there does appear to be some variation in K/Rb in the Gardar rocks, in this case the K/Rb rises slightly as K rises.

There seems no compelling reason to postulate the presence of amphibole in the mantle to explain the incompatible element content of the Gardar rocks. Partial melting of peridotite under hydrous conditions such as those required to stabilise amphibole in the mantle (Kushiro, 1970) produces silica-rich liquids, but the presence of CO_2 may cause the melt to become undersaturated in silica (Eggler, 1973), so that the presence of hydrous phases such as amphibole cannot be ruled out on the grounds of the critically undersaturated nature of the Gardar basalts.

Essentially, if both the K-rich and K-poor rocks are to be derived from a similar mantle composition, the process invoked must be capable of explaining the rather irregular appearance of the K-rich magmas, embracing those formed towards the end of a magmatic episode.

It may be significant that the enrichment factor for Na is similar in both the K-rich and K-poor rocks. This may imply the involvement of omphacitic pyroxene in production of the magmas, either in partial melting or in fractionation. The fractionation of a mixture of omphacitic pyroxene and garnet at pressures greater than ca. 25 kb has been suggested by O'Hara (1968) as a means of varying the incompatible element content of basaltic magmas. The major element composition of the eclogite is close to the composition of the liquid and thus fractionation produces little change in the major elements. O'Hara considers it would be possible to crystallise ca. 50% of the original liquid as eclogite without great changes occurring in the major element composition, although extreme fractionation could produce potassic mafic compositions, for example kimberlitic liquids.

The consequences of eclogite fractionation have been described by O'Hara and Yoder (1967). One consequence is the raising of the K/Na ratio because of the extraction of Na in omphacitic pyroxene and this is what is seen in the Gardar basaltic compositions; the K-rich rocks have a higher K/Na ratio (because similar Na) than the K-poor rocks (fig.7.7). The K/Na ratio also rises during low-pressure fractionation because Na is removed in plagioclase, but this could not produce K-rich basaltic compositions. Another effect of eclogite fractionation would be the derivation of nepheline-normative liquids from the hypersthene-normative liquids produced by partial melting at high pressure (O'Hara, 1968;

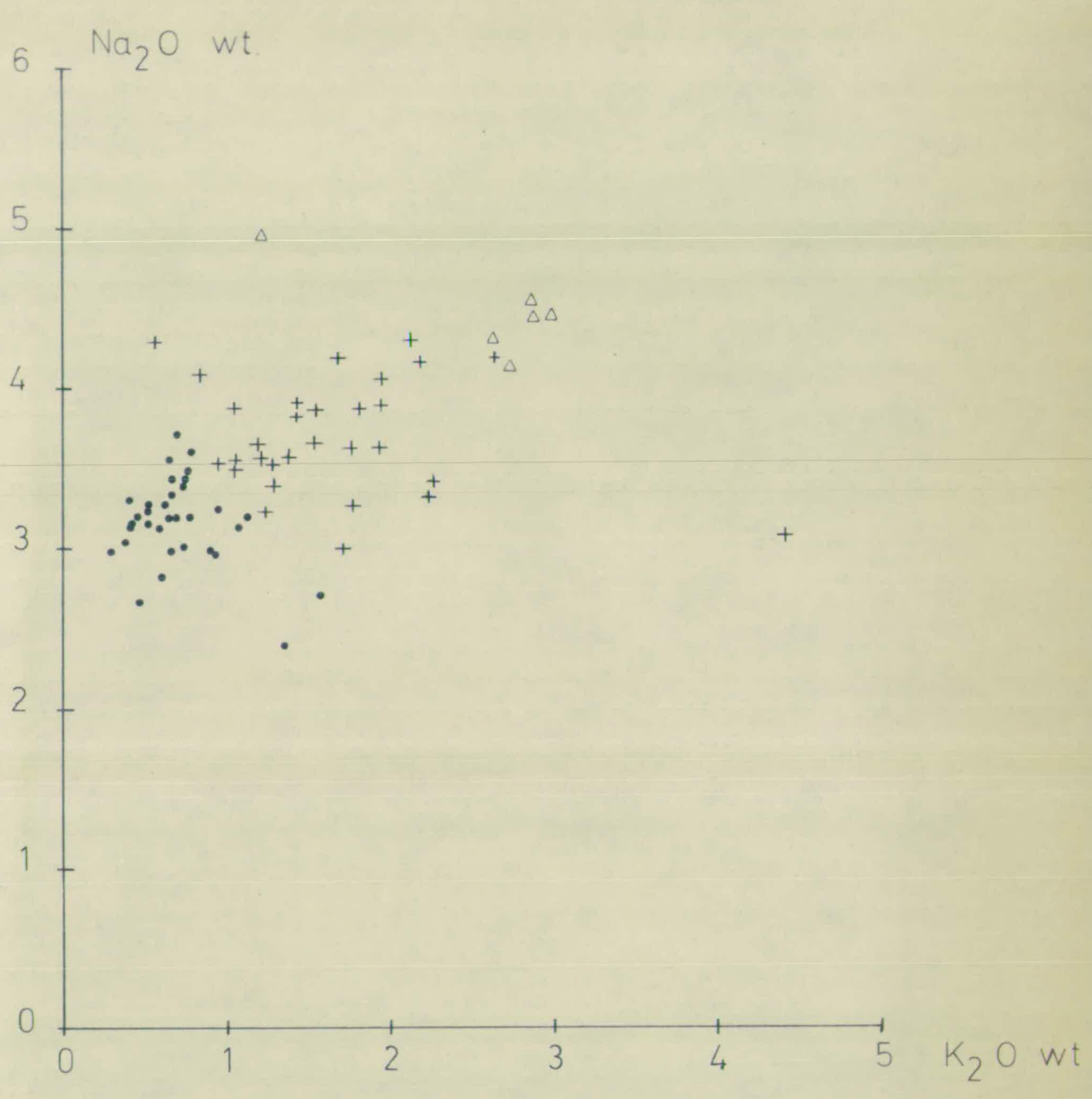
FIGURE 7.7:

Na_2O - K_2O variation diagram for Gardar dyke-rocks.

Filled circles: basaltic compositions with DI under 35.

Crosses: trachydolerites with DI between 35 and 50.

Triangles: trachydolerites and syenogabbros with DI over 50.


Na2O wt.
6
5
4
3
2
1
0
0
1
2
3
4
5
K2O wt

O'Hara and Yoder, 1967). This could explain the generally lower Si contents of the K-rich rocks relative to those of the K-poor.

In terms of a partial melting/fractionation model, using the same mantle composition and limitations on fractionation suggested for the K-poor primary magmas, the possibilities for eclogite fraction include the following:

a. 5% melting (E = 17); 25% eclogite fractionation (E = 23); 40 further fractionation (E = 38).

or

b. 10% melting (E = 9); 60% eclogite fractionation (E = 23); 40 further fractionation (E = 38).

Thus eclogite fractionation is capable of explaining the enrichment in incompatible elements and could explain the appearance of the enriched liquids later in the magmatic cycle, as liquids retained at depth. Upton and Thomas (1973) suggested that the incompatible element content of the potassic ultramafic intrusions in the Narssaq gabbro may have resulted from extensive eclogite fractionation.

The mechanism may, however, be criticised on the grounds of the volume reduction required to produce the required enrichment factors. As the original volume of the magma cannot be estimated this does not necessarily imply that eclogite fractionation could not, therefore have occurred.

Mechanisms of enrichment such as wall-rock reaction (Green and Ringwood, 1967c) and zone refining (Harris, 1957, Harris and

Middlemost, 1970), which essentially depend on the reaction of the liquid with the mantle through which it ascends, have been questioned by Gast (1968) and O'Hara (1968) on the grounds of their effectiveness over a period of magma genesis.

If wall rock reaction normally operates during the ascent of a magma batch, one might question why the earlier batches in the Ivigtut and Nunarssuit zones are comparatively poor in incompatible elements. In the case of zone refining, the degree of enrichment is proportional to the distance traversed by the magma (Harris, 1957). This would require that either the K-rich magmas had been produced at a greater depth, or that they had reached a lower pressure environment before eruption, than the K-poor rocks. Since the major element chemistry is controlled by the final pressure of equilibration the latter alternative can be discounted in the case of the Gardar rocks, which are little different in terms of major elements.

7.4.2. Conclusions

Criteria for distinguishing between the mechanisms which are suggested to be capable of producing variations in incompatible element abundances in magmas are largely absent. However, on the basis of the incompatible element abundances in the Gardar rocks, it is suggested that the variation in these elements in the basaltic parents may be produced by variable degrees of eclogite fractionation from the liquid produced by partial melting of a garnet lherzolite mantle at high pressures. Variable

degrees of melting are also capable of generating variations in incompatible element abundances, but do not explain the irregular appearance of the incompatible-element enriched magmas, including those formed towards the end of a magmatic episode.

The variation in the incompatible elements is not considered to be compatible with the significant involvement of phlogopite during melting, since this should generate high Rb/Sr ratios and would not explain the enrichment in Sr together with K, Rb and Ba.

It has been suggested that the low CaO content of the parental basaltic liquids was inherited from a period of clinopyroxene plus olivine fractionation at comparatively high pressures, perhaps equivalent to the base of the crust, but modification of the liquids by low-pressure fractionation of olivine or olivine plus plagioclase means it is difficult to estimate the extent of this proposed fractionation episode.

Fractionation of olivine and plagioclase at low pressures, (with formation of anorthosite by accumulation of the plagioclase) plus or minus magnetite, clinopyroxene and apatite produced a range of basaltic to trachybasaltic liquids which formed the basic dykes.

REFERENCES.

Ade-Hall, J. M. and Lawley, E. A. 1969. An unsolved problem: opaque petrological differences between Tertiary basaltic dykes and lavas. In: Newall, G. and Rast, N. (Eds), Mechanism of Igneous Intrusion. Geol. J. Spec. Issue 2, 217-230.

Allaart, J. H. 1967. Basic and intermediate igneous activity and its relationships to the evolution of the Julianehaab granite, South Greenland. Meddr. Grønland, 175, No. 1.

---------- 1969. The chronology and petrography of the Gardar dykes between Igaliko Fjord and Redekammem, South Greenland. Rapp. Grønlands geol. Unders., 25.

---------- 1973. Description accompanying geological map of Greenland: Julianehaab 60 V.2 Nord, 1:100,000. Greenland Geological Survey, Copenhagen.

Allaart, J. H., Bridgwater, D., and Henriksen, N. 1969. Pre-Quaternary geology of Southwest Greenland and its bearing on North Atlantic correlation problems. In: North Atlantic - Geology and Continental Drift., 859-882. Am. Assoc. Petroleum Geolog., Memoir 12.

Andermann, G. and Kemp, J. W. 1958. Scattered X-rays as internal standards in X-ray emission spectroscopy. Analyt. Chem., 30, 1306-1309.

Aoki, K. 1963. The kaersutites and oxykaersutites from alkalic rocks of Japan and surrounding areas. J. Petrology, 4, 198-210.

-------- 1970. Petrology of kaersutite-bearing mafic and ultramafic inclusions in Iki Islands, Japan. Contr. Mineral. and Petrol., 25, 270-283.

Aoki, K. and Kushiro, I. 1968. Some clinopyroxenes from ultramafic inclusions in Drieser Weiher, Eifel. Contr. Mineral. and Petrol., 18, 326-337.

Appleton, J. D. 1972. Petrogenesis of the potassium-rich lavas from the Roccamonfina volcano, Roman Region, Italy. J. Petrology, 13, 425-456.

Armstrong, R. L. 1963. K-Ar dates from West Greenland. Geol. Soc. Am. Bull., 74, 1189-1192.

Ayrton, S. N. 1963. A contribution to the geological investigations of the Ivigtût region, S. W. Greenland. Bull. Grønlands geol. Unders., 37. (Meddr. Grønlands, 172, No. 4).

Bailey, D. K. 1974. Continental rifting and alkaline magmatism. In: Sørensen, H. (Ed), The Alkaline Rocks, Interscience, New York.

Bergström, L. 1963. Petrology of the Tjörn area in western Sweden. Sveriges geol. Unders., Ser. C, No. 593.

Berlin, R. and Henderson, C. M. B. 1968. A re-interpretation of Sr and Ca fractionation trends in plagioclase from basaltic rocks. Earth Planet. Sci. Lett., 4, 79-83.

---------- 1969. Distribution of Sr and Ba between alkali feldspar, plagioclase and groundmass of porphyritic trachytes and phonolites. Geochem. Cosmochim. Acta, 33, 247-255.

Berthelsen, A. 1962. On the geology of the country around Ivigtût, S. W. Greenland. Geol. Rundsch., 52, 269-280.

Blaxland, A. B., van Breemen, O., Emeleus, C. H. and Anderson, J. G. In preparation. Age and origin of the major syenite centres in the Gardar province of South Greenland: Rb-Sr studies.

Bondesen, E. and Henriksen, N. 1965. On some Precambrian metadolerites from the central Ivigtût region, Southwest Greenland. Meddr. Grønland, 179, No. 2.

Bottinga, Y. and Weill, D. F. 1970. Densities of liquid silicate systems calculated from partial molar volumes of oxide components. Am. J. Sci., 269, 169-182.

Boyd, W. W. Jr. 1974. Geochemical investigations of composite bodies involving intermediate members of the alkali basalt - trachyte suite. Unpub. Ph. D. thesis, Edinburgh University.

Bridgwater, D. 1965. Isotopic age determinations from South Greenland and their geological setting. Meddr. Grønland, 179, No. 4.

Bridgwater, D. and Coe, K. 1969. The role of stoping in the emplacement of the giant dykes of Isortoq, South Greenland. In: Newall, G. and Rast, N. (Eds), Mechanism of Igneous Intrusion, 67-78, Geol. J. Spec. Issue 2.

Bridgwater, D. and Harry, W. T. 1968. Anorthosite xenoliths and plagioclase megacrysts in Precambrian intrusions in South Greenland. Bull. Grønlands geol. Unders., 77. (Meddr. Grønland, 185, No. 2).

Brown, G. M. 1957. Pyroxenes from the early and middle stages of fractionation of the Skaergaard intrusion, East Greenland. Mineral. Mag., 31, 511-543.

---------- 1967. Mineralogy of basaltic rocks. In: Hess, H. H., and Poldervaart, A., (Eds), Basalts, vol. 1, Interscience, New York, 103-162.

Burnham, C. W. 1967. Hydrothermal fluids at the magmatic stage. In: Barnes, H. (Ed), Geochemistry of Hydrothermal Ore Deposits, 36-76, Holt, Reinhart and Winston, Inc.

Carmichael, I. S. E. 1967. The iron-titanium oxides of salic volcanic rocks and their associated iron-magnesium silicates. Contr. Miner. and Petrol., 14, 36-64.

Carmichael, I. S. E., Turner, F. J. and Verhoogen, J. 1974. Igneous Petrology. International Series in the Earth and Planetary Sciences. McGraw-Hill, New York.

Carswell, D. A. and Dawson, J. B. 1970. South African kimberlite pipes and their petrogenesis. Contr. Mineral. Petrol., 25, 163-184.

Cawthorn, R. G., Ford, C. E., Biggar, G. M., Bravo, M. S. and Clarke, D. B. 1973. Determination of the liquid composition in experimental samples: discrepancies between microprobe analysis and other methods. Earth Planet. Sci. Lett., 21, 1-5.

Clark, S. P., Schairer, J. F. and de Neufville, J. 1962. Phase relations in the system $CaMgSi_2O_6$ - $CaAl_2SiO_6$ at low and high pressure. Carnegie Inst. Wash. Yrbk., 61, 59-68.

Clarke, D. B. 1970. Teritary basalts of Baffin Bay: possible primary magma from the mantle. Contr. Mineral. and Petrol., 25, 203-224.

Cohen, L. H., Ito, K. and Kennedy, G. C. 1967. Melting and phase relations in an anhydrous basalt up to 40kb. Am. J. Sci., 265, 475-518.

Coombes, D. S. 1963. Trends and affinites of basaltic magmas and pyroxenes as illustrated by the diopside-olivine-silica diagram. Miner. Soc. Am. Special Paper 1, 227-250.

Coombes, D. S. and Wilkinson, J. F. G. 1969. Lineages and fractionation trends in undersaturated volcanic rocks from the East Otago volcanic province (New Zealand) and related rocks. J. Petrology, 10, 440-501.

Cox, K. G. and Bell, J. D. 1972. A crystal fractionation model for the basaltic rocks of the New Georgia Group, British Solomon Islands. Contr. Miner. and Petrol., 37, 1-13.

Davis, B. T. C. and Schairer, J. F. 1965. Melting relations in the join diopside-forsterite-pyrope at 40 kilobars and at 1 atmosphere. Carnegie Inst. Wash. Yrbk., 64, 123-126.

Deer, W. A., Howie, R. A. and Zussman, J. 1966. An introduction to the rock-forming minerals. Longmans, London.

Eggler, D. H. 1973. Role of CO_2 in melting processes in the mantle. Carnegie Inst. Wash. Yrbk., 72, 457-467.

Elder, J. W. 1969. Quantitative laboratory studies of dynamical models of igneous intrusion. In: Newall, G. and Rast, N. (Eds), Mechanism of Igneous Intrusion. Geol. J. Spec. Issue 2, 245-260.

Emeleus, C. H. 1964. The Grønnedal-Ika alkaline complex, South Greenland. The structure and geological history of the complex. Bull. Grønlands geol. Unders., 45. (Meddr. Grønland, 172, No. 3).

Emeleus, C. H. and Harry, W. T. 1970. The Igaliko nepheline syenite complex. General description. Bull. Grønlands geol. Unders., 85. (Meddr. Grønland, 186, No. 3).

Emeleus, C. H. and Stephenson, D. 1970. Field work between Tunugliarfik and Tasiussaq. Rapp. Grønlands geol. Unders., 28.

Emeleus, C. H. and Upton, B. G. J. In press. The Gardar period in Southern Greenland.

Emslie, R. F. 1970. The geology of the Michikamau intrusion. Geol. Surv. Can. Pub., paper 68-57.

Emslie, R. F. and Lindsley, D. H. 1969. Experiments bearing on the origin of anorthosite inclusions. Carnegie Inst. Wash. Yrbk., 67, 108-112.

Erlank, A. J. 1968. The terrestrial abundance relationship between K and Rb. In: Ahrens, L. H. (Ed), Origin and Distribution of the Elements, 871-888. Pergamon, Oxford and New York.

Ferguson, J. and Pulvertaft, T. C. R. 1963. Contrasted styles of layering in the Gardar province of South Greenland. Min. Soc. Amer. Spec. Pap. 1 (I. M. A.), 10-21.

Flanagan, F. J. 1969. U. S. Geological Survey standards - 2. First compilation of data for the new U. S. G. S. rocks. Geochim. cosmochim. Acta, 33, 81-120.

Fleischer, M. 1969. U. S. Geological Survey standards - 1. Additional data on rocks G-1 and W-1, 1965-1967. Geochim. cosmochim. Acta, 33, 65-79.

Forbes, W. C. and Flower, M. F. 1974. Phase relations of titaniferous phlogopite: a refactory phase in the upper mantle? Earth Planet. Sci. Lett., 22, 60-66.

Fratta, M. and Shaw, D. M. 1974. Residence contamination of K, Rb, Li and Tl in diabase rocks. Can. J. Earth Sci., 11, 422-429.

Gass, I. G. 1970. Tectonic and magmatic evolution of the Afro-Arabian dome. In: Clifford, T. N. and Gass, I. G. (Eds), African Magmatism and Tectonics. Oliver and Boyd, Edinburgh, 285-300.

Gast, P. W. 1968. Trace element fractionation and the origin of tholeiitic and alkaline magma types. Geochim. cosmochim. Acta, 32, 1057-1086.

Gibb, F.G. F. 1973. The zoned clinopyroxenes of the Shiant Isles sill, Scotland. J. Petrology, 14, 203-230.

Gill R. C. O. 1972a. The geochemistry of the Grønnedal-Ika alkaline complex, South Greenland. Unpubl. Ph. D. thesis, University of Durham, England.

---------- 1972b. Chemistry of peralkaline phonolitic dykes from the Grønnedal-Ika area, South Greenland. Contr. Mineral. and Petrol., 34, 87-100.

Gorbatschev, R. 1961. Dolerites of the Eskilstuna region, Eastern central Sweden. Sveriges geol. Unders., Arsbok 55 (1961), No. 4, Ser. C, No. 580.

Green, D. H. 1973. Experimental melting studies on a model upper mantle composition at high pressure under water-saturated and water-understaurated conditions. Earth Planet. Sci. Lett., 19, 37-53.

Green, T. and Ringwood, A. E. 1967a. Crystallisation of basalt and andesite under high pressure hydrous conditions. Earth Planet. Sci. Lett., 3, 481-489.

---------- 1967b. The stability fields of aluminous pyroxene peridotite and garnet peridotite and their relevance to upper mantle structure. Earth Planet. Sci. Lett., 3, 151-160.

---------- 1967c. The genesis of basaltic magma. Contr. Mineral. and Petrol., 15, 103-190.

Griffin, W. L. and Murthy, V. R. 1969. Distribution of K, Rb, Sr and Ba in some minerals relevant to basalt genesis. Geochim. cosmochim. Acta, 33, 1389-1414.

Grout, F. F. and Schwartz, G. M. 1939. The geology of the anorthosites of the Minnesota coast of Lake Superior. Bull. geol. Surv. Minnesota, 28, 1-116.

Haggerty, S. E. and Baker, I. 1967. The alteration of olivine in basaltic and associated lavas. Part 1, high temperature alteration. Contr. Mineral. and Petrol., 16, 233-257.

Hamilton, D. L. and Anderson, G. M. 1967. Effects of water and oxygen pressure of the crystallisation of basaltic magmas. In: Hess, H. H. and Poldervaart, A. (Eds), Basalts, vol. 1, 445-482. Interscience, New York.

Hamilton, W. 1965. Diabase sheets of the Taylor Glacier region, Victoria Land, Antarctica. Prof. Pap. U. S. Geol. Surv., 456-B, 1-71.

Harris, P. G. 1957. Zone refining and the origin of potassic basalts. Geochim. cosmochim. Acta, 12, 195-208.

---------- 1967. Segregation processes in the upper mantle. In: Runcorn, S. K. (Ed), Mantles of the Earth and Terrestrial Planets, 305-317. Interscience, New York.

---------- 1969. Basalt type and African rift valley tectonism. Tectonophysics, 8, 427-436.

Harris, P. G. and Middlemost, E. A. K. 1970. The evolution of kimberlites. Lithos, 3, 77-88.

Harris, P. G., Reay, A. and White, I. G. 1967. Chemical composition of the upper mantle. J. Geophys. Res., 72, 6359-6369.

Harry, W. T. and Pulvartaft, T. C. R. 1963. The Nunarssuit intrusive complex, South Greenland. Part 1. Bull. Grønlands geol. Unders., 36. (Meddr. Grønland, 169, No. 1).

Hart, S. R. and Aldrich, L. T. 1967. Fractionation of K/Rb by amphiboles: implications regarding mantle composition. Science, 155, 325-327.

Henriksen, N. 1960. Structural analysis of a fault in Southwest Greenland. Bull. Grønland geol. Unders., 26. (Meddr. Grønland, 162, No. 9).

Higgins, A. K. and Bondesen, E. 1966. Supracrustals of pre-Ketilidian age (the Tartoq group) and their relationships with Ketilidian supracrustals in the Ivigtut region, Southwest Greenland. Rapp. Grønlands geol. Unders., 8.

Holloway, J. R. and Burnham, C. W. 1972. Melting relations of basalt with equilibrium water pressure less than total pressure. J. Petrology, 13, 1-29.

Hytonen, K. and Schairer, J. F. 1961. The plane enstatite-anorthite- diopside and its relation to basalts. Carnegie Inst. Wash. Yrbk., 60, 125-139.

Jahns, R. H. and Burnham, C. W. 1969. Experimental studies of pegmatite gensis : 1. A model for the derivation and crystallisation of granitic pegmatites. Econ. Geol., 64, 843-863.

Jamieson, B. G. and Clarke, D. B. 1970. Potassium and associated elements in tholeiitic basalts. J. Petrology, 11, 183-204.

Jenkins, R. and de Vries, J. L. 1967. Practical X-ray spectrometry. Springer-Verlag, New York. 186pp.

Kennedy, G. C. 1955. Some aspects of the role of water in rock melts. In: Poldervaart, A. (Ed), Crust of the Earth - A Symposium. Spec. Pap. geol. Soc. Am., 62, 489-503.

Kogarko, L. N. 1974. The role of volatiles. In: Sørensen, H. (Ed), The Alkaline Rocks, 474-487. Wiley-Interscience, New York.

Krokstrom, T. 1932. The Breven dolerite dyke. Bull. Geol. Inst. Uppsala, 23, 242-330.

---------- 1936. The Halleförs dolerite dyke and some problems of basaltic rocks. Bull. Geol. Inst. Uppsala, 26, 113-263.

Kushiro, I. 1962. Clinopyroxene solid solutions. Part 1. The $CaAl_2SiO_6$ component. Jap. J. Geol. Geog., 33, 213-220.

---------- 1970. Stability of amphibole and phlogopite in the upper mantle. Carnegie Inst. Wash. Yrbk., 68, 245-247.

---------- 1972. Partial melting of synthetic and natural peridotites at high pressures. Carnegie Inst. Wash. Yrbk., 71, 357-362.

Kushiro, I., Shimizu, N., Nakamura, Y. and Akimoto, S. 1972. Composition of co-existing liquid and solid phases formed upon melting of natural garnet and spinel lherzolites at high pressures: a preliminary report. Earth Planet. Sci. Lett., 14, 19-25.

Lambert, R. St. J., and Holland, J. G. 1974. Yttrium geochemistry applied to petrogenesis utilising Ca-Y relationships in minerals in rocks. Geochim. cosmochim. Acta, 38, 1393-1414.

Larsen, O. 1966. K/Ar determinations from Western Greenland. Rapp. Grønlands geol. Unders., 11, 57-67.

Le Bas, M. J. 1962. The role of aluminium in igneous clinopyroxenes in relationship to their parentage. Am. J. Sci., 260, 267-288.

Le Maitre, R. W. 1969. Kaersutite-bearing plutonic xenoliths from Tristan da Cunah, South Atlantic. Mineralog. Mag., 37, 185-197.

Lofgren, G. 1975. Temperatute induced zoning in synthetic plagioclase feldspar. In: Mackenzie, W. S. and Zussman, J. (Eds), The Feldspars. N. A. T. O. Advanced Study Institute, 362-375. Manchester University Press.

Luth, W. C. and Tuttle, O. F. 1969. The hydrous vapour phase in equilibrium with granite and granite magmas. In: Larsen, L. H. (Ed), Poldervaart Memorial volume. Geol. Soc. Amer. Mem., 115, 513-548.

Macdonald, R. 1969. The petrology of alkaline dykes from the Tugtutôq area, South Greenland. Bull. Geol. Soc. Denmark, 20, 38-58.

Macdonald, R. and Parker, A. 1969. Zirconium in alkaline dykes from the Tugtutôq region, South Greenland. Bull. Geol. Soc. Denmark, 20, 59-63.

Manson, V. 1967. Geochemistry of basaltic rocks: Major elememts. In: Hess, H. H. and Poldervaart, A. (Eds), Basalts: The poldervaart Treatise on Rocks of Basaltic Composition. Vol. 1, 215-269. Wiley-Interscience, New York.

Martignole, J. 1974. Mechanism of differentiation in the Morin Anorthosite complex. Contr. Mineral. and Petrol., 46, 99-107.

Modreski, P. J. 1972. The melting of phlogopite in the presence of enstatite, aluminous enstatite, diopside, spinel, corundum and pyrope. Carnegie Inst. Wash. Yrbk., 71, 392-396.

Mohr, P. A. 1971. Ethiopian rift and plateaus: some volcanic petrochemical differences. J. Geophys. Res., 76, 1967-1984.

Moorbath, S., Webster, R. K. and Morgan, J. W. 1960. Absolute age determinations in Southwest Greenland. Meddr. Grønland, 162, No. 9.

Morse, S. A. 1964. Age of Labrador Anorthosites. Nature, Lond., 203, 509-510.

Murthy, M. V. N. 1958. Coronites from India and their bearing on the origin of coronas. Bull. Geol. Soc. Amer., 68, 23-38.

Mysen, B. 1973. Melting in a hydrous mantle: phase relations of mantle peridotite with controlled water and oxygen fugacities. Carnegie Inst. Wash. Yrbk., 72, 467-477.

Nesbitt, R. W. and Hamilton, D. L. 1970. Crystallisation of an alkali olivine basalt under controlled pH_2O, pO_2 conditions. Physics Earth Planetary Interiors, 3, 309-315.

Nicholls, I. A. and Ringwood, A. E. 1973. Effect of water on olivine stability in tholeiites and the production of silica-saturated magmas in the island arc environment. J. Geol., 81, 285-300.

O'Hara, M. J. 1965. Primary magmas and the origin of basalts. Scot. J. Geol., 1, 19-40.

---------- 1968. The bearing of phase equilibria studies in synthetic and natural systems on the origin and evolution of basic and ultrabasic rocks. Earth-Sci. Rev., 4, 69-133.

---------- 1970. Upper mantle composition inferred from laboratory experiments and observation of volcanic products. Phys. Earth Planet. Interiors, 3, 236-245.

O'Hara, M. J., Richardson, S. W. and Wilson, G. 1971. Garnet peridotite stability and occurrence in crust and mantle. Contr. Mineral. and Petrol., 32, 48-68.

O'Hara, M. J. and Yoder, H. S. 1963. Partial melting of the mantle. Carnegie Inst. Wash. Yrbk., 62, 67-71.

---------- 1967. Formation and fractionation of basic magmas at high pressures. Scot. J. Geol., 3, 67-117.

O'Nions, R. K. and Pankhurst, R. J. 1974. Petrogenetic significance of isotope and trace-element variations in volcanic rocks from the mid-Atlantic. J. Petrology, 15, 603-634.

Philpotts, J. A. and Schnetzler, C. C. 1970. Phenocryst-matrix partition coefficients for K, Rb, Sr and Ba, with applications to anorthosite and basalt genesis. Geochim. cosmochim. Acta, 34, 307-322.

Phinney, W. C. 1969. Anorthosite occurrences in Keweenawan Rocks of northeastern Minnesota. In: Isachsen, Y. (Ed), The Origin of Anorthosites and Related Rocks, 135-147. N. Y. State Museum and Sci. Service, Mem. 18.

Poldervaart, A. and Gilkey, A. K. 1954. On clouded plagioclase. Am. Mineral., 36, 75-91.

Poulsen, V. 1964. The sandstones of the Precambrian Eriksfjord Formation in South Greenland. Rapp. Grønlands geol. Unders., 2.

Powers, H. A. 1955. Composition and origin of baslatic magma of the Hawaiian Islands. Geochim. cosmochim. Acta, 7, 77-107.

Prinz, M. 1967. Geochemistry of basaltic rocks: Trace elements. In: Hess, H. H. and Poldervaart, A. (Eds), Basalts, vol. 1, 271-324. Interscience, New York.

Pulvertaft, T. C. R. 1965. The Equaloqarfia layered dyke, Nunarssuit, South Greenland. Meddr. Grønland, 169, No. 8.

Ringwood, A. E. 1966. The chemical composition and origin of the earth. In: Hurely, P. M. (Ed), Advances in Earth Sciences. M. I. T. Press, Cambridge, Mass.

Roedder, E. 1965. Liquid CO_2 inclusions in olivine-bearing nodules and phenocrysts from basalts. Am. Mineral., 50, 1746-1782.

Roeder, P. L. and Emslie, R. F. 1970. Olivine-liquid equilibrium. Contr. Mineral. and Petrol., 29, 275-289.

Rose, H. J., Adler, I. and Flanagan, F. J. 1963. X-ray flourescence analysis of the light elements in rocks and minerals. Appl. Spectrosc., 17, 81-85.

Saether, E. 1948. On the genesis of peralkaline rock provinces. Rep. 18th. Intern. geol. Congr. Great Britain, 2, 123-130.

Shapiro, L. and Brannock, W. W. 1956. Rapid analysis of silicate rocks. Bull. U. S. geol. Surv., 1036C, 19-56.

Shaw, D. M. 1968. A review of K/Rb fractionation trends by covariance analysis. Geochim. cosmochim. Acta, 32, 573-602.

Siegel, S. 1956. Nonparametric statistics for the Behavioural Sciences. New York.

Simkin, T. and Smith, J. V. 1970. Minor element distribution in olivine. J. Geol., 78, 304-325.

Stephenson, D. 1974. Mn and Ca enriched olivines from nepheline syenites of the South Qorôq Centre, South Greenland. Lithos, 7, 35-41.

Stewart, J. W. 1964. The earlier Gardar igneous rocks of the Illimaussaq area, South Greenland. Unpubl. Ph. D. thesis, Univ. of Durham.

---------- 1970. Precambrian alkaline-ultramafic/carbonatite volcanism at Qagssiarssuk, South Greenland. Bull. Grønlands geol. Unders., 84. (Meddr. Grønland, 186, No. 4).

Sun, C., Williams, R. J. and Sun, S. 1974. Distribution coefficients of Eu and Sr for plagioclase-liquid and clinopyroxene-liquid in oceanic ridge basalt: an experimental study. Geochim. cosmochim. Acta, 38, 1415-1433.

Sutton, J. 1963. Long-term cycles in the evolution of the continents. Nature, 198, 731-735.

Sweatman, T. R. and Long, J. V. P. 1969. Quantitative electron-microprobe analysis of rock-forming minerals. J. Petrology, 10, 332-379.

Sørensen, H. 1969. On the magmatic evolution of the alkaline igneous province of South Greenland. Rapp. Grønlands geol. Unders., 7.

Taylor, S. R. 1965. The application of trace element data to problems in petrology. In: Ahrens, L. H., Press, F., Runcorn, S. K. and Urey, H. C. (Eds), Physics and Chemistry of the Earth, 6, 215-250. Pergamon, Oxford and London.

Thompson, G., Shido, F, and Miyashiro, A. 1972. Trace element distribution in fractionated oceanic basalts. Chem. Geol., 9, 89-97.

Thompson, R. N. 1972a. The 1-atmosphere melting patterns of some basaltic volcanic series. Am. J. Sci., 272, 901-932.

---------- 1974. Primary basalts and magma genesis. 1. Skye, Northwest Scotland. Contr. Mineral. and Petrol., 45, 317-341.

Thompson, R. N., Esson, J. and Dunham, A. C. 1972. Major element chemical variation in the Eocene lavas of the Isle of Skye, Scotland. J. Petrology, 13, 219-253.

Thornton, C. P. and Tuttle, O. F. 1960. Chemistry of igneous rocks. 1. Differentiation Index. Am. J. Sci., 258, 664-684.

Upton, B. G. J. 1960. The alkaline igneous complex of Kûngnât Fjeld, South Greenland. Bull. Grølands geol. Unders., 27. (Meddr. Grønland, 123, No. 4).

---------- 1962. Geology of Tugtutôq and neighbouring islands, Gouth Greenland. Part 1. Meddr. Grønland, 169, No. 8.

Upton, B. G. J. 1964a. The geology of Tugtutôq and neighbouring islands, South Greenland. Part II. Nordmarkitic syenites and related alkaline rocks. Meddr. Grønlands, 169, No. 2.

---------- 1964b. The geology of Tugtutôq and neighbouring islands, South Greenland. Part III. Olivine gabbros, syenogabbros and anorthosites. Part IV. The nepheline syenites of the Hviddalcomposite dyke. Bull. Grønlands geol. Unders., 48. (Meddr. Grønland, 169, No. 3).

---------- 1965. The petrology of a camptonite sill in South Greenland. Meddr. Grønland, 169, No. 11. (Bull. Grønlands geol. Unders., 50).

---------- 1970. Basic rocks of the Gardar igneous province. Rapp. Grønlands geol. Unders., 28, 26-29.

---------- 1971. Melting experiments on chilled gabbros and syenogabbros. Carnegie Inst. Wash. Yrbk., 70, 112-118.

---------- 1974. The alkaline province of Southwest Greenland. In: Sørensen, H. (Ed), The Alkaline Rocks, 221-238. Academic Press, New York.

Upton, B. G. J. and Thomas, J. E. 1973. Precambrian potassic ultramafic rocks, South Greenland. J. Petrology, 14, 509-534.

van Breemen, O., Aftalion, M. and Allaart, J. H. 1974. Isotopic and geochronologic studies on granites from the Ketilidian mobile belt of South Greenland. Geol. Soc. Am. Bull., 85, 403-412.

van Breemen, O. and Upton, B. G. J. 1972. The age of some Gardar intrusive complexes, South Greenland. Bull. geol. Soc. Amer., 83, 3381-3390.

Varne, R. 1970. Hornblende lherzolite and the upper mantle. Contr. Mineral. and Petrol., 27, 45-51.

Vincent, A. E. 1960. Analysis by gravimetric and volumetric methods, flame photometry, colourimetry and related techniques. In: Smales, A. A. and Wager, L. R. (Eds), Methods in Geochemistry, 33-80. Interscience, New York.

Vinogradov, A. P. 1962. Average contents of chemical elements in the principal types of igneous rocks of the earth's crust. Geokhimiya (translated), 1962, 641-664.

Wager, L. R., Vincent, E. A. and Smales, A. A. 1957. Sulphides in the Skaergaard intrusion, East Greenland. Econ. Geology, 52, 855-903.

Walton, B. J. 1965. Sanerutian appinitic rocks and Gardar dykes and diatremes north of Narssarssuaq, South Greenland. Bull. Grønlands geol. Unders., 57. (Meddr. Grønland, 179, No. 9).

Wanless, R. K., Stevens, R. D., Lachance, G. R. and Edmonds, C. M. 1967. Age determinations and geological studies, K/Ar isotopic ages, report 7. Geol. Surv. Can., paper 66-17.

Watt, W. S. 1966. Chemical analyses from the Gardar igneous province, South Greenland. Rapp. Grønlands geol. Unders., 6.

---------- 1968. Petrology and geology of the Precambrian Gardar dykes on Qaersuarssuk, South Greenland. Bull. Grønlands geol. Unders., 14.

Watt, W. S. 1969. The coast-parallel dyke swarm of South-west Greenland in relation to the opening of the Labrador Sea. Can. J. Earth Sci., 6, 1320-1321.

Watterson, J. 1965. Plutonic development of the Ilordleq area, South Greenland. Part I. Chronology and the occurrence and recognition of metamorphosed basic dykes. Bull. Grønlands geol. Unders., 51. (Meddr. Grønland, 172, No. 7).

Wegmann, C. E. 1938. Geological investigations in southern Greenland. 1. On the structural divisions of southern Greenland. Meddr. Grønland, 113, No. 2)

Welcher, F. J. (Ed) 1963. Standard methods of chemical analysis. Vol. 2: industrial and natural products and non-instrumental methods. D. Van Nostrand Co. Inc., New Jersey.

Wilkinson, J. F. G. 1961. Some aspects of the calciferous amphiboles, oxyhornblende, kaersutite and barkevikite. Am. Miner., 46, 340-354.

---------- 1974. The mineralogy and petrography of alkali basaltic rocks. In: Sørensen, H. (Ed), The Alkaline Rocks, 67-95. Academic Press, New York.

Wilson, A. D. 1955. A new method for the determination of ferrous iron in rocks and minerals. Bull. geol. Surve. Gt. Br., 9, 56-58.

Wood, C. P. 1968. A geochemical study of E. African alkaline lavas and its relevance to the petrogenesis of nephelinites. Unpubl. Ph. D. thesis, Univ. of Leeds.

Yagi, K. and Onuma, K. 1967. The join $CaMgSi_2O_6$ - $CaTiAl_2O_6$ and its bearing on the titanaugites. J. Fac. Sci. Hokkaido Univ., Ser. IV, 13, 463-483.

Yoder, H. S. 1970. Phlogopite-H_2O-CO_2: an example of the multicomponent gas problem. Carnegie Inst. Wash, Yrbk., 68, 236-240.

---------- 1973. Contemporaneous basaltic and rhyolitic magmas. Am. Miner., 58, 153-171.

Yoder, H. S. and Kushiro, I. 1969. Melting of a hydrous phase: phlogopite. Am. J. Sci., Schairer Vol., 267A, 558-582.

Yoder, H. S. and Tilley, C. E. 1962. Origin of basaltic magmas: an experimental study of natural and synthetic rock systems. J, Petrology, 3, 342-532.

-0-

Acknowledgements

I should like to thank my supervisor, Dr. B.G.J. Upton, for suggesting the study, and for his patience during the work.

Permission to work on the material was granted by the Director of the Geological Survey of Greenland.

Some analyses were kindly provided by J. Engell, Mineralogisk Institut, Danmarks Techniske Højskole, Lyngby, Denmark.

Mr. G.R. Angell and Mr. M.J. Saunders provided valuable assistance and instruction in X-ray fluorescence and analytical chemical techniques respectively. Instruction in the techniques of electron microprobe analysis was provided by Drs. P.G. Hill and B. Jeffries.

Dr. K.R. Gill kindly identified the ore minerals in several polished specimens of the dyke rocks.

I am very grateful to Mr. C. Chaplin, Laboratory Superintendent, for the preparation of photomicrographs, and to Mr. B. Jackson for the preparation of some diagrams.

Thanks are due to Mrs. Shelagh Formby, who did the typing.

Finally I wish to thank my husband for his continued support and advice during the preparation of this thesis.

The work was carried out during the tenure of a Natural Environment Research Council Studentship.

Appendix 1.

Preparation of rock powders for chemical analysis

1. Wash hand specimens (ca.500g) and scrub with bristle brush to remove surface dirt and loose material. Rinse in de-ionised water and dry.

2. Break up into chips (ca. 3-4cm) using a Cutrock hydraulic splitter, and discard weathered surfaces.

3. Crush chips to coarse powder; initially Manchester Rollers were used in this process but later a Sturtevant jaw crusher was used. Replicate samples prepared by both methods showed no significant chemical differences (Table A.1.).

4. A representative ca. 150g sample obtained by cone and quartering.

5. Reduce sample to <100 mesh B.S. by grinding in a tungsten carbide tema. Check grain size by seiving, transfer powder to bottles and dry at 105°C. for 24 hours. Seal and store.

Table A1.1

Comparative contamination tests on Manchester Rollers and Sturtevant jaw crusher.

	101425		101471	
	a.	b.	a.	b.
SiO_2	46.47	47.85	47.72	47.82
TiO_2	2.77	2.84	2.30	2.17
Al_2O_3	14.46	14.91	17.13	18.0
Fe_2O_3*	16.58	16.9	13.82	13.51
MnO	0.22	0.20	0.16	0.15
MgO	5.51	5.35	7.25	7.19
CaO	7.55	7.70	8.13	8.05
Na_2O	3.58	3.52	3.62	3.67
K_2O	1.19	1.23	1.21	1.17
P_2O_5	0.45	0.42	0.88	0.83
ppm.				
Ba	783	724	1106	1186
Zr	219	201	160	145
Y	49	59	33	48
Sr	347	379	863	957
Rb	38	43	18	21
Zn	87	99	56	67
Cu	159	128	48	36
Ni	77	67	104	119
Cr	51	58	53	59
V	312	339	174	156

Appendix 2

Analytical techniques

2.A. X-Ray spectrographic analysis

Jenkins and De Vries (1967) have discussed the theoretical background and general principles of X-ray spectrographic analysis. All major and trace elements except FeO, Na_2O, H_2O and CO_2 were determined using a Phillips PW 1212 automatic X-ray spectrometer, under standard operating conditions in use at the Grant Institute of Geology.

Correction of the raw counts for instrument drift and the calculation of a least squares regression line for the standards, against which the unknown specimens were measured, was carried out using a computer programme written by R.F. Cheeney.

For major element analysis matrix effects and mass absorbtion interference were eliminated using the method described by Rose et al. (1963), which involves the dilution of the bulk sample with lithium tetraborate and lanthanum oxide (a heavy absorber), and fusion of the mixture to a glass. The fused sample is then ground to a powder which is pressed into a disc for analysis. The sample preparation method is described below.

1. Dry bulk rock powders at 105°C for 24 hours. Dry Specure Lithium tetraborate and Lanthanum oxide separately at 400°C for 24 hours.
2. Weigh out rock powder, lanthanum oxide and lithium tetraborate in ratio 1:1:8 (0.75 g:0.75 g:6.0 g).
3. Mix thoroughly transfer to carbon crucibles and fuse the mixture in a furnace for 30 minutes at 1050°C.

4. Remove cruicibles from the furnace and when the fused mixture has solidified, transfer to a desiccator to cool completely.
5. Make up any weight lost on fusion by adding dry lithium tetraborate to the sample.
6. Crush the fused bead and grind to 200 mesh B.S. in a tungsten carbide tema. Check the grain size by seiving. Bottle the powder and dry for 24 hours at 105°C.
7. Press the powder to a disc jacketed by boric acid using a hydraulic press at 15 tons pressure for 45 seconds. Reject any disc whose powder surface is not perfect: the characteristic radiation of the lighter elements (Si, Mg, Al) has a very limited surface penetration.

Determination of the trace elements was made on bulk rock powders. The peak/background method of Anderman and Kemp (1958) was used, as interference effects are minimised by this method. Loose 100 mesh B.S. rock powders were exposed to radiation in special containers with a replaceable Mylar film base.

The precision of the major and trace element methods is shown in table A.2.1 and the accuracy calculated from the international standards AGU1, BCR1, and W1 and a departmental standard, E1 in table A.2.2.

2.B. Electron microprobe analysis

All mineral analysis were carried out using a Cambridge Scientific Instruments Microscan 5 Electron Probe Microanalyser. The procedure followed is similar to that described by Sweatman and Long (1969), under the standard operating conditions in use at Edinburgh University.

The counts obtained on the peak for each element, corrected for dead-time and with the background counts subtracted, were compared with the intensities measured on standards of simple composition. This gave a value for the apparent concentration of each element in the specimen which was converted to the real concentration using a computer programme available at Edinburgh which corrected for the atomic number, absorption and fluorescence differences between the standard and specimen.

The precision of the analysis is principally governed by the stability of the electron beam and the counting statistics. The electron beam stability was monitored by placing a Faraday cage in the path of the beam after the final aperture. The probe current was maintained to within $\pm$ 0.5% of the standard figure of 30 nanoamps.

Table A.2.1

Estimated precision of major and trace element analysis

The results are quoted as $\bar{x} \pm \frac{s}{(n)}$, where

$\bar{x}$ = the mean of n measurements

$\frac{s}{(n)}$ = the standard error of the mean

s^2 = an estimate of variance of the measurements

Major elements: specimen 101430; n = 5

wt% SiO_2	48.04 ± 0.27
TiO_2	2.79 ± 0.02
Al_2O_3	14.58 ± 0.12
Fe_2O_3*	16.08 ± 0.08
MgO	6.28 ± 0.14
CaO	8.54 ± 0.06
K_2O	0.83 ± 0.02
P_2O_5	0.51 ± 0.02

Trace elements: specimens 101394, 101489, 101419; n = 4

		101394	101489	101419
ppm.	Ba	471 ± 11	796 ± 8.75	611 ± 17
	Zr	64 ± 1.46	347 ± 4.24	149 ± 3.53
	Y	12 ± 0.79	58 ± 3.75	50 ± 2.7
	Sr	807 ± 5.73	75 ± 2.8	399 ± 4.6
	Rb	24 ± 1.03	104 ± 2.8	23 ± 2.2
	Zn	45 ± 1.07	127 ± 9.54	97 ± 6
	Cu	23 ± 1.7	11 ± 1.66	87 ± 8.16
	Ni	135 ± 4	11 ± 1.4	86 ± 2.75
	Cr	31 ± 1.4	19 ± 1.8	68 ± 1.5
	V	38 ± 1.8	74 ± 2.2	222 ± 8
wt%	MnO	0.07 ± 0.01	0.21 ± 0.02	0.19 ± 0.01

Note:- Fe_2O_3* = total Fe as Fe_2O_3.

Table A.2.2

Estimated accuracy of XRF analysis

Standard		AGV1.		BCR1.		E1		W1	
		a.	b.	a.	b.	a.	b.	a.	b.
Total	SiO_2	58.99	59.75	54.48	54.75	36.82	36.37		
	TiO_2	1.08	1.01	2.23	2.24	4.60	4.57		
	Al_2O_3	17.01	17.38	13.65	13.55	10.38	10.29		
	Fe_2O_3	6.80	7.03	13.50	13.22	27.73	27.95		
	MgO	1.49	1.20	3.28	3.15	6.55	6.56		
	CaO	4.98	4.75	6.95	6.94	7.85	8.05		
	K_2O	2.89	2.99	1.68	1.71	0.24	0.22		
	P_2O_5	0.48	0.48	0.36	0.36	1.91	1.92		
	MnO wt%			0.17	0.18	0.44	0.41	0.17	0.18
	Ba ppm			790	770	670	700	215	196
	Zr			180	192	85	110	97	100
	Y			46	57	60	40	25	30
	Sr			340	335	220	235	220	190
	Rb			45	53	5	9	22	28
	Zn			132	112	100	107	82	73
	Cu			17	-	40	74	110	133
	Ni			10	13	110	104	78	82
	Cr			25	19	65	60	120	111
	V			400	402	220	226	240	256

Note:-

a. recommended value (major element values from Flanagan (1969) and Fleischer (1969); trace elements, preferred values, Geology Department, Edinburgh University).

b. mean value obtained over period of analysis.

Appendix 2.C.

Chemical analysis: wet chemistry

1. FeO

Ferrous iron was determined using the method described by Wilson (1955). The bulk powder sample is dissolved in cold hydroflouric acid in PTFE crucibles in the presence of excess ammonium vanadate.

When the rock powder has dissolved completely (after ca. 3 days) the excess vanadate is titrated against ammonium ferrous sulphate dissolved in a mixture of boric and sulphuric acid. Sodium diphenylamine is used as an indicator. Analar or Specure reagents were used throughout. Table A.2.3 shows the precision of the method.

2. Na_2O

The method of analysis used at Edinburgh was developed by M. J. Saunders. Sodium determinations were made using an EEL flame photometer (see Vincent, 1960). The bulk powder sample, weighed into platinum crucibles, is dissolved in conc. nitric acid and hydrofluoric acid. Excess hydrofluoric acid is removed by the addition of 1 + 1 sulphuric acid and subsequent evaporation. Dilute sulphuric acid and deionised water are added to maintain all the sodium in the solution. Insoluble calcium sulphate is allowed to settle. The solution is analysed in the flame photometer, using a double Na filter to minimise interference from any calcium remaining in the solution. Analar or Specure reagents were used throughout. The precision of the method is shown in Table. A.2.3.

3. H_2O.

A modification of the method described by Shapiro and Brannock (1962) was used to determine water gravimetrically. 1g of bulk powder and 3g of flux (lead oxide: lead chromate = 2:1) were fused in a test tube and the water given off absorbed on a pre-weighed filter paper. The filter paper was reweighed to give the weight of water. The precision of the method is summarised in Table A.2.3.

4. CO_2

The method of analysis was devoloped by M. J. Saunders. It is based on the pressometric method described in 'Standard Methods in Chemical Analysis', volume 2 (Welcher, 1963).

The CO_2 evolved by the action of HCl on the rock powder produces a change in pressure in a calibrated system of constant volume. The change in pressure, measured by the change in height of a column of mercury, is proportional to the amount of CO_2 given off. This is compared with the amount of CO_2 evolved from a known weight of $CaCO_3$. Measurements on the $CaCO_3$ standard and on blanks are repeated throughout the day to allow for changes in atmospheric pressure.

The rock powder is weighed into a small flask, and 1.5ml 25% HCl, held in a small bottle, added. The flask is attached to the manometer and immersed in a water bath to allow the mercury levels to equilibrate at constant temperature. After the initial mercury level has been read the HCl is shaken over the powder in the small

flask, and the flask heated and cooled three times to ensure all the CO_2 is evolved. The flask is then allowed to cool to standard temperature in the water bath before the new mercury level is recorded. Analar or Specure reagents are used throughout. An estimate of the precision of the method is given in table A.2.3.

Table A.2.3

Estimated precision of wet-chemical analysis

Results are quoted as $\bar{x} \pm \underset{(n)}{s}$, where $\bar{x}$ = mean of n measurements, $\underset{(n)}{s}$ = the standard error of the mean and s^2 = an estimate of variance of the measurements.

FeO: n = 4. specimen no. 101339 9.16 ± 0.05 specimen no. 101381 9.94 ± 0.02

Na_2O: n = 11. specimen no. 101470 3.31 ± 0.02

H_2O: n = 6. specimen no. 101343 0.52 ± 0.02

CO_2: n = 4. specimen no. 101401 3.05 ± 0.01

APPENDIX 3

Key to analyses in Appendix 4

GGU Spec. No.	Description of dyke	Location of spec.	Spec. locality map No.
101264	ESE BD_0 (east branch)	Centre	1a.
101266	ESE BD_0 west branch	8 m from contact	1a.
101267	ESE BD_0 pegmatite, as 101266		1a.
101296	ESE BD_0	10 cm from contact	1a.
101271	ENE 22m dolerite, cuts gabbro giant dyke	chill	1a.
101272	as above	6 m from chill	1a.
101327	ESE dolerite ? BD_1	centre	1a.
101328	as above	1 m from south contact	1a.
101283	ENE 100 m gabbro dyke	2 m from north contact	1a.
101469	ENE 40 m porphyritic dolerite ENE extremity of a gabbro giant dyke		1a.
101470	15 m continuation of 101469, above basal Gardar unconformity		1a.
101471	same as above		
101277	ENE 6 m BFD	contact	1a.

GGU Spec. No.	Description of dyke	Location of Spec.	Spec. locality map No.
101287	ENE ? BFD, cuts Tugtutoq gabbro giant dyke		la.
101488	ENE 5 m composite dyke, basic margin	chill	la.
101489	quartz porphyry centre of above	centre	la.
101301	33 m quartz porphyry composite dyke	basic margin (1m)	la.
101302	as above	centre	
101248	ENE 1 m trachyte, main dyke swarm		la.
101275	ENE 13 m trachyte, main swarm	centre	la.
101312	ENE 5 m banded trachydiorite	chill	la.
101313	as above	centre	
101317	ENE 2 m flow-banded trachydiorite		la.
101320	ENE 2 m trachydiorite	chill	la.
101331	ESE 70 m BD_0	centre	lb.
101333	ESE BD_0	2 m from/chill	lb.
101345	ESE BD_0	centre	lb.
101430	E-W BD_0	20 m from S	lb.
	1	contact	
101336	ENE BD_1 (?)	8 m	lb.
101347	ENE BD_1		lb.

GGU Spec. No.	Description of dyke	Location of spec.	Map No.
101431	ENE BD_1 (?)	few m from contact	1b.
101436	NE 'Sermilik master-dyke'	near margin	1b.
101338	syenogabbro giant dyke	20 cm N chill	1b.
101349	20 m BFD, 1 m trachyte margin	10 cm	1b.
101356	ENE 16 m dolerite with anorthositic inclusions	contact	1b.
101368	16 m dolerite with plagioclase megacrysts		1b.
101369	12m dolerite, multiple intrusion with anorthositic inclusions, cuts 101368		1b.
101375	as 101369	chill	1b.
101381	40 m basic dyke		1b.
101393	large dolerite	3 m	1b.
101394	anorthositic xenolith in 101393		1b.
101339	syenogabbro /from giant dyke as 101338		1b.
101342	south margin above dyke	2 m	1b.
101361	banded syenogabbro, giant dyke	1 m	1b.
101351	giant dyke, north contact	5 m	1b.
101357	giant dyke, south contact		1b.
101366	gabbro from composite gabbro-breccia intrusion	few m	1b.

GGU Spec. No.	Description of dyke	Location of spec.	Map No.
101377	gabbro unit, composite dyke	10 m	1b.
101340	syenite unit, 101338/339 dyke		1b.
101341	drusy syenite, as above		
101343	syenite, as above	near centre	1b.
101344	pegmatitic syenite, as 101343	NW contact	1b.
101362	syenite unit, 101361 dyke	centre	1b.
101358	syenite unit, 101357 dyke	centre	1b.
101355	syenogabbro, giant dyke	30 m from S contact	1b.
101386	North Bangs Havn complex, gabbro	15 m from contact	1b.
101388	North contact, as above	contact	1b.
101370	NNE 70 m dolerite		1b.
101360	NE dolerite	contact	1b.
101380	NNE 50 M dolerite, cut by 101381		1b.
101391	NE dolerite		1b.
101406	E-W BD_0	centre	1c.
101417	ENE 70 m. dyke, 'Le Flic'	10 cm from contact	1c.
101418	as above	centre	
101427	ENE ? continuation of 'Le Flic'	centre	1c.

GGU Spec. No.	Description of dyke	Location of Spec.	Map No.
101428	as above	N contact	1c
101398	NE		1c
101419	ENE 10 m dyke cutting 'Le Flic'	margin	1c
101422	ENE dolerite		1c
101426	E-W 3 m dyke, cuts 101427/428		1c
101429	NE 15 m dyke, cuts 101427/428		1c
101400	ENE dyke, cut by trachyte		1c
101401	near above		1c
101403	ENE (BD_2) 'Gronnedal master dyke'	4 m from chill	1c
101404	as above		
101405	as above	centre	1c
101421	NE dyke, cuts Le Flic		1c
101425	as above, also cuts 101422		
101407	ENE 10 m dolerite		1c
101408	NE, 4 m slightly porphyritic dyke		1c
101409	E-W 4 m intermediate dyke	centre	1c
101411	ENE 3 m lamprophyre		1c
101412	1 m dolerite cutting 101411		1c
101413	1 m feldsparphyric dolerite		1c

GGU Spec. No.	Description of dyke	Location of spec.	Map No.
101415	NE 25 m dolerite	1 m from chill	1c
101416	NE 1 m dyke cutting 101415		1c

- -

H	Jotnian	Dala region.	NE 3 m dolerite dyke: centre.
P	dykes	" "	NE 25 m dolerite dyke: near contact.
X	Sweden	" "	N 2 m dolerite dyke : centre.

EC621A Michikamau chill specimen, Nain region, Canada: supplied by Dr. R.F. Emslie. No petrographic data.

- -

Analyses of specimens from the Bangs Havn complex, supplied by J. Engell. No petrographic data.

121201 to 121269 and 121284 : gabbro, syenogabbro and syenite from the North eastern Bangs Havn compl

121271 : aplite cutting 121269

121293a : quartz-feldspar-phyric dyke

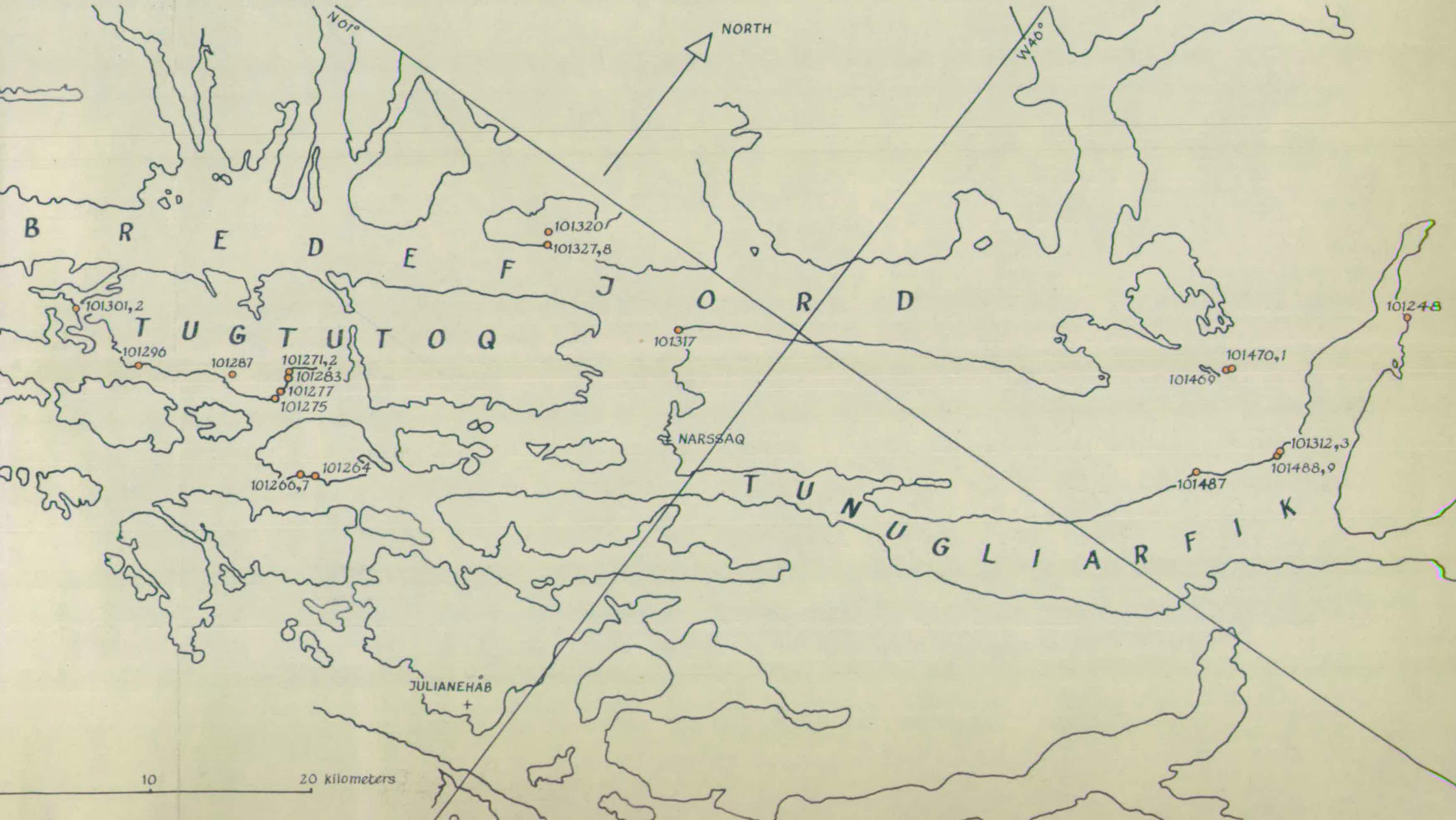
121293b : " " " "

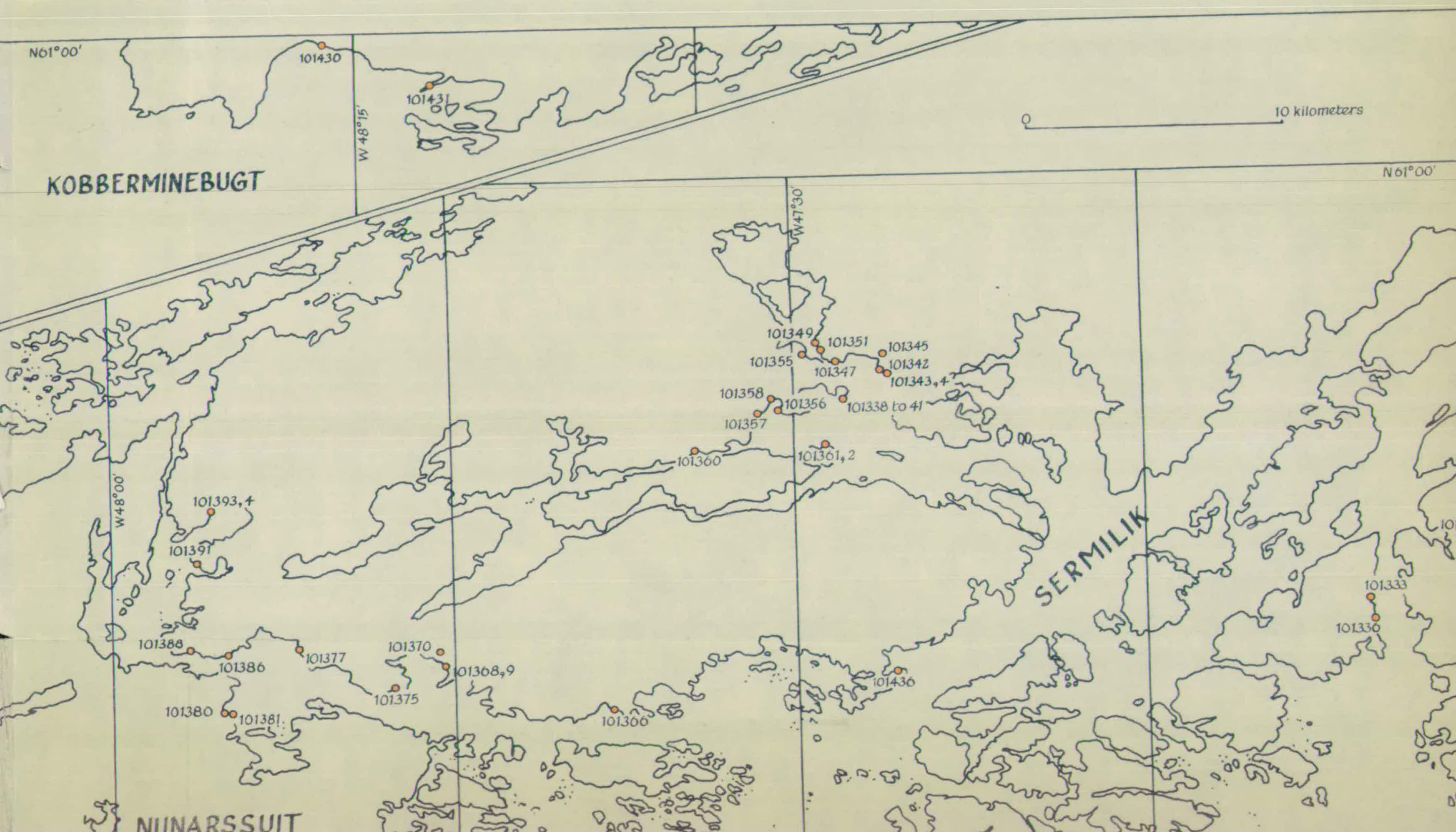
121294f : centre differentiated dyke

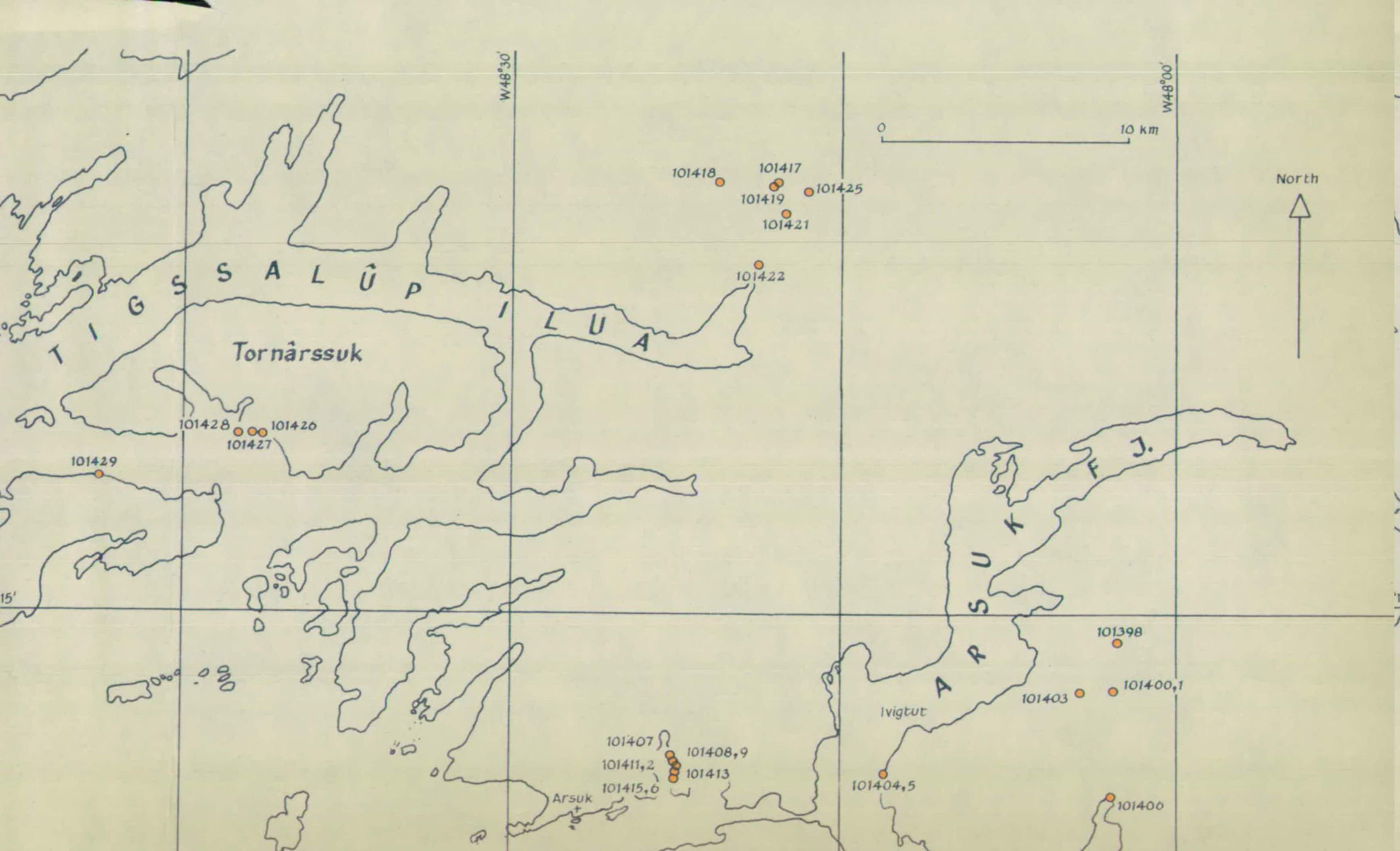
121301 : ENE dolerite dyke, older than Bangs Havn complex.

121302b to 121317 : Western Bangs Havn complex

FIGURE A3.1a, b & c (three pages):
Specimen-locality maps.


N01°
NORTH
W40°
B R E D E F J O R D
101320
101327,8
101301,2
T U G T U T O Q
101296
101287
101271,2
101283
101277
101275
101317
101470,1
101469
101248
NARSSAQ
101312,3
101488,9
101487
101264
101266,7
T U N U G L I A R F I K
JULIANEHÅB
10
20 kilometers


N61°00'
101430
101431
W 48°15'
KOBBERMINEBUGT
0
10 kilometers
N61°00'
W47°30'
101349
101351
101345
101355
101347
101342
101343,4
101358
101356
101338 to 41
101357
101360
101361,2
W48°00'
101393,4
101391
SERMILIK
101333
101330
101388
101386
101377
101370
101368,9
101375
101380
101381
101366
101436
NUNARSSUIT


W48°30'
W48°00'
0
10 km
North
101418
101417
101419
101425
101421
101422
TIGSSALÛP ILUA
Tornârssuk
101428
101426
101427
101429
ARSUKFJ.
101398
101403
101400,1
Ivigtut
101407
101408,9
101411,2
101413
101415,6
Arsuk
101404,5
101406
15'

Spec	101264	101266	101267	101296	101271	101272	101327	101328
SiO_2	46.85	48.88	50.16	50.22	46.05	46.08	54.16	39.96
Al_2O_3	11.37	18.05	12.44	15.57	15.13	14.76	17.04	15.00
Fe_2O_3	2.51	1.01	2.42	3.80	1.82	2.95	3.32	6.13
FeO	11.09	10.00	10.59	8.42	12.36	10.80	5.34	12.17
MgO	5.81	6.66	3.67	5.33	5.27	5.21	1.31	5.18
CaO	11.06	8.45	9.70	9.27	8.04	7.75	4.27	6.98
Na_2O	2.99	3.55	4.29	3.43	3.65	3.87	5.02	3.00
K_2O	0.89	0.64	0.56	0.66	1.55	1.82	4.73	1.70
H_2O^+	1.13	0.80	1.44	1.16	2.04	1.90	1.22	1.22
CO_2	0.00	0.00	0.00	0.00	0.00	0.00	0.00	0.00
TiO_2	5.15	1.19	3.50	1.79	3.05	3.14	1.62	5.40
P_2O_5	0.74	0.31	0.99	0.44	1.16	1.38	0.73	1.82
MnO	0.18	0.16	0.20	0.15	0.21	0.18	0.14	0.19
Sum	99.77	99.70	99.96	100.24	100.33	99.84	98.90	98.75
Q	0.00	0.00	0.30	0.00	0.00	0.00	0.00	0.00
wo	0.00	0.00	0.00	0.00	0.00	0.00	0.00	0.00
c	0.00	0.00	0.00	0.00	0.00	0.00	0.00	0.00
hy	5.98	3.40	9.36	15.22	0.00	0.00	0.00	0.00
ol	3.45	19.06	0.00	3.42	18.59	15.51	5.45	21.29
or	5.33	3.82	3.36	3.94	9.31	10.97	28.63	10.32
sc	0.00	0.00	0.00	0.00	0.00	0.00	0.00	0.00
ap	1.78	0.74	2.38	1.05	2.79	3.33	1.77	4.43
ab	25.64	30.37	36.83	29.34	28.14	29.93	39.00	23.57
ac	0.00	0.00	0.00	0.00	0.00	0.00	0.00	0.00
mt	3.69	1.48	3.56	3.14	2.68	4.36	3.76	5.21
an	15.17	31.77	13.22	25.41	20.66	17.88	10.23	23.05
hm	0.00	0.00	0.00	0.00	0.00	0.00	0.00	0.00
cc	0.00	0.00	0.00	0.00	0.00	0.00	0.00	0.00
ne	0.00	0.00	0.00	0.00	1.77	1.88	2.44	1.36
di	29.05	7.07	24.25	15.05	10.16	10.04	5.57	0.25
il	9.91	2.28	6.74	3.44	5.89	6.08	3.15	10.53
H_2O	1.13	0.80	1.44	1.16	2.04	1.90	1.22	1.22
Ba	538	435	374	720	1564	1559	4634	1831
Zr	276	140	431	164	155	164	324	165
Y	63	28	84	31	56	47	51	39
Sr	253	384	266	413	762	709	758	829
Rb	26	23	22	24	29	49	74	28
Zn	116	83	137	99	109	86	87	9
Cu	42	16	82	41	36	71	0	0
Ni	67	142	25	32	48	34	10	22
Cr	97	44	27	77	47	29	18	11
V	401	120	193	231	322	184	110	292

Spec	101283	101469	101470	101471	101277	101287	101488	101489
SiO_2	47.04	45.83	45.39	47.62	46.71	46.67	47.91	60.50
Al_2O_3	16.78	16.36	15.69	17.72	15.86	14.84	15.70	15.60
Fe_2O_3	3.06	2.49	5.56	1.68	3.81	2.31	0.97	3.69
FeO	10.08	11.14	9.19	10.75	9.80	9.91	11.23	4.53
MgO	4.96	4.66	4.54	7.21	4.67	6.60	4.30	0.48
CaO	7.67	7.69	7.04	8.04	7.66	9.19	6.87	1.06
Na_2O	3.63	3.41	3.31	3.64	3.61	3.19	3.07	5.41
K_2O	1.93	2.26	2.21	1.18	1.77	1.13	4.39	5.26
H_2O^+	1.24	1.22	1.67	0.62	2.05	3.40	1.36	0.92
CO_2	0.00	0.00	0.00	0.00	0.00	0.00	0.00	0.00
TiO_2	2.68	3.44	3.87	2.21	2.88	2.59	2.87	1.05
P_2O_5	0.72	1.45	1.82	0.85	1.11	0.41	1.19	0.22
MnO	0.16	0.16	0.14	0.15	0.19	0.18	0.19	0.21
Sum	99.95	100.11	100.43	101.67	100.12	100.42	100.05	98.93
Q	0.00	0.00	0.00	0.00	0.00	0.00	0.00	5.08
wo	0.00	0.00	0.00	0.00	0.00	0.00	0.00	0.00
c	0.00	0.00	0.00	0.00	0.00	0.00	0.00	0.00
hy	0.00	0.00	6.59	0.00	0.76	0.00	0.00	4.74
ol	15.70	16.52	12.37	22.19	15.17	15.61	16.44	0.00
or	11.55	13.49	13.24	6.90	10.67	6.88	26.27	31.71
sc	0.00	0.00	0.00	0.00	0.00	0.00	0.00	0.00
ap	1.73	3.47	4.37	1.99	2.68	1.00	2.85	0.53
ab	28.03	27.33	28.40	28.19	31.16	27.12	18.07	46.70
ac	0.00	0.00	0.00	0.00	0.00	0.00	0.00	0.00
mt	4.05	3.65	4.48	2.41	4.16	3.45	1.42	5.46
an	24.10	22.89	21.73	28.22	22.28	23.53	16.30	2.80
hm	0.00	0.00	0.00	0.00	0.00	0.00	0.00	0.00
cc	0.00	0.00	0.00	0.00	0.00	0.00	0.00	0.00
ne	1.67	0.99	0.00	1.23	0.00	0.37	4.46	0.00
di	8.01	5.05	1.35	4.72	7.54	16.96	8.66	0.94
il	5.16	6.60	7.45	4.15	5.58	5.07	5.52	2.03
H_2O	1.24	1.22	1.67	0.62	2.05	3.40	1.36	0.92
Ba	1381	1794	2572	1146	1442	901	1894	796
Zr	155	198	201	153	165	160	186	347
Y	37	58	46	42	39	47	54	58
Sr	787	971	927	910	675	793	691	75
Rb	49	41	46	20	50	11	186	104
Zn	87	72	78	62	122	96	116	127
Cu	17	30	37	42	32	37	31	11
Ni	54	55	32	112	49	118	33	11
Cr	48	29	18	56	38	288	29	19
V	204	306	143	165	295	168	317	74

Appendix 4

Spec	101301	101302	101248	101275	101312	101313	101317	101320
SiO_2	48.48	65.90	56.61	58.19	49.88	48.37	46.62	48.53
Al_2O_3	14.41	12.80	15.41	14.85	14.68	15.02	15.82	15.62
Fe_2O_3	2.52	3.86	2.85	3.79	1.46	2.72	1.40	3.50
FeO	10.18	3.10	7.55	5.57	10.69	10.07	8.66	7.44
MgO	4.43	0.54	0.65	0.33	2.96	4.03	5.73	4.10
CaO	6.65	0.79	2.90	2.36	6.52	6.72	7.32	6.19
Na_2O	4.29	5.20	5.90	6.38	5.21	3.90	2.91	5.28
K_2O	2.12	4.69	4.40	4.91	2.01	2.82	3.74	1.77
H_2O^+	1.43	0.67	1.06	0.89	2.44	2.69	2.65	3.09
CO_2	0.00	0.00	0.00	0.00	0.65	0.07	0.71	2.55
TiO_2	2.74	0.73	0.94	0.72	2.04	2.17	2.54	2.50
P_2O_5	1.05	0.10	0.12	0.07	0.93	0.82	0.52	0.51
MnO	0.20	0.16	0.31	0.28	0.25	0.21	0.15	0.16
Sum	98.50	98.54	98.70	98.34	99.72	99.61	98.77	101.24
Q	0.00	16.30	0.00	0.00	0.00	0.00	0.00	0.00
wo	0.00	0.00	0.00	0.00	0.00	0.00	0.00	0.00
c	0.00	0.00	0.00	0.00	0.00	0.00	0.00	0.91
hy	0.00	2.67	0.00	0.00	0.00	0.00	0.00	4.02
ol	13.99	0.00	5.57	2.60	13.83	13.70	16.23	11.54
or	12.90	28.32	26.63	29.77	12.20	17.19	22.99	10.66
sc	0.00	0.00	0.00	0.00	0.00	0.00	0.00	0.00
ap	2.56	0.24	0.29	0.17	2.26	2.00	1.28	1.23
ab	35.85	40.59	46.40	45.36	40.37	30.34	19.66	45.54
ac	0.00	3.85	0.00	4.46	0.00	0.00	0.00	0.00
mt	3.76	3.79	4.23	3.40	2.17	4.07	2.11	3.87
an	14.21	0.00	2.63	0.00	11.03	15.62	19.82	11.47
hm	0.00	0.00	0.00	0.00	0.00	0.00	0.00	0.00
cc	0.00	0.00	0.00	0.00	1.52	0.16	1.68	5.91
ne	0.83	0.00	2.56	2.69	2.67	2.00	3.23	0.00
di	10.55	2.82	9.86	10.13	9.96	10.67	7.99	0.00
il	5.36	1.42	1.83	1.40	3.98	4.25	5.02	4.84
H_2O	1.43	0.67	1.06	0.89	2.44	2.69	2.65	3.09
Ba	1227	207	983	114	537	1497	2737	577
Zr	343	919	1678	1434	378	321	231	266
Y	57	130	221	174	93	81	25	50
Sr	545	74	303	65	318	501	856	466
Rb	121	282	121	229	70	73	88	69
Zn	118	567	309	235	159	152	97	101
Cu	72	29	0	4	22	20	36	11
Ni	48	12	10	11	55	53	85	47
Cr	45	25	24	22	61	39	117	35
V	263	43	52	31	182	84	263	267

Appendix 4

Spec	101487	101331	101333	101345	101430	101336	101347	101431
SiO_2	45.82	47.98	47.58	46.72	48.04	45.84	48.46	45.43
Al_2O_3	14.86	18.19	18.34	16.67	14.58	16.72	17.98	15.62
Fe_2O_3	3.91	1.35	3.18	2.12	2.78	2.93	2.47	1.54
FeO	7.97	9.79	9.14	9.48	12.88	10.54	9.57	12.23
MgO	3.35	7.76	4.08	8.20	6.28	5.29	6.67	11.38
CaO	6.68	9.44	7.51	8.91	8.54	7.62	8.30	7.76
Na_2O	4.94	3.14	3.87	2.82	4.08	3.84	3.60	2.98
K_2O	2.39	0.53	1.04	0.59	0.83	1.56	0.77	0.28
H_2O^+	2.67	0.89	2.35	1.73	0.28	1.85	0.70	0.46
CO_2	3.00	0.00	0.00	0.00	0.00	0.00	0.00	0.00
TiO_2	2.69	1.34	2.50	1.52	2.79	2.76	1.75	1.32
P_2O_5	0.83	0.23	0.33	0.32	0.51	0.54	0.38	0.24
MnO	0.19	0.16	0.12	0.17	0.19	0.17	0.16	0.21
Sum	99.30	100.80	100.04	99.25	101.78	99.66	100.81	99.45
Q	0.00	0.00	0.00	0.00	0.00	0.00	0.00	0.00
wo	0.00	0.00	0.00	0.00	0.00	0.00	0.00	0.00
c	0.97	0.00	0.00	0.00	0.00	0.00	0.00	0.00
hy	0.00	0.55	2.83	6.79	0.00	0.00	2.57	0.00
ol	13.89	21.35	13.06	17.42	17.80	16.48	17.76	32.68
or	14.62	3.13	6.29	3.58	4.83	9.42	4.55	1.67
sc	0.00	0.00	0.00	0.00	0.00	0.00	0.00	0.00
ap	2.04	0.55	0.80	0.78	1.19	1.31	0.90	0.57
ab	42.00	26.59	33.54	24.47	29.40	26.42	30.43	23.47
ac	0.00	0.00	0.00	0.00	0.00	0.00	0.00	0.00
mt	4.37	1.96	3.59	2.90	3.97	4.15	3.26	2.26
an	9.06	34.00	30.32	31.87	18.73	24.30	30.59	28.70
hm	0.00	0.00	0.00	0.00	0.00	0.00	0.00	0.00
cc	7.06	0.00	0.00	0.00	0.00	0.00	0.00	0.00
ne	0.70	0.00	0.00	0.00	2.49	3.68	0.00	1.08
di	0.00	9.32	4.69	9.24	16.36	8.87	6.62	7.03
il	5.29	2.55	4.86	2.96	5.22	5.36	3.32	2.53
H_2O	2.67	0.89	2.35	1.73	0.28	1.85	0.70	0.46
Ba	1015	355	695	295	639	720	661	306
Zr	251	112	153	128	208	190	87	108
Y	67	33	49	34	46	48	25	22
Sr	549	385	492	366	302	485	667	370
Rb	105	18	34	22	19	47	18	14
Zn	125	98	98	86	64	70	73	75
Cu	43	0	9	86	30	167	63	55
Ni	52	158	67	203	71	60	128	276
Cr	77	81	87	81	98	44	64	45
V	113	167	389	171	296	130	143	135

Spec	101436	101338	101349	101356	101368	101369	101375	101381
SiO_2	47.33	46.48	58.13	48.31	46.65	47.74	50.42	47.72
Al_2O_3	17.52	17.34	15.67	14.30	16.32	16.99	16.35	15.44
Fe_2O_3	3.82	1.82	1.67	2.41	2.26	3.18	2.64	3.94
FeO	9.54	10.70	7.26	11.80	10.12	8.83	9.41	9.94
MgO	3.83	7.18	1.58	4.05	6.56	6.79	4.31	5.94
CaO	8.05	9.18	2.90	6.71	8.94	8.53	7.98	8.24
Na_2O	3.91	3.16	4.23	4.18	3.01	3.24	4.16	3.38
K_2O	1.42	0.41	4.99	2.64	0.72	0.94	1.68	1.30
H_2O^+	1.51	0.29	1.15	1.15	2.18	2.04	0.85	1.48
CO_2	0.00	0.00	0.00	0.00	0.00	0.00	0.00	0.00
TiO_2	3.04	1.75	1.15	3.13	2.40	1.63	1.92	2.15
P_2O_5	0.80	0.29	0.56	1.15	0.43	0.29	0.56	0.45
MnO	0.14	0.18	0.22	0.23	0.17	0.17	0.18	0.20
Sum	100.91	98.78	99.51	100.06	99.76	100.37	100.46	100.18
Q	0.00	0.00	3.09	0.00	0.00	0.00	0.00	0.00
wo	0.00	0.00	0.00	0.00	0.00	0.00	0.00	0.00
c	0.00	0.00	0.00	0.00	0.00	0.00	0.00	0.00
hy	0.00	0.16	13.88	0.00	7.45	3.40	0.00	1.77
ol	13.58	21.28	0.00	14.59	12.78	16.88	12.53	16.40
or	8.45	2.46	29.97	15.76	4.36	5.65	9.96	7.79
sc	0.00	0.00	0.00	0.00	0.00	0.00	0.00	0.00
ap	1.91	0.70	1.35	2.75	1.04	0.70	1.33	1.08
ab	32.09	27.14	36.38	30.84	26.09	27.91	35.03	29.00
ac	0.00	0.00	0.00	0.00	0.00	0.00	0.00	0.00
mt	4.00	2.68	2.46	3.53	3.36	3.23	3.80	3.93
an	26.23	32.40	9.18	12.59	29.60	29.56	21.05	23.44
hm	0.00	0.00	0.00	0.00	0.00	0.00	0.00	0.00
cc	0.00	0.00	0.00	0.00	0.00	0.00	0.00	0.00
ne	0.66	0.00	0.00	2.65	0.00	0.00	0.16	0.00
di	7.27	9.81	1.47	11.28	10.64	9.52	12.47	12.44
il	5.81	3.37	2.22	6.01	4.67	3.15	3.66	4.14
H_2O	1.51	0.29	1.15	1.15	2.18	2.04	0.85	1.48
Ba	934	304	3898	1322	434	619	1525	978
Zr	193	122	415	435	130	113	154	124
Y	52	42	75	95	38	36	54	44
Sr	448	412	215	365	471	457	578	626
Rb	35	11	57	62	31	24	30	48
Zn	62	4	116	133	100	82	119	155
Cu	45	8	0	31	134	79	71	146
Ni	46	112	6	27	119	133	42	72
Cr	22	48	17	19	59	56	55	52
V	232	195	112	256	175	184	171	236

Spec	101393	101394	101339	101342	101361	101351	101357	101366
SiO_2	47.36	49.62	48.63	48.61	52.53	46.13	47.86	51.71
Al_2O_3	19.38	23.28	13.99	14.41	15.75	14.92	13.51	15.00
Fe_2O_3	0.83	1.37	3.75	2.36	3.16	2.50	3.72	2.24
FeO	9.42	5.22	9.16	9.53	8.15	10.95	9.11	9.14
MgO	7.98	4.79	2.77	3.21	2.31	4.05	3.25	2.66
CaO	8.89	10.19	7.08	7.07	5.96	7.14	7.46	5.89
Na_2O	3.27	3.71	4.31	4.13	4.43	4.16	4.97	4.53
K_2O	0.51	0.69	2.62	2.73	2.87	2.18	1.22	2.86
H_2O^+	0.58	0.79	1.33	1.73	1.06	1.42	2.14	1.05
CO_2	0.00	0.00	0.00	0.00	0.00	0.00	0.00	0.00
TiO_2	1.01	0.79	3.00	3.03	2.56	3.58	3.20	2.69
P_2O_5	0.22	0.22	1.80	1.61	1.12	1.67	1.91	1.08
MnO	0.14	0.07	0.18	0.19	0.15	0.18	0.21	0.15
Sum	99.59	100.74	98.62	98.61	100.05	98.88	98.56	99.00
Q	0.00	0.00	0.00	0.00	0.07	0.00	0.00	0.00
wo	0.00	0.00	0.00	0.00	0.00	0.00	0.00	0.00
c	0.00	0.00	0.00	0.00	0.00	0.00	0.00	0.00
hy	0.00	0.00	1.05	0.00	12.09	0.00	1.00	5.96
ol	24.15	13.00	8.73	10.67	0.00	14.30	9.51	5.56
or	3.04	4.08	15.92	16.64	17.13	13.21	7.48	17.24
sc	0.00	0.00	0.00	0.00	0.00	0.00	0.00	0.00
ap	0.53	0.52	4.38	3.93	2.68	4.05	4.69	2.61
ab	26.17	29.98	37.50	35.90	37.86	31.85	43.61	39.11
ac	0.00	0.00	0.00	0.00	0.00	0.00	0.00	0.00
mt	1.22	1.80	4.56	3.53	4.01	3.72	4.30	3.31
an	37.06	44.85	11.40	13.12	14.76	15.99	11.35	12.39
hm	0.00	0.00	0.00	0.00	0.00	0.00	0.00	0.00
cc	0.00	0.00	0.00	0.00	0.00	0.00	0.00	0.00
ne	0.96	0.77	0.00	0.08	0.00	2.29	0.00	0.00
di	4.94	3.50	10.60	10.21	6.49	7.61	11.77	8.60
il	1.94	1.50	5.86	5.93	4.91	6.97	6.30	5.21
H_2O	0.58	0.79	1.33	1.73	1.06	1.42	2.14	1.05
Ba	422	471	2152	1563	1473	1742	2124	1535
Zr	74	64	180	215	240	213	226	250
Y	17	12	67	64	58	70	74	73
Sr	589	807	446	533	446	485	456	391
Rb	12	24	40	59	64	34	26	52
Zn	68	45	89	95	94	77	139	83
Cu	25	23	11	12	13	40	12	0
Ni	185	135	9	2	7	18	12	0
Cr	46	31	18	15	18	15	13	21
V	99	38	187	25	152	217	32	59

Appendix 4

Spec	101377	101340	101341	101343	101344	101362	101358	101355
SiO_2	53.40	57.69	57.96	57.30	62.21	58.59	56.23	51.84
Al_2O_3	14.85	15.83	15.68	15.68	15.79	15.33	15.63	14.74
Fe_2O_3	2.77	3.97	4.81	6.35	7.65	3.55	5.20	3.03
FeO	9.60	5.60	4.99	3.34	0.26	6.09	5.65	8.32
MgO	2.70	0.81	0.87	0.27	0.00	0.81	0.91	2.21
CaO	6.34	3.19	3.11	1.95	0.03	3.10	3.71	5.99
Na_2O	4.04	5.63	5.86	6.24	9.42	6.19	5.86	4.46
K_2O	1.95	4.59	4.85	5.48	2.51	4.42	4.10	2.98
H_2O^+	1.05	1.00	1.10	0.50	0.33	1.06	0.85	1.75
CO_2	0.00	0.00	0.00	2.09	0.26	0.00	0.48	0.00
TiO_2	2.80	1.30	1.31	0.96	0.07	1.37	1.43	2.37
P_2O_5	0.37	0.40	0.37	0.14	0.00	0.33	0.49	0.93
MnO	0.16	0.20	0.20	0.24	0.11	0.19	0.20	0.21
Sum	100.03	100.21	100.51	100.54	98.64	101.03	100.74	98.83
Q	3.52	0.00	1.11	5.40	1.99	0.00	0.00	0.00
wo	0.00	0.00	0.00	0.00	0.00	0.00	0.00	0.00
c	0.00	0.00	0.00	1.11	0.00	0.00	0.00	0.00
hy	12.72	3.38	1.74	0.67	0.00	0.00	1.76	6.96
ol	0.00	0.03	0.00	0.00	0.00	2.24	0.91	2.60
or	11.64	27.33	25.26	32.37	15.09	26.12	24.25	18.13
sc	0.00	0.00	0.00	1.70	0.58	0.00	0.00	0.00
ap	0.89	0.95	0.88	0.33	0.00	0.78	1.16	2.27
ab	34.53	48.01	49.87	44.39	68.40	50.71	49.63	38.86
ac	0.00	0.00	0.00	0.00	8.65	0.00	0.00	0.00
mt	3.98	5.80	7.01	8.76	1.01	5.15	7.55	4.17
an	16.80	4.40	3.95	0.00	0.00	0.99	4.24	11.74
hm	0.00	0.00	0.00	0.30	4.10	0.00	0.00	0.00
cc	0.00	0.00	0.00	3.15	0.05	0.00	1.09	0.00
ne	0.00	0.00	0.00	0.00	0.00	0.91	0.00	0.00
di	10.55	7.61	7.67	0.00	0.00	10.50	6.70	10.64
il	5.37	2.49	2.50	1.82	0.14	2.60	2.72	4.63
H_2O	1.05	1.00	1.10	0.50	0.33	1.06	0.85	1.75
Ba	917	2320	1888	336	14	1744	2819	2422
Zr	193	414	454	495	3944	384	278	224
Y	63	74	82	79	607	70	66	73
Sr	377	148	165	44	27	122	242	506
Rb	50	55	66	100	78	58	44	56
Zn	112	128	122	122	170	110	133	129
Cu	5	6	10	8	0	0	13	16
Ni	0	11	7	7	14	7	0	0
Cr	21	19	21	23	23	19	10	11
V	273	90	77	44	0	82	4	12

Appendix 4

Spec	101386	101388	101370	101360	101380	101391	101406	101417
SiO_2	47.51	46.38	46.38	47.02	48.49	47.62	49.71	47.63
Al_2O_3	16.57	16.60	17.35	16.36	16.98	16.75	13.32	16.91
Fe_2O_3	2.56	2.43	3.47	2.54	2.25	2.59	3.28	1.93
FeO	11.49	10.53	9.91	10.76	9.98	10.50	11.07	8.11
MgO	7.40	7.35	7.13	6.51	6.46	5.80	4.51	8.14
CaO	9.10	8.77	8.42	8.42	8.55	8.77	7.73	11.27
Na_2O	3.12	3.27	2.96	3.43	3.12	3.48	3.25	2.67
K_2O	0.59	0.61	0.92	0.74	1.09	1.04	1.76	0.45
H_2O^+	0.86	1.10	2.33	1.08	1.85	1.46	0.96	2.38
CO_2	0.00	0.00	0.00	0.00	0.00	0.00	0.00	0.00
TiO_2	1.99	1.80	1.97	2.21	1.72	2.40	2.87	1.63
P_2O_5	0.32	0.32	0.28	0.42	0.33	0.49	0.71	0.19
MnO	0.19	0.20	0.16	0.19	0.16	0.18	0.16	0.15
Sum	101.70	99.36	101.28	99.68	100.98	101.08	99.33	101.46
Q	0.00	0.00	0.00	0.00	0.00	0.00	0.02	0.00
wo	0.00	0.00	0.00	0.00	0.00	0.00	0.00	0.00
c	0.00	0.00	0.00	0.00	0.00	0.00	0.00	0.00
hy	2.77	0.00	2.15	1.86	7.58	0.00	18.62	1.49
ol	19.25	21.43	20.22	17.99	13.30	16.83	0.00	16.01
or	3.46	3.65	5.50	4.43	6.50	6.17	10.57	2.68
sc	0.00	0.00	0.00	0.00	0.00	0.00	0.00	0.00
ap	0.75	0.77	0.67	1.01	0.79	1.16	1.71	0.45
ab	26.18	26.83	25.34	29.43	26.63	29.47	27.96	22.81
ac	0.00	0.00	0.00	0.00	0.00	0.00	0.00	0.00
mt	3.52	3.51	3.48	3.57	3.29	3.62	4.22	2.37
an	29.22	29.19	31.70	27.44	29.36	27.11	16.83	33.14
hm	0.00	0.00	0.00	0.00	0.00	0.00	0.00	0.00
cc	0.00	0.00	0.00	0.00	0.00	0.00	0.00	0.00
ne	0.00	0.65	0.00	0.00	0.00	0.04	0.00	0.00
di	11.10	10.51	7.16	10.01	9.26	11.02	14.54	17.92
il	3.75	3.46	3.78	4.26	3.29	4.57	5.54	3.12
H_2O	0.86	1.10	2.33	1.08	1.85	1.46	0.96	2.38
Ba	385	418	499	656	668	771	738	321
Zr	128	123	81	120	117	135	325	137
Y	41	40	29	27	51	55	67	52
Sr	409	436	487	527	558	481	260	393
Rb	16	17	21	18	36	16	57	21
Zn	77	87	54	83	78	79	110	72
Cu	77	105	74	114	67	91	71	77
Ni	110	118	125	121	133	67	57	206
Cr	50	54	83	51	46	57	53	233
V	218	216	198	232	204	142	311	248

Spec	101418	101427	101428	101398	101419	101422	101426	101429
SiO_2	45.28	46.27	46.70	41.91	49.16	48.41	48.73	48.04
Al_2O_3	15.54	15.79	18.03	15.87	15.42	20.25	15.34	17.67
Fe_2O_3	2.85	2.26	1.87	4.40	2.75	1.00	3.32	1.31
FeO	13.38	10.73	10.19	10.49	10.23	8.55	9.86	9.34
MgO	7.53	5.98	6.91	6.61	5.35	7.50	6.29	7.40
CaO	7.67	8.62	8.86	9.96	8.74	9.89	8.59	9.50
Na_2O	3.18	3.47	3.33	2.39	3.19	3.04	3.38	3.13
K_2O	0.68	0.75	0.66	1.35	0.77	0.37	0.73	0.40
H_2O^+	0.80	0.97	0.58	2.53	1.04	0.64	0.83	0.47
CO_2	0.00	0.00	0.00	0.00	0.00	0.00	0.00	0.00
TiO_2	2.69	2.40	1.83	2.19	1.87	0.81	1.92	1.21
P_2O_5	0.34	0.42	0.39	0.60	0.32	0.14	0.33	0.20
MnO	0.20	0.17	0.15	0.26	0.19	0.13	0.20	0.17
Sum	100.14	97.83	99.50	98.56	99.03	100.73	99.52	98.84
Q	0.00	0.00	0.00	0.00	0.00	0.00	0.00	0.00
wo	0.00	0.00	0.00	0.00	0.00	0.00	0.00	0.00
c	0.00	0.00	0.00	0.00	0.00	0.00	0.00	0.00
hy	0.04	0.00	0.00	0.00	16.27	2.27	9.36	4.20
ol	24.36	17.52	20.71	20.40	4.31	19.81	11.07	17.50
or	4.04	4.57	3.94	8.32	4.64	2.18	4.37	2.40
sc	0.00	0.00	0.00	0.00	0.00	0.00	0.00	0.00
ap	0.81	1.03	0.93	1.48	0.77	0.33	0.79	0.48
ab	27.08	29.93	27.31	12.48	27.55	25.70	29.00	26.92
ac	0.00	0.00	0.00	0.00	0.00	0.00	0.00	0.00
mt	4.16	3.38	2.74	3.89	3.43	1.45	3.50	1.93
an	26.29	26.11	32.64	29.82	26.01	40.47	24.87	33.52
hm	0.00	0.00	0.00	0.00	0.00	0.00	0.00	0.00
cc	0.00	0.00	0.00	0.00	0.00	0.00	0.00	0.00
ne	0.00	0.20	0.63	4.67	0.00	0.00	0.00	0.00
di	8.08	12.56	7.57	14.60	13.38	6.25	13.34	10.71
il	5.14	4.70	3.51	4.34	3.63	1.54	3.70	2.34
H_2O	0.80	0.97	0.58	2.53	1.04	0.64	0.83	0.47
Ba	454	487	412	887	611	209	639	319
Zr	159	198	155	165	149	56	145	97
Y	43	45	41	62	50	12	38	28
Sr	310	327	363	1764	399	422	394	349
Rb	22	20	22	31	23	14	21	21
Zn	101	98	87	34	97	65	92	75
Cu	107	86	78	5	87	48	107	132
Ni	133	108	145	83	86	172	78	106
Cr	130	145	125	54	68	65	60	93
V	298	232	175	242	222	113	204	141

Appendix 4

Spec	101400	101401	101403	101404	101405	101421	101425	101407
SiO_2	47.42	47.68	47.83	48.37	48.03	46.24	47.39	47.40
Al_2O_3	18.77	12.03	16.81	18.43	16.31	14.49	14.76	19.15
Fe_2O_3	2.81	2.49	1.94	2.21	1.57	3.14	4.19	0.17
FeO	7.43	8.17	10.70	8.71	11.46	12.20	11.35	9.41
MgO	7.51	10.14	7.16	7.40	7.42	5.52	5.40	8.50
CaO	8.60	9.07	9.24	9.18	9.06	7.87	7.65	9.05
Na_2O	2.70	3.22	3.20	3.18	3.23	3.52	3.55	3.30
K_2O	1.57	1.23	0.44	0.66	0.51	0.94	1.22	0.39
H_2O^+	2.68	2.36	0.55	0.58	0.41	0.66	1.04	0.33
CO_2	0.00	3.06	0.00	0.00	0.00	0.00	0.00	0.00
TiO_2	1.13	2.12	1.65	1.22	1.70	2.94	2.82	0.96
P_2O_5	0.16	0.66	0.22	0.21	0.24	0.40	0.43	0.22
MnO	0.14	0.15	0.17	0.15	0.20	0.18	0.21	0.14
Sum	100.92	102.38	99.91	100.30	100.14	98.10	100.01	99.02
Q	0.00	0.00	0.00	0.00	0.00	0.00	0.00	0.00
wo	0.00	0.00	0.00	0.00	0.00	0.00	0.00	0.00
c	0.00	0.00	0.00	0.00	0.00	0.00	0.00	0.00
hy	0.63	21.35	3.75	3.19	2.61	1.45	2.98	0.00
ol	20.24	7.97	17.72	17.82	19.99	16.56	15.39	25.27
or	9.45	7.26	2.62	3.91	3.02	5.70	7.29	2.33
sc	0.00	0.00	0.00	0.00	0.00	0.00	0.00	0.00
ap	0.39	1.56	0.52	0.50	0.57	0.97	1.03	0.53
ab	23.27	27.23	27.25	26.99	27.40	30.57	30.38	25.59
ac	0.00	0.00	0.00	0.00	0.00	0.00	0.00	0.00
mt	2.78	3.61	2.83	2.81	2.28	4.30	4.41	0.25
an	35.10	14.73	30.39	34.17	28.57	21.51	20.97	36.76
hm	0.00	0.00	0.00	0.00	0.00	0.00	0.00	0.00
cc	0.00	6.95	0.00	0.00	0.00	0.00	0.00	0.00
ne	0.00	0.00	0.00	0.00	0.00	0.00	0.00	1.46
di	5.95	5.31	11.77	8.29	12.32	13.20	12.13	5.95
il	2.19	4.02	3.15	2.32	3.24	5.73	5.42	1.85
H_2O	2.68	2.36	0.55	0.58	0.41	0.66	1.04	0.33
Ba	424	1386	305	374	377	710	754	312
Zr	129	188	116	91	126	180	210	101
Y	49	46	35	19	39	54	54	19
Sr	785	1149	380	523	377	388	363	393
Rb	53	55	16	17	17	18	41	14
Zn	64	105	84	75	90	11	93	76
Cu	45	41	110	38	119	0	144	0
Ni	173	291	115	130	122	63	72	175
Cr	71	330	81	47	88	53	55	48
V	141	155	181	116	215	317	326	60

Appendix 4

Spec	101408	101409	101411	101412	101413	101415	101416	H
SiO_2	48.11	49.37	38.03	45.65	47.36	47.21	46.52	50.99
Al_2O_3	14.86	16.85	7.86	15.32	14.91	14.71	14.53	15.72
Fe_2O_3	3.61	2.37	4.51	4.10	4.03	3.57	1.15	1.52
FeO	11.28	9.96	10.45	10.29	10.65	11.78	9.32	9.55
MgO	4.59	2.71	10.61	4.69	6.19	4.98	6.16	5.83
CaO	7.54	4.41	12.78	8.40	9.83	7.58	8.75	7.34
Na_2O	3.57	5.83	2.44	3.82	2.99	3.51	3.44	3.04
K_2O	1.35	2.65	2.36	1.42	0.66	1.27	2.55	1.75
H_2O^+	1.17	1.69	1.53	1.15	1.21	1.23	2.42	3.25
CO_2	0.00	1.61	3.93	0.82	0.00	0.00	0.00	0.00
TiO_2	2.99	2.46	4.66	2.55	2.27	3.05	3.92	1.58
P_2O_5	1.19	0.68	1.31	0.42	0.31	0.55	0.52	0.30
MnO	0.19	0.12	0.20	0.21	0.21	0.19	0.16	0.20
Sum	100.45	100.71	100.67	98.84	100.62	99.63	99.44	101.07
Q	0.00	0.00	0.00	0.00	0.00	0.00	0.00	0.00
wo	0.00	0.00	0.00	0.00	0.00	0.00	0.00	0.00
c	0.00	1.75	0.00	0.00	0.00	0.00	0.00	0.00
hy	13.88	0.00	0.00	0.00	4.48	5.73	0.00	20.54
ol	6.48	14.52	17.68	15.75	13.96	12.51	12.04	3.18
or	8.03	15.81	14.06	8.60	3.93	7.63	15.53	10.57
sc	0.00	0.00	0.00	0.00	0.00	0.00	0.00	0.00
ap	2.84	1.63	3.13	1.02	0.74	1.32	1.27	0.73
ab	30.43	43.89	9.69	28.72	25.48	30.19	19.03	26.29
ac	0.00	0.00	0.00	0.00	0.00	0.00	0.00	0.00
mt	4.29	3.47	6.59	4.35	3.67	4.42	1.72	2.25
an	20.68	7.33	3.55	20.96	25.50	20.97	17.18	24.61
hm	0.00	0.00	0.00	0.00	0.00	0.00	0.00	0.00
cc	0.00	3.70	9.01	1.91	0.00	0.00	0.00	0.00
ne	0.00	3.20	6.02	2.38	0.00	0.00	5.94	0.00
di	7.65	0.00	21.35	11.35	17.90	11.34	19.62	8.76
il	5.72	4.72	8.92	4.96	4.34	5.89	7.67	3.07
H_2O	1.17	1.69	1.53	1.15	1.21	1.23	2.42	3.25
Ba	676	1390	1047	591	411	815	1381	698
Zr	245	344	400	206	166	221	767	166
Y	68	39	63	63	50	58	46	50
Sr	336	1487	1157	463	287	373	627	546
Rb	49	45	59	42	22	54	68	56
Zn	75	167	138	120	84	90	86	121
Cu	39	8	159	47	88	74	16	23
Ni	44	15	369	66	82	54	128	96
Cr	55	16	171	91	120	57	199	45
V	159	196	461	180	289	289	390	206

Spec	P	X	EC621A	121201	121203	121219	121244	121247
SiO_2	52.51	49.78	49.11	44.52	48.30	47.76	57.08	61.65
Al_2O_3	16.11	15.45	18.60	10.26	18.17	18.53	12.69	14.32
Fe_2O_3	1.42	5.20	0.55	3.72	2.60	2.71	5.40	6.57
FeO	8.88	6.54	11.06	16.32	9.07	9.18	8.90	2.47
MgO	6.85	6.04	6.91	4.12	3.52	5.40	0.34	0.26
CaO	7.78	6.87	12.29	8.29	9.44	9.37	4.15	2.49
Na_2O	3.33	2.73	1.37	3.50	3.88	3.48	5.16	4.90
K_2O	1.70	2.65	0.00	1.41	1.01	0.67	3.44	3.85
H_2O^+	1.63	2.51	0.20	0.00	0.00	0.00	0.00	0.00
CO_2	0.00	0.00	0.00	0.00	0.00	0.00	0.00	0.00
TiO_2	1.24	4.03	0.90	4.20	2.60	2.19	1.46	0.99
P_2O_5	0.29	0.49	0.33	1.91	0.52	0.35	0.35	0.21
MnO	0.16	0.23	0.21	0.28	0.15	0.15	0.31	0.20
Sum	101.90	102.52	101.53	98.53	99.26	99.79	99.28	97.91
Q	0.00	0.00	0.00	0.00	0.00	0.00	4.62	14.73
wo	0.00	0.00	0.00	0.00	0.00	0.00	0.00	1.48
c	0.00	0.00	0.00	0.00	0.00	0.00	0.00	0.00
hy	14.90	16.18	29.57	3.52	0.00	0.67	3.05	0.00
ol	7.57	5.38	0.10	14.01	10.54	15.35	0.00	0.00
or	10.02	16.00	0.00	8.45	6.01	3.97	20.47	23.23
sc	0.00	0.00	0.00	0.00	0.00	0.00	0.00	0.00
ap	0.68	1.19	0.77	4.59	1.24	0.83	0.83	0.51
ab	28.10	23.60	11.44	30.03	31.87	29.52	43.97	42.34
ac	0.00	0.00	0.00	0.00	0.00	0.00	0.00	0.00
mt	2.05	3.57	0.79	5.47	3.33	3.15	7.88	5.87
an	23.92	22.56	44.01	8.23	29.40	33.04	1.31	5.83
hm	0.00	0.00	0.00	0.00	0.00	0.00	0.00	2.66
cc	0.00	0.00	0.00	0.00	0.00	0.00	0.00	0.00
ne	0.00	0.00	0.00	0.00	0.65	0.00	0.00	0.00
di	10.40	7.38	11.64	17.62	11.98	9.30	15.07	1.43
il	2.35	4.15	1.69	8.09	4.97	4.17	2.79	1.92
H_2O	1.63	2.51	0.20	0.00	0.00	0.00	0.00	0.00

Ba	637	1007	761
Zr	153	216	101
Y	50	58	53
Sr	451	342	858
Rb	41	90	6
Zn	101	131	83
Cu	6	6	68
Ni	135	50	12
Cr	118	43	39
V	195	295	265

Appendix 4

Spec	121252	121261	121262	121266	121268	121269	121271	121284
SiO_2	57.90	55.52	58.30	63.94	53.89	52.82	50.97	53.49
Al_2O_3	15.57	14.06	14.22	13.73	14.29	16.68	13.54	12.20
Fe_2O_3	1.50	3.08	6.25	4.03	5.47	2.44	4.12	2.02
FeO	6.20	7.90	5.01	4.15	6.92	7.36	8.87	13.55
MgO	3.19	2.95	0.43	0.39	1.66	3.89	2.55	0.61
CaO	4.99	5.88	3.01	1.86	5.26	6.91	6.09	5.26
Na_2O	4.28	3.90	6.07	5.16	4.64	3.88	4.88	4.61
K_2O	2.71	2.18	3.63	4.38	2.54	2.00	1.99	3.39
H_2O^+	0.00	0.00	0.00	0.00	0.00	0.00	0.00	0.00
CO_2	0.00	0.00	0.00	0.00	0.00	0.00	0.00	0.00
TiO_2	1.34	2.47	1.24	0.91	2.26	1.80	2.57	1.65
P_2O_5	0.31	0.44	0.28	0.15	0.88	0.34	0.87	0.49
MnO	0.13	0.16	0.28	0.22	0.19	0.15	0.22	0.34
Sum	98.12	98.54	98.72	98.92	98.00	98.27	96.67	97.61
Q	6.06	6.91	4.36	13.19	5.93	0.71	0.00	0.00
wo	0.00	0.00	1.70	0.00	0.00	0.00	0.00	0.00
c	0.00	0.00	0.00	0.00	0.00	0.00	0.00	0.00
hy	13.30	12.43	0.00	1.14	5.03	15.55	5.95	3.27
ol	0.00	0.00	0.00	0.00	0.00	0.00	4.49	7.87
or	16.32	13.08	21.72	26.16	15.31	12.03	12.17	20.52
sc	0.00	0.00	0.00	0.00	0.00	0.00	0.00	0.00
ap	0.75	1.06	0.67	0.36	2.13	0.82	2.13	1.19
ab	36.90	33.51	52.02	44.13	40.04	33.41	42.74	39.95
ac	0.00	0.00	0.00	0.00	0.00	0.00	0.00	0.00
mt	2.22	3.53	9.18	5.91	8.09	3.11	4.55	3.00
an	15.56	14.64	0.84	1.38	10.87	22.58	9.48	2.65
hm	0.00	0.00	0.00	0.00	0.00	0.00	0.00	0.00
cc	0.00	0.00	0.00	0.00	0.00	0.00	0.00	0.00
ne	0.00	0.00	0.00	0.00	0.00	0.00	0.00	0.00
di	6.30	10.08	7.12	5.98	8.21	8.31	13.43	18.35
il	2.59	4.76	2.39	1.75	4.38	3.48	5.05	3.21
H_2O	0.00	0.00	0.00	0.00	0.00	0.00	0.00	0.00
Ba								
Zr								
Y								
Sr								
Rb								
Zn								
Cu								
Ni								
Cr								
V								

Appendix 4

Spec	121293	121293	121294	121301	121302	121305	121317
SiO_2	75.97	75.88	67.11	44.05	49.97	45.23	51.97
Al_2O_3	11.87	11.56	15.04	15.40	16.37	13.06	12.86
Fe_2O_3	1.87	1.76	0.95	2.13	2.53	3.22	1.44
FeO	0.97	1.02	2.78	10.25	9.08	11.00	12.76
MgO	0.08	0.11	1.11	10.84	4.43	3.58	1.91
CaO	0.03	0.10	1.98	7.65	7.14	8.98	5.21
Na_2O	4.44	4.07	4.81	2.34	4.11	3.69	4.90
K_2O	3.80	4.30	3.88	0.54	1.27	1.22	2.51
H_2O^+	0.00	0.00	0.00	0.00	0.00	0.00	0.00
CO_2	0.00	0.00	0.00	0.00	0.00	0.00	0.00
TiO_2	0.07	0.15	0.65	1.50	2.04	4.09	2.33
P_2O_5	0.00	0.02	0.17	0.36	0.33	1.68	0.86
MnO	0.03	0.04	0.09	0.17	0.16	0.20	0.27
Sum	99.13	99.01	98.57	95.23	97.43	95.95	97.02
Q	35.65	35.67	17.72	0.00	0.00	0.00	0.00
wo	0.00	0.00	0.00	0.00	0.00	0.00	0.00
c	0.40	0.08	0.00	0.00	0.00	0.00	0.00
hy	0.38	0.52	5.96	7.87	7.82	4.44	4.13
ol	0.00	0.00	0.00	24.83	8.21	7.19	10.27
or	22.65	25.66	23.26	3.35	7.70	7.51	15.28
sc	0.00	0.00	0.00	0.00	0.00	0.00	0.00
ap	0.00	0.05	0.41	0.90	0.80	4.15	2.10
ab	37.90	34.78	41.29	20.79	35.69	32.53	42.71
ac	0.00	0.00	0.00	0.00	0.00	0.00	0.00
mt	2.74	2.58	1.40	3.01	3.56	4.21	2.15
an	0.15	0.37	8.10	31.42	23.06	16.11	5.85
hm	0.00	0.00	0.00	0.00	0.00	0.00	0.00
cc	0.00	0.00	0.00	0.00	0.00	0.00	0.00
ne	0.00	0.00	0.00	0.00	0.00	0.00	0.00
di	0.00	0.00	0.61	4.84	9.19	15.77	12.94
il	0.13	0.29	1.25	2.99	3.98	8.09	4.56
H_2O	0.00	0.00	0.00	0.00	0.00	0.00	0.00
Ba							
Zr							
Y							
Sr							
Rb							
Zn							
Cu							
Ni							
Cr							
V							

Appendix 5

Mineral analyses

Explanation of symbols and abbreviations

Name	D	= dolerite
	TD	= trachydolerite
	SG	= syenogabbro
	Tdi	= trachydiorite
	A	= anorthosite
Occur.	pc	= phenocryst core
	gr	= groundmass rim
Rock	Greenland Geological Survey specimen numbers.	
FeO*	= total Fe as FeO	
nd	= not determined	

an analyses marked * is the mean of 2 or more analyses

in table A.5.1, 101419a to d are analyses from the core to the rim of one phenocryst.

Table A.5.1

Feldspar analyses

Name	D	D	D	D	D	D	D	D
Occur.	p	g	g	pc	p	p	pr	g
Rock	101413a*	101413 b	101413c	101419a	101419b	101419c	101419d	101419e
SiO_2	52.25	53 .68	53.25	51.84	50.89	51.06	50.74	53.87
Al_2O_3	29.57	27.99	28.25	29.90	30.26	30.37	30.48	28.05
TiO_2	0.07	0.10	0.15	0.05	0.06	0.05	0.09	0.10
FeO*	0.62	0.91	0.98	0.45	0.45	0.44	0.57	0.67
MgO	0.22	0.18	0.26	0.13	0.13	0.12	0.13	0.11
CaO	13.23	11.81	12.26	13.22	13.83	14.07	14.17	11.27
Na_2O	3.91	4.39	4.18	3.89	3.52	3.50	3.44	4.91
K_2O	0.15	0.22	0.21	0.14	0.13	0.13	0.12	0.26
BaO	nd	nd	nd	nd	nd	nd	nd	nd
Sum	100.02	99.28	99.53	99.62	99.27	99.74	99.74	99.24
Mol%								
An	64.6	59.0	61.0	64.7	67.9	68.4	69.0	55.1
Ab	34.5	39.7	37.7	34.5	31.3	30.8	30.3	43.4

Name	TD	TD	TD	TD	TD	TD	TD	TD	TD
Occur.	p	p	g	g	pc	pr	p?	p	p
Rock	101469a	101469b	101469c	101412a	101412b	101412c	101412d	101277a	101277b
SiO_2	54.60	55.62	58.72	51.85	52.19	51.95	53.43	53.56	53.31
Al_2O_3	27.77	27.01	25.14	29.86	29.41	29.33	28.33	28.29	27.97
TiO_2	0.14	0.14	0.20	0.10	0.09	0.10	0.15	0.17	0.19
FeO*	0.31	0.24	0.44	0.60	0.47	0.53	1.29	0.45	0.75
MgO	0.06	0.07	0.05	0.14	0.15	0.14	0.45	0.11	0.13
CaO	10.24	9.40	7.33	13.53	13.00	12.88	11.28	11.75	11.33
Na_2O	5.23	5.62	6.80	3.27	3.97	3.89	4.87	4.75	4.68
K_2O	0.57	0.72	0.75	0.17	0.21	0.19	0.22	0.41	0.43
BaO	0.14	0.16	0.35	nd	nd	nd	nd	nd	nd
Sum	99.06	98.98	99.80	99.52	99.49	99.01	100.02	99.32	98.79
Mol%									
An	50.3	46.0	35.7	66.1	63.6	63.9	55.4	57.3	55.8
Ab	46.4	49.8	59.9	32.9	35.2	34.9	43.3	40.3	41.7
Or	3.3	4.2	4.4	1.0	1.2	1.2	1.3	2.4	2.5

Name	TD	TD	TD	TD	TD	TD	TD	TD	TD
Occur.	g	p	pr	pc	p	p	g	pc	pr
Rock	101277c	101375a	101375b	101375c	101375d	101375e	101375f	101356a	101356b
SiO_2	55.10	52.38	54.15	54.00	53.57	55.51	62.61	56.85	57.93
Al_2O_3	27.49	29.03	27.85	27.87	28.16	26.49	21.09	26.15	25.10
TiO_2	0.24	0.06	0.12	0.09	0.06	0.13	0.16	0.18	0.21
FeO*	0.66	0.58	0.62	0.52	0.60	0.88	0.71	0.56	0.76
MgO	0.08	0.08	0.04	0.07	0.09	0.05	0.38	0.07	0.06
CaO	10.15	12.58	11.54	11.27	11.63	10.05	6.24	8.85	7.75
Na_2O	5.66	4.10	4.43	4.56	4.60	5.45	8.72	6.19	6.82
K_2O	0.28	0.36	0.43	0.42	0.45	0.52	0.29	0.54	0.55
Sum	99.65	99.17	99.18	98.80	99.16	99.08	100.2	99.3 9	99.18
Mol%									
An	49.0	61.6	57.3	56.3	56.8	49.0	27.9	42.7	37.4
Ab	49.4	36.3	40.0	41.2	40.6	48.0	70.6	54.2	59.5
Or	1.6	2.1	2.7	2.5	2.6	3.0	1.5	3.1	3.2

Name	TD	TD	TD	TD	TD	A	A	A
Occur.	pc	pr	g	pc	pr	pc	pr	g
Rock	101356c	101356d	101356e	86029a	86029b	101394a	101394b	101394c
SiO_2	55.49	56.05	56.24	59.61	63.00	54.32	54.69	51.88
Al_2O_3	27.12	26.87	26.57	24.26	22.27	27.94	27.83	30.04
TiO_2	0.16	0.14	0.19	0.12	0.17	0.10	0.11	0.12
FeO*	0.58	0.54	0.82	0.25	0.37	0.42	0.46	0.46
MgO	0.09	0.08	0.05	0.03	0.04	0.08	0.08	0.08
CaO	10.16	9.38	8.48	6.25	3.48	11.37	11.18	13 .33
Na_2O	5.64	5.95	6.29	7.54	9.13	4.89	4.96	4.05
K_2O	0.48	0.44	0.22	0.76	0.81	0.43	0.46	0.24
Sum	99.72	99.45	98.88	98.82	99.27	99.55	99.77	100.20
Mol%								
An	48.6	45.3	42.1	30.1	16.6	54.8	54.0	63.6
Ab	48.7	52.2	56.6	65.6	78.8	42.7	43.4	35.0
Or	2.7	2.5	1.3	4.4	4.6	2.5	2.6	1.4

Name	D	D	D	D	D	D	D	D	D
Occur.	g	gc	gr	gc	gr	g	g	g	gc
Rock	101393a	101393b	101393c	101393d	101393e	101331a	101331b	101331c	101418a
SiO_2	52.09	55.01	53.51	53.59	54.39	53.86	55.81	51.74	52.78
Al_2O_3	30.42	29.62	28.85	28.99	28.12	28.57	27.40	30.21	29.24
TiO_2	0.13	0.13	0.16	0.13	0.14	0.13	0.14	0.05	0.09
FeO*	0.38	0.46	0.45	0.43	0.20	0.64	0.53	0.49	0.52
MgO	0.06	0.07	0.11	0.04	0.02	0.05	0.03	0.07	0.09
CaO	12.95	10.76	11.90	11.96	10.93	11.88	9.97	13.65	12.49
Na_2O	4.50	5.20	4.61	4.47	5.09	4.49	5.25	3.63	4.39
K_2O	0.20	0.50	0.36	0.30	0.27	0.36	0.3 6	0.27	0.28
Sum	100.73	101.75	99.95	99.91	99.16	99.98	99.49	100.11	99.88
Mol%									
An	60.7	51.8	57.6	58.6	53.4	58.1	50.0	66.4	60.1
Ab	38.2	45.3	40.4	39.6	45.0	39.8	47.8	32.0	38.3
Or	1.1	2.9	2.0	1.8	1.6	2.1	2.2	1.6	1.6

Name	D	D	D	TD	TD	TD	TD	TD
Occur.	gr	g	g	g	g	g	g	g
Rock	101418b	101418c	101418d	30736	101266a	101266b	101401a	101401b
SiO_2	53.28	55.02	57.97	53.02	53.99	55.02	54.79	54.51
Al_2O_3	28.35	27.62	25.84	27.32	28.59	28.08	27.51	27.74
TiO_2	0.14	0.15	0.14	0.18	0.09	0.09	0.14	0.15
FeO*	0.45	0.52	0.42	0.15	0.51	0.60	0.51	0.46
MgO	0.09	0.39	0.05	0.05	0.06	0.07	0.12	0.10
CaO	11.85	10.92	7.91	11.60	11.69	10.77	10.49	10.43
Na_2O	4.39	5.15	6.68	4.90	4.90	5.36	5.33	5.27
K_2O	0.44	0.40	0.74	0.23	0.39	0.37	0.39	0.39
Sum	98.99	100.17	99.75	97.45	100.76	100.36	99.28	99.05
Mol%								
An	58.3	52.7	37.9	55.9	55.6	51.5	50.9	51.0
Ab	39.1	45.0	57.9	42.8	42.2	46.4	46.8	46.7
Or	2.6	2.3	4.2	1.3	2.2	2.1	2.3	2.3

Name	SG	SG	SG	Tdi	Tdi
Occur.	g	gc	gr	p	g
Rock	101361a	101361b	101361c	101319a	101319b
SiO_2	57.92	57.24	64.15	55.69	67.16
Al_2O_3	25.11	26.40	19.47	27.06	21.0
TiO_2	0.13	0.12	0.14	0.07	0.27
FeO*	0.37	0.32	0.16	0.34	0.29
MgO	0.04	0.04	0.02	0.07	0.02
CaO	7.93	8.70	1.16	9.90	1.27
Na_2O	6.88	6.37	3.88	5.40	6.74
K_2O	0.55	0.46	9.87	0.96	2.10
Sum	98.93	99.65	98.77	99.49	98.85
Mol%					
An	37.7	41.9	5.8	47.5	8.0
Ab	59.2	55.5	35.2	47.0	76.4
Or	3.1	2.6	59.0	5.5	15.6

Table A.5.2

Olivine analyses

Name	D	TD	TD	TD	TD	TD	TD	TD	TD
Occur.	p	p	p	p	g	p	g	g	p
Rock	101413	30736a	30736b	30736c	30736d	101469a*	101469b	101469c	86029
SiO_2	38.63	35.66	35.92	36.23	35.74	36.82	36.13	35.37	35.77
TiO_2	0.04	0.06	0.08	0.07	0.10	0.07	0.05	0.11	0.08
Al_2O_3	0.05	0.06	0.05	0.05	0.06	0.08	0.07	0.06	0.05
FeO*	22.89	34.13	34.87	34.45	35.64	29.35	35.97	40.42	37.0
MnO	nd	nd	nd	nd	nd	0.36	nd	0.66	nd
MgO	38.40	29.84	29.96	29.23	28.39	33.51	28.23	24.39	27.08
CaO	0.40	0.40	0.41	0.44	0.32	0.28	0.32	0.49	0.37
Na_2O	0.01	0.02	0.04	0.03	0.02	0.02	0.02	0.02	0.05
K_2O	-	-	-	-	-	-	-	-	-
Sum	100.42	99.81	101.33	100.5	100.27	100.49	100.79	101.52	100.4
Mol%									
Fo	75.0	60.9	60.5	60.2	58.7	67.0	58.3	51.8	56.6
Fa	25.0	39.1	39.5	39.8	41.3	33.0	41.7	48.2	43.4

Name	A	A	D	D	D	D	TD	SG
Occur.	g	g	g	g	g	g	g	g
Rock	101394a	101394b	101393*	101418*	101331a*	101331b*	101266	101361
SiO_2	37.45	36.97	36.09	36.16	36.25	35.93	35.99	32.22
TiO_2	0.03	0.06	0.04	0.06	0.05	0.07	0.02	0.06
Al_2O_3	0.04	0.08	0.03	0.09	0.05	0.03	0.05	0.05
FeO*	28.30	31.11	34.14	35.25	35.90	37.53	37.13	55.84
MgO	33.84	31.95	29.41	28.48	27.58	26.94	26.98	11.75
CaO	0.30	0.31	0.36	0.30	0.16	0.16	0.14	0.14
Na_2O	0.02	0.01	0.03	-	0.05	0.02	0.01	-
K_2O	-	-	-	0.01	-	-	0.02	-
								1.16(MnO)
Sum	99.98	100.49	100.01	100.36	100.05	100.68	100.34	101.22
Mol%								
Fo	68.0	65.0	61.5	58.9	58.0	56.0	56.5	26.9
Fa	32.0	35.0	39.5	41.1	42.0	44.0	43.5	73.1 (+ Mn)

Table A.5.3

Pyroxene analyses

Name	D	D	D	D	D	D	A	D	D
ccur.	E	E	E	E	E	E	E	E	E
Rock	101266	101331	101418a	101418b	101393a	101393b	101394	101413a	101413 b
SiO_2	49.17	49.95	50.64	49.26	49.54	50.92	49.75	48.17	46.99
l_2O_3	2.78	2.97	2.07	3.04	3.30	2.39	2.58	4.48	5.10
TiO_2	1.81	1.91	1.27	1.53	1.91	1.39	1.60	1.86	2.43
e_2O_3	1.12	1.34	1.31	1.32	1.65	1.35	1.74	1.37	1.46
FeO	10.14	9.58	10.24	10.81	8.51	8.73	10.13	10.95	10.97
FeO*	11.15	10.80	11.42	12.00	9.99	9.94	11.71	12.18	12.27
MgO	12.98	13.25	12.70	12.30	12.67	13.80	12.22	11.94	11.67
CaO	19.95	20.43	20.12	19.85	21.81	21.29	20.79	19.80	20.10
Na_2O	0.43	0.51	0.51	0.51	0.62	0.53	0.67	0.53	0.55
K_2O	0.02	-	-	-	0.03	-	0.01	0.01	0.02
Sum	98.94	99.94	99.49	98.62	100.04	100.40	99.49	99.11	99.29
Mol%									
CaO	42.71	43.60	43.10	42.90	46.20	44.10	44.30	43.10	43.80
MgO	38.65	38.40	37.80	36.90	37.30	39.80	36.20	36.20	35.40
FeO*	18.63	18.00	19.10	20.20	16.50	16.10	19.50	20.70	20.90
				NUMBER OF IONS ON THE BASIS OF 6 OXYGENS					
Si	1.893	1.883	1.931	1.891	1.869	1.906	1.896	1.844	1.803
Al	.107	.117	.069	.109	.131	.094	.104	.156	.197
Al	.018	.015	.024	.028	.015	.011	.012	.046	.033
Ti	.052	.054	.036	.044	.054	.039	.046	.054	.070
Fe^{3+}	.032	.038	.038	.038	.047	.038	.050	.040	.042
Fe^{2+}	.323	.302	.326	.347	.269	.273	.323	.351	.352
Mg	.737	.725	.722	.704	.713	.769	.694	.681	.667
Ca	.814	.825	.822	.816	.882	.853	.849	.812	.826
Na	.032	.038	.038	.038	.045	.038	.050	.039	.041
K	.001	-	-	-	.002	-	.001	.001	.001

Name	TD	TD	TD	SG		Tdi	Tdi	Tdi	Tdi
ccur.	p	g	g	g		p	g	gc	gr
Rock	86029a	86029b	101469	101361		101319a	101319b	101313a	101313b
SiO_2	51.23	50.38	46.96	50.25		50.07	46.28	46.77	48.52
l_2O_3	1.67	2.32	4.79	2.01		3.24	6.64	5.44	3.85
TiO_2	0.82	1.84	3.13	1.23		0.97	3.64	2.93	1.92
e_2O_3	1.39	1.70	1.96	1.21		1.84	1.42	1.43	1.58
FeO	10.21	10.94	9.73	11.66		12.70	8.15	9.54	10.20
eO*	11.46	12.47	11.49	12.75		14.36	9.43	10.82	11.62
MgO	11.84	10.71	10.36	12.49		10.20	11.73	10.92	10.81
CaO	21.63	21.64	21.40	20.33		20.39	21.36	21.81	21.57
a_2O	0.54	0.66	0.76	0.47		0.70	0.53	0.54	0.59
K_2O	-	-	-	-		0.02	0.03	0.02	0.03
Sum	99.33	100.19	99.09	99.65		100.13	99.78	99.40	99.07
ol%									
CaO	45.98	46.77	47.79	42.66		44.53	47.43	48.00	47.00
MgO	35.01	32.19	32.18	36.46		31.00	36.23	33.50	33.00
eO*	19.01	21.04	20.03	20.89	FeO	24.47	16.34	18.50	20.00
			NUMBER OF IONS ON THE BASIS OF 6 OXYGENS						
Si	1.951	1.915	1.808	1.915		1.913	1.751	1.790	1.863
Al^{iv}	0.049	0.085	0.192	0.085	Al	.087	.249	.210	.137
Al^{vi}	0.026	0.019	0.026	0.006	Al	.059	.047	.035	.037
Ti	0.024	0.053	0.091	0.035		.028	.104	.084	.055
Fe^{3+}	0.040	0.049	0.057	0.035		.053	.040	.041	.046
Fe^{2+}	0.325	0.348	0.313	0.372		.406	.258	.305	.328
Mg	0.672	0.607	0.594	0.709		.581	.662	.623	.619
Ca	0.883	0.881	0.883	0.830		.835	.866	.894	.887
Na	0.040	0.049	0.057	0.035		.052	.039	.040	.044
K	-	-	-	-		.001	.001	.001	.001

Table A.5.4

Proportions of end member molecules, clinopyroxenes

Rock	Wo	En	Fs	Ct	Tt	Ac
101266	37.59	36.84	16.15	1.06	5.19	3.18
101331	37.73	36.99	15.02	1.17	5.38	3.71
101418a	39.93	36.21	16.39	1.01	3.66	3.79
101418b	37.16	34.96	17.24	2.45	4.40	3.78
101393a	39.89	35.15	13.24	1.90	5.35	4.47
101393b	39.68	37.99	13.48	1.33	3.86	3.80
101394	39.11	34.31	15.96	1.20	4.35	4.89
101413a	35.14	33.66	17.32	4.71	5.30	3.89
101413b	34.81	32.66	17.22	4.43	6.86	4.02
86029a	42.34	33.63	16.29	1.40	2.36	3.99
86029b	41.80	30.55	17.51	-	5.33	4.90
101469	38.47	29.53	15.56	1.79	9.01	5.63
101361	38.77	35.01	18.35	0.98	3.48	3.44
101319a	38.14	29.06	20.31	4.50	2.79	5.19
101319b	35.70	32.87	12.82	4.43	10.31	3.87
101313a	38.10	30.75	15.08	3.79	8.33	3.95
101313b	39.86	30.78	16.31	3.15	5.51	4.39

Wo	Wollastonite	$(Ca_2Si_2O_6)$
En	Enstatite	$(Mg_2Si_2O_6)$
Fs	Ferrosilite	$(Fe_2Si_2O_6)$
Ct	Ca-Tschermak	$(Ca\ Al_2\ SiO_6)$
Tt	Ti-Tschermak	$(Ca\ Ti\ Al_2O_6)$
Ac	Acmite	$(Na\ Fe^{3+}\ Si_2O_6)$

Table A.5.5

Clinopyroxene norms

Rock	101266	101331	101418a	101418b	101393a	101393b	101394	101413a
or	0.12	-	-	-	0.18	-	0.06	0.06
ab	3.70	4.32	4.37	4.38	1.17	4.47	4.72	3.75
an	5.69	5.82	3.40	6.09	6.13	4.13	4.02	9.90
le	-	-	-	-	-	-	-	-
ne	-	-	-	-	2.21	-	0.53	0.42
di	76.63	76.96	78.97	76.04	81.86	81.18	80.57	72.08
hy	3.32	2.20	7.17	3.25	-	0.06	-	-
ol	5.40	5.13	1.74	5.36	2.44	5.60	4.50	6.79
cs	-	-	-	-	-	-	-	-
mt	1.65	1.94	1.92	1.94	2.39	1.95	2.54	2.13
il	3.49	3.63	2.44	2.95	3.63	2.63	3.05	4.65

Rock	101413b	86029a	86029b	101469	101361	101319a	101319b	1013_13a	101313b
or	0.12	-	-	-	-	0.12	-	-	0.18
ab	0.48	4.60	5.26	-	3.99	5.92	-	-	1.00
an	11.47	2.15	3.36	9.72	3.99	5.63	15.68	12.43	7.84
le	-	-	-	-	-	-	0.14	0.09	-
ne	2.28	-	0.17	3.51	-	-	2.43	2.49	2.19
di	72.08	85.96	84.42	77.33	79.59	78.33	67.17	72.19	81.24
hy	-	2.11	-	-	3.63	1.28	-	-	-
ol	6.79	1.58	0.84	0.17	5.31	4.22	3.63	2.99	1.56
cs	-	-	-	0.42	-	-	1.95	2.12	-
mt	2.13	2.03	2.46	2.86	1.76	2.66	2.06	2.09	2.31
il	4.65	1.57	3.49	5.98	2.34	1.84	6.93	5.60	3.68

Table A.5.6

Kaersutite

Rock	101319	No. ions on basis 23 Oxygen	
SiO_2	38.17	5.787 2.212 (Al^{iv})	Z
Al_2O_3	13.1	0.129 (Al^{iv})	
TiO_2	6.67	0.771	
FeO*	13.06	1.656	Y
MgO	10.72	2.422	
CaO	11.18	1.816	
Na_2O	2.25	0.661	X
K_2O	1.51	0.292	
Tot.	96.66		

CIPW Norms (wt%)

	a	b
ne	0.54	1.58
hy	-	-
di	25.64	8.51
ol	17.48	16.29
or	8.25	9.09
ab	16.62	16.47
an	19.59	21.58
il	11.87	-
hm	-	14.77

Norms: a. = analysis totally oxidised

b. = analysis totally reduced

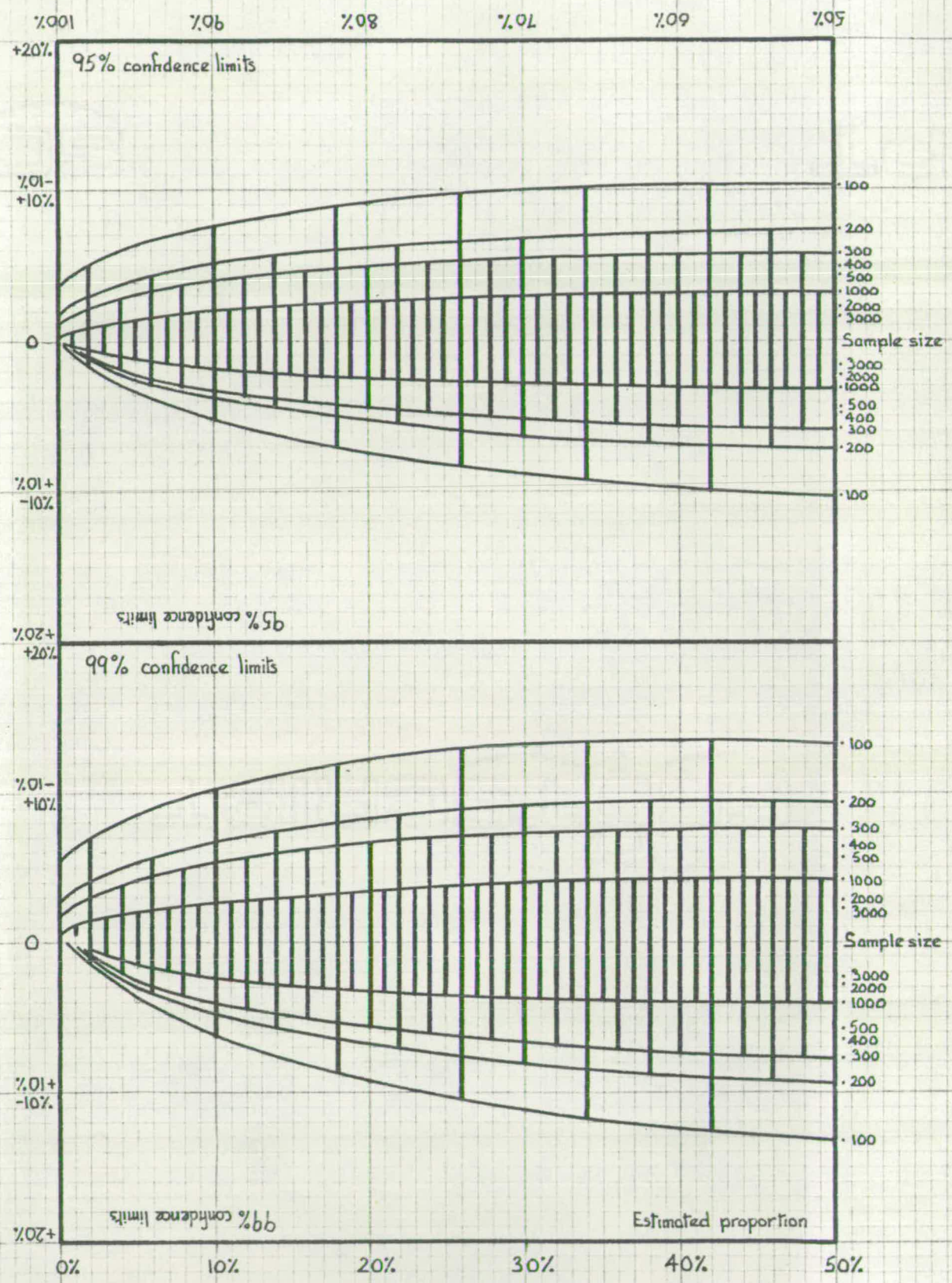
Appendix 6

Optical determinations

Plagioclase compositions were determined on a flat-stage microscope, using the Michel-Levy method.

Modal data was determined on a flat stage microscope fitted with a point-counting stage. Either 200 or 300 points were counted, depending on grain-size. Figure A.6.1 was used to estimate the standard error of the determinations.

FIGURE A6.1:
Confidence-limit chart to be used in conjunction with Table A6.1.



Turn the graphs upside down for proportions over 50%

RFC 1974 December 3

CONFIDENCE LIMITS FOR ESTIMATING PROPORTIONS BY COUNTING

Explanation of/abbreviations and symbols used in Appendix 6,

Table A6.1.

D	dolerite
G	gabbro
TD	trachydolerite
SG	syenogabbro
MS	mafic syenite
B	Benmoreite
GA	gabbro anorthosite
Tdi	trachydiorite
T	trachyte
S	syenite
R	rhyolite
DP	dolerite pegmatite
AK	augite kersantite
p/g	phenocryst/groundmass
+	constituent present
ep	epidote
rieb	riebeckite
o	ocelli
hbl	hornblende
gt	garnet
cc	calcite
ab	albite
ag	aegirine
he	haematite

Modal analyses of rocks in Appendix 4

Spec. No.	Oliv p/g	Plag p/g	Alk p/g	Cpx p/g	Ore p/g	Ap p/g	Bi/chl g	Qz p/g	Other g	Rock Type
101264	0/8	0/32	0/25	0/18	0/6	0/1	10			TD
101266	0/15	0/64	0/13	0/4	0/2	0/+	2			D
101267		0/31	0/30	0/28	0/3	0/2	6			DP
101296	0/8	0/53	0/13	0/11	0/6	0/+	10			D
101271	3/+	14/+	0/?	0/+	+/+	0/?	+			TD
101272	0/4	0/36	0/29	0/8	0/7	0/3	13			TD
101327	0/+	0/10	0/75	0/4	0/2	0/1	4		ep	MS
101328	0/9	0/53	0/12	0/2	0/15	0/3	5			TD
101283	0/13	0/50	0/19	0/8	0/6	0/1	3			TD
101469	1/8	3/43	0/27	0/5	0/6	0/1	6			TD
101470	0/11	2/48	0/16	0/7	0/8	0/4	4			TD
101471	0/15	0/56	0/11	0/7	0/3	0/2	4			D
101277	4/?	12/+	0/?	0/+	1/+	0/?	+			TD
101287	0/?	0/37	0/16	0/17	0/5	0/+	19		ep	TD
101488	0/?	4/+	0/?	0/?	1/+	0/?	+			TD
101489			6/74	0/+	1/+	1/?	+	2/+	rieb	R
101301	+/?	19/+	0/?	0/+	+/+	0/?	+			TD
101302			13/+		0/+			2/+	rieb	R
101248			0/57	0/1	0/2	0/+			rieb	T
101275			0/78		0/+				rieb	T
101312	5/?	8/+	0/+	0/+	+/+	0/?	+		o 5	Tdi
101313	0/?	0/26	0/24	0/18	0/12	0/+	17		ep	Tdi

101317	4/+	10/19	0/25	4/14	0/5	0/?	14		ep	Tdi
101320	2/?	6/+	0/?	0/+	1/+	0/?	+		o 3	Tdi
101487	6/?	16/+	0/?	0/+	3/+	0/?	+		o 5	Tdi
101331	0/17	0/60	0/6	0/6	0/3	0/+	2			D
101333	0/7	0/63	0/12	0/10	0/5	0/+	3			TD
101345	0/15	0/53	0/9	0/11	0/7	0/+	5			D
101430	0/12	0/55	0/10	0/10	0/4	0/1	8			TD
101336	0/10	0/61	0/9	0/9	0/6	0/1	4			TD
101347	0/12	0/56	0/9	0/10	0/5	0/+	8			D
101431	0/20	0/62	0/5	0/6	0/3	0/+	4			D
101436	0/7	0/52	0/16	0/7	0/8	0/+	10			TD
101338	0/12	0/59	0/8	0/7	0/7	0/+	7			D
101349		0/+	8/+	0/+	1/+	+/+	+	0/+	hbl	B
101356	+/+	+/+	0/?	0/+	+/+	0/?	+			TD
101368	0/12	0/58	0/6	0/10	0/6	0/1	7			D
101369	0/11	0/60	0/5	0/11	0/4	0/+	9			D
101375	+/?	5/+	0/?	0/+	+/+	0/?	+			TD
101381	0/7	0/51	0/10	0/15	0/7	0/1	9			TD
101393	0/18	0/64	0/10	0/3	0/2	0/+	3			D
101394	0/14	60/21	0/?	0/4	0/1	0/+	+			GA
101339	0/3	0/35	0/40	0/7	0/9	0/2	4			SG
101342	0/5	0/32	0/29	0/14	0/5	0/3	12			SG
101361	0/4	0/33	0/37	0/10	0/6	0/3	7	0/+		SG
101351	0/9	0/34	0/30	0/9	0/10	0/4	4			SG
101357	0/+	0/28	0/45	0/8	0/7	0/3	5		ep 4	SG
101366	0/?	0/25	0/35	0/12	0/7	0/2	19			SG

101377	0/+	0/27	0/30	0/17	0/9	0/+	17			SG
101340	0/+	0/7	0/64	0/12	0/6	0/1	10			S
101341	0/+	0/11	0/69	0/9	0/4	0/1	6		gt	S
101343		0/6	0/75	0/6	0/6	0/1	6			S
101344	0/+	/70ab	0/10	/17ag	0/he		3			S
101362	0/	0/6	0/72	0/8	0/5	0/1	5		hbl/3	S
101358	0/+	0/15	0/70	0/4	0/4	0/+	7			S
101355	0/2	0/18	0/49	0/13	0/5	0/1	12			SG
101386	0/12	0/54	0/9	0/12	0/5	0/+	8			D
101388	0/15	0/49	0/12	0/13	0/3	0/+	8			D
101370	0/14	0/54	0/11	0/8	0/7	0/+	6			D
101360	0/13	0/59	0/13	0/7	0/5	0/1	2			D
101380	0/11	0/52	0/11	0/13	0/4	0/+	9			D
101391	0/8	0/49	0/14	0/10	0/5	0/+	14			TD
101406	0/5	0/35	0/23	0/17	0/10	0/3	3	0/1		TD
101417	2/+	4/+	0/?	0/+	0/+	0/?	+			D
101418	0/14	0/52	0/5	0/17	0/8	0/+	4			G
101427	0/9	0/58	0/9	0/8	0/6	0/1	9			G
101428	0/13	0/60	0/9	0/7	0/3	0/+	8			D
101398	0/12	0/52	0/8	0/12	0/10	0/+	6			D
101419	0/9	+/55	0/5	0/16	0/8	0/+	7			D
101422	0/14	0/67	0/7	0/6	0/3	0/+	3			D
101426	0/10	+/55	0/6	0/14	0/7	0/+	8			D
101429	0/14	0/62	0/4	0/9	0/3	0/+	8			D
101400	0/16	0/54	0/12	0/5	0/2	0/+	11			D
101401	3/+	0/23	0/30	12/+	0/9	0/+	12			TD

01403	0/16	0/55	0/8	0/13	0/4	0/+	4			D
01404	0/13	0/58	0/6	0/12	0/7	0/+	4			D
01405	0/15	0/60	0/6	0/7	0/5	0/+	7			D
01421	0/10	0/53	0/12	0/10	0/9	0/1	5			TD
01425	0/8	0/46	0/18	0/12	0/11	0/1	4			TD
01407	0/18	0/59	0/6	0/10	0/3	0/+	4			D
01408	0/5	+/50	0/15	0/12	0/11	0/2	5			TD
01409		0/20	0/49	0/	0/8	0/1	17		hbl/cc	Tdi
01411		0/45		0/19	0/9	0/2	25		cc	AK
01412	+/?	2/+	0/?	0/+	+/+	0/+	+			TD
01413	3/+	7/+	0/?	0/+	0/+	0/?	+			D
01415	0/7	0/56	0/13	0/10	0/7	0/+	7			TD
01416	4/?	+/45		6/15	+/14	0/+	14		hbl/cc	AK

Swedish dykes. Jotnian age.

	0/7	0/55	0/12	0/15	0/6	0/1	4			TD
	0/+	3/+	0/?	0/+	0/+	0/+	+	0/+		TD
	0/8	0/49	0/9	0/17	0/8	0/+	9			TD

- - - - - - - - - - - - - - -

ERRATA:

page 116: the sentence on lines 2 and 3 should read '40% fractionation from liquids with enrichment factors of between 4 and 17 produces enrichment factors in the residual liquid of 8 to 28.'

page 7: third line from the foot of the page: Bridgwater and Coe (1970) should read Bridgwater and Coe (1969).

page 9: line 9 and throughout: Sorensen (1969) should read Sorensen (1966).

page 11: second line from the foot of the page: Gill (1972) should read Gill (1972 b).

page 12: tenth line from the foot of the page: reference missing.

Ferguson, J. 1964. Geology of the Ilimaussaq intrusion, south Greenland. Bull. Grønlands geol. Unders., 39 (Meddr. Grønland, 172).

page 14: line nine: Watt (1969) should read Watt (1966).

page 18: line five: reference missing. Welin, E. and Blomqvist, G. 1966. Further age measurements on radioactive minerals from Sweden. Geol. Fören. Stockholm Forhandlingar, 88, 3-18.

page 20: line two: Mohr (1970) should read Mohr (1971).

page 36: line three: 'defined' should read 'deflected'.

page 37: ninth line from the foot of the page: Emeleus and Stevenson (1969) should read Emeleus and Stevenson (1970).

explanation of fig. 4.3., opposite page 59: two references missing.

Wilkinson, J.F.G. 1956. Clinopyroxenes of alkali olivine basalt magma. Am. Mineralogist, 41, 724-743.

Brown, G.M. and Vincent, E.A. 1963. Pyroxenes from the late stages of fractionation of the Skaergaard intrusion, E. Greenland. J. Petrology, 4, 175-197.

page 71: line 6: Emslie and Roeder (1970) should read Roeder and Emslie (1970).

page 83: ninth line from the foot of the page: reference missing. Kogarko, L.N., Ryabchikov, I.D. and Sørensen, H. 1974. Liquid fractionation. In: The Alkaline Rocks, Sorensen, H. (Ed.), 488-499. Wiley Interscience, New York.

page 88: line three: Thompson et. al. (1972) refers to Thompson, G. et al.

page 90: line three: reference missing. Chao, E.C.T. and Fleischer, M. 1960. The abundance of zirconium in igneous rocks. Twenty-first International Geological Congress Report, 1, 106-131.

page 108: third line form the foot of the page: reference missing. Ito, K. and Kennedy, G.C. 1967. Melting and phase relations in a natural peridotite to 40 kilobars. Am. J. Sci., 265, 519-539.

page 113: line nine: Thompson, et al. (1972) refers to Thompson, R.N.

" " line twelve: Kushiro (1969) should read Kushiro (1970).

" " ninth line from the foot of the page: Yoder (1969) should read Yoder (1970).

Al_2O_3 wt

MgO wt

TiO_2 wt

MgO wt

Na_2O wt

MgO wt

MnO wt

MgO wt

P_2O_5

MgO wt

K_2O wt

MgO wt

SiO_2 wt

MgO wt

CaO wt

MgO wt

$Fe_2O_3 + FeO$ wt

MgO wt

Sr ppm.
200
400
0
2 3 4 5 6 7 8 9 10 11 12 MgO wt

Ba ppm
3000
2000
1000
0
2 3 4 5 6 7 8 9 10 11 12 MgO wt

V ppm.
500
300
100
0
2 3 4 5 6 7 8 9 10 11 12 MgO wt.

Rb ppm
200
100
0
2 4 6 8 10 12 MgOwt

Zn ppm
160
80
0
2 4 6 8 10 12 MgOwt

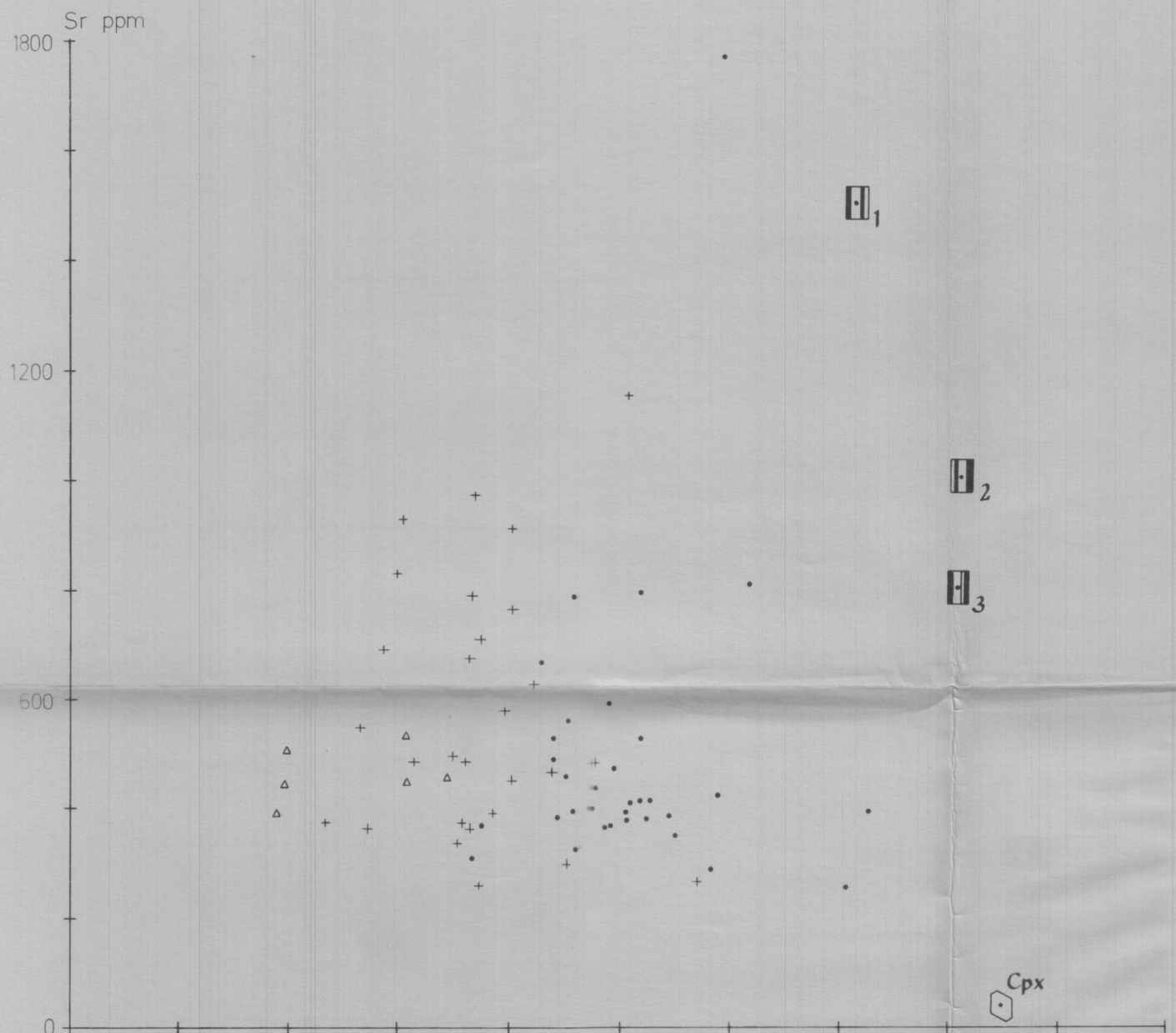
Zr ppm
500
300
100
0
2 4 6 8 10 12 MgOwt

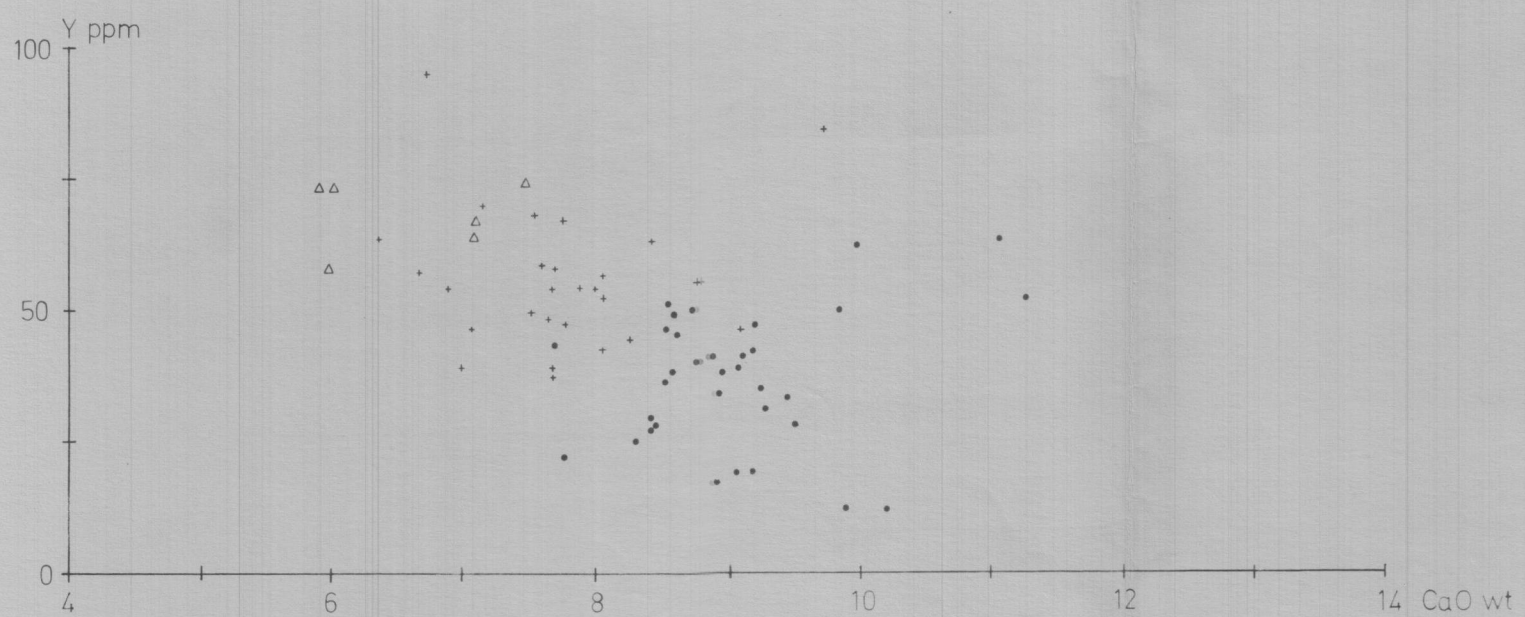
Y ppm
100
50
0
2 4 6 8 10 12 MgOwt

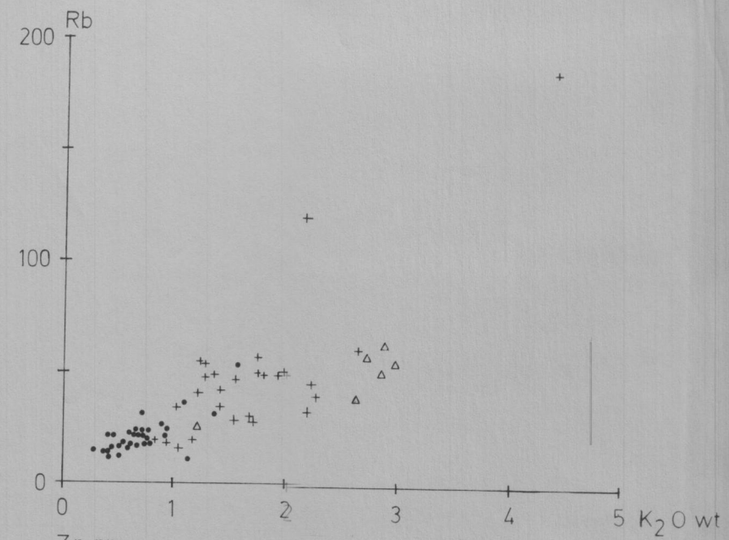
Cu ppm
180
120
60
0
2 4 6 8 10 12 MgOwt

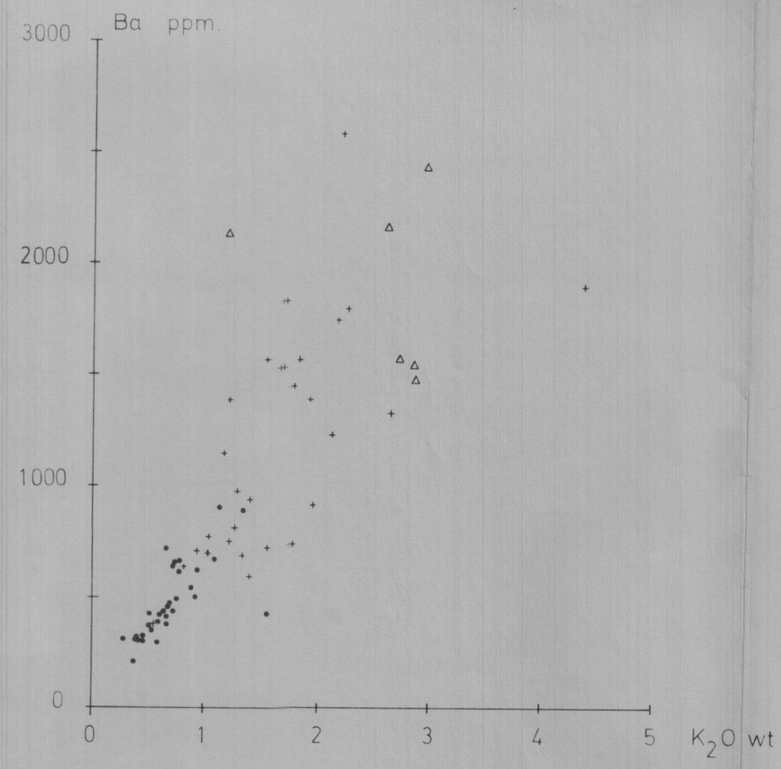
Cr ppm
360
240
120
0
2 4 6 8 10 12 MgO wt

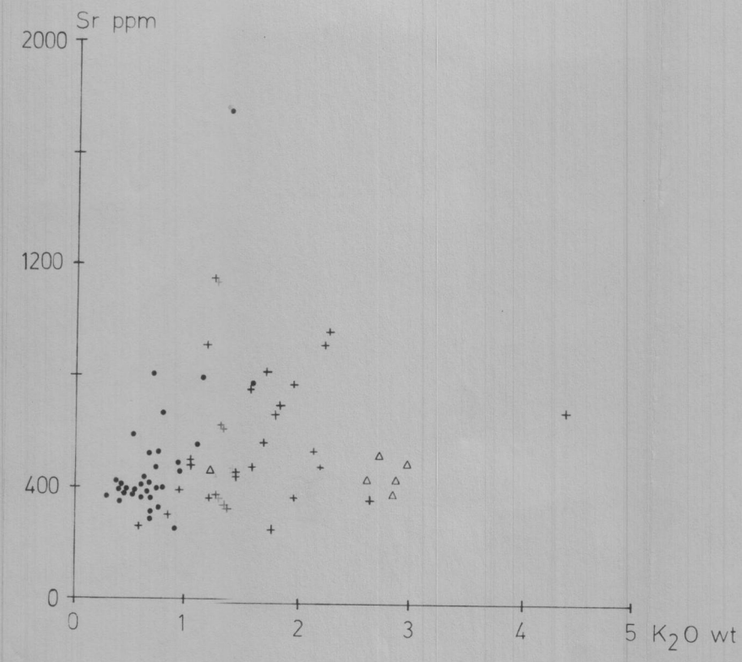
Ni ppm
300
200
100
0
2 3 4 5 6 7 8 9 10 11 12 MgO wt

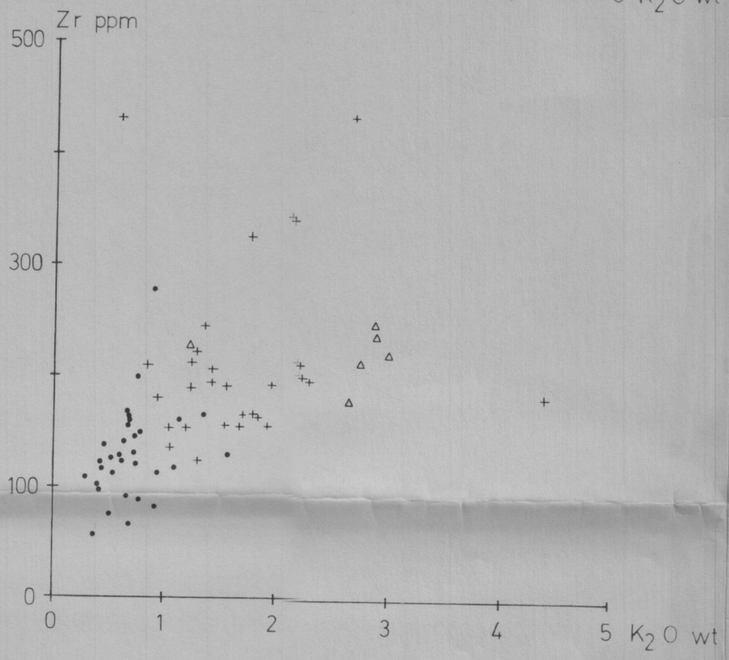

Sr ppm
1800
1200
600
0
0
6
8
10
12
14 CaO wt
1
2
3
Cpx

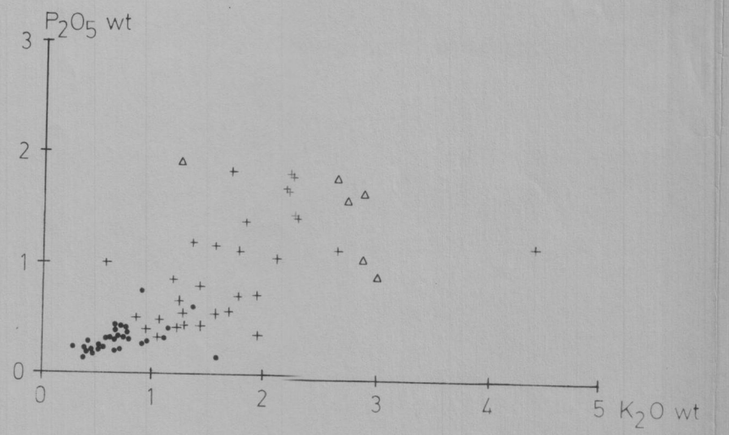

Y ppm
100
50
0
4
6
8
10
12
14 CaO wt

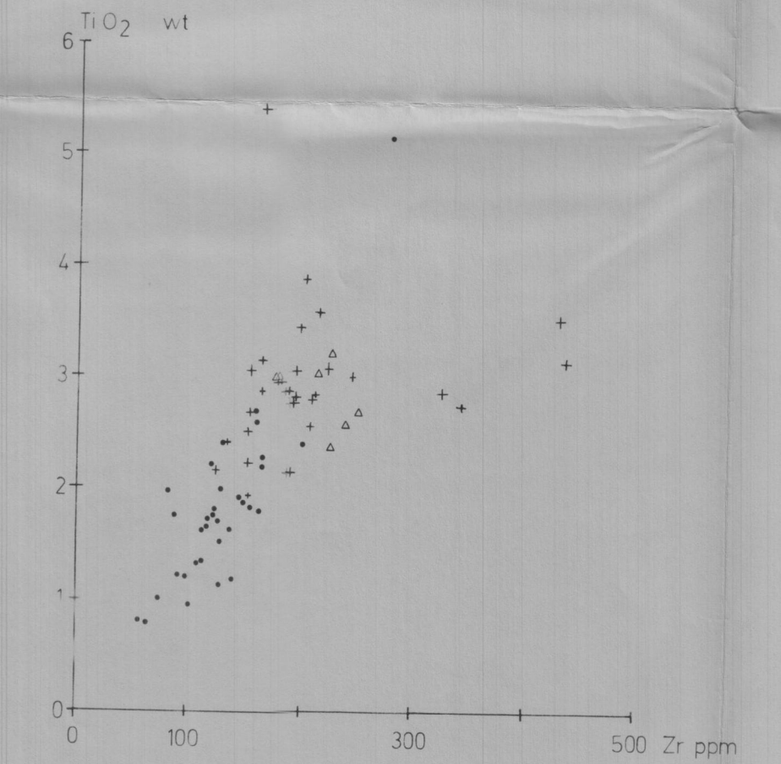

Rb
200
100
0
0
1
2
3
4
5 K_2O wt

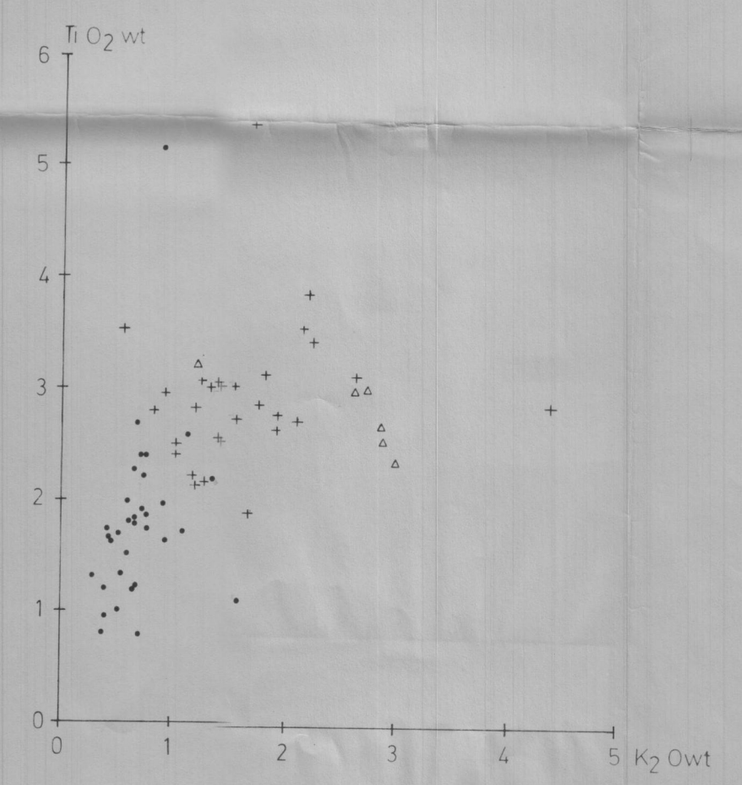

Ba ppm
3000
2000
1000
0
0
1
2
3
4
5 K_2O wt


Sr ppm
2000
1200
400
0
0
1
2
3
4
5 K_2O wt


Zr ppm
500
300
100
0
0
1
2
3
4
5 K_2O wt


P_2O_5 wt
3
2
1
0
0
1
2
3
4
5 K_2O wt


TiO_2 wt
6
5
4
3
2
1
0
0
100
300
500 Zr ppm


TiO_2 wt
6
5
4
3
2
1
0
0
1
2
3
4
5 K_2O wt